ABSTRACT

Title of Thesis:	BEHAVIOR OF FIBER REINFORCED POLYMER PILES WITH OCTAGONAL CROSS-SECTIONS IN INTEGRAL ABUTMENT BRIDGE FOUNDATIONS
	Kavach Gupta, Master of Science, 2020
Thesis Directed By:	Professor Amde M. Amde Department of Civil and Environmental Engineering

Billions of dollars worth of losses are incurred due to corrosion and degradation of bridges in the United States. In a conventional bridge, deicing salts and chemicals cause rapid degradation in expansion joints, stiffeners, and other structural components. One of the solutions to tackle such a problem is to eliminate expansion joints in the system and design the whole bridge as an integral abutment bridge. In this type of bridge, the abutment and the deck act as a monolithic system. An integral abutment bridge has no expansion joints. Movement due to thermal expansion and contraction is accommodated by the abutments, which in turn transfer the movement to the piles. The maintenance costs of integral abutment bridges are considerably lower than the traditional jointed bridges; therefore, most state highway departments

in the United States recommend the use of integral abutment bridges whenever possible.

Using alternatives to conventional piling materials is another solution discussed in this thesis and will be the main focus of the same. Fiber Reinforced Polymer (FRP) piles have some advantages in corrosion resistance and hence can be economical in aggressive environments. In this thesis, FRP piles with octagonal cross-sections were analyzed for their behavior in integral abutment bridges. The octagonal section can easily be manufactured using a vast array of manufacturing methods, especially by the filament winding method, which is a cheaper manufacturing option as compared to other methods like pultrusion. Octagonal sections provide flat surfaces that make operations like bolting easy. In addition to this, irregular octagonal sections can provide stiffness and flexibility about two perpendicular axes simultaneously. Three-dimensional models were made and analyzed using ANSYS Workbench with the help of ANSYS Composite PrePost (ACP) modules. Over 300 soil-pile models were analyzed in this study. The results in this thesis depict the trends captured by varying different parameters for various soil-pile models.

BEHAVIOR OF FIBER REINFORCED POLYMER COMPOSITE PILES WITH OCTAGONAL CROSS SECTIONS IN INTEGRAL ABUTMENT BRIDGE FOUNDATIONS

by

Kavach Gupta

Thesis submitted to the Faculty of the Graduate School of the
University of Maryland, College Park, in partial fulfillment
of the requirements for the degree of
Master of Science
2020

Advisory Committee:
Professor Amde M. Amde, Chair
Professor M. Sherif Aggour
Professor Chung C. Fu

Dedication

This thesis is wholeheartedly dedicated to my beloved parents, who have been a constant source of inspiration and encouragement for me.

Acknowledgments

First and foremost, I would like to express my heartfelt gratitude towards my advisor and mentor, Dr. Amde M. Amde, for his continuous support throughout the course of this study. Without his able guidance, I cannot think of being able to have done this study.

I would also like to thank my advisory committee: Dr. M. Sherif Aggour and Dr. Chung C. Fu, for agreeing to be a part of the committee. A special thanks to Dr. Aggour, whose ENCE 641 class taught me necessary concepts in pile foundations, which were very useful in this thesis.

I would also like to thank Dr. Yahya Aliabadizadeh, for guiding me throughout this study. I would also like to thank Mr. Dustin Troutman of Creative Pultrusions for agreeing to share engineering data from their firm.

I would also like to thank my friend Ms. Priya Ashok for proofreading my thesis document by taking out time from her busy schedule and also for her emotional support throughout the course of study.

Last but not least I would like to thank my mother Neena Gupta, my father Suresh Gupta, my grandmother Chanchal Gupta, my uncle Parvesh Gupta, my aunt Radha Gupta, my sisters Kokila Gupta and Kishika Gupta and my brothers Chaitanaya Mahajan and Kashish Gupta, without whose support I would not have been able to attend the graduate school at all. A special thanks to my nephew Ihit for the positive vibes of his presence that made his uncle able to finish this study on time.

I would take this opportunity to remember my late grandfather, who would be happy in heaven, seeing me succeed.

Table of Contents

List of Tables

List of Figures

1 Introduction

We live in an era of rapid infrastructure development, and bridges are an essential component of the same. The conventional bridges have led to billions of dollars worth of losses in repair and maintenance (Iskander et al., 1998), especially in aggressive environments (like marine environment). The deterioration of concrete, steel, and timber is hence a severe disadvantage of constructing bridges in such aggressive environments. Fiber reinforced polymer (FRP) can be used as a reliable piling material against corrosion.

It has also been found that installation and maintenance of expansion joints and bearings are expensive since deicing chemicals and salts are prevalent through these locations, which eventually corrode the bridge. Designing bridges as integral abutment bridges prove to be effective for this problem.

In this study, integral abutment bridges with FRPs were analyzed. Insufficient performance history and present experimental prominence to the subject have restricted the use of FRP piles to fendering and similar lightweight applications only. For heavy load usage, there is still room for research in order to explore the possibility of using FRP piles in bridges.

Recent research (Jaradat, 2005) analyzed soil-pile behavior in integral abutment bridges for FRP piles, which paved the way for future research. The benefits of elliptical cross-sections (Aliabadizadeh,2016) were analyzed in comparison to the circular FRP piles, further strengthening the research. These studies found that FRP piles were effective against lateral movements caused in integral abutment bridges. This thesis analyzes FRP piles with octagonal cross-sections for use in integral abutment bridges. A finite element analysis of over 300 three-dimensional models was done using ANSYS Workbench.

1.1 Integral Abutment Bridges

Thermal strains cause expansion and contraction in bridges. These movements are generally accommodated by using expansion joints and roller supports. Installation and maintenance of joints and bearings are expensive. Since these joints start leaking over time, they become main sites of deterioration due to deicing chemicals and salts, especially in aggressive environments.

A possible solution to the above problems is designing a bridge as an integral abutment bridge, where the deck and abutment act as a monolithic system. Integral abutment bridges are found to be cost-effective and hence are widely popular throughout the United States.

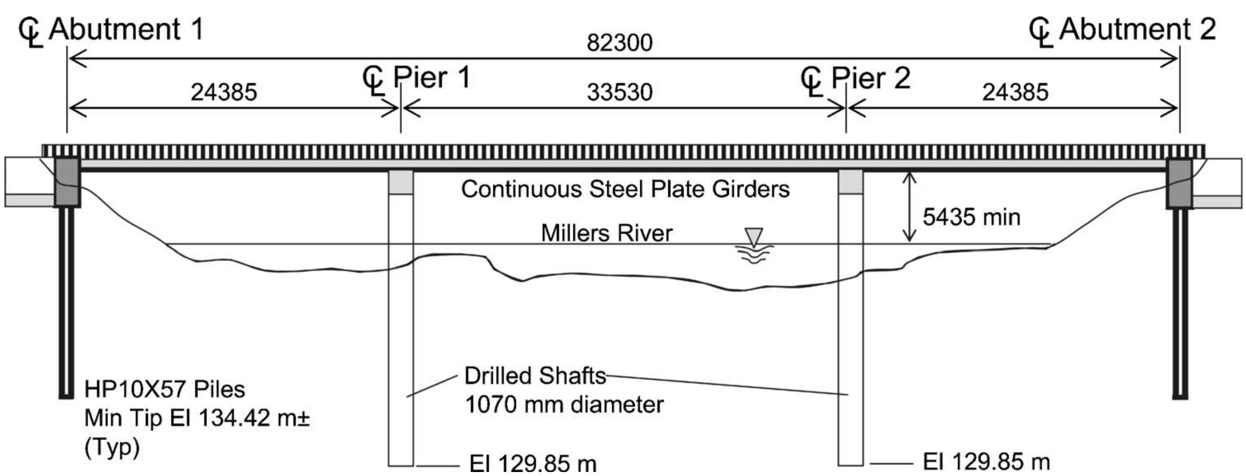

Figure 1: Side view schematic of Orange-Wendell Bridge, an Integral Abutment Bridge (Civjan, Bonczar, et al., 2007)

Since the abutments are directly supported on piles, the lateral movement in the abutment is accommodated by lateral movement in piles. This eliminates the need for expansion joints in the bridge. In addition to this, IABs save bridge owners a considerable amount of money and time compared to conventional bridges. Colorado was the first U.S. state to build an IAB in the 1920s, followed by California. Many other states like Massachusetts, Kansas, Ohio, Oregon, Pennsylvania, and South Dakota followed suit in the following years (Kunin and Alampalli 1999). A study in University of Maryland (Paraschos and Amde 2011) has shown that 41 states in the U.S. have been using integral abutment bridges as of 2008. This number has shown an increasing trend since its introduction to the country and is still gaining more acceptance.

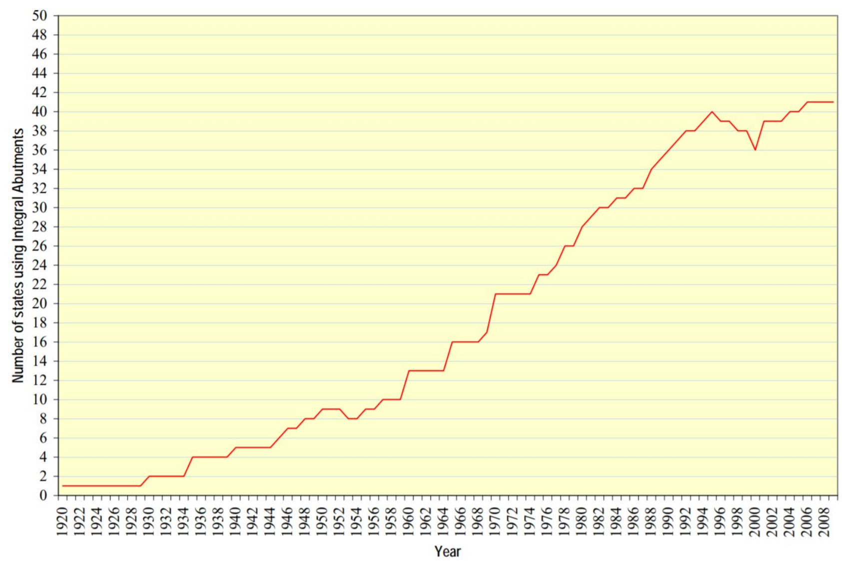

Figure 2: Evolution of IAB in U.S. (Paraschos and Amde 2011)

Kunin and Alampalli (2000) have found that the benefits of integral abutment bridges include reduced initial costs and long term maintenance expenses, resistance against deicing chemicals and salts, decreased impact loads, improved riding quality, simple construction procedures, and structural continuity which resists seismic events and overloads. All these benefits have encouraged designers to prefer IABs over conventional bridges wherever feasible. Overall, the performance of IABs has been rated between good to excellent irrespective of problems like cracking and settlement of bridge approaches and lack of a set design standard across agencies and states.

However, since the system is monolithic, the temperature and other forces generate lateral movement, which is directly transferred to the piles. Hence, the engineers need to make sure that the piles are designed for such loads. Most agencies use the following equation to estimate the thermal movement:

$$\Delta\, Length = Length \times \Delta\, Temperature \times Coefficient\ of\ thermal\ expansion$$

It has been found that H or HP piles generally serve the purpose, but in aggressive environments, corrosion plays a significant role in discouraging the use of such piles. That is where using FRP piles can prove to be effective due to their corrosion-resistant properties.

1.2 Fiber Reinforced Polymer (FRP)

Fiber reinforced polymer (FRP) is a composite material made of two phases, namely matrix phase, and the reinforcing phase. The reinforcing phase consists of fibers, which are usually the load-bearing component of the composite material. The fibers used are generally glass, carbon, aramid, etc. Sometimes other fibers like wood, asbestos, or paper might be used as well. The matrix phase provides protection and support to fibers and facilitates stress transfer within the section. The matrix usually consists of epoxy, vinyl ester or polyester thermosetting plastic.

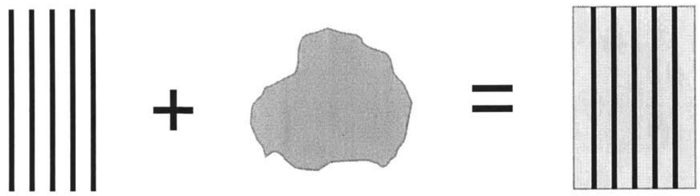

Figure 3: Formation of FRP (Tuakta, 2004)

The reinforcing fibers are combined with the resin matrix in different forms to create laminate. Initially developed for aerospace research and manufacturing, FRPs are gaining wide popularity in the civil engineering industry, especially in marine and bridge applications. Structural engineers are gaining more confidence in using this technology as more and more advances are happening in this field.

1.2.1 Structure of FRP Composites

FRP composite system can is a system of two or more phases on a macroscopic level that decide the properties of the resulting composite material. As discussed earlier, the properties of the resulting composite material are superior to those of the individual constituent materials. The phase that is usually stiffer, discontinuous, and more robust, is called the reinforcing phase, and the other phase, which is less stiff but continuous is called the matrix. Some chemical interactions between the two phases may result in the formation of interphase at the union of two phases.

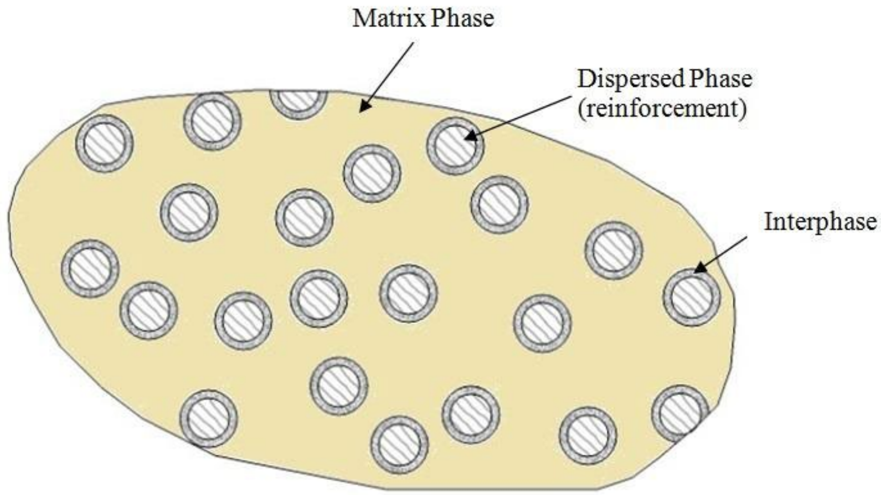

Figure 4: Phases of a composite material (Daniel and Ishai, 1994)

The properties of the resultant composite material are dependent on the properties of its constituents, their geometry, and the phase distribution. One of the most critical parameters is the volume fraction of the reinforcing fibers. Also, the distribution determines the homogeneity of the material system. (Daniel and Ishai, 1994)

1.2.2 Lamina (Ply) and Laminates

A lamina also called ply, is a plane or curved layer of unidirectional fibers or woven fibers in a matrix. If the fibers are unidirectional, the lamina is referred to as unidirectional lamina (UD) and would be the main focus of the analysis throughout this thesis. A lamina is considered to be an orthotropic material that has a longitudinal, a transverse (in-plane), and a normal principal axis.

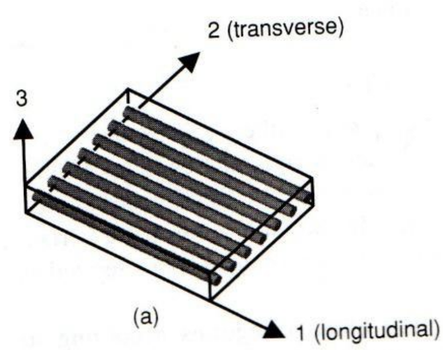

Figure 5: Unidirectional Lamina (Daniel and Ishai, 1994)

A laminate is formed by stacking up layers of unidirectional laminae. These laminae can be stacked up in different orientations to yield different properties, which is shown in the upcoming sections. Because of the complexity of multilayered geometry, it is recommended to use a fixed coordinate system (x, y, z). This way, the orientation of the ply can also be determined by observing its angle from the reference x-axis.

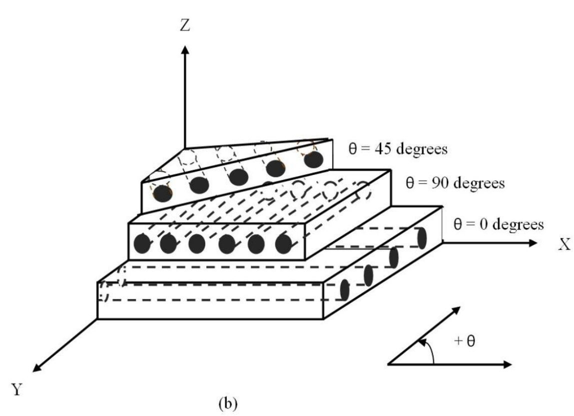

Figure 6: Coordinate system in multidirectional laminate (Daniel and Ishai, 1994)

1.2.3 Types of fibers

Fibers constitute the reinforcing materials in an FRP composite. It is generally made into a long filament with a diameter in the order of 10 micrometers. Generally, the fiber occupies 30-70% of the matrix volume in composites (Aliabadizadeh, 2016). We have the flexibility to use fibers in either continuous or discontinuous form (Shaia, 2013). For structural applications, the most commonly used fibers are glass fiber, aramid fibers, carbon, boron, ultrahigh molecular weight polyethylene. The main functions of the fibers are to carry the load and provide stiffness, strength, thermal stability, and other structural properties in the FRP. Thus, the fibers in FRP must have a high modulus of elasticity, high ultimate strength, a low variation of strength among fibers, high stability of their strength during handling, and high uniformity of diameter and surface dimension among fibers (Tuakta, 2004).

In the civil engineering industry, there are three classes of fibers which are widely used :

i. Glass Fibers.
ii. Carbon Fibers.
iii. Aramid Fibers.

The properties of the most commonly used fibers are tabulated below:

Table 1: Properties of some common fibers (Tuakta, 2004)

Material	**Density (g/cm^3)**	**Tensile Modulus (E) (GPa)**	**Tensile Strength (σ) (GPa)**	**Specific Modulus (E/σ)**	**Specific Strength**	**Relative Cost**
E-glass	2.54	70	3.45	27	1.35	Low
S-glass	2.5	86	4.5	34.5	1.8	Moderate
Graphite, high modulus	1.9	400	1.8	200	0.9	High
Graphite, high strength	1.7	240	2.6	140	1.5	High
Boron	2.6	400	3.5	155	1.3	High
Kevlar 29	1.45	80	2.8	55.5	1.9	Moderate
Kevlar 49	1.45	130	2.8	89.5	1.9	Moderate

1.2.3.1 Glass Fibers

Glass fibers the most commonly used reinforcing materials of all in the civil engineering industry. They are formed when thin strands of silica-based or other formulation glass are extruded into many fibers with small diameters. The process and technique of drawing glass into small fibers have been known for a considerable amount of time, but the process of using them in fabric applications is very recent (Aliabadizadeh, 2016).

Five forms of glass fiber strands are used in composite applications: chopped fibers, chopped strands, chopped strand mats, woven fabric, and surface tissue. Further, three classes of glass fibers are identified:

i. E-glass.
ii. S-glass.
iii. C-glass.

Figure 7: Fiberglass being used in filament winding process (Fibrex FRP Piping Systems, 2020)

The E-glass stands for glass fiber designated for electrical use, S for high strength, and C for high corrosion resistance. Out of all. E-glass is most commonly used in the civil engineering industry, and C-glass is least used. E-glass is produced from lime-alumina-borosilicate, which uses readily available raw materials like sand. The glass fiber strength and modulus can degrade with increasing temperature and has a lower thermal expansion coefficient than that of steel. (Tang, 1997)

Table 2: Typical cured epoxy/glass mechanical properties. (Composite Material Handbook, DoD)

E Glass, Woven 7781 Style	Standard Structural	Dual Purpose Structural/Adhesive
Tensile Strength, ksi (Mpa)	63 (430)	48 (330)
Tensile Modulus, Msi (Gpa)	3.8 (36)	2.8 (19)
Compressive Strength, ksi (MPa)	60 (410)	50 (340)
Compressive Modulus, Msi (GPa)	3.6 (25)	3.2 (22)
Flexural Strength ksi, (MPa)	80 (550)	65 (450)
Flexural Modulus Msi, (GPa)	3.7 (26)	3.3 (23)
Interlaminar Shear ksi, (MPa)	2.6 (18)	3.8 (26)
Sandwich Peel, lb/in width (N/m width)	N/A	30 (3.4)
Metal-to-Metal Peel, lb/lin. in. (N/lin. m)	N/A	55 (6.3)
Specific Gravity gm/cm3 (lb/in3)	1.8 (0.065)	1.6 (0.058)
Cured Resin Content % Wt.	33	48

1.2.3.2 Aramid Fibers

Aromatic polyamide fiber, also known as aramid fibers, is a high-performance fiber used in civil engineering applications. The manufacturing process includes extruding a solution of aromatic polyamide at low temperatures of (-50 degree Celsius to -80 degree Celsius) onto a hot cylinder at 200 degrees Celsius. Fibers left after evaporation are then stretched and drawn to increase their strength and stiffness. During this process, molecules become highly oriented in the longitudinal direction. They possess higher strength and toughness among the reinforcing fibers and have high static, dynamic fatigue, and impact strengths (Tuakta, 2004). The most commonly used aramid fibers are Kevlar® 29 and Kevlar® 49.

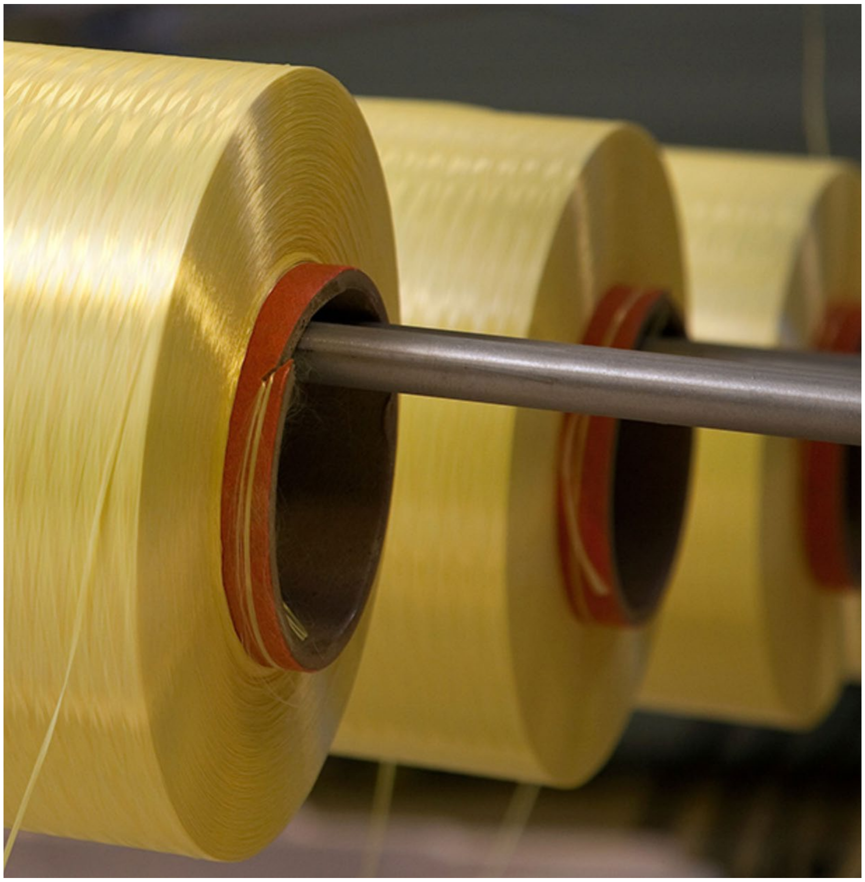

Figure 8:Kevlar® Fibers (Dupont, 2020)

1.2.3.3 Carbon Fibers

Carbon fibers are also high-performance fibers used in the civil engineering industry. They are selected to achieve a high modulus in order to get a stiffer composite. With the economic point of view, the carbon fibers are much expensive than the glass fibers making their use limited to certain specific cases. We can choose from three precursors for carbon fibers: polyacrylonitrile (PAN), rayon, and pitch precursors. Their stress-strain curve is linear until the point of rupture, and they have lower thermal expansion coefficients than both glass and aramid fibers. Carbon fibers also have very high fatigue and creep resistance.

The carbon fiber becomes brittle at higher modulus. It becomes critical in joint and connection details, which have high stress concentrations. As a result of this phenomenon, composites made out of carbon fibers are more effective with adhesive bonding that eliminates mechanical fasteners. (Aliabadizadeh, 2016)

Figure 9: Some carbon fiber FRP profiles (Creative Pultrusions, 2020)

1.2.4 Types of Resins

Resins are generally used as the matrix in FRP composites. There are broadly three classes of resins that are used in an FRP composite, thermoplastic resin, thermosetting resin, and phenolic resin.

1.2.4.1 Thermoplastic Resin

Thermoplastic resins can be heated and remolded into other shapes since they have a defined melting point and can retain this new shape when allowed to cool. Thermoplastics have low creep resistance, even at moderate temperatures.

1.2.4.2 Thermosetting Resins

Thermosetting resins do not have a defined melting point; therefore, they cannot be heated and formed again. They can take the shape of the die and harden after cooling. However, thermosetting composites disintegrate when subjected to extreme heating.

1.2.4.3 Phenolic Resins

These are resins made of phenyl formaldehyde and have been there for long. However, they are relatively very new to the composites. They are used if superior fire resistance, and minimum smoke emissions are required. They are well suited for E-glass and carbon fibers.

1.2.5 Methods of FRP Manufacture

This thesis deals with the properties of FRP piles. Understanding the method of manufacture of a particular pile plays a crucial role in judging its behavior in many aspects like shear between the layers. The fibers are used as a composite with resin, as discussed earlier. In an FRP pile system, the fibers provide reinforcement and necessary strength, whereas the resin used decides properties like corrosion resistance, flame resistance, and the maximum operating temperature. In the sections below, methods of FRP manufacture are discussed, namely: hand layup, filament winding, pultrusion, and compression mold.

1.2.5.1 Hand Layup Process

The hand layup method is one of the oldest molding methods for making FRP products. It is a time and labor-intensive method. It is especially suitable for large parts such as FRP vessels. The mold carries the structural shape of the product desired and is designed to have a corresponding surface finish as required in the final product. For example, if the outer surface of the product is smooth, the product is made inside the female mold, and if the inner surface is smooth, the male mold is used. The mold has to be free of defects, as this decides the quality of the final product as well.

Figure 10: Hand layup process (DOFRP, 2020)

Since this is a low volume, labor-intensive process, it is suitable for FRP vessels, fiberglass car bodies, FRP furniture, etc. A variety of shapes can be made using this method. This method does not require any expensive machinery set up to start working. On the other hand, there is a significant quality control issue with this method. It is highly subjective to the operator's skills and hence not suitable for mass production.

1.2.5.2 Filament Winding Method

In this process, continuous fiber filaments are saturated with catalyzed resin and helically wound around a mandrel using a device that moves up and down the length of the rotating mandrel. This method generally makes products with the least voids possible and gives it a high fiber volume ratio of up to 80 percent. After the layers of fibers are wounded, the components of the composite are solidified. Thermosetting resins like polyester, vinyl ester, epoxy resin, and phenolic resins are preferred for this method.

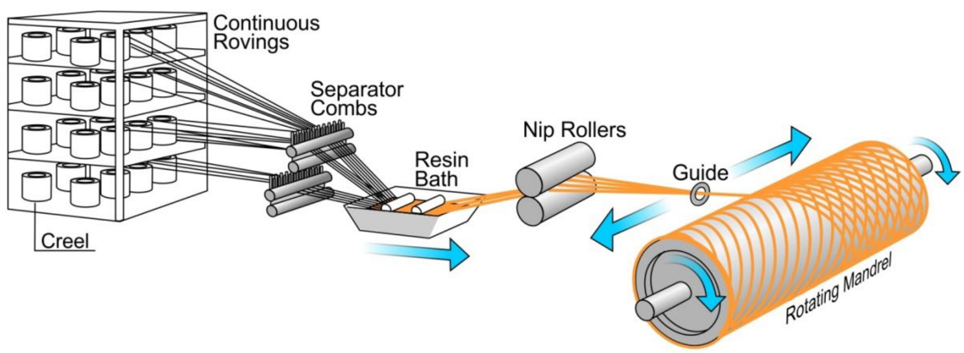

Figure 11: Filament Winding Method (Aliabadizadeh, 2016)

Because we can control the fiber placement using this method, we can reach the highest strength of FRP products. This process is semi-automatic; hence the manufacture can be completed in an orderly manner with fewer workers. By using this method, large diameters of about 15 meters can be accommodated. At the same time, this method is not suitable for complex FRP profiles since this method is suitable for only circular or close to circular sections. In this thesis, since the octagonal profile is analyzed, filament winding is recommended because of lower cost and high fiber density.

1.2.5.3 Pultrusion Process

In this method, resin-impregnated fibers are pulled through a heated steel forming die using a continuous pulling die. The fibers are placed in axial direction using this process. As the material meets the heating mold, the resin changes from liquid to gel and eventually solidifies to hard plastic. The traction device grasps the FRP material and pulls the material through the mold. After passing through it, the products are sawed to the required length.

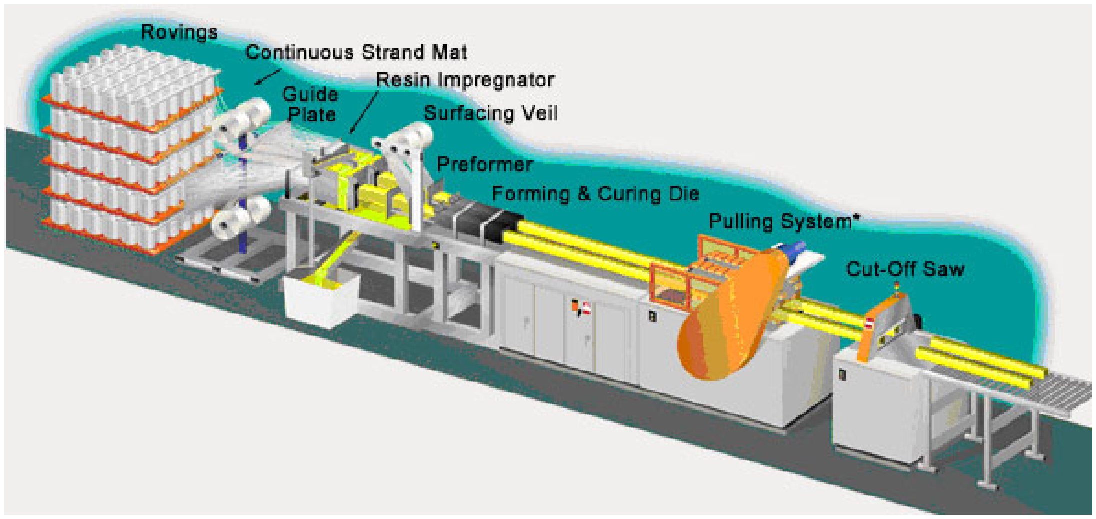

Figure 12: Pultrusion Process (Advanced Fiber Products, 2020)

The resin content can be accurately controlled in the pultrusion process. Laminate quality is excellent, and since the resin impregnation area can be enclosed, the volatile emissions are less hence promoting a better work environment. On the other hand, the cost to set up and maintain pultrusion machinery is prohibitive. Moreover, the pultrusion method is limited to near-constant cross-section components.

1.2.5.4 Compression Molding

This method is standard for the manufacture of car body parts like wheels, bumpers, utility hole covers, and plate-spring. Broadly, this process involves converting sheet plastic into FRP finish by using pressure to press it inside the mold. This method is particularly advantageous and fast for the manufacture of complex geometric shapes.

Figure 13: Compression Molding (DOFRP, 2020)

Some advantages of this method include a superior finish on all surfaces, fast production, fully automates the process as well as the ability to make products of uniform quality. On the other hand, since the setup is costly, it is not suitable for low yield. Moreover, this process is not relevant to very large FRP composites.

1.2.6 Mechanical Properties of FRP Composites

The mechanical properties of FRP composites depend on a variety of factors like fiber-ratio, the properties of individual components, the method of manufacture, fiber-orientation, fiber continuity, etc. (Tuakta, 2004)

Table 3: Typical mechanical properties of long directionally aligned fiber-reinforced composites manufactured by an automated process (epoxy resin) (Tuakta, 2004)

Material	Specific Weight	Tensile Strength (Mpa)	Tensile Modulus (Gpa)	Flexural Strength (Mpa)	Flexural Modulus (Gpa)
E-Glass	1.9	760-1030	41	1448	41
S-2 Glass	1.8	1690	52	-	-
Aramid 58	1.45	1150-1380	70-107	-	-
Carbon (PAN)	1.6	1930-2689	130-172	1593	110
Carbon (Pitch)	1.8	1380-1480	331-440	-	-

An FRP composite is considered to be an orthotropic material, and its Young's modulus can be estimated using the volumetric fractions of the two phases in the composite:

$$E_c = v_f E_f + v_r E_r$$

Where v_f and v_r are the volume fractions of fiber and resin respectively, and the subscripts c, f, and r denote the composite, fiber and the resin. The stress-strain relationship of FRP composites is almost linear, and they do not yield plastically. However, non-linearity might also be observed due to the formation of cracks in resin, fiber buckling in compression, fiber debonding, viscoelastic deformation of matrix, fiber, or both. Therefore, a yield point in composite materials signifies the departure from the linear stress-strain relationship (Tuakta, 2004). The axial tensile and compressive strengths are dependent on the fiber properties as they are responsible for taking most of the load. They are stiffer than the matrix. The transverse strength properties are influenced primarily by the matrix strength characteristics, fiber-matrix bond strength, and the internal properties like voids and internal stresses, etc. The matrix helps stabilize the fibers in compression by preventing buckling at a lower stress level.

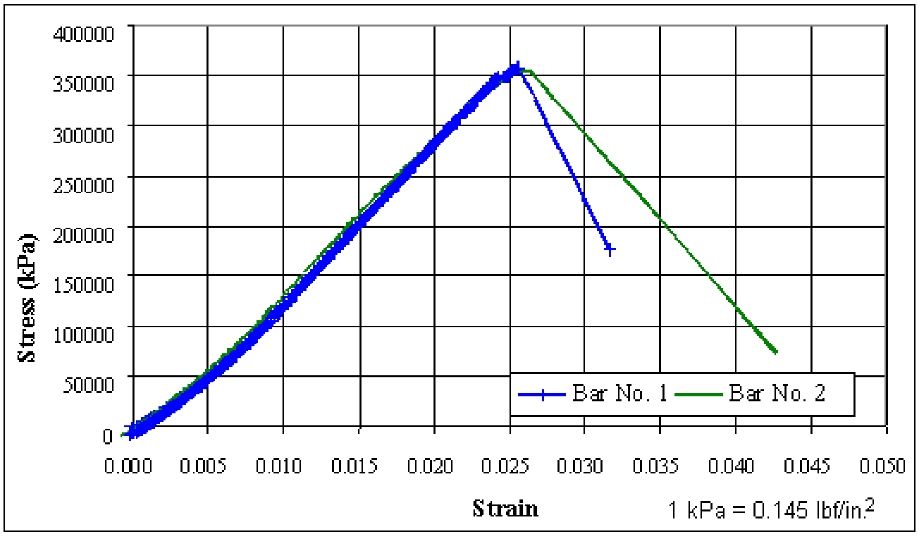

Figure 14:Stress-strain relationship of fiberglass bars (FHWA, 2006)

According to Tuakta (2004), the properties of discontinuous fiber composites are affected by fiber length and diameter, in addition to those which affect the unidirectional composites. Due to the lower fiber ratio in discontinuous fiber composites, the mechanical properties of continuous fiber composites are better.

To sum up, there are three potential causes of FRP failure:

i. Design errors.
ii. Faulty fabrication and processes.
iii. Fracture, which depends on fiber type and orientation.

1.2.7 Benefits of FRP

For an infrastructure project, FRP offers five key benefits: (Composite Advantage, 2020)

- Faster installation time.
- Lightweight material.

- Resistance to corrosion and very little maintenance.
- Cost savings.
- Design flexibility.

It can be noted that conventional building materials might seem to be cost-effective in the short term, but FRP materials prove to be economical in the long term.

1.2.7.1 Faster Installation Time

Construction of infrastructure projects might affect the day to day life of civilians, hence dragging a project for too long might be rather inconvenient for the public. Most of the FRP products are prefabricated and can be installed very swiftly, saving up majorly on the construction hours.

1.2.7.2 Lightweight Material

Components made of FRP are over eight times lighter than the precast concrete (Composite Advantage, 2020). Hence they are significantly safer and easier to work with. They require cheaper transport and require less equipment to move around. For example, FRP decking for cantilever sidewalks with a dead load of 4-9 ksf, can be up to 90 percent lighter than reinforced concrete panels.

1.2.7.3 Resistance to Corrosion and Little Maintenance Requirement

FRP products are durable and hence can last long. In environments with high concentrations of salt and other chemicals, FRP structures can last nearly 80-100 years since they are highly resistant to corrosion. To this date, this corrosion-resistant property of FRPs is greatly utilized in waterfront areas as fender piles. FRP structures need very little or no maintenance throughout their life cycle.

1.2.7.4 Cost Savings

In the short term, FRP structures may seem expensive. However, FRP components are explicitly designed to increase profitability and long-term savings. This comes in light considering the facts that FRP structures have superior durability, have low maintenance requirements, have an enhanced service life as well as they can be positioned swiftly and cheaply.

1.2.7.5 Design Flexibility

Generally, FRPs are ideal for any type of job that requires customization. Be it a complex geometry or specific feature; an FRP component can be engineered to meet those specifications with characteristic ease. This allows designers to be more versatile.

2 FRP Composite Piles

Piles are structures that are used predominantly to support structures subject to vertical and lateral loads. The load-bearing capacity of the piles depends on the site conditions, soil properties, pile-properties, etc. This is why soil-pile interaction is an important area to explore in the study of behavior of piles. The piles can be installed by either driving, which disturbs the soil, or the other method where soil displacement is not necessary. The FRP piles follow the former process of installation.

The piles can be made of materials, some of them conventional like steel, pre-cast concrete, timber, etc., and some may be made of novel materials like fiber reinforced polymer. Concrete, timber, and steel piles corrode, especially in marine environments, due to which heavy losses are incurred. Timber is treated for marine environments using chemicals like creosote, which poses a threat to marine life due to toxic nature (Iskander and Hassan, 1998). So there is not just an economic perspective involved, but there are significant environmental issues as well, which need to be addressed.

Figure 15: Marine borers (Limnoria) attacking untreated timber piles (FHWA, 2006)

Figure 16: Complete corrosion of steel H piles supporting a harbor pier (FHWA, 2006)

Composite piling industry is experiencing rapid growth in modern times with its extensive use as structures like fender piles, etc. At the same time, composite piling turns out to be expensive to acquire, which might discourage some stakeholders. However, manufacturers claim that the composite piling costs less to maintain, lasts twice as long as conventional materials like treated timber, and does not pose environmental problems (Iskander and Hassan, 1998). Another problem that has been observed with composite piling is less driving efficiency than the conventional piling. This problem will also be addressed in the upcoming sections.

2.1 Some Commonly Available Composite Piles

There are some piling products which the composite manufacturers are creating today. They can be classified as steel pipe core piling, structurally reinforced plastic matrix, fiberglass pipe pile, fiberglass-pultruded piling, and fiber reinforced plastic piling. They are discussed below:

2.1.1 Steel Pipe Core Piling

It is considered to be amongst the first plastic piling products in the American market. The piles consist of a recycled plastic shell that covers an inner steel core. The steel core is responsible for the structural strength of the pile.

2.1.2 Structurally Reinforced Plastic Matrix Piling

This type of pile typically consists of a recycled plastic matrix, reinforced with fiberglass or steel rods. Typically, the plastic matrix is chemically treated with antioxidants and ultraviolet inhibitors to retard the effects of UV light on the plastic. If reinforced with glass fibers, the piling is nonmagnetic and recyclable.

2.1.3 Fiberglass Pipe Pile

This type of pile is the prime focus of this thesis and consists of a fiberglass tubular section. The fiberglass shell provides structural strength and is highly resistant to corrosion and other damage. The fibers are impregnated with the resin and laid in designed orientations according to the required properties.

2.1.4 Fiberglass Pultruded Piling

This type of pile is nearly the same as the previous one, with the exception that this method involves a particular manufacturing method called pultrusion. In Pultrusion, as already discussed above, is the process in which wet fibers are pulled through a die and then solidified.

2.1.5 Fiber Reinforced Plastic Piling

This kind of piling consists of a recycled plastic matrix with randomly distributed fiberglass reinforcement in the matrix.

2.2 Structural Behavior of FRP Piles

Many researchers have studied the structural behavior of FRP piles. The researchers have specifically focused on studying the short-term structural behavior of the FRP piles. Many state highway departments have also shown interest in such studies. A brief account of the structural behavior of FRP piles is given below:

2.2.1 Short-Term Structural Behavior

2.2.1.1 Axial Behavior

As discussed above, the short term structural behavior has been a distinct interest for the researchers and the agencies. Fam and Rizkalla (2001) studied the behavior of concrete-filled FRP piles and proposed a confinement model.

The FRP shell in a concrete-filled composite contributes structurally to the pile by primarily providing confinement to the concrete core. Fam and Rizkalla (2001) developed a confinement model and studied the effects of confining concrete in an FRP tube. The capacity of the resulting composite exceeds the load sharing capacity of individual materials, as shown in the figure.

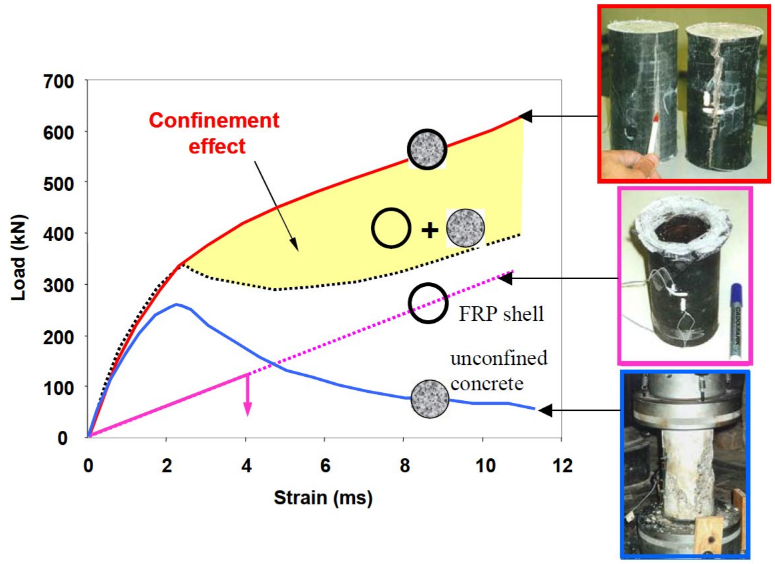

Figure 17: Confinement effect on load-strain behavior of concrete (Fam and Rizkalla, 2001)

The load-strain curve starts to depart from the unconfined concrete curve in the vicinity of the unconfined concrete strength. Here, the concrete core starts to experience significant micro-cracking, as well as increased lateral expansion, and the FRP shell applies a radial confining pressure in response (Pando, Lesko, et al., 2002). This confining pressure exerted by the FRP tube increases due to its linear elastic properties. The second slope of the load-strain curve is a function of the hoop tensile stiffness of the FRP shell, and the ultimate peak strength is governed by the hoop tensile strength of the shell. Fam and Rizkalla (2001) proposed a confinement model by which short term axial capacity of concrete-filled FRP tubes can be predicted. The results from this model were in close agreement with the experimental results, as shown in figure 18.

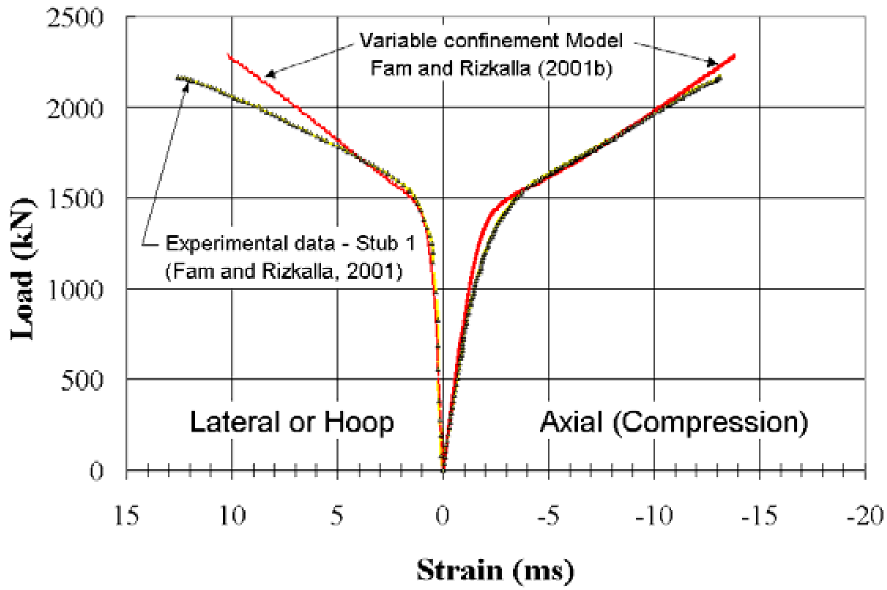

Figure 18: Experimental versus predicted axial load-strain curves using the Fam and Rizkalla model (Pando, 2002)

2.2.1.2 Flexural Behavior

Concrete-filled FRP piles can be used to resist bending moments. However, the benefits of concrete confinement are less in this case. FRP tube acts as a non-corrosive reinforcement, and the concrete provides internal resistance force in the compression zone, and increases the stiffness of the member. The concrete core also prevents the local buckling of the FRP shell.

2.2.1.3 Long-term Behavior

In marine environments, piles made of conventional building materials degrade typically over a period of 20 years. On the other hand, the manufacturers of FRP piles estimate the design life of FRP piles to be at least 75 years. This makes the life-cycle cost of FRP piles considerably low even though the initial cost for FRP piles may be high.

2.3 Drivability of FRP Piles

The drivability of FRP piles has been found to be a key issue with their usability. Many experimental and numerical analyses have been done to address this issue. Lawrence (2015), in his experimental study with GFRP piles, found that during driving, varying levels of damage was experienced in the piles. After encountering hard-driving, the hollow piles experienced a brooming failure at the head and the toe. The piles with a concrete plug at the toe experienced less severe damage. Concrete-filled FRP piles did not show much damage in the field. However, the concrete-FRP bond failed during the flexural testing.

Ashford and Jakrapiyanun (2001) found that the reason for these drivability limitations for GFRP piles is their low impedance. The impedance of a pile is the primary factor that controls pile drivability. It is calculated as the product of mass density, the cross-sectional area, and the compression wave velocity (Ashford and Jakrapiyanun, 2001). The low mass density and the high elastic modulus of the GFRPs, combined with small cross-sectional areas required due to high strengths, result in having a low pile impedance. The drivability issues may limit the ability of GFRP piles to serve as bearing piles.

2.3.1 Solutions and Recommendations

One of the conventional solutions to the problem of low impedance is increasing the thickness of the FRP shell. It was found that doubling the wall thickness essentially doubled the impedance. Another standard solution that can help increase the impedance is filling the FRP shell with concrete. Experimental results have found concrete-filled FRP piles to have better drivability. This is because the mass density and cross-sectional area increase simultaneously, which leads to an increase in impedance. Ashford and Jakrapiyanun (2001) have recommended using a high-frequency vibratory driver for installation to overcome the low impedance problem. Another recommendation is to use a steel mandrel to essentially drag the pile into place. Varying the fiber orientation was found to help optimize compression wave velocity as it is a function of elastic modulus.

Driven piles are generally installed by striking a hammer at the pile head. Sakr et al. (2004) suggested a novel toe driving technique for thin-walled FRP piles. It involves an independent penetration of the pile toe and the pile itself using a special driving head. The driving head is connected to the hammer through a long anvil. The ram of the hammer hits the anvil that transfers the impact shock to a loading plate. The loading plate is connected to a conical tip to facilitate pushing soil away. Details of the driving mechanism are shown in the figure:

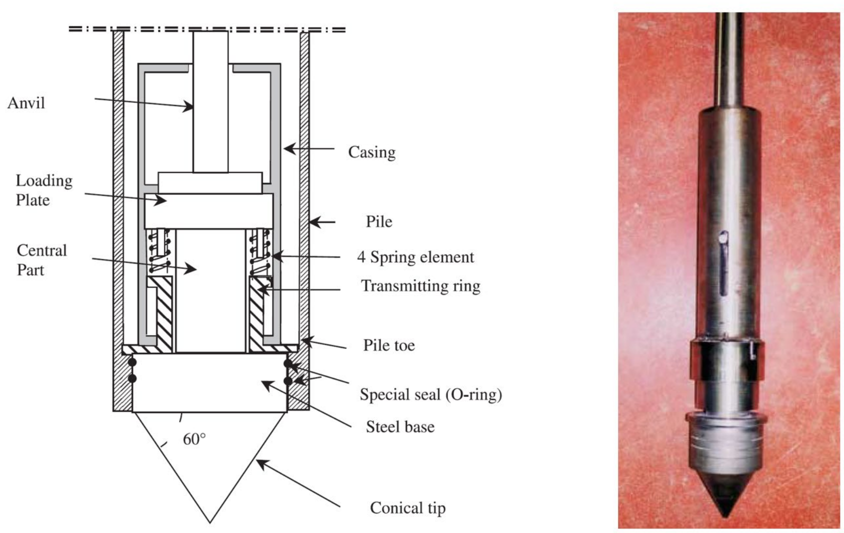

Figure 19: Toe-driving Mechanism (Sakr et al., 2004)

The main difference between toe driving and head driving is that in toe driving, the toe resistance is mobilized first, and the initial tension wave is strongly attenuated as it travels upwards to the pile head.

On the contrary, in traditional driving, the shaft resistance is mobilized first in the pile-soil interface, which leads to subsequent disturbance of surrounding soil. The initial compression wave travels downwards to the pile toe, and then the soil layer is compressed, creating a stress field around the pile and an increase in shaft resistance. Some of the main advantages of using toe driving are:

- Since the tensile strength of FRP composites is much more than its compressive strength, toe-driving utilizes its high tensile strength.
- The wall thickness of the piles can be reduced since the impact loads are transferred directly to the soil.
- The directional stability is enhanced since the center of gravity of the pile and hammer is much low.
- Piles can be easily driven through hard soils and strata as the force is concentrated at the toe.
- It is suitable for urban areas since noise levels are much lesser than traditional hammer driving.

In easy driving conditions as in soft soils, the gain in driving efficiency is not much appreciable.

2.4 Factors Affecting FRP Pile Capacity

There are certain factors that affect the capacity of FRP piles. Some of them can be varied as parameters in the numerical models, and some are environmental factors which might not be considered in the modeling. For the latter case, the choice of equipment and building materials should be made by giving due consideration to these environmental factors. Some of the most important factors are explained below:

2.4.1 Fiber Materials

Once it is decided that FRP piles are to be used for a project, choosing the right type of fibers is essential. Different fibers have different properties, and they are selected according to the usage of that particular pile in the project. For example, carbon fibers can be used to get a stiffer composite, whereas aramid fibers can be used for their higher dynamic fatigue strength.

2.4.2 Type of Resin

The type of resin is also a vital factor that affects the pile capacity. The resins are responsible for the composite's resistance against creep, temperature, etc. Moreover, the resins control the mechanism of load distribution and transfer within the section, which can significantly affect the load capacity of the composite pile.

2.4.3 Fiber Orientation or Ply Angle

The fiber orientation is the angle from the reference axis at which the fibers are wound around the pile's vertical axis. The fiber orientation has been found to affect the stresses generated in a pile, as it can be seen from the analysis results. Moreover, fiber orientation affects the drivability of the pile as well since the compression wave velocity is dependent on the fiber orientation. The choice of manufacturing method becomes very critical as some manufacturing methods have a limit to the fiber orientation.

2.4.4 Number of Layers

The number of layers decides the thickness of an FRP pile is a significant factor that affects the pile capacity. A higher number of layers is seen to add on to the pile capacity. Moreover, thicker piles show better drivability properties than thinner piles. Increasing the number of layers decreases the stress in a pile for a given set of loading conditions. Choosing a manufacturing method is also very important in deciding the number of layers. For instance, if it is decided to add on more layers to an existing composite, the pultrusion method cannot be used. On the other hand, the filament winding method would be a practical solution in case changes in the number of layers are required.

2.4.5 Pile Dimensions

Pile dimensions have an immediate impact on the stresses generated in a pile and hence the pile capacity as well. Piles having larger dimensions are found to have better capacity than their smaller counterparts.

2.4.6 Horizontal Load and Horizontal Displacement

Horizontal load and horizontal displacement were found to reduce a pile’s axial capacity since the stresses increase in piles even at lower axial loads. In this thesis, since the FRP piles are used for integral abutment bridges, horizontal load plays an essential part in deciding the pile capacity.

2.5 Primary Reasons for Choosing an Octagonal Cross-section

There is a limited amount of research that has been done on FRP piles until now. Out of those, the majority of work has been done on cylindrical piles, which is justified keeping in view the limited amount of data available for conventional piles in other shapes. Aliabadizadeh (2016), nevertheless attempted to study the behavior of elliptical FRP piles using numerical modeling in his research. His research methodology has paved the way for the study of the behavior of more unconventional sectional shapes.

In this thesis, an attempt has been made to study the behavior of octagonal piles using numerical analysis. The choice was made, keeping in mind several factors like feasibility, industrial acceptability potential, and similar available data to compare with. Some of the factors are explained below:

2.5.1 Close to a circular shape

An octagonal shape is very close to a circular shape. It gives us the advantage of using pre-existing data for circular shapes for comparison. Another significant advantage of being close to circular shape us that it can be easily manufactured using less expensive filament winding method. In addition to being a cheaper manufacturing method, the filament winding method allows adding on additional layers to a composite if required.

2.5.2 Can be made to provide flexibility and stiffness in two perpendicular axes simultaneously

The octagonal piles can be made to provide flexibility and stiffness in two perpendicular axes simultaneously, by elongating it in one direction. The advantage of such a property is that the piles can be oriented such that the weak axis is perpendicular to the centerline of an integral abutment bridge. Such an orientation makes sure that higher flexibility is provided for their movement, and minimum resistance is provided to bridge movement due to thermal expansion or contraction (Najib and Amde, 2010).

2.5.3 Multiple flat surfaces for bolting and other operations

A common problem with the rounded FRP sections is their inability to provide flat and stable surfaces for bolting. Many engineers have identified this issue, and according to FRP pile manufacturers, octagonal piles can prove to be a solution to such a problem since multiple flat surfaces are available for bolting.

2.5.4 Easier shape control

According to FRP manufacturers, cross-sectional shapes like circles and polygons are simpler to control to match the exact specifications. Complex shapes like ellipse can prove to be harder to control and implement precisely as per the specifications.

2.5.5 Use in support of excavation (SoE) systems

Pile walls are an integral part of SoE systems. In tangent pile walls, the use of octagonal shape can prove to provide a better inter-pile contact surface and thus prove to be more effective than the typical circular shape. Interactions with some engineers working in the geo-structural design have endorsed the claim.

3 Failure Criteria

Failure criteria for homogeneous isotropic materials are well established. Macro mechanical failure theories for composites have been proposed by extending and adapting isotropic failure theories to account for the anisotropy in stiffness and strength of the composite.

Azzi and Tsai in 1965 adapted Hill's theory for homogeneous anisotropic ductile materials to anisotropic heterogeneous and brittle composites and introduced the Tsai-Hill theory. In 1971, Tsai-Wu theory was introduced and is extensively used today. In this thesis, some of these criteria were used to determine failure for FRP pile models.

Daniel and Ishai (2006) have classified the lamina failure theories into three groups:

1. **Limit or non-interactive theories:** These are the failure theories in which specific failure modes are predicted by comparing individual lamina stresses or strains with corresponding strengths or ultimate strains. Maximum stress and maximum strain theories are examples of such theories. No interaction among different stress components on failure is considered.
2. **Interactive theories**: These are the theories in which all the stress components are included in one expression. Overall failure is predicted without reference to particular failure modes. Tsai-Hill and Tsai-Wu criteria are examples of such kind of theories.
3. **Partially interactive or failure mode based theories**: These theories give separate criteria for fiber or inter-fiber failures. Puck theory is a typical example of such theories.

Some main failure criteria are discussed below:

3.1 Maximum Stress Theory

According to this criterion, failure will occur if one of the principal stresses components exceeds the allowable strength of the material in that direction. This is a non-interactive failure criterion.

The following conditions must be satisfied:

$$\sigma_1 \leq X_t \quad \sigma_2 \leq Y_t$$

$$\sigma_1 \leq X_c \quad \sigma_2 \leq Y_c$$

$$\tau_{12} \leq S$$

Where:

σ_1= Stress in the fiber direction

σ_2= Stress perpendicular to the fiber direction

τ_{12}= Shear stress

X_t= Tensile strength in the fiber direction

X_c= Compressive strength in the fiber direction

Y_t= Tensile strength in the transverse direction

Y_c= Compressive strength in the transverse direction

S = Shear strength

3.2 Maximum Strain Theory

This theory predicts failure when principal strains in any direction exceed the corresponding maximum allowable strains.

The following conditions must be satisfied:

$$\varepsilon_1 \leq \varepsilon_{1t} \quad \varepsilon_2 \leq \varepsilon_{2t}$$

$$\varepsilon_1 \leq \varepsilon_{1c} \quad \varepsilon_2 \leq \varepsilon_{2c}$$

$$|\gamma_{12}| \leq \gamma$$

Where:

ε_1= Strain in the fiber direction

ε_2= Strain perpendicular to the fiber direction

γ_{12}= Shear strain

ε_{1t}= Maximum tensile strain in the fiber direction

ε_{1c}= Maximum compressive strain in the fiber direction

ε_{2t}= Maximum tensile strain in the transverse direction

ε_{2c}= Maximum compressive strain in the transverse direction

γ = Maximum shear strain

3.3 Tsai-Hill Failure Criterion

In the previous two theories, the stress and strain are assumed to act independently, such that a failure will occur if any individual limit is exceeded. The Tsai-Hill criterion assumes an interaction between the three different stresses so that a failure envelope is obtained by combinations of all element stresses. The expression for this criterion is:

$$\frac{\sigma_1^2}{X^2} - \frac{\sigma_1\sigma_2}{X^2} + \frac{\sigma_2^2}{Y^2} + \frac{\tau_{12}^2}{S^2} = 1$$

3.4 Tsai-Wu Failure Criterion

The Tsai-Wu Failure criterion, also known as interactive tensor polynomial theory, predicts the failure of orthotropic materials using the concept of strength tensors. The proposed form of the criterion is:

$$f_1\sigma_1 + f_2\sigma_2 + f_6\sigma_6 + f_{11}\sigma_1^2 + f_{22}\sigma_2^2 + f_{66}\sigma_6^2 + 2f_{12}\sigma_1\sigma_2 = 1$$

Where:

$$f_1 = \frac{1}{X_t} + \frac{1}{X_c} \quad f_2 = \frac{1}{Y_t} + \frac{1}{Y_c}$$

$$f_{11} = -\frac{1}{X_tX_c} \quad f_{22} = -\frac{1}{Y_tY_c}$$

$$f_6 = 0 \quad f_{22} = \frac{1}{S^2}$$

$$f_{11} = \frac{1}{2\sigma^2}\left[1 - \left(\frac{1}{X_t} + \frac{1}{X_c} + \frac{1}{Y_t} + \frac{1}{Y_c}\right)\sigma + \left(\frac{1}{X_tX_c} + \frac{1}{Y_tY_c}\right)\sigma^2\right]$$

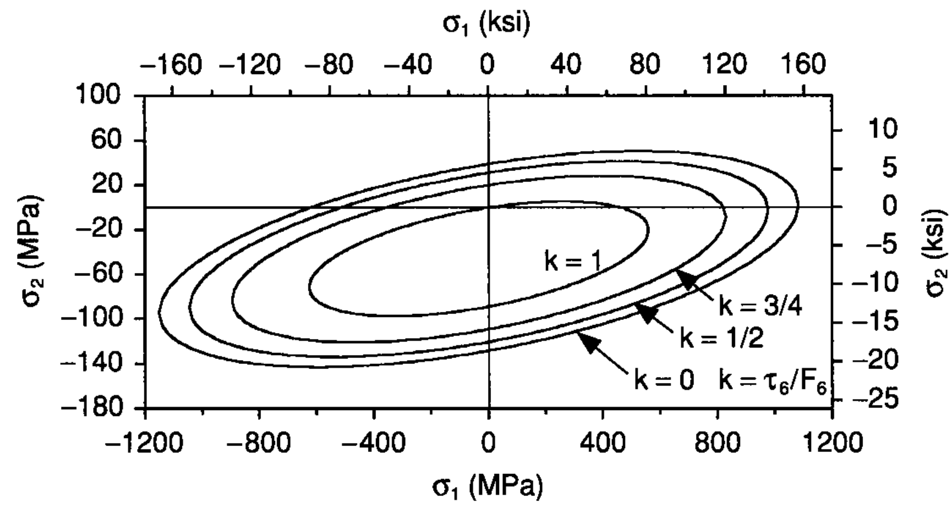

Figure 20: Tsai-Wu Criterion: Failure envelopes for Epoxy E-glass UD lamina under biaxial loading with different levels of shear stress (Daniel and Ishai, 2006)

This criterion has several desirable features. Firstly, it is operationally simple and readily amenable to computational procedures. Secondly, the stress interaction terms can be treated as independent material properties determined by appropriate experiments, unlike the Tsai-Hill theory, where the interaction terms are fixed as functions of other terms. Also, this theory, through its linear terms, accounts for the difference between tensile and compressive strengths.

3.5 Puck Failure Criterion

This criterion is a failure mode based criterion. Puck theory identifies fiber failure and inter-fiber failure in a unidirectional composite. It further separates inter-fiber failure into three different physical modes and further separates fiber failure into two different physical modes. Puck works with action planes in which the composite fails in three inter-fiber fracture modes.

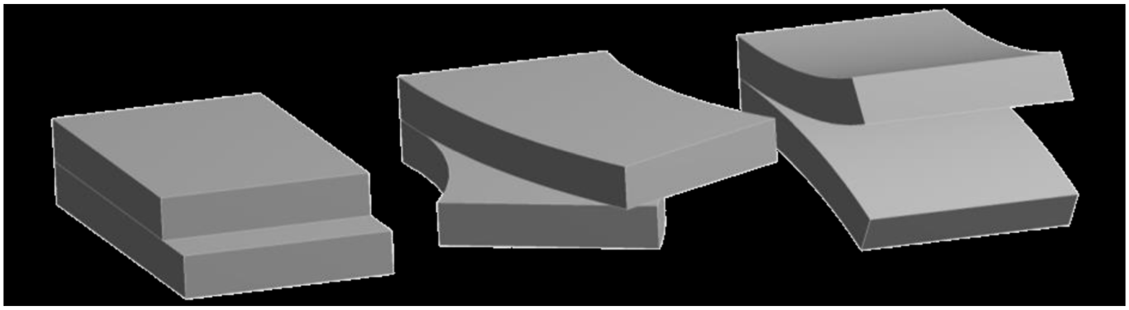

Figure 21: Inter-fiber fracture modes B, C and A (Aliabadizadeh, 2016)

4 Soil Behavior

In this thesis, the soil is assumed to have a non-linear behavior. As already discussed, the soil was represented as a set of springs spread around the pile. Three types of soil resistance-displacement curves can describe the soil characteristics – lateral resistance-displacement (p-y) curves, longitudinal load-slip (f-z) curves, and pile tip load-settlement (q-z) curves.

The p-y curves represent the relationship between the lateral soil pressure against the pile and the corresponding lateral pile displacement. The f-z curves describe the relationship between skin friction and relative vertical displacement. The q-z curves describe the bearing stress at the toe of the pile and the settlement at the toe tip. These three types of curves can be developed from basic soil parameters using the modified Ramberg-Osgood model.

4.1 Lateral Resistance Curves (p-y)

The p-y curves are developed using the modified Ramberg-Osgood model, as discussed above. The parameters needed for the modified equation are the initial lateral stiffness k_h, the ultimate lateral soil resistance p_u and a shape parameter n.

For cohesive soils, the initial lateral stiffness and ultimate lateral soil resistance will be assumed to have a constant value for all depths.

$$k_h = 67c_u$$

$$p_u = 9c_uB$$

For cohesionless soils, both the initial lateral stiffness and ultimate lateral soil resistance will be assumed to vary linearly with depth.

$$k_h = c_u x$$

$$n_h = \frac{J\gamma}{1.35}$$

$$p_u = \left(3\gamma B k_p\right)x$$

where:

k_h=Initial Lateral Stiffness

p= Generalized soil resistance

p_u= Ultimate lateral soil resistance

n= Shape factor

y= Generalized displacement

n_h= Constant of subgrade reaction

B= Pile width

x= Depth from the surface

The p-y relationship can be represented as:

$$p = \frac{k_h y}{\left(1 + \left|\frac{y}{y_n}\right|^n\right)^{\frac{1}{n}}}$$

Where:

$$y_u = \frac{p_u}{k_h}$$

The lateral resistance data for various clays used in this thesis are as follows:

Blow Count	Unit Weight	Undrained Cohesion	Shape Parameter	Pile Width	Depth from Surface	Ultimate Lateral soil resistance		Simplified Ultimate Lateral Resistance	Initial Lateral Stiffness	Simplified Initial lateral Stiffness	Ultimate Displacement	Generalized Displacement	Generalized Lateral Resistance
N	γ (pcf)	C_u (psf)	n	B (ft)	x (ft)	P_u (klf)	P_u (k/in)	$P_u = 9 c_u B$ (klf)	k_h (ksf)	$k_h = 67c_u$ (ksf)	$y_u = p_u/k_h$ (in)	y (in)	p (klf)
3	100	405	1	2	0	2.4	0.2	7.29	24	27.135	0.2687	0.00	0.00
3	100	405	1	2	1	2.8	0.233	7.29	28.05	27.135	0.2687	0.25	0.29
3	100	405	1	2	2	3.2	0.267	7.29	32.1	27.135	0.2687	0.50	0.40
3	100	405	1	2	3	3.6	0.3	7.29	36.15	27.135	0.2687	0.75	0.45
3	100	405	1	2	4	4	0.333	7.29	40.2	27.135	0.2687	1.00	0.48
3	100	405	1	2	5	4.4	0.367	7.29	44.25	27.135	0.2687	1.25	0.50
3	100	405	1	2	6	4.8	0.4	7.29	48.3	27.135	0.2687	1.50	0.52
3	100	405	1	2	7	5.2	0.433	7.29	52.35	27.135	0.2687	1.75	0.53
3	100	405	1	2	8	5.6	0.467	7.29	56.4	27.135	0.2687	2.00	0.54
3	100	405	1	2	9	6	0.5	7.29	60.45	27.135	0.2687	2.25	0.54
3	100	405	1	2	10	6.4	0.533	7.29	64.5	27.135	0.2687	2.50	0.55
3	100	405	1	2	11	6.8	0.567	7.29	68.55	27.135	0.2687	2.75	0.55
3	100	405	1	2	12	7.2	0.6	7.29	72.6	27.135	0.2687	3.00	0.56
3	100	405	1	2	13	7.2	0.6	7.29	73	27.135	0.2687	3.25	0.56
3	100	405	1	2	14	7.2	0.6	7.29	73	27.135	0.2687	3.50	0.56
3	100	405	1	2	15	7.2	0.6	7.29	73	27.135	0.2687	3.75	0.57
3	100	405	1	2	16	7.2	0.6	7.29	73	27.135	0.2687	4.00	0.57

Table 4: Lateral resistance data for Soft Clay (Aliabadizadeh, 2016)

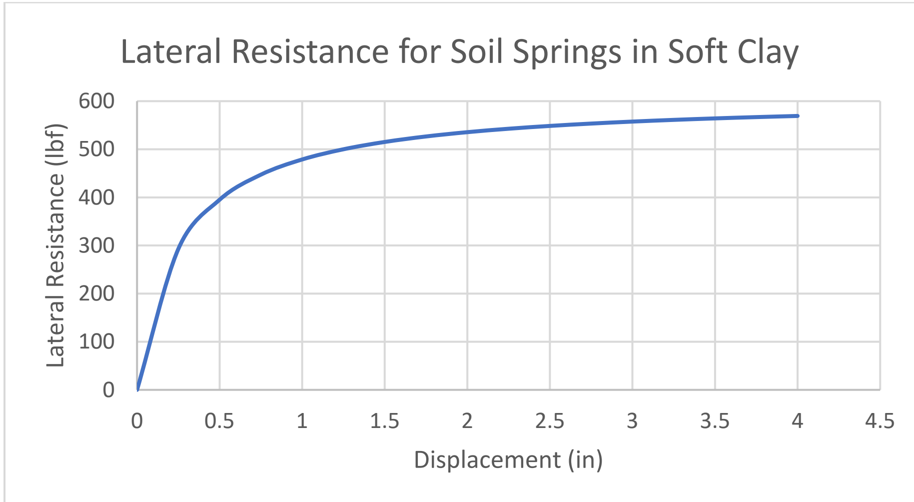

Figure 22: Lateral resistance in soft clay

Table 5: Lateral resistance data for stiff clay

Blow Count	Unit Weight	Undrained Cohesion	Shape Parameter	Pile Width	Depth from Surface	Ultimate Lateral soil resistance		Simplified Ultimate Lateral Resistance	Initial Lateral Stiffness	Simplified Initial lateral Stiffness	Ultimate Displacement	Generalized Displacement	Generalized Lateral
N	γ (pcf)	C_u (psf)	n	B (ft)	x (ft)	P_u (klf)	P_u (k/in)	$P_u = 9 c_u B$ (klf)	k_h (ksf)	$k_h = 67c_u$ (ksf)	$y_u = p_u/k_h$ (in)	y (in)	p (klf)
15	120	1569	1	2	0	9.4	0.783	28.242	190	105.123	0.2687	0.00	0.00
15	120	1569	1	2	1	10.42	0.868	28.242	210.3	105.123	0.2687	0.25	1.13
15	120	1569	1	2	2	11.44	0.953	28.242	230.6	105.123	0.2687	0.50	1.53
15	120	1569	1	2	3	12.46	1.038	28.242	250.9	105.123	0.2687	0.75	1.73
15	120	1569	1	2	4	13.48	1.123	28.242	271.2	105.123	0.2687	1.00	1.86
15	120	1569	1	2	5	14.5	1.208	28.242	291.5	105.123	0.2687	1.25	1.94
15	120	1569	1	2	6	15.52	1.293	28.242	311.8	105.123	0.2687	1.50	2.00
15	120	1569	1	2	7	16.54	1.378	28.242	332.1	105.123	0.2687	1.75	2.04
15	120	1569	1	2	8	17.56	1.463	28.242	352.4	105.123	0.2687	2.00	2.07
15	120	1569	1	2	9	18.58	1.548	28.242	372.7	105.123	0.2687	2.25	2.10
15	120	1569	1	2	10	19.6	1.633	28.242	393	105.123	0.2687	2.50	2.13
15	120	1569	1	2	11	20.62	1.718	28.242	413.3	105.123	0.2687	2.75	2.14
15	120	1569	1	2	12	21.64	1.803	28.242	433.6	105.123	0.2687	3.00	2.16
15	120	1569	1	2	13	22.66	1.888	28.242	453.9	105.123	0.2687	3.25	2.17
15	120	1569	1	2	14	23.68	1.973	28.242	474.2	105.123	0.2687	3.50	2.19
15	120	1569	1	2	15	24.7	2.058	28.242	494.5	105.123	0.2687	3.75	2.20
15	120	1569	1	2	16	25.72	2.143	28.242	514.8	105.123	0.2687	4.00	2.21

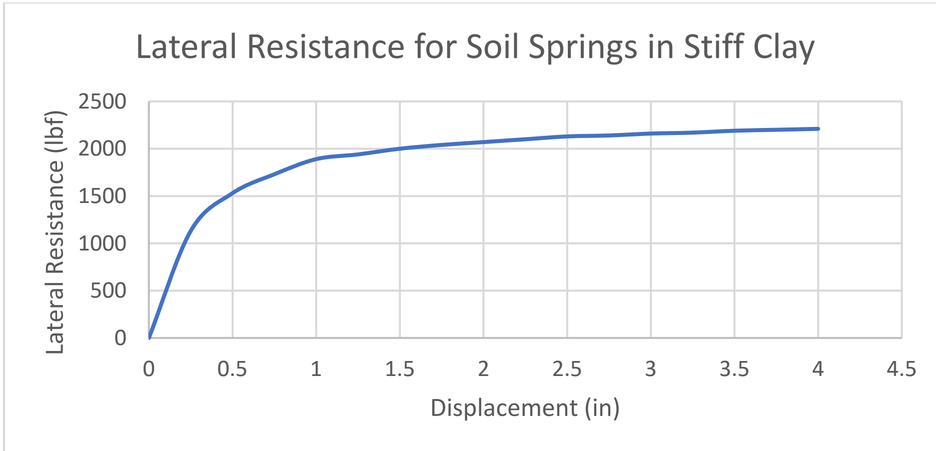

Figure 23: Lateral resistance in stiff clay

Table 6: Lateral resistance data for very stiff clay

Blow Count	Unit Weight	Undrained Cohesion	Shape Parameter	Pile Width	Depth from Surface	Ultimate Lateral soil resistance		Simplified Ultimate Lateral Resistance	Initial Lateral Stiffness	Simplified Initial lateral Stiffness	Ultimate Displacement	Generalized Displacement	Generalized Lateral Resistance
N	γ (pcf)	C_u (psf)	n	B (ft)	x (ft)	P_u (klf)	P_u (k/in)	$P_u = 9 c_u B$ (klf)	k_h (ksf)	$k_h = 67c_u$ (ksf)	$y_u = p_u/k_h$ (in)	y (in)	p (klf)
50	130	5000	2	2	0	2.4	0.2	90	24	335	0.2687	0.00	0.00
50	130	5000	2	2	1	2.8	0.233	90	28.05	335	0.2687	0.25	5.11
50	130	5000	2	2	2	3.2	0.267	90	32.1	335	0.2687	0.50	6.61
50	130	5000	2	2	3	3.6	0.3	90	36.15	335	0.2687	0.75	7.06
50	130	5000	2	2	4	4	0.333	90	40.2	335	0.2687	1.00	7.24
50	130	5000	2	2	5	4.4	0.367	90	44.25	335	0.2687	1.25	7.33
50	130	5000	2	2	6	4.8	0.4	90	48.3	335	0.2687	1.50	7.38
50	130	5000	2	2	7	5.2	0.433	90	52.35	335	0.2687	1.75	7.41
50	130	5000	2	2	8	5.6	0.467	90	56.4	335	0.2687	2.00	7.43
50	130	5000	2	2	9	6	0.5	90	60.45	335	0.2687	2.25	7.45
50	130	5000	2	2	10	6.4	0.533	90	64.5	335	0.2687	2.50	7.46
50	130	5000	2	2	11	6.8	0.567	90	68.55	335	0.2687	2.75	7.46
50	130	5000	2	2	12	7.2	0.6	90	72.6	335	0.2687	3.00	7.47
50	130	5000	2	2	13	7.2	0.6	90	73	335	0.2687	3.25	7.47
50	130	5000	2	2	14	7.2	0.6	90	73	335	0.2687	3.50	7.48
50	130	5000	2	2	15	7.2	0.6	90	73	335	0.2687	3.75	7.48
50	130	5000	2	2	16	7.2	0.6	90	73	335	0.2687	4.00	7.48

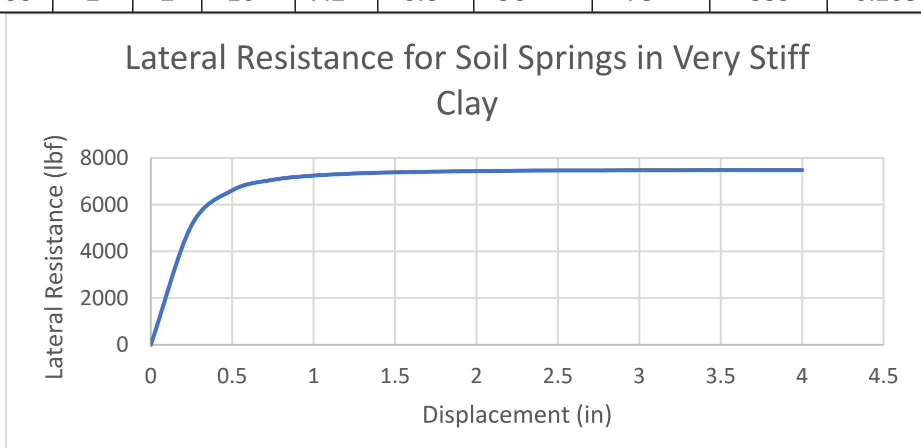

Figure 24: Lateral resistance in very stiff clay

Table 7: Lateral resistance data for loose sand

Unit Weight	Angle of Friction	Shape Parameter	Pile Width	Depth from surface	Ultimate Lateral soil resistance	Passive Pressure Coefficient	Simplified Ultimate Lateral Resistance	Initial Lateral Stiffness	Cohesionless soil parametes		Initial lateral Stiffness (Simplified)	Ultimate Displacement	Generalized Displacement	Generalized Lateral Resistance
γ (pcf)	φ (deg)	n	B (ft)	x (ft)	P_u (klf)	kp	$P_u = (3 \gamma B k_p)$ x (klf)	k_h (ksf)	J	$n_h = J \gamma / 1.35$	$k_h = n_h$ x (ksf)	$y_u = p_u / k_h$ (in)	y (in)	p (klf)
110	30	3	2	0	0.0058	3.00	0	0.16	200	16,296	0	0.1215	0.00	0.00
110	30	3	2	1	0.72	3.00	2	16	200	16,296	16	0.1215	0.25	0.16
110	30	3	2	2	1.72	3.00	4	32	200	16,296	33	0.1215	0.50	0.33
110	30	3	2	3	3	3.00	6	48	200	16,296	49	0.1215	0.75	0.49
110	30	3	2	4	4.56	3.00	8	64	200	16,296	65	0.1215	1.00	0.66
110	30	3	2	5	6.4	3.00	10	80	200	16,296	81	0.1215	1.25	0.82
110	30	3	2	6	8.52	3.00	12	96	200	16,296	98	0.1215	1.50	0.99
110	30	3	2	7	10.92	3.00	14	112	200	16,296	114	0.1215	1.75	1.15
110	30	3	2	8	13.6	3.00	16	128	200	16,296	130	0.1215	2.00	1.32
110	30	3	2	9	16.56	3.00	18	144	200	16,296	147	0.1215	2.25	1.48
110	30	3	2	10	19.8	3.00	20	160	200	16,296	163	0.1215	2.50	1.65
110	30	3	2	11	23.32	3.00	22	176	200	16,296	179	0.1215	2.75	1.81
110	30	3	2	12	27.12	3.00	24	192	200	16,296	196	0.1215	3.00	1.98
110	30	3	2	13	31.2	3.00	26	208	200	16,296	212	0.1215	3.25	2.14
110	30	3	2	14	35.56	3.00	28	224	200	16,296	228	0.1215	3.50	2.31
110	30	3	2	15	40.2	3.00	30	240	200	16,296	244	0.1215	3.75	2.47
110	30	3	2	16	45.12	3.00	32	256	200	16,296	261	0.1215	4.00	2.64

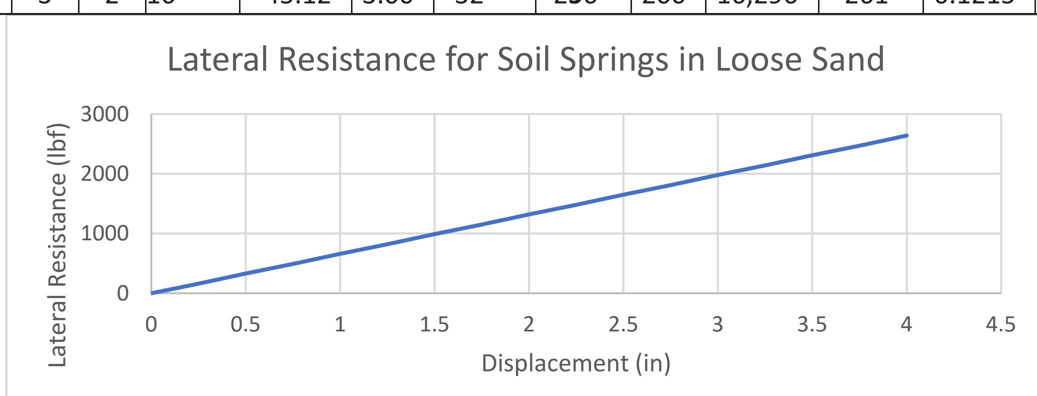

Figure 25: Lateral resistance in loose sand

Table 8: Lateral resistance data for medium sand

Unit Weight	Angle of Friction	Shape Parameter	Pile Width	Depth from surface	Ultimate Lateral soil resistance	Passive Pressure Coefficient	Simplified Ultimate Lateral Resistance	Initial Lateral Stiffness	Cohesionless soil parametes		Initial lateral Stiffness (Simplified)	Ultimate Displacement	Generalized Displacement	Generalized Lateral Resistance
γ (pcf)	φ (deg)	n	B (ft)	x (ft)	P_u (klf)	kp	$P_u = (3\ \gamma B\ k_p)$ x (klf)	k_h (ksf)	J	$n_h = J\ \gamma/1.35$	$k_h = n_h$ x (ksf)	$y_u = p_u / k_h$ (in)	y (in)	p (klf)
120	35	3	2	0	0.0082	3.69	0	0.53	600	53,333	1	0.0498	0.00	0.00
120	35	3	2	1	1.13	3.69	3	53	600	53,333	53	0.0498	0.25	0.22
120	35	3	2	2	2.88	3.69	5	106	600	53,333	107	0.0498	0.50	0.44
120	35	3	2	3	5.25	3.69	8	159	600	53,333	160	0.0498	0.75	0.66
120	35	3	2	4	8.24	3.69	11	212	600	53,333	213	0.0498	1.00	0.89
120	35	3	2	5	11.85	3.69	13	265	600	53,333	267	0.0498	1.25	1.11
120	35	3	2	6	16.08	3.69	16	318	600	53,333	320	0.0498	1.50	1.33
120	35	3	2	7	20.93	3.69	19	371	600	53,333	373	0.0498	1.75	1.55
120	35	3	2	8	26.4	3.69	21	424	600	53,333	427	0.0498	2.00	1.77
120	35	3	2	9	32.49	3.69	24	477	600	53,333	480	0.0498	2.25	1.99
120	35	3	2	10	39.2	3.69	27	530	600	53,333	533	0.0498	2.50	2.21
120	35	3	2	11	46.53	3.69	29	583	600	53,333	587	0.0498	2.75	2.44
120	35	3	2	12	54.48	3.69	32	636	600	53,333	640	0.0498	3.00	2.66
120	35	3	2	13	63.05	3.69	35	689	600	53,333	693	0.0498	3.25	2.88
120	35	3	2	14	72.24	3.69	37	742	600	53,333	747	0.0498	3.50	3.10
120	35	3	2	15	82.05	3.69	40	795	600	53,333	800	0.0498	3.75	3.32
120	35	3	2	16	92.48	3.69	43	848	600	53,333	853	0.0498	4.00	3.54

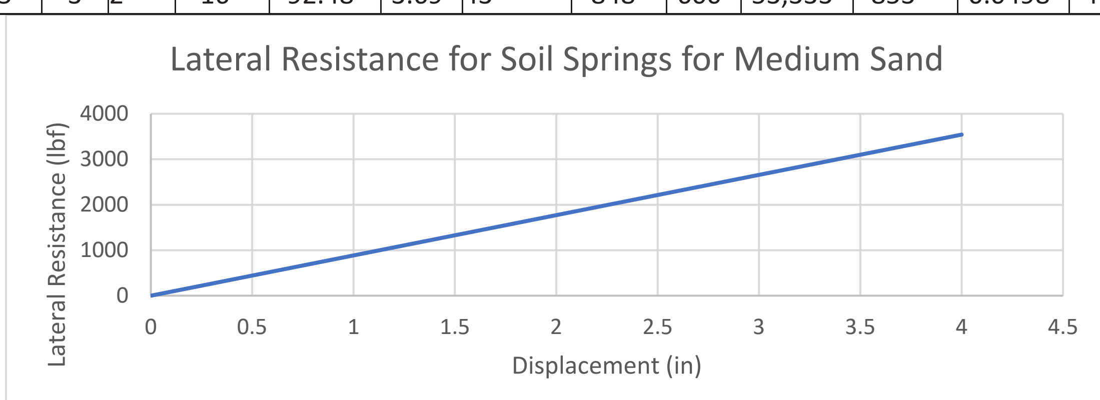

Figure 26: Lateral resistance in medium sand

Table 9:Lateral resistance data for dense sand

Unit Weight	Angle of Friction	Shape Parameter	Pile Width	Depth from surface	Ultimate Lateral soil resistance	Passive Pressure Coefficient	Simplified Ultimate Lateral Resistance	Initial Lateral Stiffness	Cohesionless soil parametes		Initial lateral Stiffness (Simplified)	Ultimate Displacement	Generalized Displacement	Generalized Lateral Resistance
γ (pcf)	φ (deg)	n	B (ft)	x (ft)	$_u$ (klf)	kp	$P_u = (3\ \gamma\ B\ k_p)\ x$ (klf)	k_h (ksf)	J	$n_h = J\ \gamma/1.35$	$k_h = n_h\ x$ (ksf)	$y_u = p_u / k_h$ (in)	y (in)	p (klf)
130	40	3	2	0	0.0115	4.60	0	1.4	1500	144,444	1	0.0248	0.00	0.00
130	40	3	2	1	1.65	4.60	4	140	1500	144,444	144	0.0248	0.25	0.30
130	40	3	2	2	4.32	4.60	7	280	1500	144,444	289	0.0248	0.50	0.60
130	40	3	2	3	8.01	4.60	11	420	1500	144,444	433	0.0248	0.75	0.90
130	40	3	2	4	12.72	4.60	14	560	1500	144,444	578	0.0248	1.00	1.20
130	40	3	2	5	18.45	4.60	18	700	1500	144,444	722	0.0248	1.25	1.49
130	40	3	2	6	25.2	4.60	22	840	1500	144,444	867	0.0248	1.50	1.79
130	40	3	2	7	32.97	4.60	25	980	1500	144,444	1,011	0.0248	1.75	2.09
130	40	3	2	8	41.76	4.60	29	1120	1500	144,444	1,156	0.0248	2.00	2.39
130	40	3	2	9	51.57	4.60	32	1260	1500	144,444	1,300	0.0248	2.25	2.69
130	40	3	2	10	62.4	4.60	36	1400	1500	144,444	1,444	0.0248	2.50	2.99
130	40	3	2	11	74.25	4.60	39	1540	1500	144,444	1,589	0.0248	2.75	3.29
130	40	3	2	12	87.12	4.60	43	1680	1500	144,444	1,733	0.0248	3.00	3.59
130	40	3	2	13	101.01	4.60	47	1820	1500	144,444	1,878	0.0248	3.25	3.89
130	40	3	2	14	115.92	4.60	50	1960	1500	144,444	2,022	0.0248	3.50	4.19
130	40	3	2	15	131.85	4.60	54	2100	1500	144,444	2,167	0.0248	3.75	4.48
130	40	3	2	16	148.8	4.60	57	2240	1500	144,444	2,311	0.0248	4.00	4.78

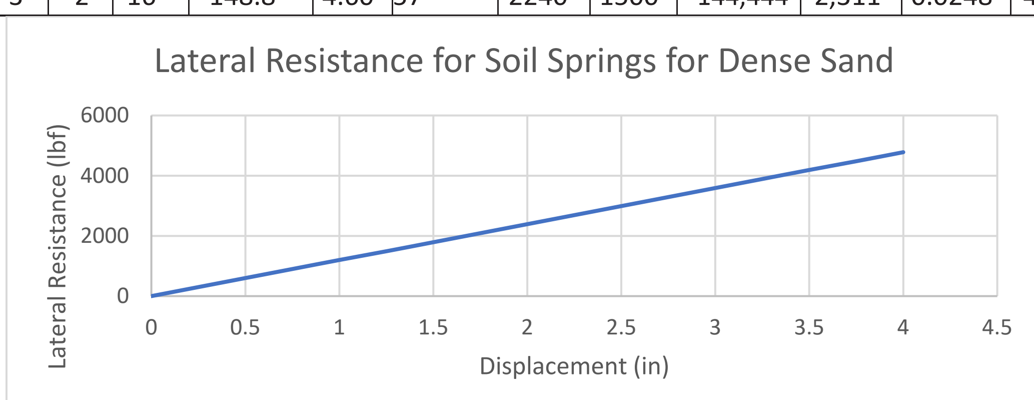

Figure 27: Lateral resistance in dense sand

4.2 Slip Resistance Curves (f-z)

As discussed earlier, f-z curves describe the relationship between skin friction and the relative vertical displacement between pile and soil. The modified Ramberg-Osgood model has been used to generate the curves. The parameters needed for the slip resistance curves are the initial vertical stiffness k_v, the maximum shear stress f_{max}, and the shape parameter n. Factor $\alpha = 1.0$ is used to obtain the soil-pile adhesion.

The f-z relationship is given as:

$$f = \frac{k_v z}{\left(1 + \left|\frac{z}{z_u}\right|^n\right)^{\frac{1}{n}}}$$

Where:

$$z_u = \frac{f_{max}}{k_v}$$

k_v= initial slip resistance

q = generalized soil resistance

f_{max}= ultimate soil slip resistance

n= shape parameter

z= generalized displacement

Table 10: Vertical slip resistance data for soft clay

Blow Count	Shape Parameter	Gross Perimeter of pile	Undrained Cohesion of Clay	Shear Strength Reduction Factor	Adhesion of soil and pile	Maximum Shear Stress	Simplified Maximum Shear Stress	Relative Displacement to develop f_{max}	Initial Vertical Stiffness	Simplified Initial Vertical Stiffness		Generalized Displacement	Generalized Slip Resistance
N	n	l_g (ft)	C_u = 97 N+114 (psf)	α	$C_a = \alpha C_a$ (psf)	f_{max} = min(l_g c_u, l_g c_a) (klf)	f_{max} (klf)	z_c (in)	k_v= 10 f_{max} / z_c (ksf)	k_v (ksf)	z_u = f_{max}/k_v (in)	z (in)	q (klf)
3	1	5	405	1	405	1.96	1.34	0.25	939.6	640	0.0251	0.00	0.00
3	1	5	405	1	405	1.96	1.34	0.25	939.6	640	0.0251	0.25	1.22
3	1	5	405	1	405	1.96	1.34	0.25	939.6	640	0.0251	0.50	1.28
3	1	5	405	1	405	1.96	1.34	0.25	939.6	640	0.0251	0.75	1.30
3	1	5	405	1	405	1.96	1.34	0.25	939.6	640	0.0251	1.00	1.31
3	1	5	405	1	405	1.96	1.34	0.25	939.6	640	0.0251	1.25	1.31
3	1	5	405	1	405	1.96	1.34	0.25	939.6	640	0.0251	1.50	1.32
3	1	5	405	1	405	1.96	1.34	0.25	939.6	640	0.0251	1.75	1.32
3	1	5	405	1	405	1.96	1.34	0.25	939.6	640	0.0251	2.00	1.32
3	1	5	405	1	405	1.96	1.34	0.25	939.6	640	0.0251	2.25	1.33
3	1	5	405	1	405	1.96	1.34	0.25	939.6	640	0.0251	2.50	1.33
3	1	5	405	1	405	1.96	1.34	0.25	939.6	640	0.0251	2.75	1.33
3	1	5	405	1	405	1.96	1.34	0.25	939.6	640	0.0251	3.00	1.33
3	1	5	405	1	405	1.96	1.34	0.25	939.6	640	0.0251	3.25	1.33
3	1	5	405	1	405	1.96	1.34	0.25	939.6	640	0.0251	3.50	1.33
3	1	5	405	1	405	1.96	1.34	0.25	939.6	640	0.0251	3.75	1.33
3	1	5	405	1	405	1.96	1.34	0.25	939.6	640	0.0251	4.00	1.33

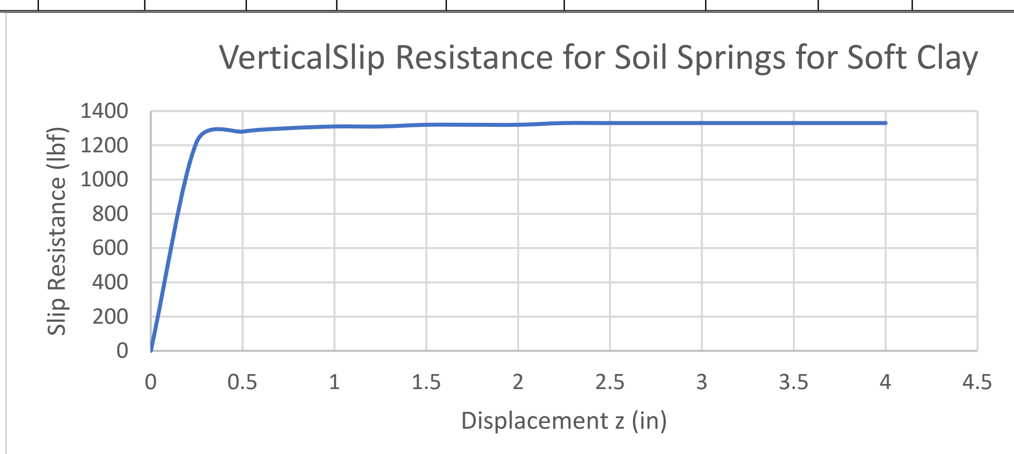

Figure 28: Slip Resistance for Soft Clay

Table 11: Vertical slip resistance data for stiff clay

Blow Count	Shape Parameter	Gross Perimeter of pile	Undrained Cohesion of Clay	Shear Strength Reduction Factor	Adhesion of soil and pile	Maximum Shear Stress	Simplified Maximum Shear Stress	Relative Displacement to develop f_{max}	Initial Vertical Stiffness	Simplified Initial Vertical Stiffness		Generalized Displacement	Generalized Slip Resistance
N	n	l_g (ft)	C_u = 97 N+114 (psf)	α	$C_a = \alpha C_a$ (psf)	$f_{max} = \min(l_g c_u, l_g c_a)$ (klf)	f_{max} (klf)	z_c (in)	$k_v = 10\, f_{max} / z_c$ (ksf)	k_v (ksf)	$z_u = f_{max}/k_v$ (in)	z (in)	q (klf)
15	1	5	1569	1	1569	7.58	3.86	0.25	3640.1	1850	0.0250	0.00	0.00
15	1	5	1569	1	1569	7.58	3.86	0.25	3640.1	1850	0.0250	0.25	3.51
15	1	5	1569	1	1569	7.58	3.86	0.25	3640.1	1850	0.0250	0.50	3.68
15	1	5	1569	1	1569	7.58	3.86	0.25	3640.1	1850	0.0250	0.75	3.74
15	1	5	1569	1	1569	7.58	3.86	0.25	3640.1	1850	0.0250	1.00	3.77
15	1	5	1569	1	1569	7.58	3.86	0.25	3640.1	1850	0.0250	1.25	3.78
15	1	5	1569	1	1569	7.58	3.86	0.25	3640.1	1850	0.0250	1.50	3.80
15	1	5	1569	1	1569	7.58	3.86	0.25	3640.1	1850	0.0250	1.75	3.81
15	1	5	1569	1	1569	7.58	3.86	0.25	3640.1	1850	0.0250	2.00	3.81
15	1	5	1569	1	1569	7.58	3.86	0.25	3640.1	1850	0.0250	2.25	3.82
15	1	5	1569	1	1569	7.58	3.86	0.25	3640.1	1850	0.0250	2.50	3.82
15	1	5	1569	1	1569	7.58	3.86	0.25	3640.1	1850	0.0250	2.75	3.83
15	1	5	1569	1	1569	7.58	3.86	0.25	3640.1	1850	0.0250	3.00	3.83
15	1	5	1569	1	1569	7.58	3.86	0.25	3640.1	1850	0.0250	3.25	3.83
15	1	5	1569	1	1569	7.58	3.86	0.25	3640.1	1850	0.0250	3.50	3.83
15	1	5	1569	1	1569	7.58	3.86	0.25	3640.1	1850	0.0250	3.75	3.83
15	1	5	1569	1	1569	7.58	3.86	0.25	3640.1	1850	0.0250	4.00	3.84

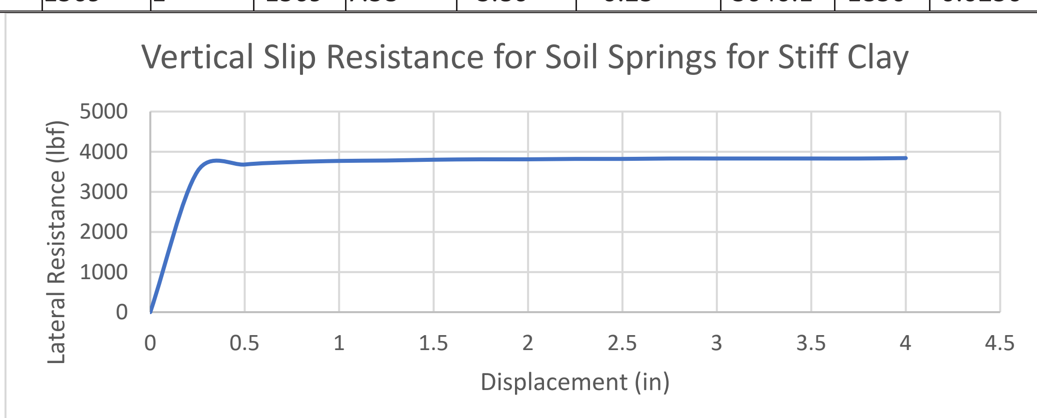

Figure 29: Slip resistance for stiff clay

Table 12: Vertical slip resistance data for very stiff clay

Blow Count	Shape Parameter	Gross Perimeter of pile	Undrained Cohesion of Clay	Shear Strength Reduction Factor	Adhesion of soil and pile	Maximum Shear Stress	Simplified Maximum Shear Stress	Relative Displacement to develop f_{max}	Initial Vertical Stiffness	Simplified Initial Vertical Stiffness		Generalized Displacement	Generalized Slip Resistance
N	n	l_g (ft)	$C_u = 97$ N+114 (psf)	α	$C_a = \alpha C_a$ (psf)	f_{max} = min(l_g c_u , l_g c_a) (klf)	f_{max} (klf)	z_c (in)	$k_v = 10$ f_{max} / z_c (ksf)	k_v (ksf)	$z_u = f_{max}/k_v$ (in)	z (in)	q (k f)
50	1	5	4964	1	4964	23.99	6.22	0.25	11516.5	2960	0.0252	0.00	0.00
50	1	5	4964	1	4964	23.99	6.22	0.25	11516.5	2960	0.0252	0.25	5.65
50	1	5	4964	1	4964	23.99	6.22	0.25	11516.5	2960	0.0252	0.50	5.92
50	1	5	4964	1	4964	23.99	6.22	0.25	11516.5	2960	0.0252	0.75	6.02
50	1	5	4964	1	4964	23.99	6.22	0.25	11516.5	2960	0.0252	1.00	6.07
50	1	5	4964	1	4964	23.99	6.22	0.25	11516.5	2960	0.0252	1.25	6.10
50	1	5	4964	1	4964	23.99	6.22	0.25	11516.5	2960	0.0252	1.50	6.12
50	1	5	4964	1	4964	23.99	6.22	0.25	11516.5	2960	0.0252	1.75	6.13
50	1	5	4964	1	4964	23.99	6.22	0.25	11516.5	2960	0.0252	2.00	6.14
50	1	5	4964	1	4964	23.99	6.22	0.25	11516.5	2960	0.0252	2.25	6.15
50	1	5	4964	1	4964	23.99	6.22	0.25	11516.5	2960	0.0252	2.50	6.16
50	1	5	4964	1	4964	23.99	6.22	0.25	11516.5	2960	0.0252	2.75	6.16
50	1	5	4964	1	4964	23.99	6.22	0.25	11516.5	2960	0.0252	3.00	6.17
50	1	5	4964	1	4964	23.99	6.22	0.25	11516.5	2960	0.0252	3.25	6.17
50	1	5	4964	1	4964	23.99	6.22	0.25	11516.5	2960	0.0252	3.50	6.18
50	1	5	4964	1	4964	23.99	6.22	0.25	11516.5	2960	0.0252	3.75	6.18
50	1	5	4964	1	4964	23.99	6.22	0.25	11516.5	2960	0.0252	4.00	6.18

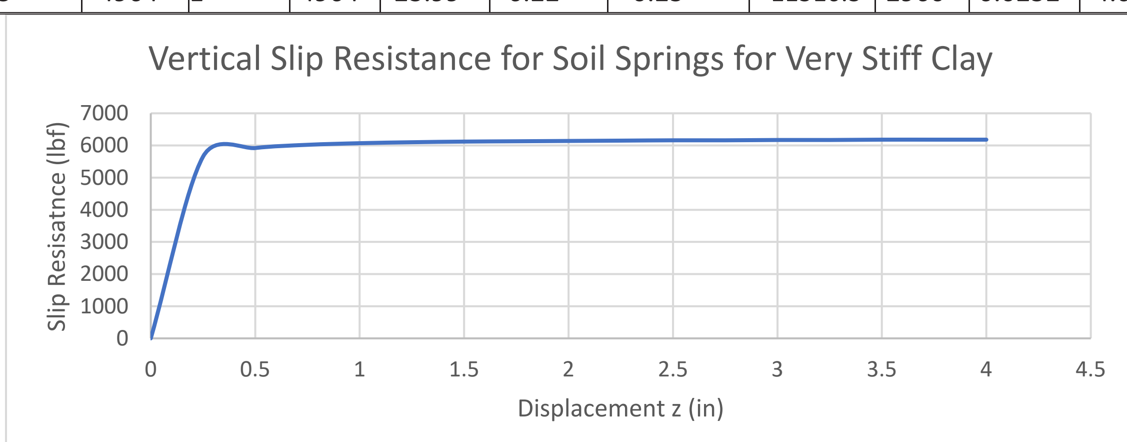

Figure 30: Slip resistance in very stiff clay

Table 13: Vertical slip resistance data for loose sand

Blow Count	Shape Parameter	Gross Perimeter of pile	Maximum Shear Stress	Simplified Maximum Shear Stress	Relative Displacement to develop f_{max}	Initial Vertical Stiffness	Simplified Initial Vertical Stiffness		Generalized Displacement	Generalized Slip Resistance
N	n	l_g (ft)	$f_{max} = 0.04\ N\ l_g$ (klf)	f_{max} (klf)	z_c (in)	$k_v = 10\ f_{max} / z_c$ (ksf)	k_v (ksf)	$z_u = f_{max}/k_v$ (in)	z (in)	q (klf)
5	1	5	0.97	0.50	0.4	290.0	150	0.0400	0.00	0.00
5	1	5	0.97	0.50	0.4	290.0	150	0.0400	0.25	0.43
5	1	5	0.97	0.50	0.4	290.0	150	0.0400	0.50	0.46
5	1	5	0.97	0.50	0.4	290.0	150	0.0400	0.75	0.47
5	1	5	0.97	0.50	0.4	290.0	150	0.0400	1.00	0.48
5	1	5	0.97	0.50	0.4	290.0	150	0.0400	1.25	0.48
5	1	5	0.97	0.50	0.4	290.0	150	0.0400	1.50	0.49
5	1	5	0.97	0.50	0.4	290.0	150	0.0400	1.75	0.49
5	1	5	0.97	0.50	0.4	290.0	150	0.0400	2.00	0.49
5	1	5	0.97	0.50	0.4	290.0	150	0.0400	2.25	0.49
5	1	5	0.97	0.50	0.4	290.0	150	0.0400	2.50	0.49
5	1	5	0.97	0.50	0.4	290.0	150	0.0400	2.75	0.49
5	1	5	0.97	0.50	0.4	290.0	150	0.0400	3.00	0.49
5	1	5	0.97	0.50	0.4	290.0	150	0.0400	3.25	0.49
5	1	5	0.97	0.50	0.4	290.0	150	0.0400	3.50	0.49
5	1	5	0.97	0.50	0.4	290.0	150	0.0400	3.75	0.49
5	1	5	0.97	0.50	0.4	290.0	150	0.0400	4.00	0.50

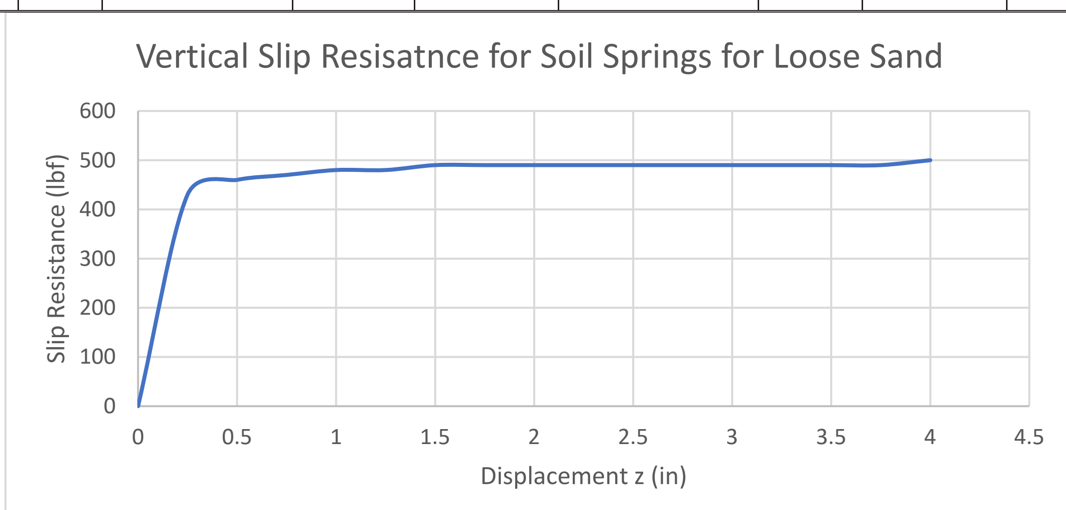

Figure 31: Slip resistance loose sand

Table 14: Vertical resistance data for medium sand

Blow Count	Shape Parameter	Gross Perimeter of pile	Maximum Shear Stress	Simplified Maximum Shear Stress	Relative Displacement to develop f_{max}	Initial Vertical Stiffness	Simplified Initial Vertical Stiffness		Generalized Displacement	Generalized Slip Resistance
N	n	l_g (ft)	$f_{max} = 0.04\ N\ l_g$ (klf)	f_{max} (klf)	z_c (in)	$k_v = 10\ f_{max} / z_c$ (ksf)	k_v (ksf)	$z_u = f_{max}/k_v$ (in)	z (in)	q (klf)
15	1	5	2.90	1.50	0.4	870.0	450	0.0400	0.00	0.00
15	1	5	2.90	1.50	0.4	870.0	450	0.0400	0.25	1.29
15	1	5	2.90	1.50	0.4	870.0	450	0.0400	0.50	1.39
15	1	5	2.90	1.50	0.4	870.0	450	0.0400	0.75	1.42
15	1	5	2.90	1.50	0.4	870.0	450	0.0400	1.00	1.44
15	1	5	2.90	1.50	0.4	870.0	450	0.0400	1.25	1.45
15	1	5	2.90	1.50	0.4	870.0	450	0.0400	1.50	1.46
15	1	5	2.90	1.50	0.4	870.0	450	0.0400	1.75	1.47
15	1	5	2.90	1.50	0.4	870.0	450	0.0400	2.00	1.47
15	1	5	2.90	1.50	0.4	870.0	450	0.0400	2.25	1.47
15	1	5	2.90	1.50	0.4	870.0	450	0.0400	2.50	1.48
15	1	5	2.90	1.50	0.4	870.0	450	0.0400	2.75	1.48
15	1	5	2.90	1.50	0.4	870.0	450	0.0400	3.00	1.48
15	1	5	2.90	1.50	0.4	870.0	450	0.0400	3.25	1.48
15	1	5	2.90	1.50	0.4	870.0	450	0.0400	3.50	1.48
15	1	5	2.90	1.50	0.4	870.0	450	0.0400	3.75	1.48
15	1	5	2.90	1.50	0.4	870.0	450	0.0400	4.00	1.49

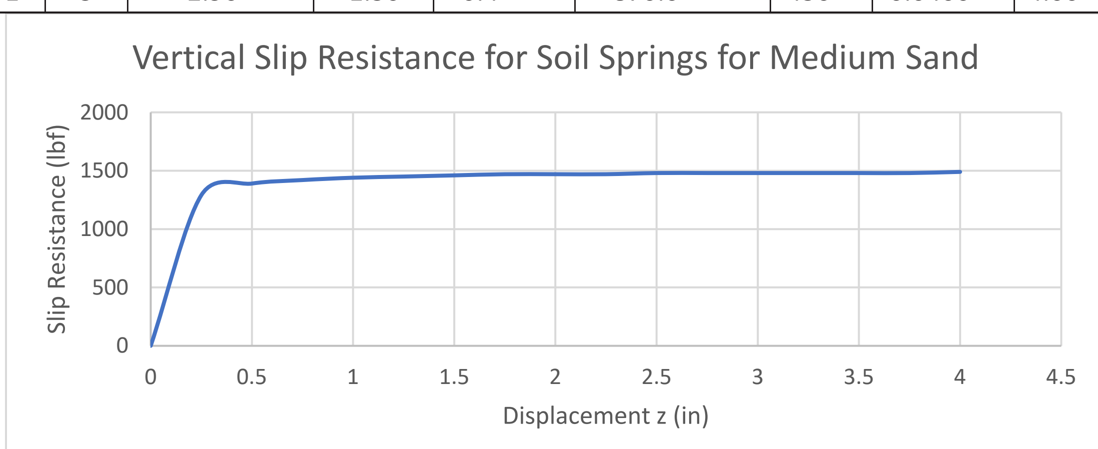

Figure 32: Slip resistance in medium sand

Table 15: Vertical slip resistance data for dense sand

Blow Count	Shape Parameter	Gross Perimeter of pile	Maximum Shear Stress	Simplified Maximum Shear Stress	Relative Displacement to develop f_{max}	Initial Vertical Stiffness	Simplified Initial Vertical Stiffness		Generalized Displacement	Generalized Slip Resistance
N	n	l_g (ft)	$f_{max} = 0.04\ N\ l_g$ (klf)	f_{max} (klf)	z_c (in)	$k_v = 10\ f_{max} / z_c$ (ksf)	k_v (ksf)	$z_u = f_{max}/k_v$ (in)	z (in)	q (klf)
30	1	5	5.80	3.00	0.4	1740.0	900	0.0400	0.00	0.00
30	1	5	5.80	3.00	0.4	1740.0	900	0.0400	0.25	2.59
30	1	5	5.80	3.00	0.4	1740.0	900	0.0400	0.50	2.78
30	1	5	5.80	3.00	0.4	1740.0	900	0.0400	0.75	2.85
30	1	5	5.80	3.00	0.4	1740.0	900	0.0400	1.00	2.88
30	1	5	5.80	3.00	0.4	1740.0	900	0.0400	1.25	2.91
30	1	5	5.80	3.00	0.4	1740.0	900	0.0400	1.50	2.92
30	1	5	5.80	3.00	0.4	1740.0	900	0.0400	1.75	2.93
30	1	5	5.80	3.00	0.4	1740.0	900	0.0400	2.00	2.94
30	1	5	5.80	3.00	0.4	1740.0	900	0.0400	2.25	2.95
30	1	5	5.80	3.00	0.4	1740.0	900	0.0400	2.50	2.95
30	1	5	5.80	3.00	0.4	1740.0	900	0.0400	2.75	2.96
30	1	5	5.80	3.00	0.4	1740.0	900	0.0400	3.00	2.96
30	1	5	5.80	3.00	0.4	1740.0	900	0.0400	3.25	2.96
30	1	5	5.80	3.00	0.4	1740.0	900	0.0400	3.50	2.97
30	1	5	5.80	3.00	0.4	1740.0	900	0.0400	3.75	2.97
30	1	5	5.80	3.00	0.4	1740.0	900	0.0400	4.00	2.97

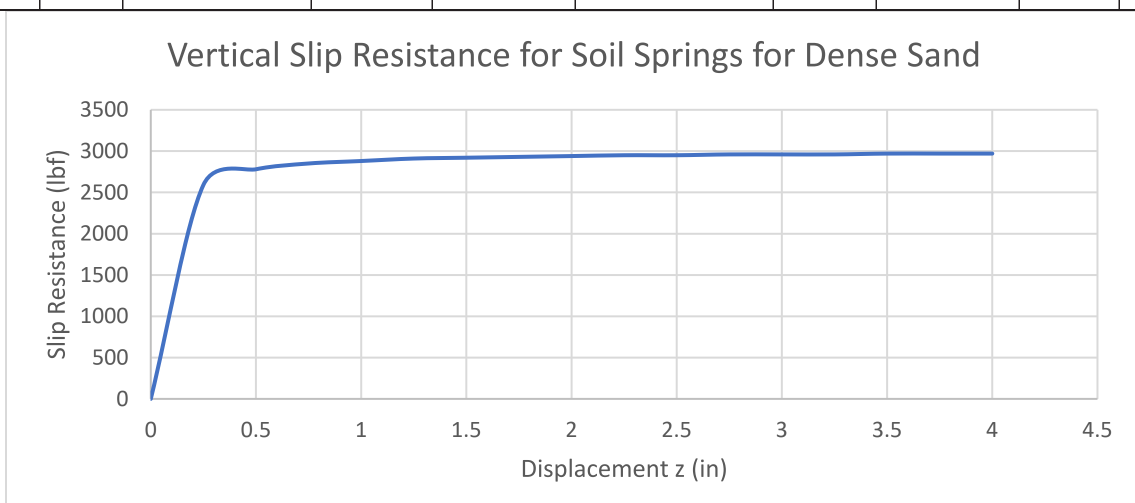

Figure 33: Slip resistance for dense sand

4.3 Bearing Resistance Curves (q-z)

These curves describe the relationship between bearing stress at the pile tip and the pile tip settlement. The parameters needed to generate such a curve are the initial point stiffness k_q, the maximum bearing stress q_{max}, and the shape parameter n.

The q-z relationship is:

$$q = \frac{k_q z}{\left(1 + \left|\frac{z}{z_u}\right|^n\right)^{\frac{1}{n}}}$$

Where:

$$z_u = \frac{q_{max}}{k_q}$$

k_q= initial point stiffness

q = generalized soil resistance

q_{max}= ultimate soil bearing resistance

n= shape parameter

z= generalized displacement

Table 16: Vertical end bearing resistance data for soft clay

Blow Count	Shape Parameter	Undrained Cohesion of Clay	Maximum Bearing Stress	Simplified Maximum Bearing Stress	Relative Displacement to develop q_{max}	Initial Point Stiffness	Simplified Initial Point Stiffness		Generalized displacement	Generalized Resistance
N	n	C_u = 97 N+114 (psf)	q_{max} =9 c_u (ksf)	q_{max} (ksf)	z_c (in)	k_q= 10 q_{max} / z_c (kcf)	k_q (ksf)	z_u = q_{max}/k_q (in)	z (in)	q (klf)
3	1	405	4	3.60	0.25	1749.6	1700	0.0254	0.00	0.00
3	1	405	4	3.60	0.25	1749.6	1700	0.0254	0.25	3.27
3	1	405	4	3.60	0.25	1749.6	1700	0.0254	0.50	3.43
3	1	405	4	3.60	0.25	1749.6	1700	0.0254	0.75	3.48
3	1	405	4	3.60	0.25	1749.6	1700	0.0254	1.00	3.51
3	1	405	4	3.60	0.25	1749.6	1700	0.0254	1.25	3.53
3	1	405	4	3.60	0.25	1749.6	1700	0.0254	1.50	3.54
3	1	405	4	3.60	0.25	1749.6	1700	0.0254	1.75	3.55
3	1	405	4	3.60	0.25	1749.6	1700	0.0254	2.00	3.55
3	1	405	4	3.60	0.25	1749.6	1700	0.0254	2.25	3.56
3	1	405	4	3.60	0.25	1749.6	1700	0.0254	2.50	3.56
3	1	405	4	3.60	0.25	1749.6	1700	0.0254	2.75	3.57
3	1	405	4	3.60	0.25	1749.6	1700	0.0254	3.00	3.57
3	1	405	4	3.60	0.25	1749.6	1700	0.0254	3.25	3.57
3	1	405	4	3.60	0.25	1749.6	1700	0.0254	3.50	3.57
3	1	405	4	3.60	0.25	1749.6	1700	0.0254	3.75	3.58
3	1	405	4	3.60	0.25	1749.6	1700	0.0254	4.00	3.58

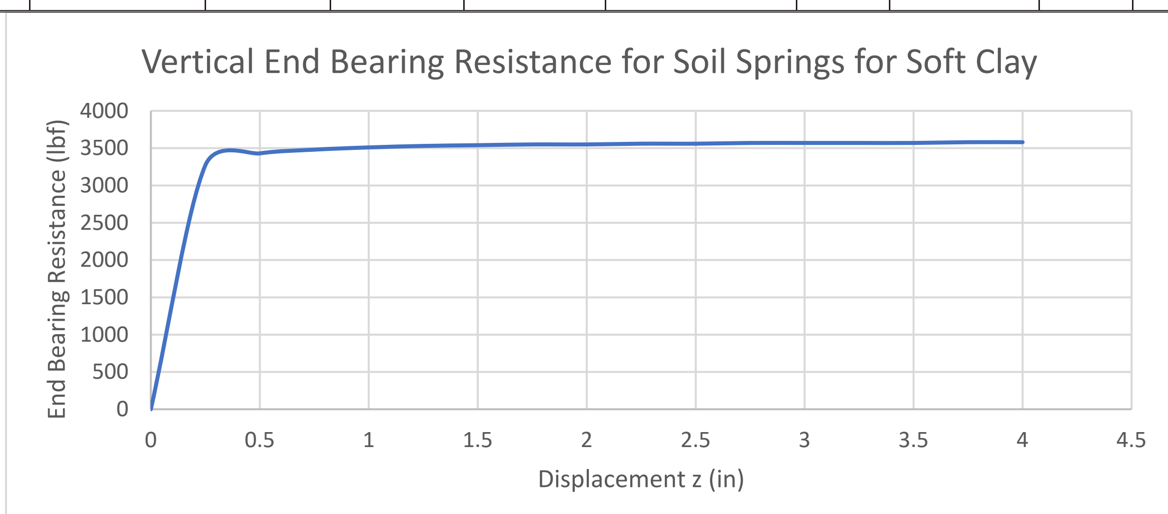

Figure 34: End bearing resistance in soft clay

Table 17: Vertical end bearing resistance data for stiff clay

Blow Count	Shape Parameter	Undrained Cohesion of Clay	Maximum Bearing Stress	Simplified Maximum Bearing Stress	Relative Displacement to develop q_{max}	Initial Point Stiffness	Simplified Initial Point Stiffness		Generalized displacement	Generalized Resistance
N	n	C_u = 97 N+114 (psf)	q_{max} =9 c_u (ksf)	q_{max} (ksf)	z_c (in)	k_q= 10 q_{max} / z_c (kcf)	k_q (ksf)	z_u = q_{max}/k_q (in)	z (in)	q (klf)
15	1	1569	14	14.00	0.25	6778.1	6700	0.0251	0.00	0.00
15	1	1569	14	14.00	0.25	6778.1	6700	0.0251	0.25	12.72
15	1	1569	14	14.00	0.25	6778.1	6700	0.0251	0.50	13.33
15	1	1569	14	14.00	0.25	6778.1	6700	0.0251	0.75	13.55
15	1	1569	14	14.00	0.25	6778.1	6700	0.0251	1.00	13.66
15	1	1569	14	14.00	0.25	6778.1	6700	0.0251	1.25	13.72
15	1	1569	14	14.00	0.25	6778.1	6700	0.0251	1.50	13.77
15	1	1569	14	14.00	0.25	6778.1	6700	0.0251	1.75	13.80
15	1	1569	14	14.00	0.25	6778.1	6700	0.0251	2.00	13.83
15	1	1569	14	14.00	0.25	6778.1	6700	0.0251	2.25	13.85
15	1	1569	14	14.00	0.25	6778.1	6700	0.0251	2.50	13.86
15	1	1569	14	14.00	0.25	6778.1	6700	0.0251	2.75	13.87
15	1	1569	14	14.00	0.25	6778.1	6700	0.0251	3.00	13.88
15	1	1569	14	14.00	0.25	6778.1	6700	0.0251	3.25	13.89
15	1	1569	14	14.00	0.25	6778.1	6700	0.0251	3.50	13.90
15	1	1569	14	14.00	0.25	6778.1	6700	0.0251	3.75	13.91
15	1	1569	14	14.00	0.25	6778.1	6700	0.0251	4.00	13.91

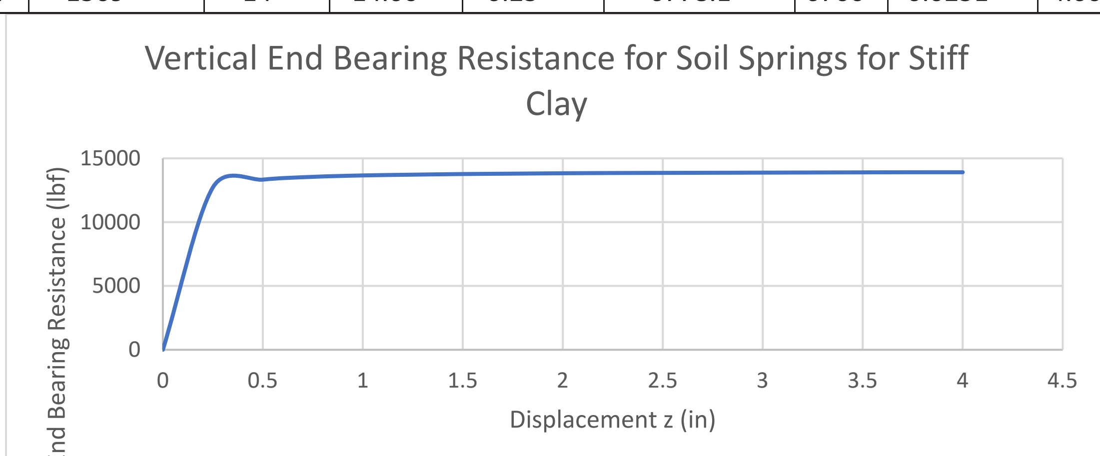

Figure 35: End bearing resistance in stiff clay

Table 18: Vertical end bearing resistance data for very stiff clay

Blow Count	Shape Parameter	Undrained Cohesion of Clay	Maximum Bearing Stress	Simplified Maximum Bearing Stress	Relative Displacement to develop q_{max}	Initial Point Stiffness	Simplified Initial Point Stiffness		Generalized displacement	Generalized Resistance
N	n	C_u = 97 N+114 (psf)	q_{max} =9 c_u (ksf)	q_{max} (ksf)	z_c (in)	k_q= 10 q_{max} / z_c (kcf)	k_q (ksf)	z_u = q_{max}/k_q (in)	z (in)	q (klf)
50	1	4964	45	45.00	0.25	21444.5	21000	0.0257	0.00	0.00
50	1	4964	45	45.00	0.25	21444.5	21000	0.0257	0.25	40.80
50	1	4964	45	45.00	0.25	21444.5	21000	0.0257	0.50	42.80
50	1	4964	45	45.00	0.25	21444.5	21000	0.0257	0.75	43.51
50	1	4964	45	45.00	0.25	21444.5	21000	0.0257	1.00	43.87
50	1	4964	45	45.00	0.25	21444.5	21000	0.0257	1.25	44.09
50	1	4964	45	45.00	0.25	21444.5	21000	0.0257	1.50	44.24
50	1	4964	45	45.00	0.25	21444.5	21000	0.0257	1.75	44.35
50	1	4964	45	45.00	0.25	21444.5	21000	0.0257	2.00	44.43
50	1	4964	45	45.00	0.25	21444.5	21000	0.0257	2.25	44.49
50	1	4964	45	45.00	0.25	21444.5	21000	0.0257	2.50	44.54
50	1	4964	45	45.00	0.25	21444.5	21000	0.0257	2.75	44.58
50	1	4964	45	45.00	0.25	21444.5	21000	0.0257	3.00	44.62
50	1	4964	45	45.00	0.25	21444.5	21000	0.0257	3.25	44.65
50	1	4964	45	45.00	0.25	21444.5	21000	0.0257	3.50	44.67
50	1	4964	45	45.00	0.25	21444.5	21000	0.0257	3.75	44.69
50	1	4964	45	45.00	0.25	21444.5	21000	0.0257	4.00	44.71

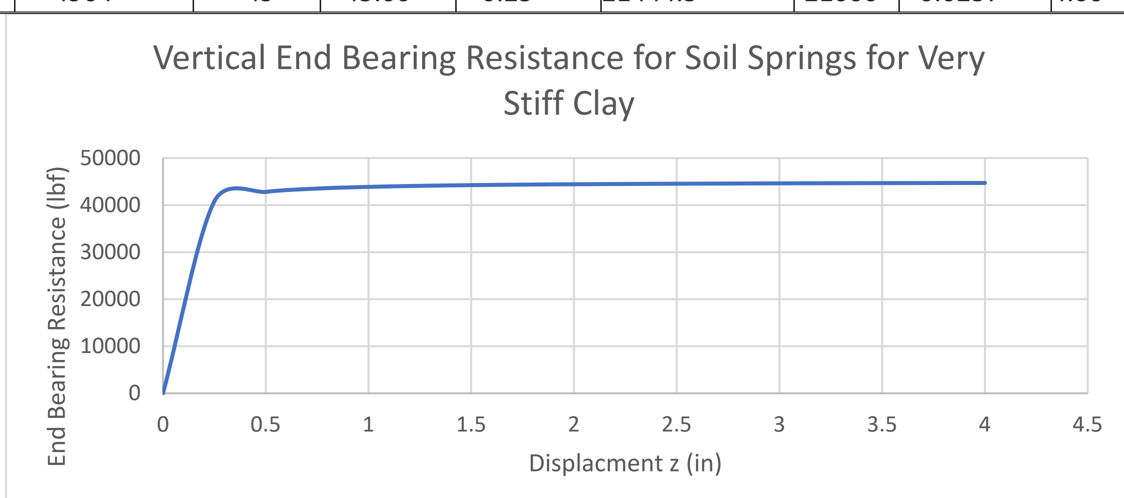

Figure 36: End bearing resistance in very stiff clay

Table 19: Vertical end bearing resistance data for loose sand

Blow Count	Shape Parameter	Corrected Standard Penetration at depth of pile tip	Maximum Bearing Stress	Simplified Maximum Bearing Stress	Relative Displacement to develop q_{max}	Initial Point Stiffness	Simplified Initial Point Stiffness		Generalized displacement	Generalized Resistance
N	n	N_{corr}	$q_{max} = 8\ N_{corr}$ (ksf)	q_{max} (ksf)	z_c (in)	$k_q = 10\ q_{max} / z_c$ (kcf)	k_q (ksf)	$z_u = q_{max}/k_q$ (in)	z (in)	q (klf)
5	1	5	40	40.00	0.4	12000.0	12000	0.0400	0.00	0.00
5	1	5	40	40.00	0.4	12000.0	12000	0.0400	0.25	34.48
5	1	5	40	40.00	0.4	12000.0	12000	0.0400	0.50	37.04
5	1	5	40	40.00	0.4	12000.0	12000	0.0400	0.75	37.97
5	1	5	40	40.00	0.4	12000.0	12000	0.0400	1.00	38.46
5	1	5	40	40.00	0.4	12000.0	12000	0.0400	1.25	38.76
5	1	5	40	40.00	0.4	12000.0	12000	0.0400	1.50	38.96
5	1	5	40	40.00	0.4	12000.0	12000	0.0400	1.75	39.11
5	1	5	40	40.00	0.4	12000.0	12000	0.0400	2.00	39.22
5	1	5	40	40.00	0.4	12000.0	12000	0.0400	2.25	39.30
5	1	5	40	40.00	0.4	12000.0	12000	0.0400	2.50	39.37
5	1	5	40	40.00	0.4	12000.0	12000	0.0400	2.75	39.43
5	1	5	40	40.00	0.4	12000.0	12000	0.0400	3.00	39.47
5	1	5	40	40.00	0.4	12000.0	12000	0.0400	3.25	39.51
5	1	5	40	40.00	0.4	12000.0	12000	0.0400	3.50	39.55
5	1	5	40	40.00	0.4	12000.0	12000	0.0400	3.75	39.58
5	1	5	40	40.00	0.4	12000.0	12000	0.0400	4.00	39.60

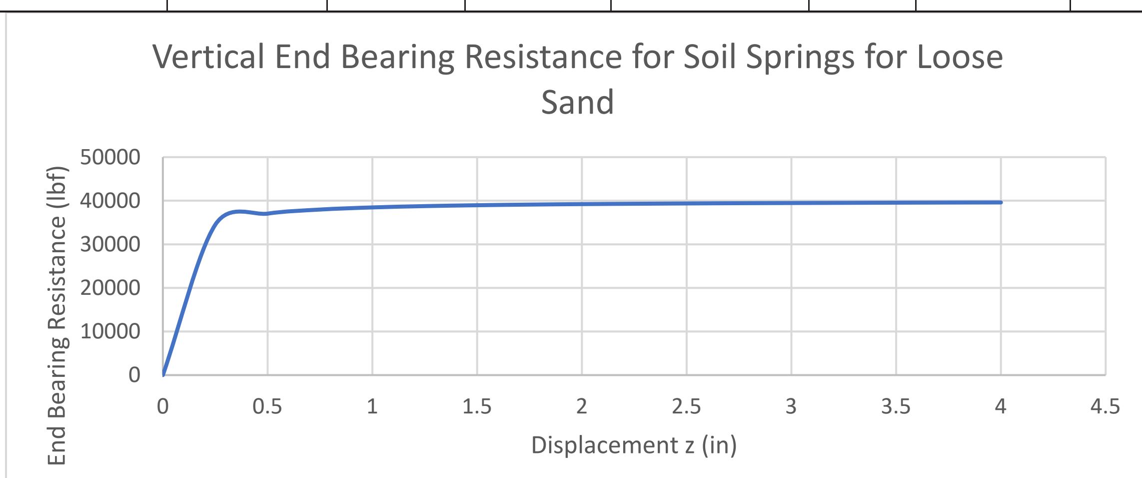

Figure 37: End bearing resistance in loose sand

Table 20: Vertical end bearing resistance data for medium sand

Blow Count	Shape Parameter	Corrected Standard Penetration at depth of pile tip	Maximum Bearing Stress	Simplified Maximum Bearing Stress	Relative Displacement to develop q_{max}	Initial Point Stiffness	Simplified Initial Point Stiffness		Generalized displacement	Generalized Resistance
N	n	N_{corr}	$q_{max} = 8 N_{corr}$ (ksf)	q_{max} (ksf)	z_c (in)	$k_q = 10\, q_{max} / z_c$ (kcf)	k_q (ksf)	$z_u = q_{max}/k_q$ (in)	z (in)	q (klf)
15	1	15	120	120.00	0.4	36000.0	36000	0.0400	0.00	0.00
15	1	15	120	120.00	0.4	36000.0	36000	0.0400	0.25	103.45
15	1	15	120	120.00	0.4	36000.0	36000	0.0400	0.50	111.11
15	1	15	120	120.00	0.4	36000.0	36000	0.0400	0.75	113.92
15	1	15	120	120.00	0.4	36000.0	36000	0.0400	1.00	115.38
15	1	15	120	120.00	0.4	36000.0	36000	0.0400	1.25	116.28
15	1	15	120	120.00	0.4	36000.0	36000	0.0400	1.50	116.88
15	1	15	120	120.00	0.4	36000.0	36000	0.0400	1.75	117.32
15	1	15	120	120.00	0.4	36000.0	36000	0.0400	2.00	117.65
15	1	15	120	120.00	0.4	36000.0	36000	0.0400	2.25	117.90
15	1	15	120	120.00	0.4	36000.0	36000	0.0400	2.50	118.11
15	1	15	120	120.00	0.4	36000.0	36000	0.0400	2.75	118.28
15	1	15	120	120.00	0.4	36000.0	36000	0.0400	3.00	118.42
15	1	15	120	120.00	0.4	36000.0	36000	0.0400	3.25	118.54
15	1	15	120	120.00	0.4	36000.0	36000	0.0400	3.50	118.64
15	1	15	120	120.00	0.4	36000.0	36000	0.0400	3.75	118.73
15	1	15	120	120.00	0.4	36000.0	36000	0.0400	4.00	118.81

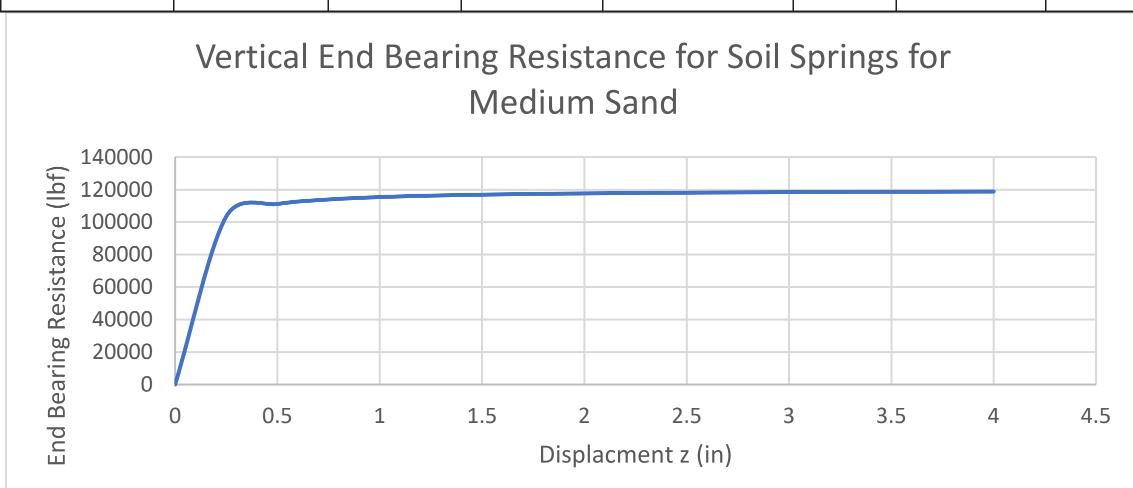

Figure 38: End bearing resistance in medium sand

Table 21: Vertical end bearing resistance data for dense sand

Blow Count	Shape Parameter	Corrected Standard Penetration at depth of pile tip	Maximum Bearing Stress	Simplified Maximum Bearing Stress	Relative Displacement to develop q_{max}	Initial Point Stiffness	Simplified Initial Point Stiffness		Generalized displacement	Generalized Resistance
N	n	N_{corr}	$q_{max} = 8\ N_{corr}$ (ksf)	q_{max} (ksf)	z_c (in)	$k_q = 10\ q_{max} / z_c$ (kcf)	k_q (ksf)	$z_u = q_{max}/k_q$ (in)	z (in)	q (klf)
30	1	23	180	180.00	0.4	54000.0	55000	0.0393	0.00	0.00
30	1	23	180	180.00	0.4	54000.0	55000	0.0393	0.25	155.56
30	1	23	180	180.00	0.4	54000.0	55000	0.0393	0.50	166.89
30	1	23	180	180.00	0.4	54000.0	55000	0.0393	0.75	171.04
30	1	23	180	180.00	0.4	54000.0	55000	0.0393	1.00	173.20
30	1	23	180	180.00	0.4	54000.0	55000	0.0393	1.25	174.52
30	1	23	180	180.00	0.4	54000.0	55000	0.0393	1.50	175.41
30	1	23	180	180.00	0.4	54000.0	55000	0.0393	1.75	176.05
30	1	23	180	180.00	0.4	54000.0	55000	0.0393	2.00	176.53
30	1	23	180	180.00	0.4	54000.0	55000	0.0393	2.25	176.91
30	1	23	180	180.00	0.4	54000.0	55000	0.0393	2.50	177.22
30	1	23	180	180.00	0.4	54000.0	55000	0.0393	2.75	177.47
30	1	23	180	180.00	0.4	54000.0	55000	0.0393	3.00	177.67
30	1	23	180	180.00	0.4	54000.0	55000	0.0393	3.25	177.85
30	1	23	180	180.00	0.4	54000.0	55000	0.0393	3.50	178.00
30	1	23	180	180.00	0.4	54000.0	55000	0.0393	3.75	178.13
30	1	23	180	180.00	0.4	54000.0	55000	0.0393	4.00	178.25

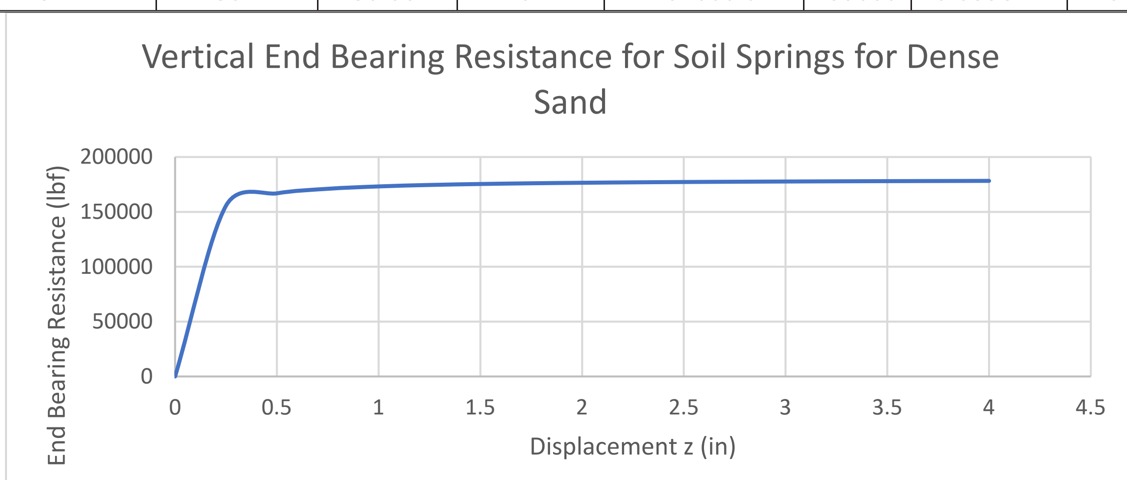

Figure 39: End bearing resistance in dense sand

5 Finite Element Analysis of the Pile Models using ANSYS Workbench

ANSYS software packages have been in use in the civil engineering industry for long. ANSYS Parametric Design Language (APDL) was earlier used to model structures. It gained popularity as a reliable finite element modeling software. In the old times, computers with limited computing power and graphical capabilities used to run the software at that time. So the modeling was based on the programming inputs. ANSYS unveiled ANSYS Workbench in the early 2000s, which had a better interface and a better user experience.

ANSYS Workbench is the user-friendly alternative of older APDL. Although APDL is still running, Workbench a more popular choice in the industry as well as academia due to its tendency to serve many engineering fields, from civil engineering to aerospace industry. ANSYS Workbench uses APDL in the background but provides the user with many built-in modules. APDL provides the capability of having a wide array of FE element types, suitable for the standard and unique model types. ANSYS Workbench has established itself as one of the most prominent and capable finite element analysis software in the market.

For this thesis, since composite materials are involved, the ANSYS Composite PrePost (ACP) module was used. It was unveiled in 2013 as an add-on module to the ANSYS Workbench. ACP allows users to model layered composites, with changing parameters from size to layers and batch process multiple similar models. This was very necessary for the kind of analysis that was required for this thesis. For structural analysis, the static structural module was employed.

The process starts in the ACP pre-processing tab, where the materials are assigned first. Then the model geometry, meshing, and boundary conditions are decided. ACP setup is used to define the composite properties. This data is transferred to the static structural module, where the static analysis has to be done. In the imported model, soil conditions are modeled, and loads are assigned to obtain results of static analysis. The results are then transferred to the ACP post-processing tab, where the composite results can be analyzed. A project schematic is shown below, which depicts the transfer of data between different modules:

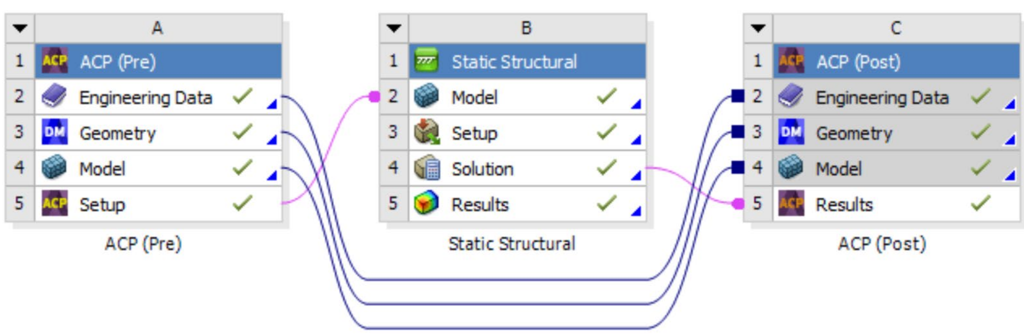

Figure 40: Typical view of project schematic in ANSYS Workbench

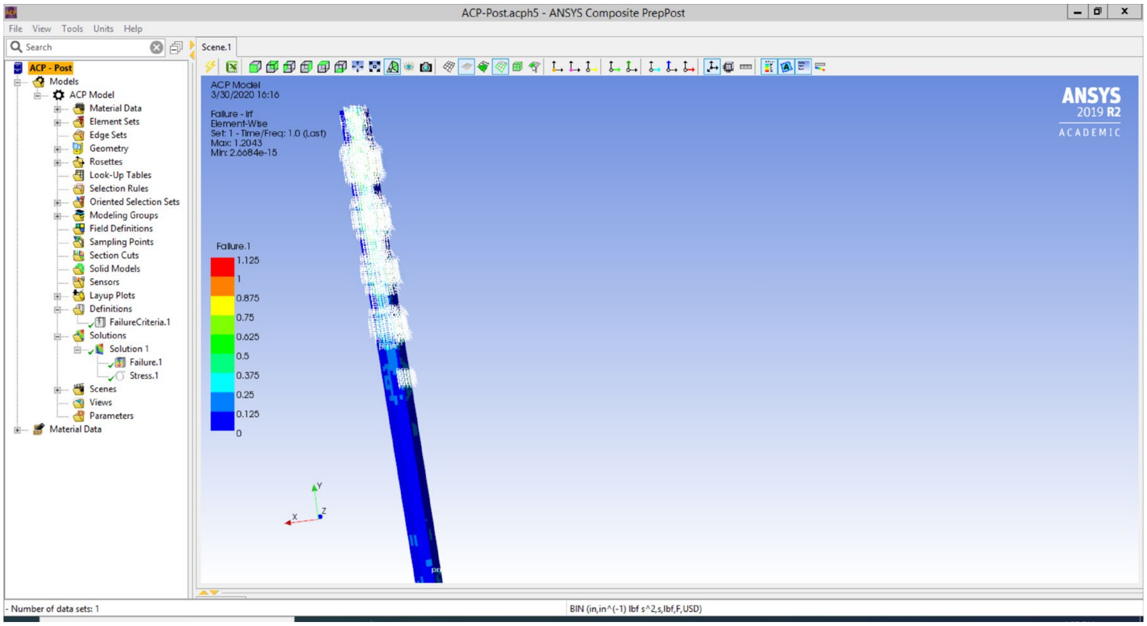

Figure 41: Typical view of ACP Post Processing

5.1 Model Initiation and Pre Processing

In ANSYS Workbench, the model was initiated in the ACP Pre Processing tab since a composite section had to be modeled. The following steps were taken to generate each model:

5.1.1 Engineering Data

The materials to be used in the piles can be chosen from the engineering data sources where a vast array of materials has been listed. ANSYS Workbench also allows a user to edit the properties of a particular material according to the project needs.

ANSYS Workbench can be used to define orthotropic elastic materials. It cannot define orthotropic and non-linear materials. It has been seen that most of the composite materials stay elastic before fracture, and hence orthotropic elasticity is a close approximation for composite material definition (Aliabadizadeh, 2016).

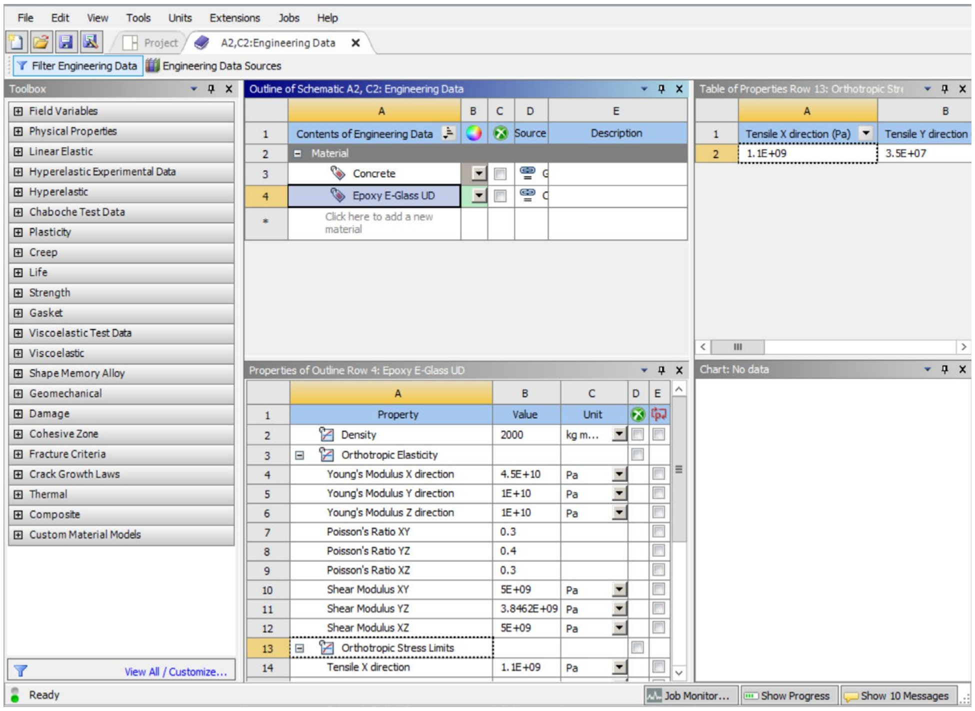

Figure 42: Typical view of engineering data mode

5.1.2 Setting up the Geometry

The next step is to define the geometry of the pile. ANSYS Workbench gives two options for a modeling environment, SpaceClaim and DesignModeler. For this study, DesignModeler was used for geometry definition. the resulting geometry is shown in the figure:

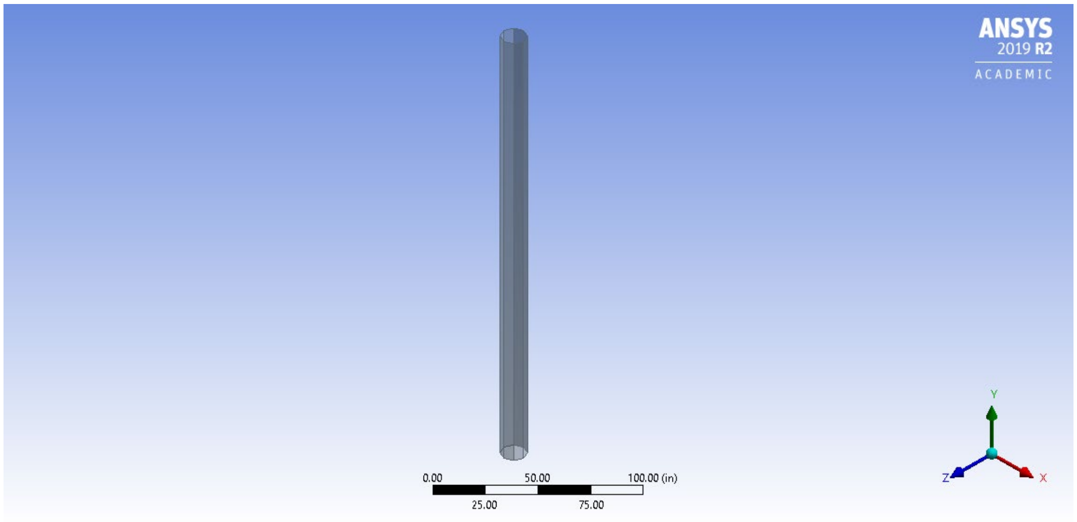

Figure 43: Typical view of pile geometry in DesignModeler

5.1.3 Meshing

Once the geometry has been defined, meshing is done. It is essential for finite element analysis that the entire volume of the structure is divided into smaller elements. Mesh sizes have to be defined with due consideration. A coarse mesh may give inaccurate results, whereas too fine mesh can increase the computation time drastically.

For this study, the automatic meshing method was used in quad/tri dominant mode. Without refinement, it was seen that the results were inaccurate. On the other hand, a mesh with multiple levels of refinement led to a server timeout. Finally, an adequate mesh refinement level was chosen. For the FRP shell, the rectangular mesh was found to be the most effective. In concrete-filled sections, tetrahedral meshing was found to be the most accurate for the concrete core.

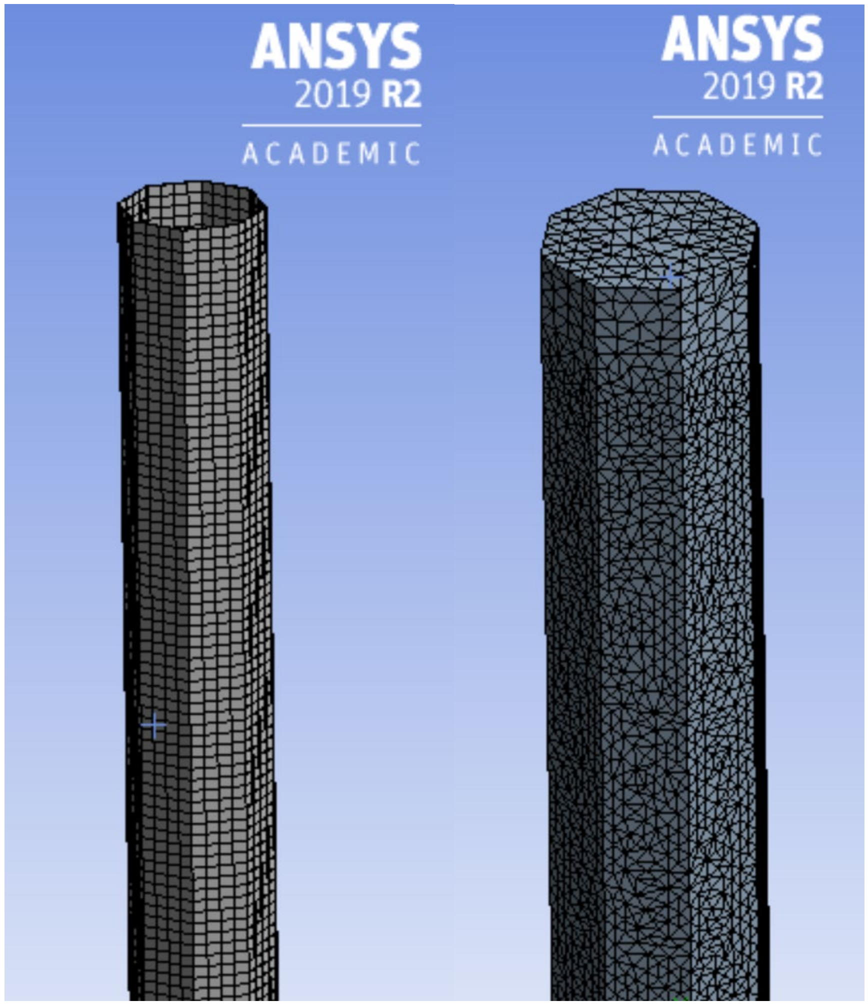

Figure 44: Meshing for (a) FRP Shell (b) Concrete Core

5.2 ACP Pre Processing

ACP Pre-Processing tab is used to define the properties of composite layers in a system. ACP Pre allows us to define the fabric properties, create the ply stack up as well as allows us to define the layup properties. Following steps were followed to set up the composite shell of the pile:

5.2.1 Material Data

This tab allows the users to define the fabric and stackup data. Fabric data is pulled out directly from the engineering data, and the user can set fabric thickness. For this thesis, Epoxy E-Glass UD was chosen. Then the stackup tab allows a user to decide the fiber orientation in individual layers.

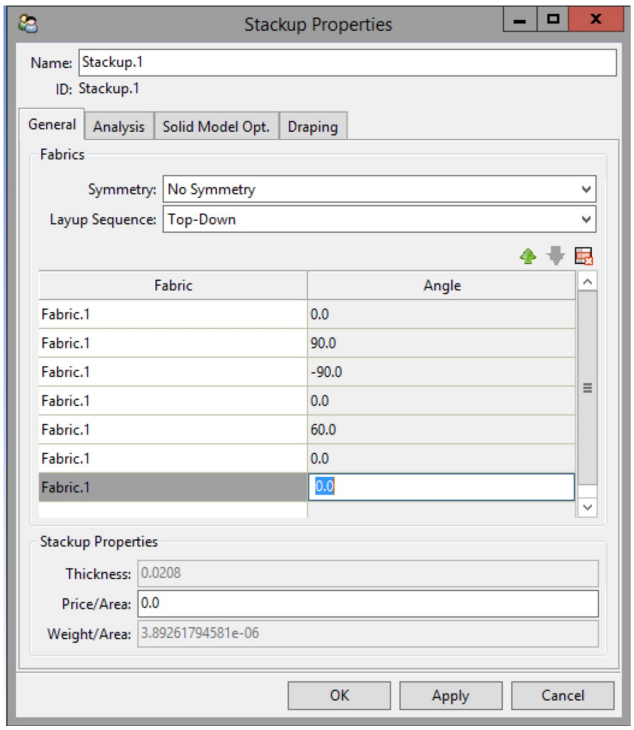

Figure 45: Typical view of Stackup Properties menu

5.2.2 Defining Rosettes

Rosettes define the direction of the composite layup. The inputs for rosettes include origin coordinates, direction 1 (the 0° direction for the composite layup), and direction 2 (90° direction for the composite layup). The set of rosettes tells the program in which direction the ply layup should happen in the laminate. For this thesis, a set of 3 rosettes was defined.

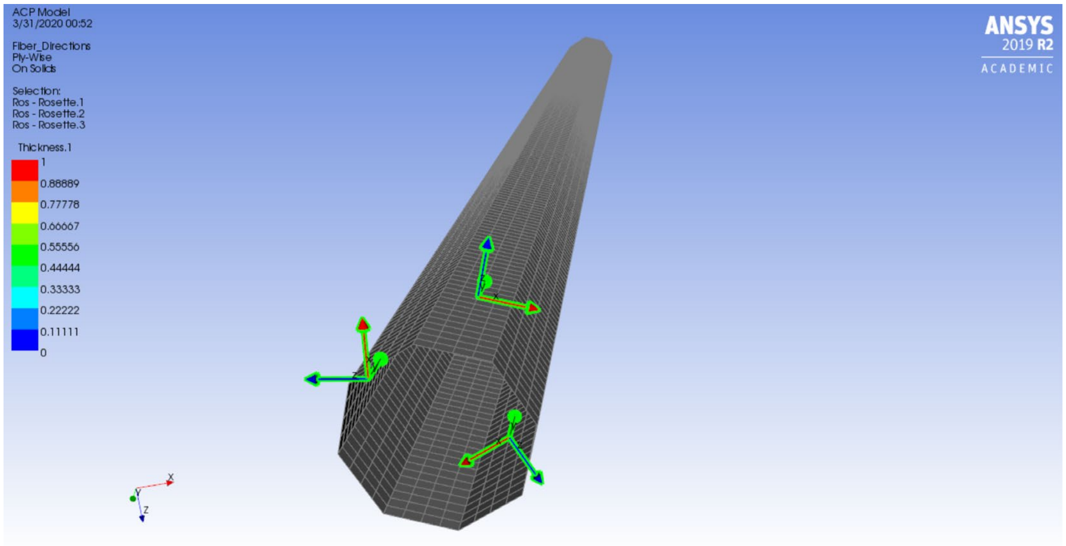

Figure 46: Rosettes

The next figure illustrates the reference directions that are generated after the rosettes are defined. Yellow-colored arrows define the direction 1.

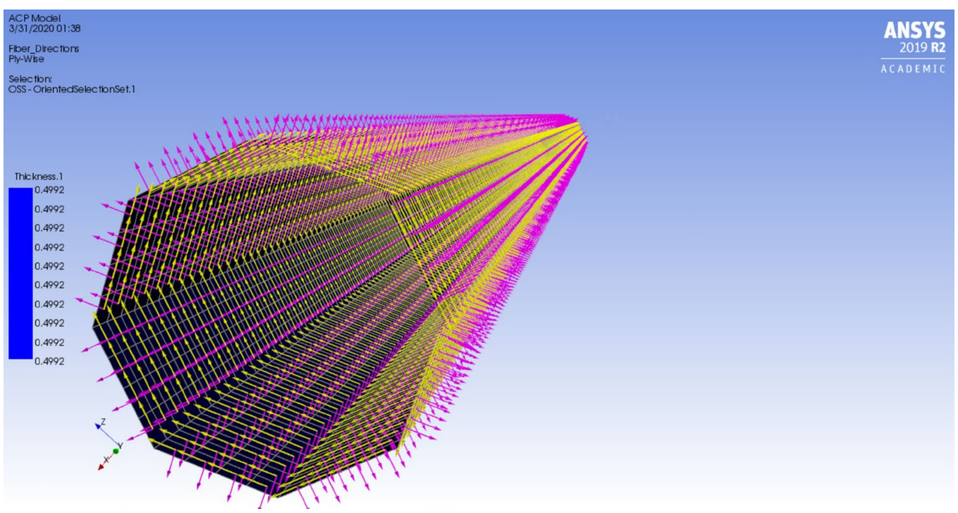

Figure 47: Reference directions after the rosettes are defined

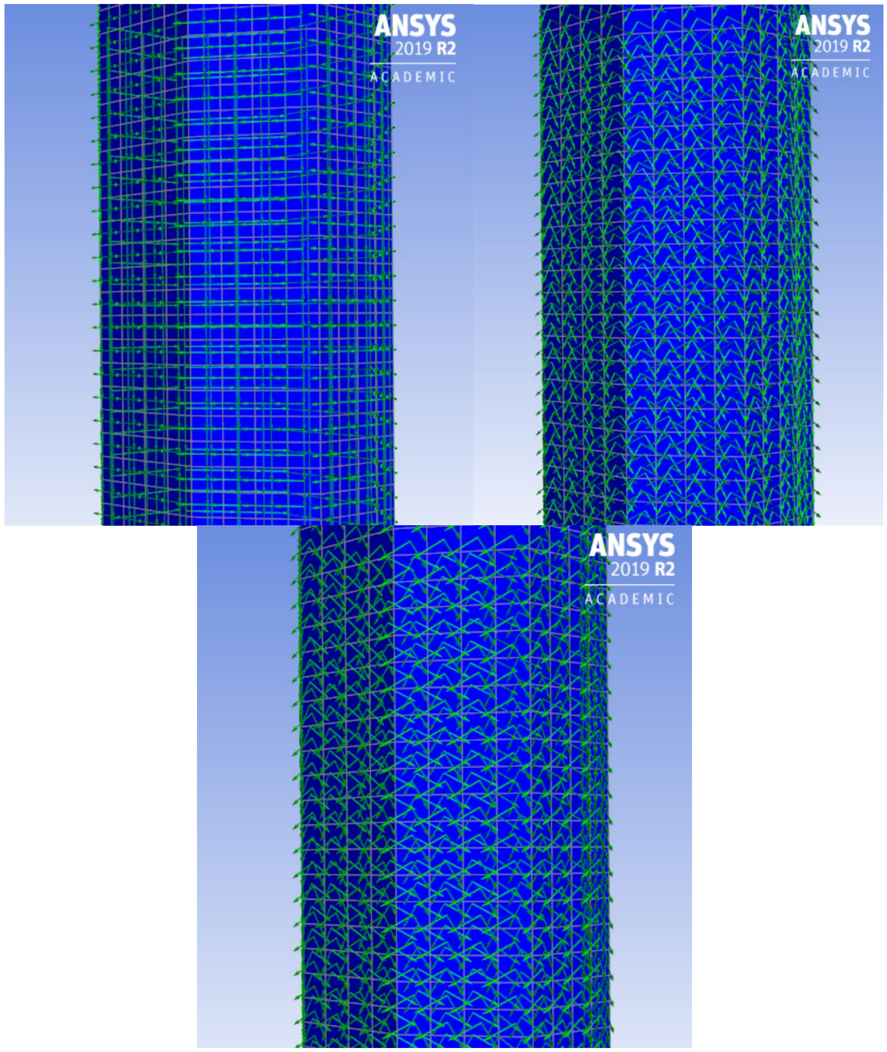

Figure 48: Fibers oriented at different angles

Now, on the completion of the ACP setup, the "composite shell data" was transferred to the static structural module.

5.3 Static Structural Analysis

The data from the ACP setup is transferred to the Static Structural module. Static Structural runs using ANSYS Mechanical. The inputs for this module are force, displacement, boundary conditions, connections, etc. For the output, in addition to the stress and strain results, the composite failure tool was also used to determine the failure ratio for various cases. The steps involved are described in the sections that follow.

5.3.1 Load and Horizontal Displacement

In this thesis, multiple combinations of vertical loads and horizontal displacements were tested. The lateral load has been presented as forced horizontal displacement. Horizontal displacement was given in the X direction at the pile head and was limited to 4 inches and applied in half an inch steps. A load is applied in the negative Y direction. The scope of the point of application of the vertical load and horizontal displacement is limited to the top face. ANSYS distributes the force and displacement evenly throughout that face, including edges.

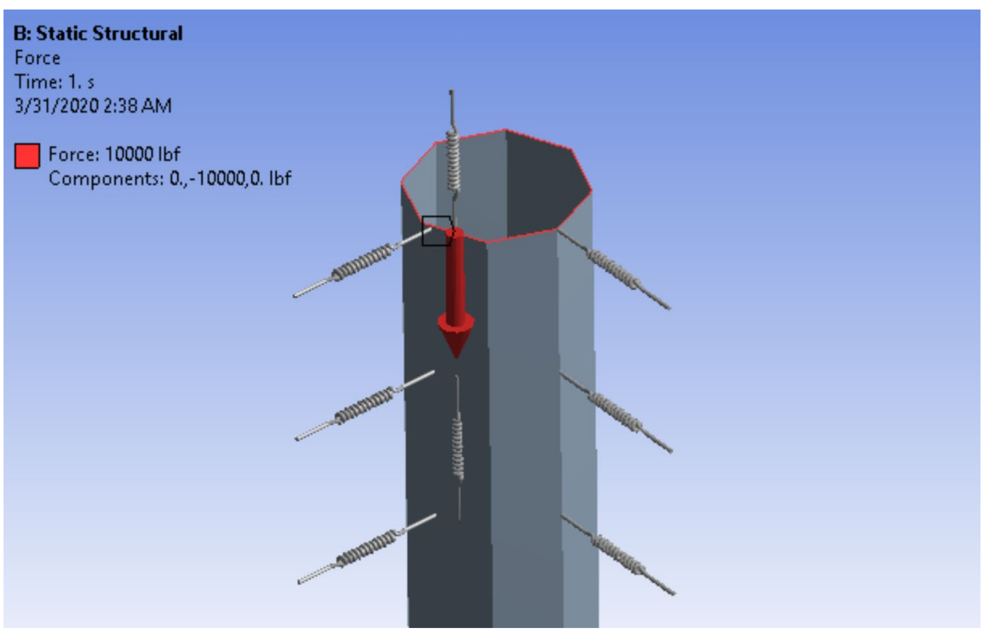

Figure 49: Force applied evenly amongst all of the top edges

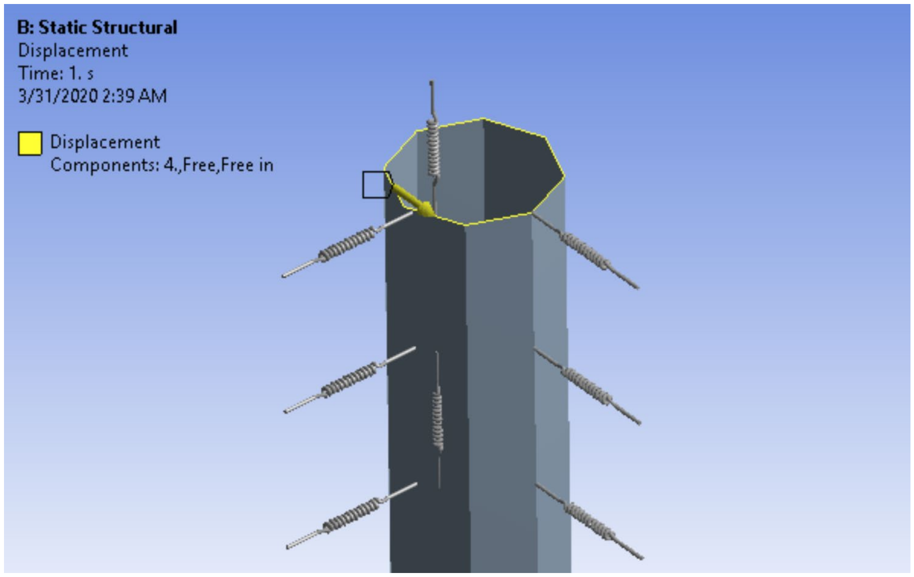

Figure 50: Horizontal displacement at the pile head

5.3.2 Modeling Soil Behavior

The soil around the pile is modeled as non-linear springs. The springs are based on modified Ramberg-Osgood models. Springs had an area of influence of 12 in, and the influence of spring was spread using a pinball region of appropriate diameter. Three kinds of springs were used:

- Lateral resistance springs, based on p-y curves.
- Slip resistance springs, based on f-z curves.
- End bearing springs, based on q-z curves.

The p-y curves represent the relationship between the lateral soil pressure against the pile and the corresponding lateral pile displacement. The f-z curves describe the relationship between skin friction and the relative vertical displacement between pile and soil. The q-z curves describe the relationship between bearing stress at tip and pile tip settlement.

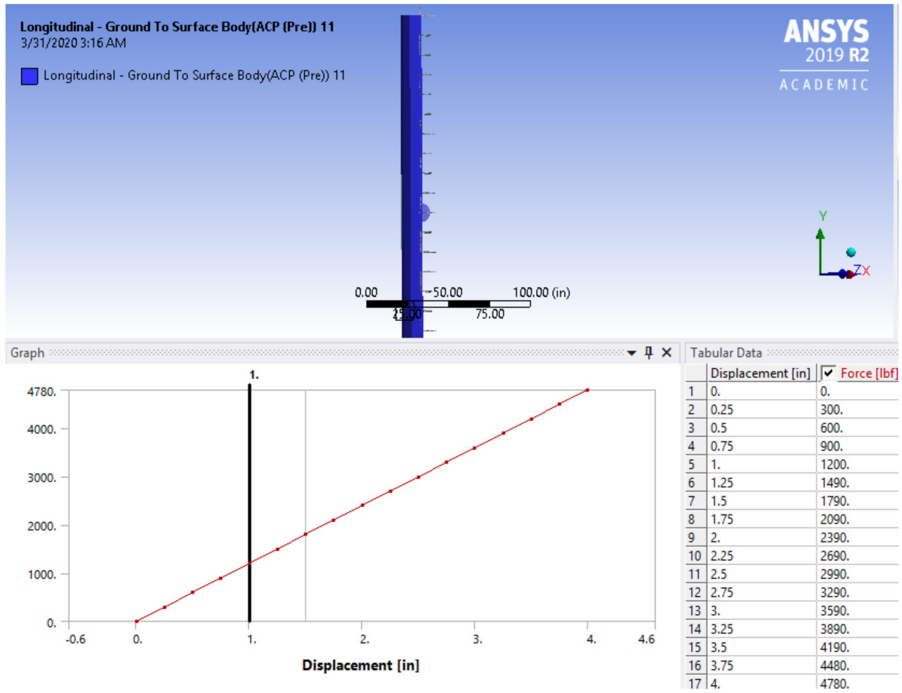

Figure 51: Lateral resistance soil spring model for dense sand

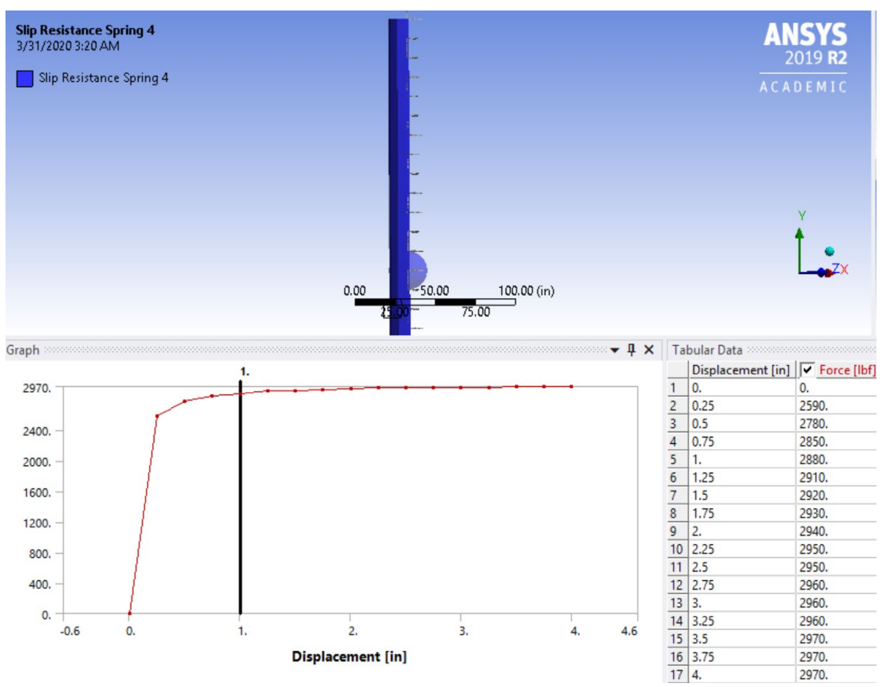

Figure 52: Slip resistance soil springs for dense sand

5.3.3 Setting Composite Failure Criteria

In the composite failure tool, the required failure criteria can be chosen and assigned weights. A point to note here is that this step can be also be skipped here as this functionality is available in ACP Post Processing as well.

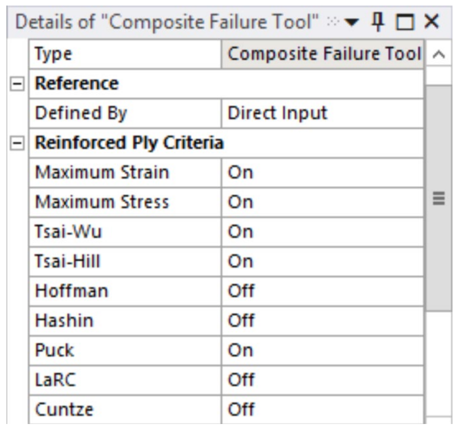

Figure 53: Choosing failure criteria in static structural module

As already discussed, for this thesis, the failure criteria that were used are:

- Maximum stress.
- Maximum strain.
- Tsai-Wu.
- Tsai-Hill.
- Puck.

5.3.4 Output Results

The results of the analysis of the pile against the given load and displacement conditions can be seen in the solution tab. Maximum principal stress and maximum shear stress are two major categories of results in which we are interested. In addition to the stress values, we also observe failure ratios to obtain trends for change in failure ratio by varying parameters.

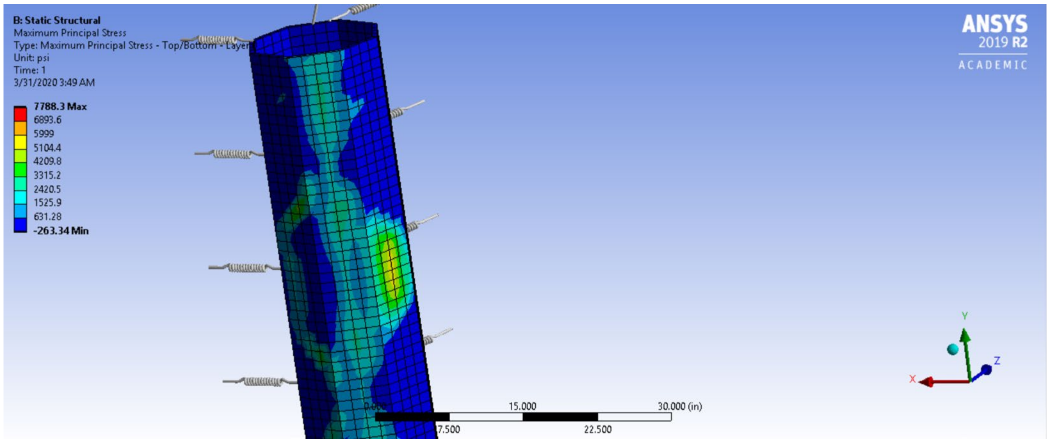

Figure 54: Maximum Principal Stress

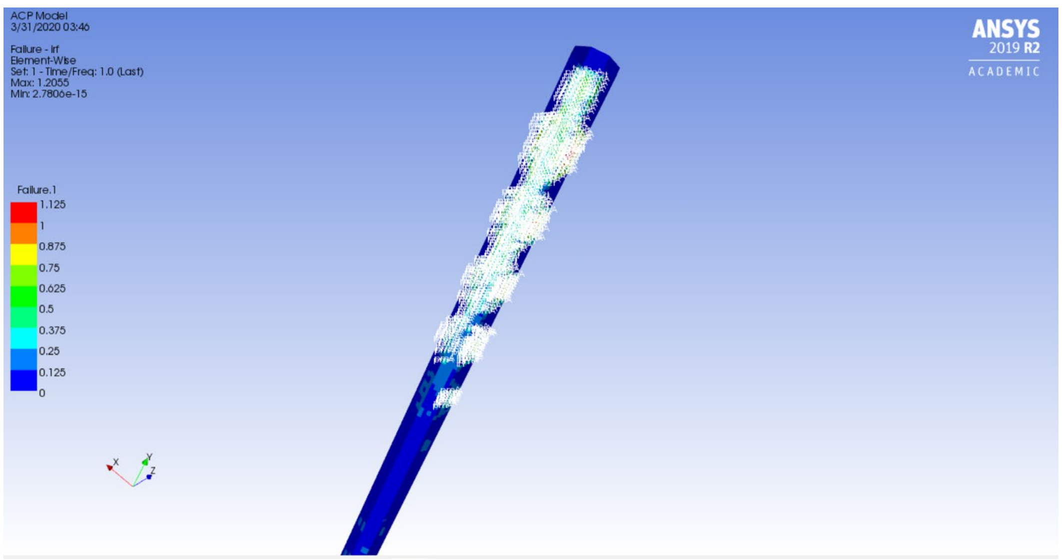

Figure 55: Governing failure criterion (From ACP Post)

5.4 Model Validation

The soil-pile modeling technique was validated against two available resources:

i. Available data from previous research.

ii. Available data from the Industry.

The validation results are discussed in the sections below.

5.4.1 Validation using Data from Previous Research

For one of the results, Jaradat (2005) analyzed concrete-filled rectangular sections in dense sand.

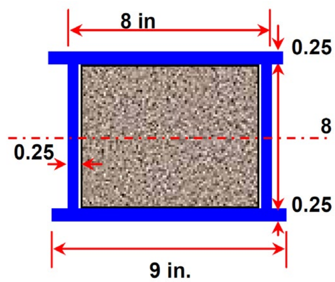

Figure 56: Section used by Jaradat (2005

The laminate structure for 12 layers was [0,0,90,90,0,0,0,0.90,90,0,0]. The pile height was 20 ft. A similar section was reproduced using the algorithm used in this theory.

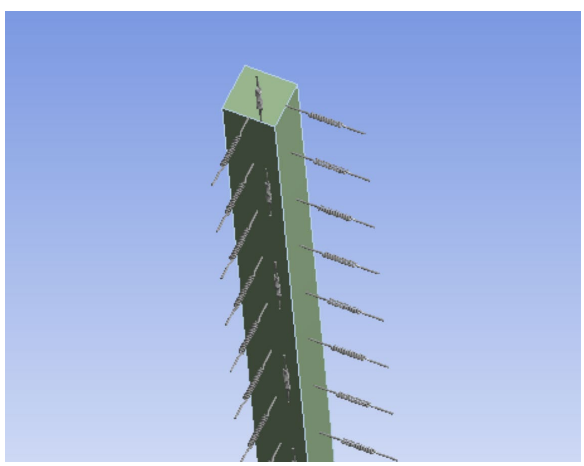

Figure 57: Section reproduced for analysis in ANSYS

The loading conditions were also kept similar: an axial load of 300 kips and a horizontal displacement of 2 inches was applied. The pile stress generated in these conditions was found to be 12205.3 psi (12.205 ksi), which is in agreement with the results in the referred research (12.5 ksi).

5.4.2 Validation using Data from the Industry

A pipe pile brochure by Creative Pultrusions, Inc. depicts some mechanical properties of a standard FRP octagonal section. The sides of the octagon were 8 inches long, and the edge thickness was 0.25 inches. The model was reproduced in ANSYS, as shown in the figure:

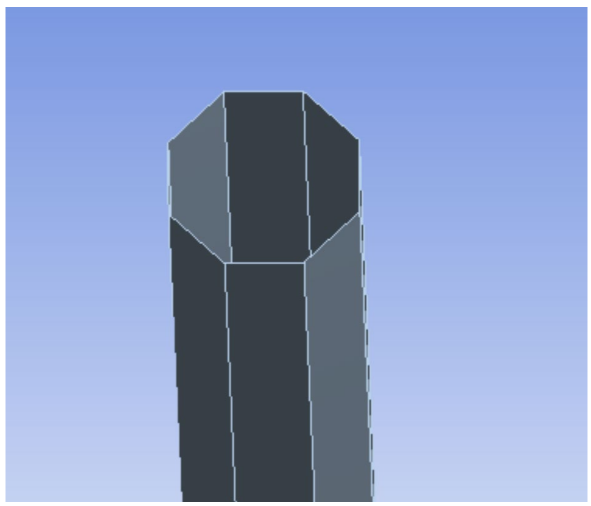

Figure 58: Octagonal test model

The average shear strength of the pile according to analysis on ANSYS was 12381 psi which is in close agreement with the value provided by the firm, i.e., 12554 psi.

6 Results and Discussion

The soil-pile models in ANSYS were studied in an attempt to capture the trends of variation in properties by varying certain parameters.

6.1 *Behavior of FRP piles in different soil types subjected to constant vertical load and horizontal displacement*

In this section, piles were analyzed for a constant vertical load with varying fiber orientation and soil types. The piles had a constant horizontal displacement at the head.

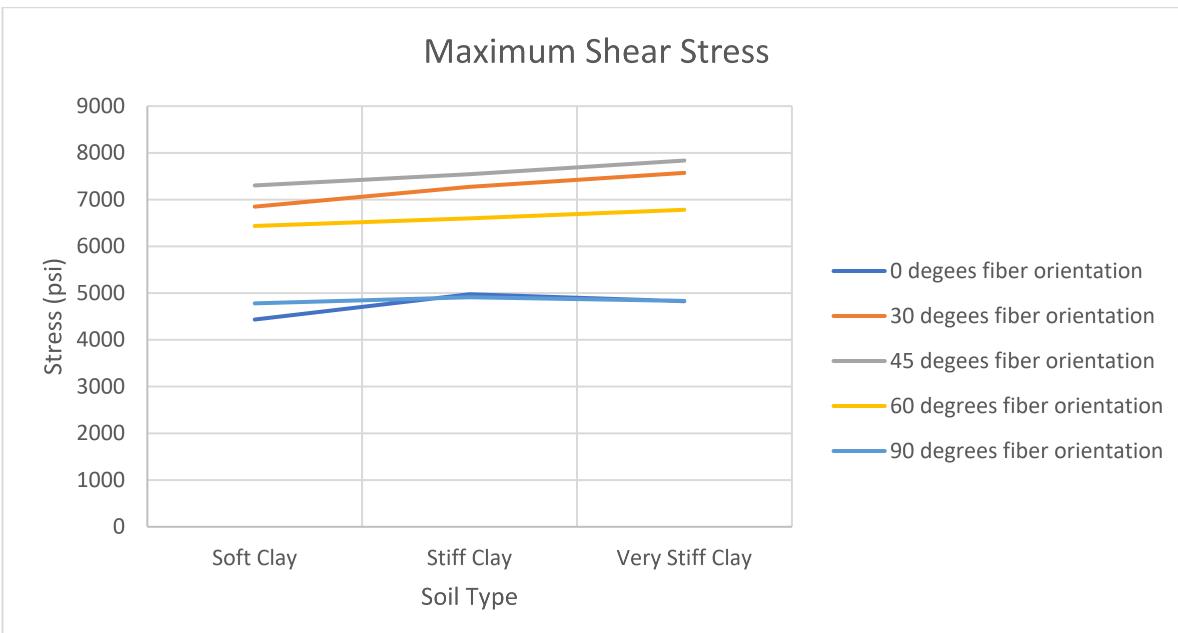

Figure 59: Comparison of maximum shear stress in different clays

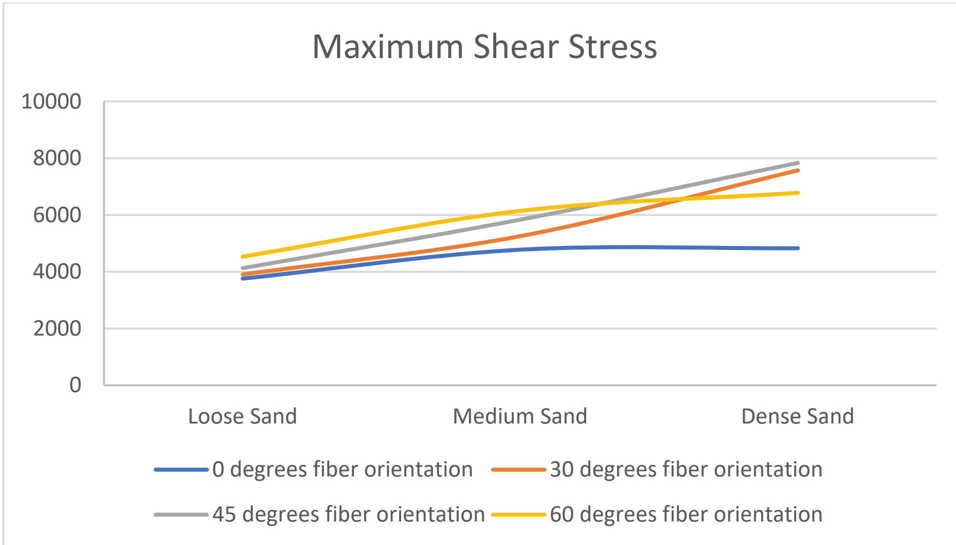

Figure 60: Comparison of maximum shear stress in different soil sands

It is evident from the curves that stiffer the soil; more are the stresses generated in a pile. This is because soft soils accommodate lateral displacements better as they offer less resistance to the lateral movement resulting in lower stresses. It was also observed that the vertical displacements in loose sands are considerably high. Fiber orientation does not affect the vertical deformation in piles.

6.2 Behavior of FRP piles with varying vertical load subjected to constant horizontal displacement

In this section, results for the analysis of an FRP pile section for varying vertical load and fiber orientation are discussed. The pile was given a horizontal displacement of 4 in. for the analysis.

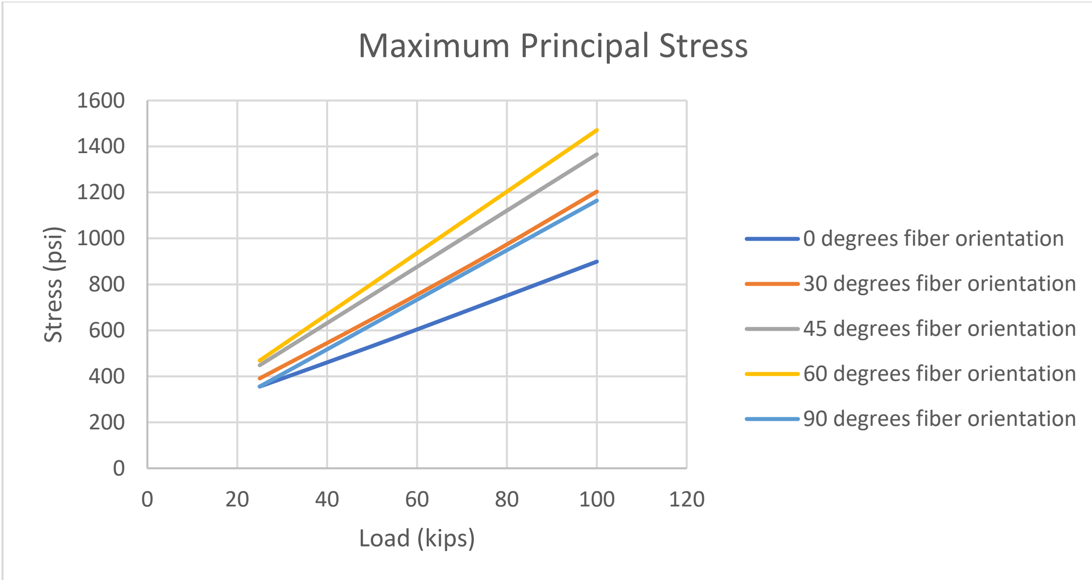

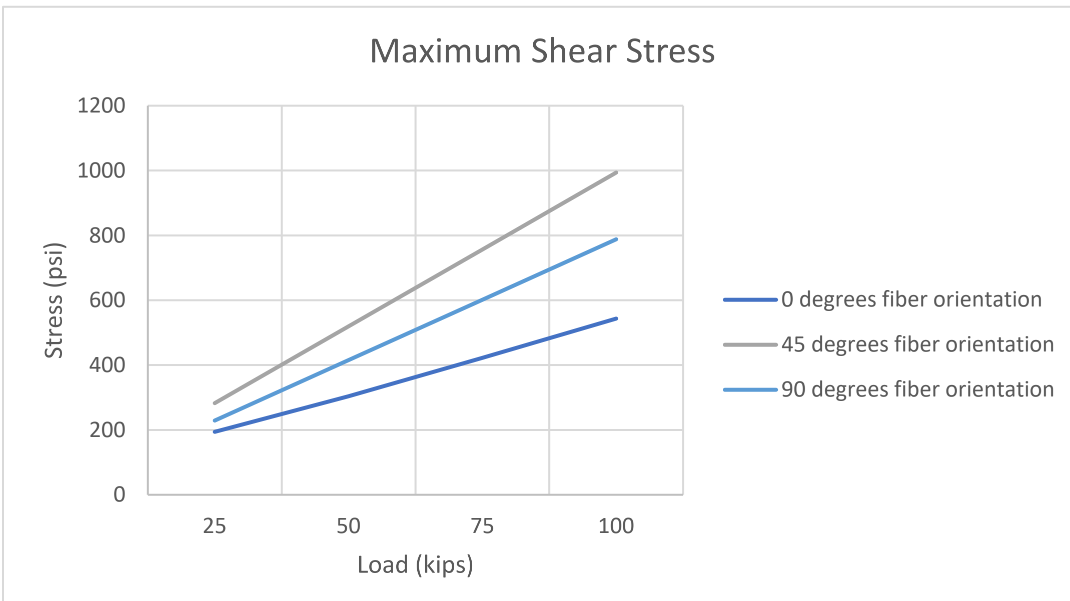

Figure 61: Variation in pile stresses against varying vertical load

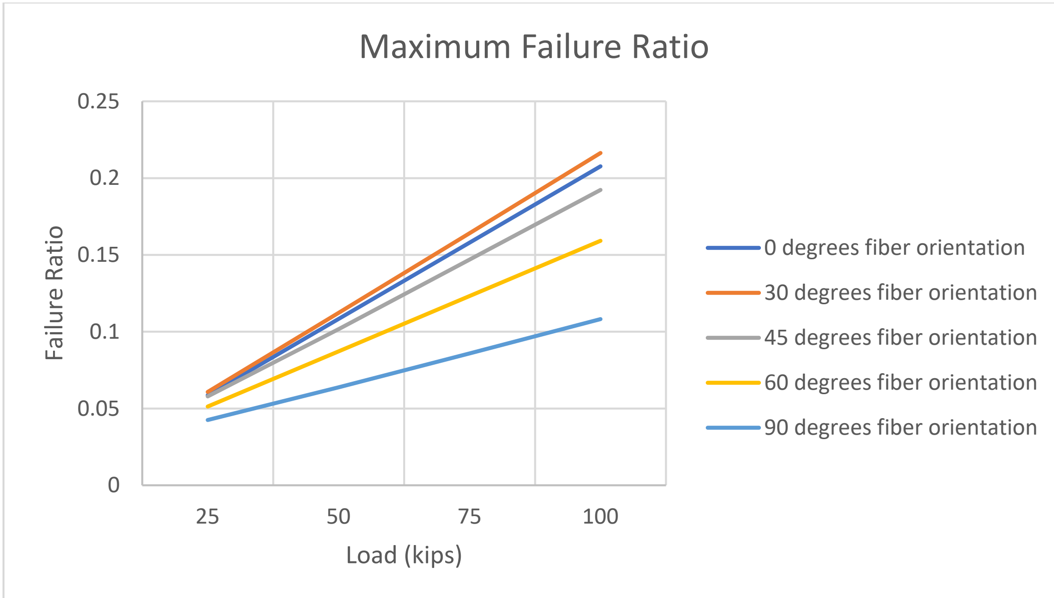

Figure 62: Variation in maximum failure ratio against variation in vertical load

As it is clear from the curves that the stress in piles as well as the failure ratio increase linearly with an increase in the axial load applied. The rate of increase of failure ratio for the pile decreases with an increase in fiber orientation.

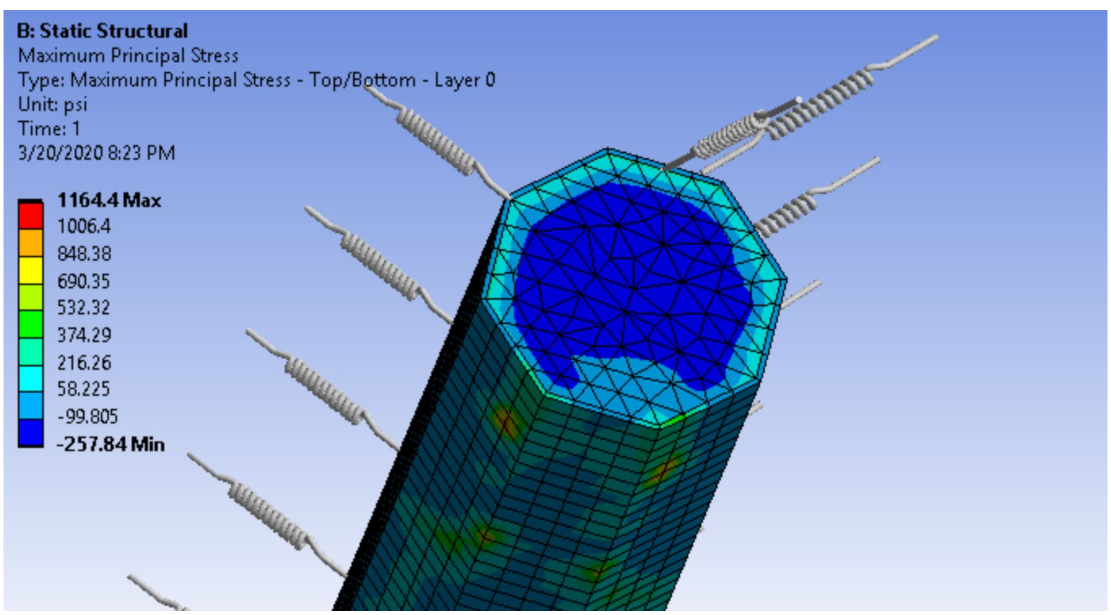

Figure 63: Typical view of analysis window

6.3 Comparison of behavior of concrete-filled FRP piles and hollow FRP piles subject to similar loading conditions

In this section, we will discuss the results of the comparison between hollow FRP sections and concrete-filled sections. All the other parameters, like vertical load, the number of layers, and horizontal displacement, were kept the same for comparison.

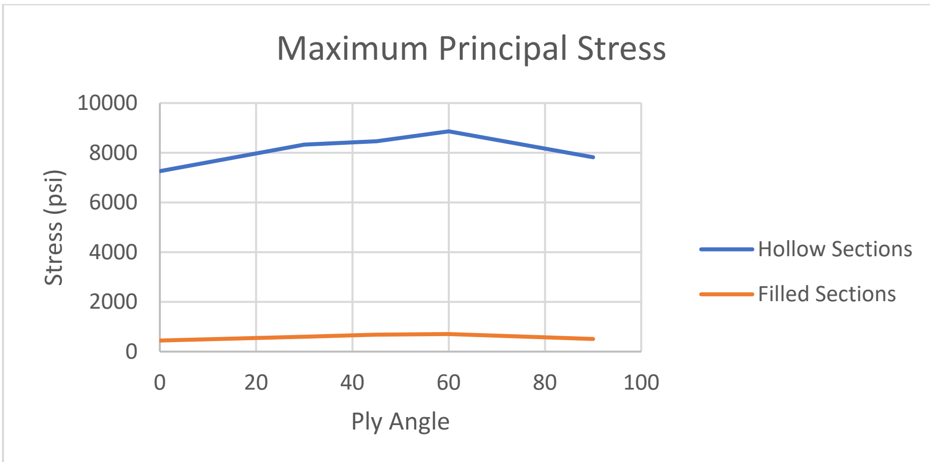

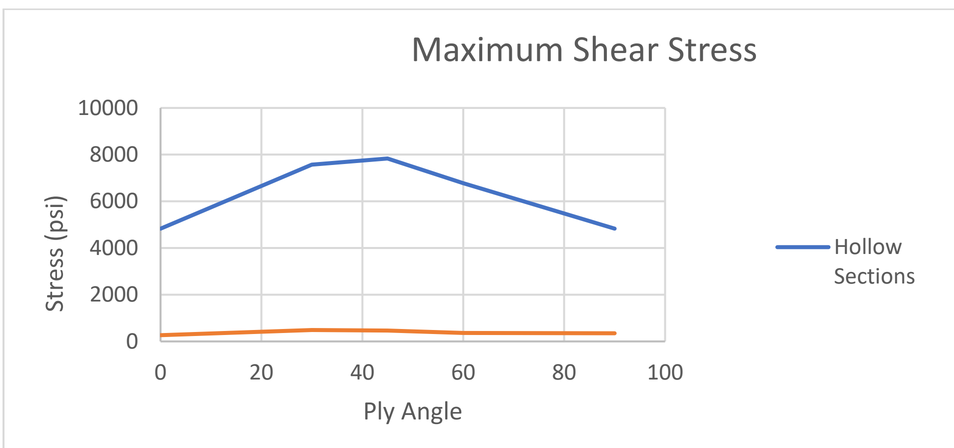

Figure 64: Comparison of stresses in concrete-filled and hollow FRP piles

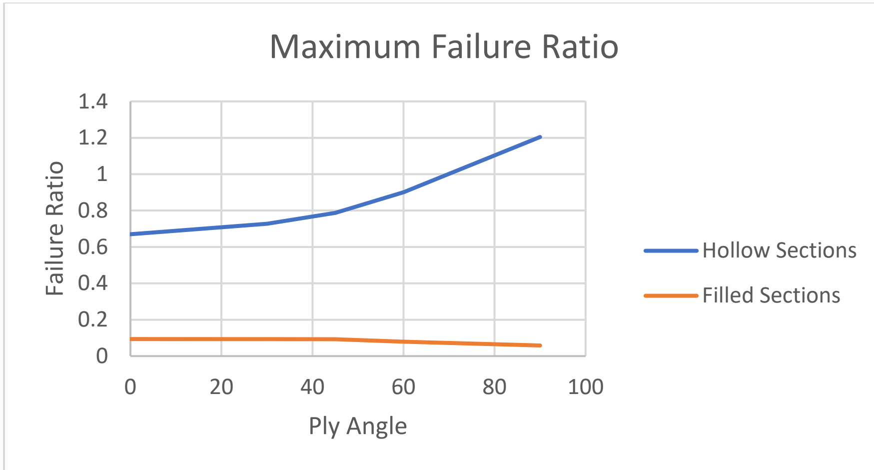

Figure 65: Comparison of maximum failure ratios in concrete-filled and hollow FRP piles

It is evident from the curves above that concrete fill decreases the stresses in the piles significantly. The failure ratio also decreases with the introduction of concrete fill. Hence it can be said that concrete filling has a considerable effect in pile capacity and failure. It was also seen that the vertical deformations were much lower in concrete-filled sections than the hollow sections.

6.4 Behavior of FRP piles with varying number of ply layers subjected to similar loading conditions

In this section, the results of the analysis of FRP piles with variable fiber orientation and the number of FRP layers are discussed.

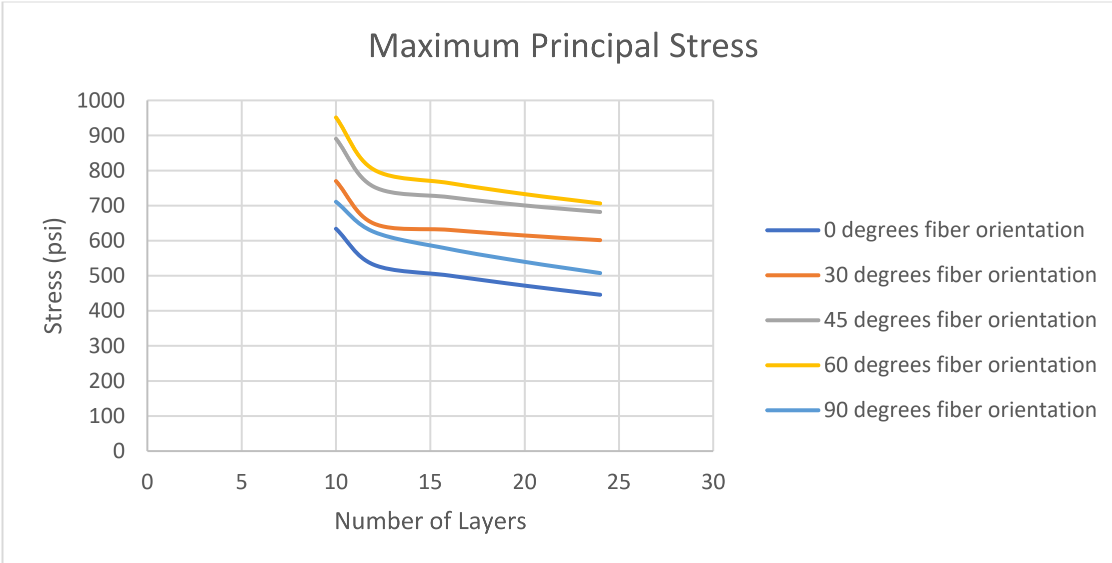

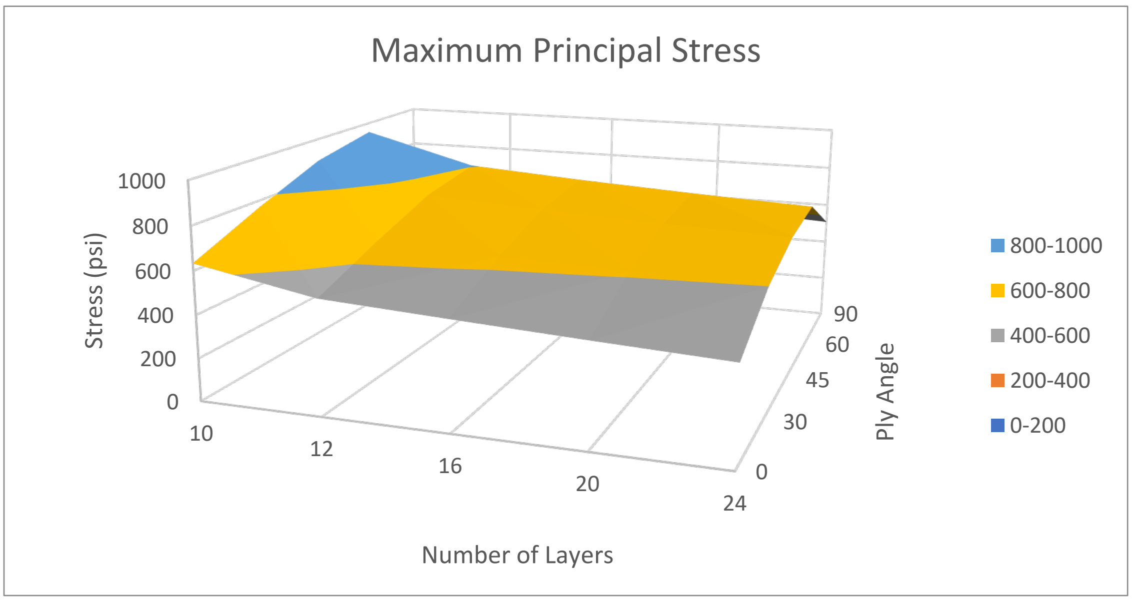

Figure 66: Comparison of pile stresses with varying number of ply layers

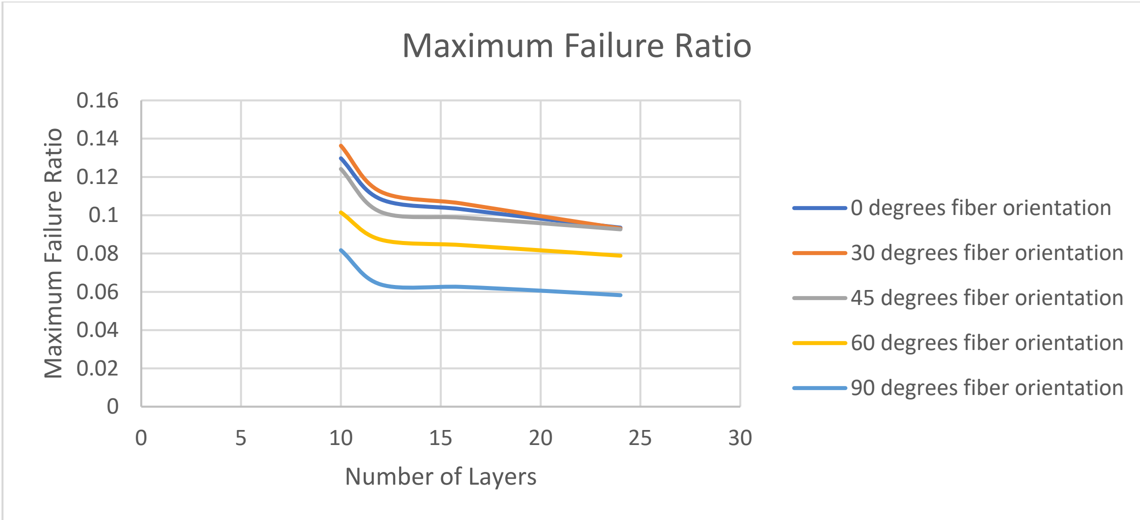

Figure 67: Comparison of maximum failure ratio with varying number of ply layers

As can be seen from the curves, the pile stresses and maximum failure ratio decrease rapidly until a shell thickness of about 0.25 inch, and the rate of decrease becomes gradual afterward. It should be noted that the variation of pile stresses with the number of ply layers is linear. The maximum principal stress achieves maxima at 60° fiber orientation, and the maximum shear stress achieves a maximum at 45°.

6.5 Behavior of FRP piles subjected to constant vertical load but varying horizontal displacement at the pile-head

In this section, we will discuss the results of the analysis of varying horizontal displacement and fiber orientation for a given octagonal pile profile.

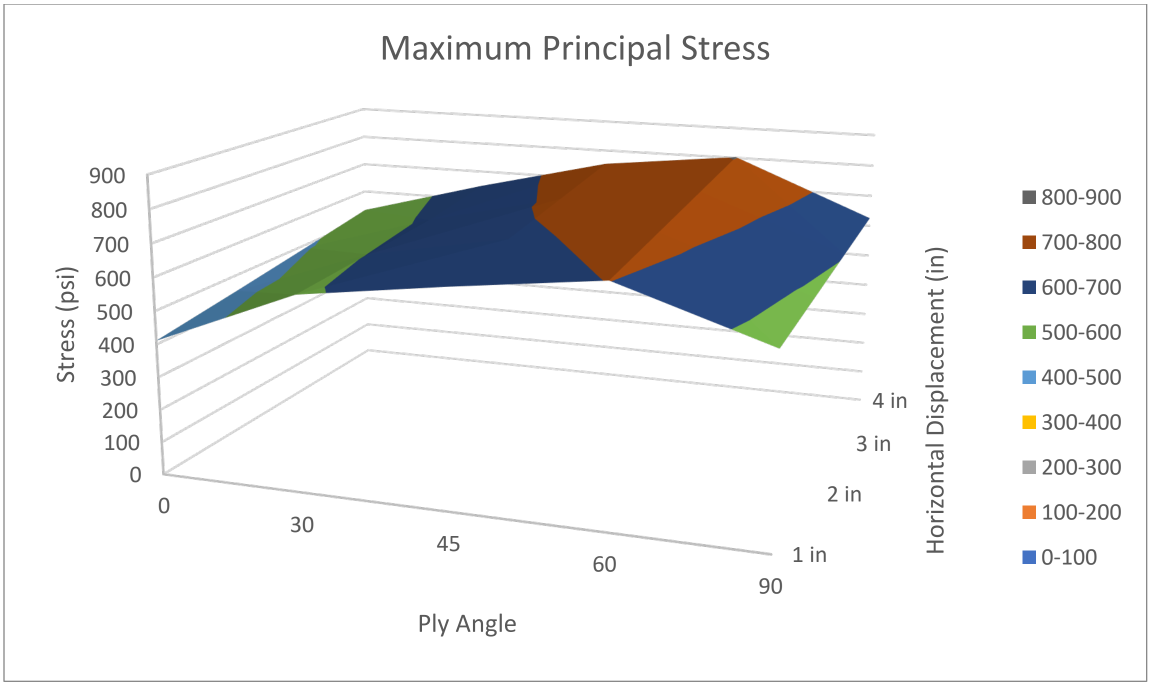

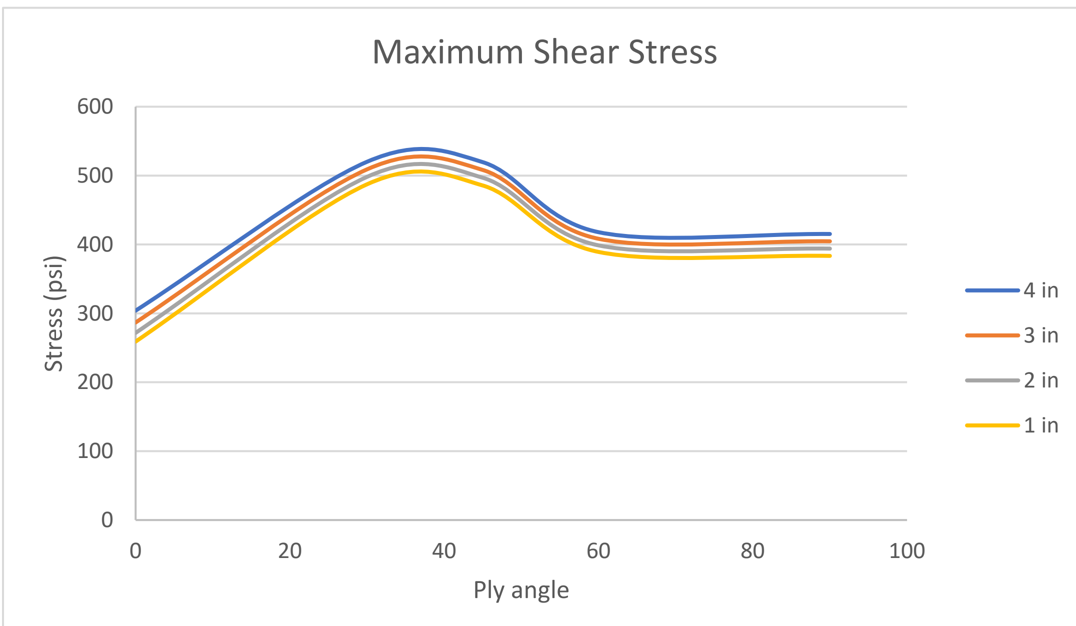

Figure 68: Variation in pile stresses against varying horizontal displacement and fiber orientation

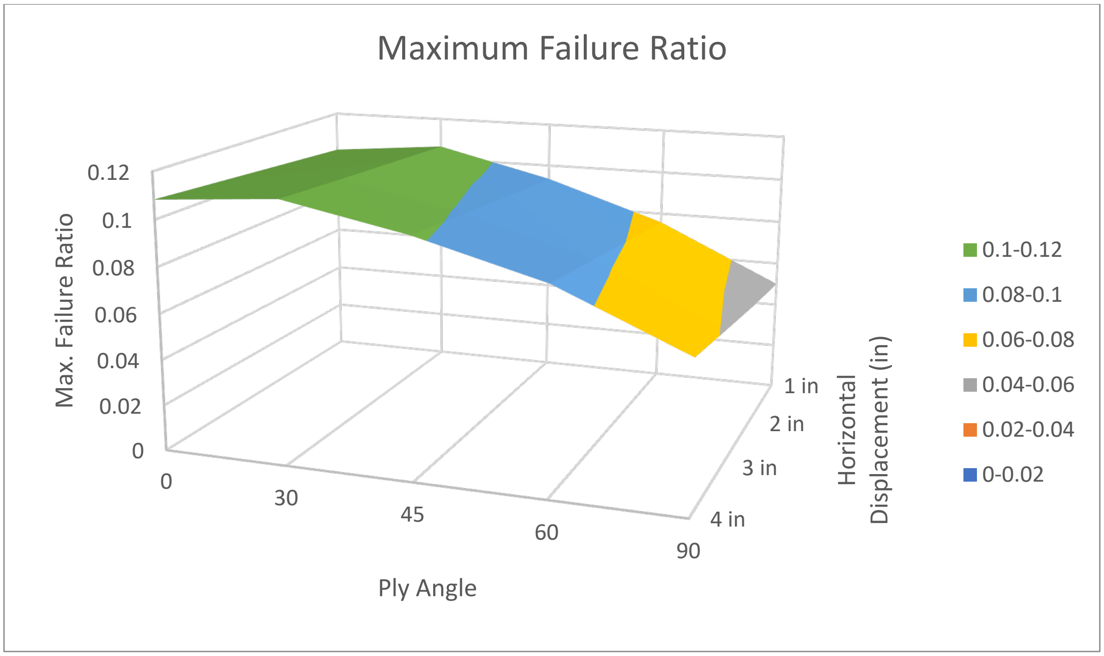

Figure 69: Variation in maximum failure ratio against varying horizontal displacement and fiber orientation

As shown in the curves above, for concrete-filled FRP pile sections, the maximum principal stress approaches maxima at 40°, and the maximum shear stress approaches maxima at 60°. A similar result was obtained by Aliabadizadeh (2016) for his analysis of elliptical piles. It can also be seen that pile stresses increase linearly with the horizontal displacement at the head of the pile. The maximum failure ratio achieves maxima at 30° and decreases from there on with increasing fiber orientation. A linear increase in maximum failure ratio with an increase in horizontal displacement was also observed, as was expected.

6.6 Comparison of FRP piles having circular cross-sections and FRP piles having an octagonal cross-section

The most commonly used piles have a circular cross-section. Hence, it becomes necessary to compare the octagonal sections analyzed in this study with circular sections under similar conditions. The piles of both shapes had equal perimeters to ensure that the amount of material used is the same. The piles were subjected to the same soil conditions, vertical load, and horizontal displacement.

The stresses generated in the octagonal piles were lesser than the stresses in circular piles. Moreover, the failure ratio in octagonal piles was lesser than the circular piles. An irregular octagonal section was also tested where it was elongated along one of the axes (longer diagonals) keeping the perimeter the same. For such piles, the failure ratio was observed to be higher. This does not mean that the circular section is a better choice but instead means that increasing section width increases the width of the soil profile, and therefore the soil resistance increases. The narrower side in an irregular octagonal pile can be oriented in the direction of lateral displacement to achieve the desired lower stiffness, which in turn reduces the soil resistance.

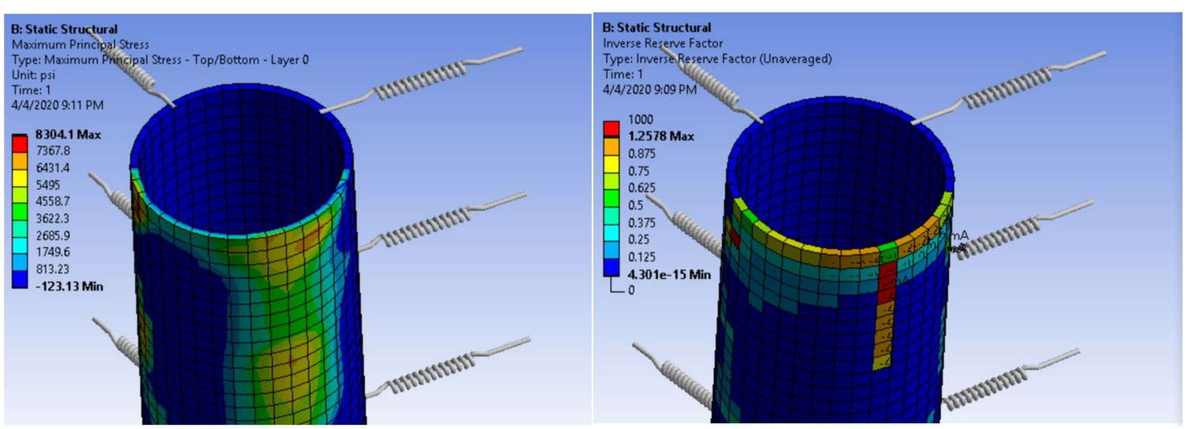

Figure 70:FRP piles with circular cross-sections

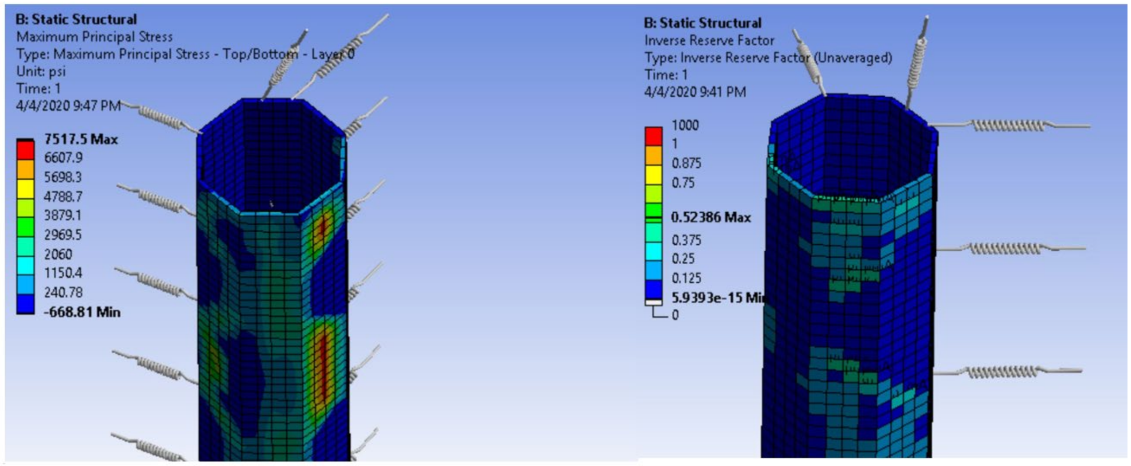

Figure 71: FRP piles with octagonal cross-section

7 Conclusions

This work is a record of an extensive study investigating the use of FRP piles with octagonal cross-sections for integral abutment bridges. Although the initial cost of installing FRP piles is high, manufacturers claim that the lifecycle cost of an FRP structure is considerably low. Experimental results have found limitations in the drivability of FRP piles as well, but novel methods like toe-driving have been devised to improve the same.

Octagonal sections were chosen due to their compatibility to cheaper manufacturing methods and for their ability to provide stiffness and flexibility in two perpendicular axes simultaneously. Interaction with engineers working in the industry revealed that octagonal sections might prove useful since they offer stable flat surfaces for operations like bolting. These were the primary reasons to start with an octagonal cross-section. A numerical analysis revealed that various parameters, such as fiber orientation, dimensions, loading conditions, and soil conditions, affect the capacity of FRP piles.

Following are some general trends and observations from the study:

- The type of soil at the site has a considerable effect on the pile behavior for an IAB. The stiffer the soil, the more are the stresses generated in a pile. This is because horizontal displacement generates more forces in stiffer soils. Therefore, softer soils are favorable for integral abutment bridges as they offer less resistance to the lateral movement, and hence lesser stresses are generated in the piles.

- The results also suggest that loose soils are more suitable as end-bearing piles since they do not offer enough skin friction. The study observed high vertical displacement in loose sand, which makes loose sands unsuitable for FRP piles. If a layer of dense soil or a rock stratum is encountered near the pile toe, then FRP piles can be used in loose sands.
- For piles subjected to the same horizontal displacement at the top and having the same fiber orientation, the stresses increase linearly with an increasing vertical load. The failure ratio also increases linearly with the vertical load. The rate of increase of failure ratio for the pile decreases with an increase in fiber orientation.
- Concrete-filled FRP sections have considerably lower stresses than hollow FRP sections. This is because the stress is drastically reduced in the composite and is transferred to the concrete fill.
- The vertical deformation in a concrete-filled FRP pile section is considerably lower than a hollow FRP pile section. Fiber orientation does not affect the vertical deformation.
- For piles subjected to constant horizontal displacement and having a varying number of ply layers, the pile stresses decrease linearly with an increasing number of layers. The rate of decrease is drastic in thinner layers, and after a certain point, the rate of decrease becomes gradual. In the case of fiberglass, this change occurred at 0.25 inches thickness.

- For piles subjected to constant vertical load and varying horizontal displacement at the head, the stresses in the piles increase linearly with an increase in horizontal displacement.
- For piles subjected to constant vertical load, a maximum shear point was observed at 30° fiber orientation, and the maximum principal stress achieved maxima at 60° fiber orientation. The maximum failure ratio achieves maxima at 30° and then decreases for increasing fiber orientation.
- A comparison of circular and octagonal sections with the same perimeter revealed that the octagonal sections have the least failure ratio.
- However, for an irregular octagonal section elongated along one of the longer diagonals, the failure ratio was observed to be higher than the circular section. This does not mean that the circular section is better, but instead means that the width of the soil profile in contact has increased. The narrower side of the irregular pile can be oriented in the direction of displacement to achieve the desired lower stiffness, which in turn reduces the soil resistance.

Although FRPs are gaining popularity, there is still a lot to be done for them to gain acceptance in the piling industry. New materials like FRPs can replace conventional building materials only if dedicated research is done on the subject. Lack of usage guidelines is another factor that discourages the use of FRP in the piling industry. This study was one attempt to introduce an FRP pile section, which is economical, has certain usability benefits, and is faster to produce.

8 Appendices

8.1 Solver Output

```
ANSYS Academic Research

*-----------------------------------------------------------------*
|                                                                   |
|   W E L C O M E   T O   T H E   A N S Y S (R) P R O G R A M       |
|                                                                   |
*-----------------------------------------------------------------*



***************************************************************
   *            ANSYS 2019 R2          LEGAL NOTICES           *
***************************************************************
*                                                              *
   * Copyright 1971-2019 ANSYS, Inc. All rights reserved.       *
   * Unauthorized use, distribution or duplication is           *
   * prohibited.                                                *
*                                                              *
   * Ansys is a registered trademark of ANSYS, Inc. or its      *
   * subsidiaries in the United States or other countries.      *
   * See the ANSYS, Inc. online documentation or the ANSYS, Inc. *
   * documentation CD or online help for the complete Legal     *
   * Notice.                                                    *
*                                                              *
***************************************************************
*                                                              *
   * THIS ANSYS SOFTWARE PRODUCT AND PROGRAM DOCUMENTATION      *
   * INCLUDE TRADE SECRETS AND CONFIDENTIAL AND PROPRIETARY     *
   * PRODUCTS OF ANSYS, INC., ITS SUBSIDIARIES, OR LICENSORS.   *
   * The software products and documentation are furnished by   *
   * ANSYS, Inc. or its subsidiaries under a software license   *
   * agreement that contains provisions concerning              *
   * non-disclosure, copying, length and nature of use,         *
   * compliance with exporting laws, warranties, disclaimers,   *
   * limitations of liability, and remedies, and other          *
   * provisions.  The software products and documentation may be *
   * used, disclosed, transferred, or copied only in accordance  *
   * with the terms and conditions of that software license     *
   * agreement.                                                 *
*                                                              *
   * ANSYS, Inc. is a UL registered                             *
* ISO 9001:2015 company.                                        *
*                                                              *
***************************************************************
*                                                              *
   * This product is subject to U.S. laws governing export and  *
   * re-export.                                                 *
*                                                              *
   * For U.S. Government users, except as specifically granted  *
   * by the ANSYS, Inc. software license agreement, the use,    *
   * duplication, or disclosure by the United States Government  *
   * is subject to restrictions stated in the ANSYS, Inc.       *
   * software license agreement and FAR 12.212 (for non-DOD     *
   * licenses).                                                 *
*                                                              *
******************************************

******************** 2019 R2

Point Releases and Patches installed:

ANSYS, Inc.
Products 2019
R2 SpaceClaim
2019 R2
AIM 2019 R2
Live (includes
SpaceClaim)
2019 R2
Autodyn 2019
R2
CFD-Post only 2019 R2
CFX (includes
CFD-Post) 2019
R2 Chemkin
2019 R2
FENSAP-ICE 2019 R2
Fluent
(includes CFD-
Post) 2019 R2
Forte 2019 R2
Polyflow
(includes CFD-
Post) 2019 R2
TurboGrid 2019
R2
I
C
```

E
M
C
F
D
2
0
1
9
R
2
A
q
w
a
2
0
1
9
R
2
Customization Files for User
Programmable Features 2019 R2
Mechanical Products 2019 R2
Additive 2019 R2
Icepak
(includes CFD-
Post) 2019 R2
Viewer 2019 R2
ACIS Geometry
Interface 2019
R2 AutoCAD
Geometry
Interface 2019
R2
Catia, Version 5
Geometry Interface
2019 R2 Catia,
Version 6 Geometry
Interface 2019 R2
Creo Elements/Direct Modeling
Geometry Interface 2019 R2 Creo
Parametric Geometry Interface 2019
R2
Inventor
Geometry
Interface
2019 R2
JTOpen
Geometry
Interface
2019 R2 NX
Geometry
Interface
2019 R2
Parasolid
Geometry
Interface 2019
R2 Solid Edge
Geometry
Interface 2019
R2 SOLIDWORKS
Geometry
Interface 2019
R2 ANSYS, Inc.
License Manager
2019 R2

***** ANSYS COMMAND LINE
ARGUMENTS ***** BATCH MODE
REQUESTED (-b) = NOLIST
INPUT FILE COPY
MODE (-c) = COPY DISTRIBUTED MEMORY PARALLEL REQUESTED
2 PARALLEL PROCESSES REQUESTED WITH SINGLE
THREAD PER PROCESS TOTAL OF 2 CORES
REQUESTED
DESIGNXPLORER REQUESTED
INPUT FILE NAME = \\engrfs904v\VCL.userspace\kavach\Documents\Thesis Sections\Octagonal\V Stiff
Clay_ProjectScratch\ScrD3F9\dummy.dat OUTPUT FILE NAME = U:\Documents\Thesis Sections\Octagonal\V Stiff
Clay_ProjectScratch\ScrD3F9\solve.out

```
START-UP FILE MODE               = NOREAD
STOP FILE MODE                   = NOREAD

RELEASE= 2019 R2                 BUILD= 19.4      UP20190416 VERSION=WINDOWS x64
CURRENT JOBNAME=file0 17:45:10 APR 03,  2020 CP=  0.141


PARAMETER _DS_PROGRESS =        999.0000000

/INPUT FILE= ds.dat  LINE=          0



*** NOTE ***                               CP =       0.234 TIME= 17:45:11
The /CONFIG,NOELDB command is not valid in a Distributed ANSYS
solution. Command is ignored.

*GET _WALLSTRT FROM ACTI ITEM=TIME WALL VALUE= 17.7530556

TITLE=
Longer pile--Static Structural (B3)


SET PARAMETER DIMENSIONS ON _WB_PROJECTSCRATCH_DIR
TYPE=STRI  DIMENSIONS=          248        1        1

PARAMETER _WB_PROJECTSCRATCH_DIR(1) = U:\Documents\Thesis Sections\Octagonal\V Stiff Clay\_ProjectScratch\ScrD3F9\ SET

PARAMETER DIMENSIONS ON  _WB_SOLVERFILES_DIR
TYPE=STRI  DIMENSIONS=          248        1        1

PARAMETER _WB_SOLVERFILES_DIR(1) = U:\Documents\Thesis Sections\Octagonal\V Stiff Clay\Longer pile_files\dp0\SYS\MECH\ SET

PARAMETER DIMENSIONS ON  _WB_USERFILES_DIR
TYPE=STRI  DIMENSIONS=          248        1        1

PARAMETER _WB_USERFILES_DIR(1) = U:\Documents\Thesis Sections\Octagonal\V Stiff Clay\Longer pile_files\user_files\
--- Data in consistent BIN units. See Solving Units in the help system for more

U.S. CUSTOMARY INCH UNITS SPECIFIED FOR INTERNAL
LENGTH          = INCHES (IN)
MASS            = LBF-S**2/IN
TIME            = SECONDS (SEC)
TEMPERATURE = FAHRENHEIT
TOFFSET         = 460.0
FORCE           = LBF
HEAT            = IN-LBF
PRESSURE        = PSI (LBF/IN**2)
ENERGY          = IN-LBF
POWER           = IN-LBF/SEC

   INPUT UNITS ARE ALSO SET TO BIN

   *** ANSYS - ENGINEERING ANALYSIS SYSTEM RELEASE 2019 R2          19.4   ***
   DISTRIBUTED ANSYS Academic Research

   00427805 VERSION=WINDOWS x64 17:45:11 APR 03, 2020 CP=         0.234

   Longer pile--Static Structural (B3)



***** ANSYS ANALYSIS DEFINITION (PREP7) *****
*********** Nodes for the whole assembly ***********
*********** Nodes for all Remote Points ***********
*********** Elements for Body 1 "Surface Body(ACP (Pre))" ***********
*********** Send User Defined Coordinate System(s) ***********
*********** Set Reference Temperature ***********
*********** Send Materials ***********
*********** Send Sheet Properties ***********
*********** Sending Coordinate Systems for External Layered Section***********
*********** Sending Materials for External Layered Section***********
*********** Send External Layered Section Properties ***********
*********** Create Elastic Support ***********
*********** Define Force Using Surface Effect Elements ***********
*********** Create Remote Point "Internal Remote Point 2" ***********
*********** Create Remote Point "Internal Remote Point 2" ***********
*********** Create Remote Point "Internal Remote Point 2" ***********
*********** Create Remote Point "Internal Remote Point 2" ***********
*********** Create Remote Point "Internal Remote Point 2" ***********
*********** Create Remote Point "Internal Remote Point 2" ***********
*********** Create Remote Point "Internal Remote Point 2" ***********
*********** Create Remote Point "Internal Remote Point 2" ***********
*********** Create Remote Point "Internal Remote Point 2" ***********
*********** Create Remote Point "Internal Remote Point 2" ***********
*********** Create Remote Point "Internal Remote Point 2" ***********
*********** Create Remote Point "Internal Remote Point 2" ***********
*********** Create Remote Point "Internal Remote Point 2" ***********
*********** Create Remote Point "Internal Remote Point 2" ***********
*********** Create Remote Point "Internal Remote Point 2" ***********
*********** Create Remote Point "Internal Remote Point 2" ***********
*********** Create Remote Point "Internal Remote Point 2" ***********
*********** Create Remote Point "Internal Remote Point 2" ***********
*********** Create Remote Point "Internal Remote Point 2" ***********
*********** Create Remote Point "Internal Remote Point 2" ***********
*********** Create Remote Point "Internal Remote Point 2" ***********
*********** Create Remote Point "Internal Remote Point 2" ***********
*********** Create Remote Point "Internal Remote Point 2" ***********
*********** Create Remote Point "Internal Remote Point 2" ***********
*********** Create Remote Point "Internal Remote Point 2" ***********
*********** Create Remote Point "Internal Remote Point 2" ***********
*********** Create Remote Point "Internal Remote Point 2" ***********
*********** Create Remote Point "Internal Remote Point 2" ***********
*********** Create Remote Point "Internal Remote Point 2" ***********
*********** Create Remote Point "Internal Remote Point 2" ***********
*********** Create Remote Point "Internal Remote Point 2" ***********
```

```
*********** Create Remote Point "Internal Remote Point 2" ***********
*********** Create Remote Point "Internal Remote Point 2" ***********
*********** Create Remote Point "Internal Remote Point 2" ***********
*********** Create Remote Point "Internal Remote Point 2" ***********
*********** Create Remote Point "Internal Remote Point 2" ***********
```

```
*********** Create Remote Point "Internal Remote Point 2" ***********
*********** Create Remote Point "Internal Remote Point 2" ***********
*********** Create Remote Point "Internal Remote Point 2" ***********
*********** Create Remote Point "Internal Remote Point 2" ***********
*********** Create Remote Point "Internal Remote Point 2" ***********
*********** Create Remote Point "Internal Remote Point 2" ***********
*********** Create Remote Point "Internal Remote Point 2" ***********
*********** Create Remote Point "Internal Remote Point 2" ***********
*********** Create Remote Point "Internal Remote Point 2" ***********
*********** Create Remote Point "Internal Remote Point 2" ***********
*********** Create Remote Point "Internal Remote Point 2" ***********
*********** Create Remote Point "Internal Remote Point 2" ***********
*********** Create Remote Point "Internal Remote Point 2" ***********
*********** Create Remote Point "Internal Remote Point 2" ***********
*********** Create Remote Point "Internal Remote Point 2" ***********
*********** Create Remote Point "Internal Remote Point 2" ***********
*********** Create Remote Point "Internal Remote Point 2" ***********
*********** Create Remote Point "Internal Remote Point 2" ***********
*********** Create Remote Point "Internal Remote Point 2" ***********
*********** Create Remote Point "Internal Remote Point 2" ***********
*********** Create Remote Point "Internal Remote Point 2" ***********
*********** Create Remote Point "Internal Remote Point 2" ***********
*********** Create Remote Point "Internal Remote Point 2" ***********
*********** Create Remote Point "Internal Remote Point 2" ***********
*********** Create Remote Point "Internal Remote Point 2" ***********
*********** Create Remote Point "Internal Remote Point 2" ***********
*********** Create Remote Point "Internal Remote Point 2" ***********
*********** Create Remote Point "Internal Remote Point 2" ***********
*********** Create Remote Point "Internal Remote Point 2" ***********
*********** Create Remote Point "Internal Remote Point 2" ***********
*********** Create Remote Point "Internal Remote Point 2" ***********
*********** Create Remote Point "Internal Remote Point 2" ***********
*********** Create Remote Point "Internal Remote Point 2" ***********
*********** Create Remote Point "Internal Remote Point 2" ***********
*********** Create Remote Point "Internal Remote Point 2" ***********
*********** Create Remote Point "Internal Remote Point 2" ***********
*********** Create Remote Point "Internal Remote Point 2" ***********
*********** Create Remote Point "Internal Remote Point 2" ***********
*********** Create Remote Point "Internal Remote Point 2" ***********
*********** Create Remote Point "Internal Remote Point 2" ***********
*********** Create Remote Point "Internal Remote Point 2" ***********
*********** Create Remote Point "Internal Remote Point 2" ***********
*********** Create Remote Point "Internal Remote Point 2" ***********
*********** Create Spring Connection "Longitudinal - Ground To Surface Body(ACP
Real Constant Set For Above Spring Connection Is 165
*********** Create Spring Connection "Longitudinal - Ground To Surface Body(ACP
Real Constant Set For Above Spring Connection Is 166
*********** Create Spring Connection "Longitudinal - Ground To Surface Body(ACP
Real Constant Set For Above Spring Connection Is 167
*********** Create Spring Connection "Longitudinal - Ground To Surface Body(ACP
Real Constant Set For Above Spring Connection Is 168
*********** Create Spring Connection "Longitudinal - Ground To Surface Body(ACP
Real Constant Set For Above Spring Connection Is 169
*********** Create Spring Connection "Longitudinal - Ground To Surface Body(ACP
Real Constant Set For Above Spring Connection Is 170
*********** Create Spring Connection "Longitudinal - Ground To Surface Body(ACP
Real Constant Set For Above Spring Connection Is 171
*********** Create Spring Connection "Longitudinal - Ground To Surface Body(ACP
Real Constant Set For Above Spring Connection Is 172
*********** Create Spring Connection "Longitudinal - Ground To Surface Body(ACP
Real Constant Set For Above Spring Connection Is 173
*********** Create Spring Connection "Longitudinal - Ground To Surface Body(ACP
Real Constant Set For Above Spring Connection Is 174
*********** Create Spring Connection "Longitudinal - Ground To Surface Body(ACP
Real Constant Set For Above Spring Connection Is 175
*********** Create Spring Connection "Longitudinal - Ground To Surface Body(ACP
Real Constant Set For Above Spring Connection Is 176
*********** Create Spring Connection "Longitudinal - Ground To Surface Body(ACP
Real Constant Set For Above Spring Connection Is 177
*********** Create Spring Connection "Longitudinal - Ground To Surface Body(ACP
Real Constant Set For Above Spring Connection Is 178
*********** Create Spring Connection "Longitudinal - Ground To Surface Body(ACP
Real Constant Set For Above Spring Connection Is 179
*********** Create Spring Connection "Longitudinal - Ground To Surface Body(ACP
Real Constant Set For Above Spring Connection Is 180
*********** Create Spring Connection "Longitudinal - Ground To Surface Body(ACP
Real Constant Set For Above Spring Connection Is 181
*********** Create Spring Connection "Longitudinal - Ground To Surface Body(ACP
Real Constant Set For Above Spring Connection Is 182
*********** Create Spring Connection "Longitudinal - Ground To Surface Body(ACP
Real Constant Set For Above Spring Connection Is 183
*********** Create Spring Connection "Longitudinal - Ground To Surface Body(ACP
Real Constant Set For Above Spring Connection Is 184
*********** Create Spring Connection "Longitudinal - Ground To Surface Body(ACP
Real Constant Set For Above Spring Connection Is 185
*********** Create Spring Connection "Z Axis Spring" *********** Real
Constant Set For Above Spring Connection Is 186
*********** Create Spring Connection "Z Axis Spring 2" ***********
Real Constant Set For Above Spring Connection Is 187
*********** Create Spring Connection "Z Axis Spring 3" ***********
Real Constant Set For Above Spring Connection Is 188
*********** Create Spring Connection "Z Axis Spring 4" ***********
Real Constant Set For Above Spring Connection Is 189
*********** Create Spring Connection "Z Axis Spring 5" ***********
Real Constant Set For Above Spring Connection Is 190
*********** Create Spring Connection "Z Axis Spring 6" ***********
Real Constant Set For Above Spring Connection Is 191
*********** Create Spring Connection "Z Axis Spring 7" ***********
Real Constant Set For Above Spring Connection Is 192
*********** Create Spring Connection "Z Axis Spring 8" ***********
Real Constant Set For Above Spring Connection Is 193
*********** Create Spring Connection "Z Axis Spring 9" ***********
Real Constant Set For Above Spring Connection Is 194
*********** Create Spring Connection "Z Axis Spring 10" ***********
Real Constant Set For Above Spring Connection Is 195
*********** Create Spring Connection "Z Axis Spring 11" ***********
```

```
Real Constant Set For Above Spring Connection Is 196
*********** Create Spring Connection "Z Axis Spring 12" ***********
Real Constant Set For Above Spring Connection Is 197
*********** Create Spring Connection "Z Axis Spring 13" ***********
Real Constant Set For Above Spring Connection Is 198
```

```
*********** Create Spring Connection "Z Axis Spring 14" ***********
Real Constant Set For Above Spring Connection Is 199
*********** Create Spring Connection "Z Axis Spring 15" ***********
Real Constant Set For Above Spring Connection Is 200
*********** Create Spring Connection "Z Axis Spring 16" ***********
Real Constant Set For Above Spring Connection Is 201
*********** Create Spring Connection "Z Axis Spring 17" ***********
Real Constant Set For Above Spring Connection Is 202
*********** Create Spring Connection "Z Axis Spring 18" ***********
Real Constant Set For Above Spring Connection Is 203
*********** Create Spring Connection "Z Axis Spring 19" ***********
Real Constant Set For Above Spring Connection Is 204
*********** Create Spring Connection "Z Axis Spring 20" ***********
Real Constant Set For Above Spring Connection Is 205
*********** Create Spring Connection "Z Axis Spring 21" ***********
Real Constant Set For Above Spring Connection Is 206
*********** Create Spring Connection "Slip Resistance Spring" *********** Real
Constant Set For Above Spring Connection Is 207
*********** Create Spring Connection "Slip Resistance Spring 2" ***********
Real Constant Set For Above Spring Connection Is 208
*********** Create Spring Connection "Slip Resistance Spring 3" ***********
Real Constant Set For Above Spring Connection Is 209
*********** Create Spring Connection "Slip Resistance Spring 4" ***********
Real Constant Set For Above Spring Connection Is 210
*********** Create Spring Connection "Slip Resistance Spring 5" ***********
Real Constant Set For Above Spring Connection Is 211
*********** Create Spring Connection "Slip Resistance Spring 6" ***********
Real Constant Set For Above Spring Connection Is 212
*********** Create Spring Connection "Slip Resistance Spring 7" ***********
Real Constant Set For Above Spring Connection Is 213
*********** Create Spring Connection "Slip Resistance Spring 8" ***********
Real Constant Set For Above Spring Connection Is 214
*********** Create Spring Connection "Slip Resistance Spring 9" ***********
Real Constant Set For Above Spring Connection Is 215
*********** Create Spring Connection "Slip Resistance Spring 10" *********** Real
Constant Set For Above Spring Connection Is 216
*********** Create Spring Connection "Longitudinal - Ground To Surface Body(ACP
Real Constant Set For Above Spring Connection Is 217
*********** Create Spring Connection "End Bearing Spring" *********** Real
Constant Set For Above Spring Connection Is 218
*********** Create Spring Connection "Slip Resistance Spring 11" *********** Real
Constant Set For Above Spring Connection Is 219
*********** Create Spring Connection "Slip Resistance Spring 12" *********** Real
Constant Set For Above Spring Connection Is 220
*********** Create Spring Connection "Slip Resistance Spring 13" *********** Real
Constant Set For Above Spring Connection Is 221
*********** Create Spring Connection "Slip Resistance Spring 14" *********** Real
Constant Set For Above Spring Connection Is 222
*********** Create Spring Connection "Slip Resistance Spring 15" *********** Real
Constant Set For Above Spring Connection Is 223
*********** Create Spring Connection "Longitudinal - Ground To Surface Body(ACP
Real Constant Set For Above Spring Connection Is 224
*********** Create Spring Connection "Longitudinal - Ground To Surface Body(ACP
Real Constant Set For Above Spring Connection Is 225
*********** Create Spring Connection "Longitudinal - Ground To Surface Body(ACP
Real Constant Set For Above Spring Connection Is 226
*********** Create Spring Connection "Longitudinal - Ground To Surface Body(ACP
Real Constant Set For Above Spring Connection Is 227
*********** Create Spring Connection "Longitudinal - Ground To Surface Body(ACP
Real Constant Set For Above Spring Connection Is 228
*********** Create Spring Connection "Longitudinal - Ground To Surface Body(ACP
Real Constant Set For Above Spring Connection Is 229
*********** Create Spring Connection "Longitudinal - Ground To Surface Body(ACP
Real Constant Set For Above Spring Connection Is 230
*********** Create Spring Connection "Longitudinal - Ground To Surface Body(ACP
Real Constant Set For Above Spring Connection Is 231
*********** Create Spring Connection "Longitudinal - Ground To Surface Body(ACP
Real Constant Set For Above Spring Connection Is 232
*********** Create Spring Connection "Longitudinal - Ground To Surface Body(ACP
Real Constant Set For Above Spring Connection Is 233
*********** Create Spring Connection "Z Axis Spring 22" ***********
Real Constant Set For Above Spring Connection Is 234
*********** Create Spring Connection "Z Axis Spring 23" ***********
Real Constant Set For Above Spring Connection Is 235
*********** Create Spring Connection "Z Axis Spring 24" ***********
Real Constant Set For Above Spring Connection Is 236
*********** Create Spring Connection "Z Axis Spring 25" ***********
Real Constant Set For Above Spring Connection Is 237
*********** Create Spring Connection "Z Axis Spring 26" ***********
Real Constant Set For Above Spring Connection Is 238
*********** Create Spring Connection "Z Axis Spring 27" ***********
Real Constant Set For Above Spring Connection Is 239
*********** Create Spring Connection "Z Axis Spring 28" ***********
Real Constant Set For Above Spring Connection Is 240
*********** Create Spring Connection "Z Axis Spring 29" ***********
Real Constant Set For Above Spring Connection Is 241
*********** Create Spring Connection "Z Axis Spring 30" ***********
Real Constant Set For Above Spring Connection Is 242
*********** Create Spring Connection "Z Axis Spring 31" ***********
Real Constant Set For Above Spring Connection Is 243
*** Create a component for all grounded springs ***


***** ROUTINE COMPLETED *****  CP =           2.047


--- Number of total nodes = 9406
--- Number of contact elements = 19620
--- Number of spring elements = 0
--- Number of bearing elements = 0
--- Number of solid elements = 9216
--- Number of condensed parts = 0
--- Number of total elements = 29026

*GET _WALLBSOL FROM ACTI ITEM=TIME WALL VALUE= 17.7533333
****************************************************************************
```

```
*************************        SOLUTION       *********************************
*******************************************************************************

***** ANSYS SOLUTION ROUTINE  *****
```

```
PERFORM A STATIC ANALYSIS THIS
WILL BE A NEW ANALYSIS

USE SPARSE MATRIX DIRECT SOLVER

CONTACT INFORMATION PRINTOUT LEVEL          1

DO NOT COMBINE ELEMENT MATRIX FILES (.emat) AFTER DISTRIBUTED PARALLEL SOLUTION

DO NOT COMBINE ELEMENT SAVE DATA FILES (.esav) AFTER DISTRIBUTED PARALLEL SOLUTION

NLDIAG: Nonlinear diagnostics CONT option is set to ON.
Writing frequency : each ITERATION.

DEFINE RESTART CONTROL FOR LOADSTEP LAST
AT FREQUENCY OF LAST AND NUMBER FOR OVERWRITE IS       0

DELETE RESTART FILES OF ENDSTEP
****************************************************
****************** SOLVE FOR LS 1 OF 1 ****************

SELECT          FOR ITEM=TYPE COMPONENT=
IN RANGE             6 TO          6 STEP          1

32  ELEMENTS (OF                 29026 DEFINED) SELECTED BY ESEL COMMAND.

SELECT         ALL NODES HAVING ANY ELEMENT IN ELEMENT SET.

32 NODES (OF                  9406 DEFINED) SELECTED FROM
32 SELECTED ELEMENTS BY NSLE COMMAND.

SPECIFIED SURFACE LOAD PRES FOR ALL SELECTED ELEMENTS LKEY = 1 KVAL = 1
VALUES =            0.0000         0.0000         0.0000         0.0000

SPECIFIED SURFACE LOAD PRES FOR ALL SELECTED ELEMENTS LKEY = 2 KVAL = 1
VALUES =           -2500.0        -2500.0        -2500.0        -2500.0

SPECIFIED SURFACE LOAD PRES FOR ALL SELECTED ELEMENTS LKEY = 3 KVAL = 1
VALUES =            0.0000         0.0000         0.0000         0.0000

ALL SELECT FOR ITEM=NODE COMPONENT=
IN RANGE             1 TO      45191 STEP          1

9406  NODES (OF                9406 DEFINED) SELECTED BY NSEL COMMAND.

ALL SELECT FOR ITEM=ELEM COMPONENT=
IN RANGE             1 TO      57941 STEP          1

29026  ELEMENTS (OF              29026 DEFINED) SELECTED BY ESEL  COMMAND.
*** Set Displacements ***
CMBLOCK read of NODE component _CM276UX_XP completed

SELECT         COMPONENT _CM276UX_XP

SPECIFIED CONSTRAINT UX  FOR SELECTED NODES               1 TO       45191 BY           1
REAL=  4.00000000          IMAG=  0.00000000

ALL SELECT FOR ITEM=NODE COMPONENT=
IN RANGE             1 TO      45191 STEP          1

9406  NODES (OF                9406 DEFINED) SELECTED BY NSEL  COMMAND.
*** Component For All Non-Zero UX Displacements ***

SELECT         COMPONENT _CM276UX_XP

DEFINITION OF COMPONENT = _DISPNONZEROUX ENTITY=NODE

ALL SELECT FOR ITEM=NODE COMPONENT=
IN RANGE             1 TO      45191 STEP          1

9406  NODES (OF                9406 DEFINED) SELECTED BY NSEL COMMAND.

PRINTOUT RESUMED BY /GOP

USE AUTOMATIC TIME STEPPING THIS LOAD STEP

USE          1 SUBSTEPS INITIALLY THIS LOAD STEP FOR ALL  DEGREES OF FREEDOM
FOR AUTOMATIC TIME STEPPING:
USE          10 SUBSTEPS AS A MAXIMUM
USE           1 SUBSTEPS AS A MINIMUM

TIME=  1.0000

ERASE THE CURRENT DATABASE OUTPUT CONTROL TABLE.


WRITE ALL ITEMS TO THE DATABASE WITH A FREQUENCY OF NONE FOR
ALL APPLICABLE ENTITIES

WRITE NSOL ITEMS TO THE DATABASE WITH A FREQUENCY OF ALL FOR
ALL APPLICABLE ENTITIES

WRITE RSOL ITEMS TO THE DATABASE WITH A FREQUENCY OF ALL FOR
ALL APPLICABLE ENTITIES

WRITE EANG ITEMS TO THE DATABASE WITH A FREQUENCY OF ALL FOR
ALL APPLICABLE ENTITIES

WRITE ETMP ITEMS TO THE DATABASE WITH A FREQUENCY OF ALL FOR
ALL APPLICABLE ENTITIES

WRITE VENG ITEMS TO THE DATABASE WITH A FREQUENCY OF ALL FOR
ALL APPLICABLE ENTITIES

WRITE STRS ITEMS TO THE DATABASE WITH A FREQUENCY OF ALL FOR
```

ALL APPLICABLE ENTITIES

WRITE EPEL ITEMS TO THE DATABASE WITH A FREQUENCY OF ALL FOR
ALL APPLICABLE ENTITIES

```
WRITE EPPL ITEMS TO THE DATABASE WITH A FREQUENCY OF ALL FOR
ALL APPLICABLE ENTITIES

WRITE CONT ITEMS TO THE DATABASE WITH A FREQUENCY OF ALL FOR
ALL APPLICABLE ENTITIES

PRINTOUT RESUMED BY /GOP

WRITE MISC ITEMS TO THE DATABASE WITH A FREQUENCY OF ALL
FOR THE ENTITIES DEFINED BY COMPONENT _ELMISC

*GET  ANSINTER_  FROM ACTI  ITEM=INT           VALUE=  0.00000000

*IF  ANSINTER_                           ( =   0.00000     )  NE
0                                        ( =   0.00000     )  THEN

*ENDIF

*** NOTE ***                             CP =       2.125 TIME= 17:45:12
The automatic domain decomposition logic has selected the MESH domain
decomposition method with 2 processes per solution.

*****  ANSYS SOLVE       COMMAND  *****

*** WARNING ***                          CP =       2.125 TIME= 17:45:12
Element shape checking is currently inactive. Issue SHPP,ON or
SHPP,WARN to reactivate, if desired.

*** NOTE ***                             CP =       2.188 TIME= 17:45:12
The model data was checked and warning messages were found.
Please review output or errors file ( U:\Documents\Thesis
Sections\Octagonal\V Stiff Clay\_ProjectScratch\ScrD3F9\file0.err )
for these warning messages.

*** SELECTION OF ELEMENT TECHNOLOGIES FOR APPLICABLE ELEMENTS ***
--- GIVE SUGGESTIONS AND RESET THE KEY OPTIONS ---

ELEMENT  TYPE  1  IS  SHELL181.  IT  IS  ASSOCIATED  WITH  ELASTOPLASTIC
MATERIALS ONLY. KEYOPT(8) IS ALREADY SET AS SUGGESTED. KEYOPT(3)=2 IS
SUGGESTED FOR HIGHER ACCURACY OF MEMBRANE STRESSES; OTHERWISE,
KEYOPT(3)=0 IS SUGGESTED. KEYOPT(3) CAN NOT BE RESET HERE. PLEASE RESET IT
MANUALLY IF NECESSARY.


*** ANSYS - ENGINEERING ANALYSIS SYSTEM RELEASE 2019 R2             19.4     ***
DISTRIBUTED ANSYS Academic Research

00427805 VERSION=WINDOWS x64 17:45:12 APR 03, 2020 CP=           2.219

Longer pile--Static Structural (B3)


S O L U T I O N O P T I O N S PROBLEM DIMENSIONALITY. .

. . . . . . . . . . .3-D
DEGREES OF FREEDOM. . . . . . UX UY UZ ROTX ROTY ROTZ
ANALYSIS TYPE . . . . . . . . . . . . . . . . .STATIC (STEADY-STATE)
OFFSET TEMPERATURE FROMABSOLUTE ZERO ...............459.67
EQUATION SOLVER OPTION............................SPARSE
NEWTON-RAPHSON OPTION . . . . . . . . . . . . .PROGRAM CHOSEN
GLOBALLY ASSEMBLED MATRIX .........................SYMMETRIC

*** NOTE ***                             CP =       2.250 TIME= 17:45:12
Poisson's ratio PR input has been converted to NU input.

*** WARNING ***                          CP =       2.281 TIME= 17:45:12
Material number 165 (used by element 38057) should normally have at
least one MP or one TB type command associated with it. Output of
energy by material may not be available.

*** NOTE ***                             CP =       2.375 TIME= 17:45:12
The step data was checked and warning messages were found.
Please review output or errors file ( U:\Documents\Thesis
Sections\Octagonal\V Stiff Clay\_ProjectScratch\ScrD3F9\file0.err )
for these warning messages.

*** NOTE ***                             CP =       2.375 TIME= 17:45:12
This nonlinear analysis defaults to using the full Newton-Raphson
solution procedure. This can be modified using the NROPT command.

*** NOTE ***                             CP =       2.438 TIME= 17:45:12
Internal nodes from 45192 to 45270 are created.
79 internal nodes are used for handling degrees of freedom on pilot
nodes of rigid target surfaces.

*** NOTE ***                             CP =       2.531 TIME= 17:45:12
Internal nodes from 45192 to 45270 are created.
79 internal nodes are used for handling degrees of freedom on pilot
nodes of rigid target surfaces.
*WARNING*: Node 7686 has been used on different contact pairs (real ID
7 & 9). These two pairs will be merged. Please check the model
carefully.
*WARNING*: Some MPC/Lagrange based elements (e.g.47459) in real
constant set 7 overlap with other MPC/Lagrange based elements
(e.g.51362) in real constant set 79 which can cause overconstraint.

*** NOTE ***                             CP =       3.359 TIME= 17:45:13
Rigid-constraint surface identified by real constant set 7 and contact
element type 7 has been set up. The degrees of freedom of the rigid
surface are driven by the pilot node 45055 which connects to other
element 38067. Internal MPC will be built.
This pair will be merged with other pair defined by real constant set 163.
The used degrees of freedom set is UX UY UZ ROTX ROTY ROTZ
*WARNING*: Certain contact elements (for example 47530&51820) overlap each
```

other.
****

```
*** NOTE ***                            CP =       3.359 TIME= 17:45:13
Rigid-constraint surface identified by real constant set 9 and contact
element type 9 has been set up. The degrees of freedom of the rigid
surface are driven by the pilot node 45057 which connects to other
element 38068. Internal MPC will be built.
This pair will be merged with other pair defined by real constant set 81.
The used degrees of freedom set is UX UY UZ ROTX ROTY ROTZ
*WARNING*: Certain contact elements (for example 47605&49111) overlap each
other.
****************************************


*** NOTE ***                            CP =       3.359 TIME= 17:45:13
Rigid-constraint surface identified by real constant set 11 and contact
element type 11 has been set up. The degrees of freedom of the rigid
surface are driven by the pilot node 45059 which connects to other
element 38069. Internal MPC will be built.
This pair will be merged with other pair defined by real constant set 83.
The used degrees of freedom set is UX UY UZ ROTX ROTY ROTZ
*WARNING*: Certain contact elements (for example 47680&49195) overlap each
other.
****************************************


*** NOTE ***                            CP =       3.359 TIME= 17:45:13
Rigid-constraint surface identified by real constant set 13 and contact
element type 13 has been set up. The degrees of freedom of the rigid
surface are driven by the pilot node 45061 which connects to other
element 38070. Internal MPC will be built.
This pair will be merged with other pair defined by real constant set 83.
The used degrees of freedom set is UX UY UZ ROTX ROTY ROTZ
*WARNING*: Certain contact elements (for example 47755&49264) overlap each
other.
****************************************


*** NOTE ***                            CP =       3.359 TIME= 17:45:13
Rigid-constraint surface identified by real constant set 15 and contact
element type 15 has been set up. The degrees of freedom of the rigid
surface are driven by the pilot node 45063 which connects to other
element 38071. Internal MPC will be built.
This pair will be merged with other pair defined by real constant set 85.
The used degrees of freedom set is UX UY UZ ROTX ROTY ROTZ
*WARNING*: Certain contact elements (for example 47830&52256) overlap each
other.
****************************************


*** NOTE ***                            CP =       3.359 TIME= 17:45:13
Rigid-constraint surface identified by real constant set 17 and contact
element type 17 has been set up. The degrees of freedom of the rigid
surface are driven by the pilot node 45065 which connects to other
element 38072. Internal MPC will be built.
This pair will be merged with other pair defined by real constant set 85.
The used degrees of freedom set is UX UY UZ ROTX ROTY ROTZ
*WARNING*: Certain contact elements (for example 47907&49417) overlap each
other.
****************************************


*** NOTE ***                            CP =       3.359 TIME= 17:45:13
Rigid-constraint surface identified by real constant set 19 and contact
element type 19 has been set up. The degrees of freedom of the rigid
surface are driven by the pilot node 45067 which connects to other
element 38073. Internal MPC will be built.
This pair will be merged with other pair defined by real constant set 87.
The used degrees of freedom set is UX UY UZ ROTX ROTY ROTZ
*WARNING*: Certain contact elements (for example 47982&52625) overlap each
other.
****************************************


*** NOTE ***                            CP =       3.359 TIME= 17:45:13
Rigid-constraint surface identified by real constant set 21 and contact
element type 21 has been set up. The degrees of freedom of the rigid
surface are driven by the pilot node 45069 which connects to other
element 38074. Internal MPC will be built.
This pair will be merged with other pair defined by real constant set 87.
The used degrees of freedom set is UX UY UZ ROTX ROTY ROTZ
*WARNING*: Certain contact elements (for example 48057&49570) overlap each
other.
****************************************


*** NOTE ***                            CP =       3.359 TIME= 17:45:13
Rigid-constraint surface identified by real constant set 23 and contact
element type 23 has been set up. The degrees of freedom of the rigid
surface are driven by the pilot node 45071 which connects to other
element 38075. Internal MPC will be built.
This pair will be merged with other pair defined by real constant set 89.
The used degrees of freedom set is UX UY UZ ROTX ROTY ROTZ
*WARNING*: Certain contact elements (for example 48132&52996) overlap each
other.
****************************************


*** NOTE ***                            CP =       3.359 TIME= 17:45:13
Rigid-constraint surface identified by real constant set 25 and contact
element type 25 has been set up. The degrees of freedom of the rigid
surface are driven by the pilot node 45073 which connects to other
element 38076. Internal MPC will be built.
This pair will be merged with other pair defined by real constant set 91.
```

```
The used degrees of freedom set is UX UY UZ ROTX ROTY ROTZ
*WARNING*: Certain contact elements (for example 48211&53458) overlap each
other.
****************************************


*** NOTE ***                            CP =       3.359 TIME= 17:45:13
Rigid-constraint surface identified by real constant set 27 and contact
element type 27 has been set up. The degrees of freedom of the rigid
surface are driven by the pilot node 45075 which connects to other
element 38077. Internal MPC will be built.
This pair will be merged with other pair defined by real constant set 113.
The used degrees of freedom set is UX UY UZ ROTX ROTY ROTZ
*WARNING*: Certain contact elements (for example 48288&53759) overlap each
other.
****************************************


*** NOTE ***                            CP =       3.359 TIME= 17:45:13
Rigid-constraint surface identified by real constant set 29 and contact
element type 29 has been set up. The degrees of freedom of the rigid
surface are driven by the pilot node 45077 which connects to other
element 38078. Internal MPC will be built.
This pair will be merged with other pair defined by real constant set 95.
The used degrees of freedom set is UX UY UZ ROTX ROTY ROTZ
*WARNING*: Certain contact elements (for example 48329&50054) overlap each
other.
****************************************


*** NOTE ***                            CP =       3.359 TIME= 17:45:13
Rigid-constraint surface identified by real constant set 31 and contact
element type 31 has been set up. The degrees of freedom of the rigid
surface are driven by the pilot node 45079 which connects to other
element 38079. Internal MPC will be built.
This pair will be merged with other pair defined by real constant set 97.
The used degrees of freedom set is UX UY UZ ROTX ROTY ROTZ
*WARNING*: Certain contact elements (for example 48407&50090) overlap each
other.
****************************************


*** NOTE ***                            CP =       3.359 TIME= 17:45:13
Rigid-constraint surface identified by real constant set 33 and contact
element type 33 has been set up. The degrees of freedom of the rigid
surface are driven by the pilot node 45081 which connects to other
element 38080. Internal MPC will be built.
This pair will be merged with other pair defined by real constant set 99.
The used degrees of freedom set is UX UY UZ ROTX ROTY ROTZ
*WARNING*: Certain contact elements (for example 48482&50421) overlap each
other.
****************************************


*** NOTE ***                            CP =       3.359 TIME= 17:45:13
Rigid-constraint surface identified by real constant set 35 and contact
element type 35 has been set up. The degrees of freedom of the rigid
surface are driven by the pilot node 45083 which connects to other
element 38081. Internal MPC will be built.
This pair will be merged with other pair defined by real constant set 103.
The used degrees of freedom set is UX UY UZ ROTX ROTY ROTZ
*WARNING*: Certain contact elements (for example 48557&50462) overlap each
other.
****************************************


*** NOTE ***                            CP =       3.359 TIME= 17:45:13
Rigid-constraint surface identified by real constant set 37 and contact
element type 37 has been set up. The degrees of freedom of the rigid
surface are driven by the pilot node 45085 which connects to other
element 38082. Internal MPC will be built.
This pair will be merged with other pair defined by real constant set 125.
The used degrees of freedom set is UX UY UZ ROTX ROTY ROTZ
*WARNING*: Certain contact elements (for example 48631&50791) overlap each
other.
****************************************


*** NOTE ***                            CP =       3.359 TIME= 17:45:13
Rigid-constraint surface identified by real constant set 39 and contact
element type 39 has been set up. The degrees of freedom of the rigid
surface are driven by the pilot node 45087 which connects to other
element 38083. Internal MPC will be built.
This pair will be merged with other pair defined by real constant set 147.
The used degrees of freedom set is UX UY UZ ROTX ROTY ROTZ
*WARNING*: Certain contact elements (for example 48708&50834) overlap each
other.
****************************************


*** NOTE ***                            CP =       3.359 TIME= 17:45:13
Rigid-constraint surface identified by real constant set 41 and contact
element type 41 has been set up. The degrees of freedom of the rigid
surface are driven by the pilot node 45089 which connects to other
element 38084. Internal MPC will be built.
This pair will be merged with other pair defined by real constant set 157.
The used degrees of freedom set is UX UY UZ ROTX ROTY ROTZ
*WARNING*: Certain contact elements (for example 48782&51163) overlap each
other.
****************************************


*** NOTE ***                            CP =       3.359 TIME= 17:45:13
```

```
Rigid-constraint surface identified by real constant set 43 and contact
element type 43 has been set up. The degrees of freedom of the rigid
surface are driven by the pilot node 45091 which connects to other
element 38085. Internal MPC will be built.
This pair will be merged with other pair defined by real constant set 159.
The used degrees of freedom set is UX UY UZ ROTX ROTY ROTZ
*WARNING*: Certain contact elements (for example 48857&51199) overlap each
other.
****************************************


*** NOTE ***                            CP =       3.359 TIME= 17:45:13
Rigid-constraint surface identified by real constant set 45 and contact
element type 45 has been set up. The degrees of freedom of the rigid
surface are driven by the pilot node 45093 which connects to other
element 38086. Internal MPC will be built.
This pair will be merged with other pair defined by real constant set 161.
The used degrees of freedom set is UX UY UZ ROTX ROTY ROTZ
*WARNING*: Certain contact elements (for example 48932&51534) overlap each
other.
****************************************


*** NOTE ***                            CP =       3.359 TIME= 17:45:13
Rigid-constraint surface identified by real constant set 47 and contact
element type 47 has been set up. The degrees of freedom of the rigid
surface are driven by the pilot node 45095 which connects to other
element 38087. Internal MPC will be built.
This pair will be merged with other pair defined by real constant set 163.
The used degrees of freedom set is UX UY UZ ROTX ROTY ROTZ
*WARNING*: Certain contact elements (for example 49006&51570) overlap each
other.
****************************************


*** NOTE ***                            CP =       3.359 TIME= 17:45:13
Rigid-constraint surface identified by real constant set 49 and contact
element type 49 has been set up. The degrees of freedom of the rigid
surface are driven by the pilot node 45097 which connects to other
element 38088. Internal MPC will be built.
This pair will be merged with other pair defined by real constant set 81.
The used degrees of freedom set is UX UY UZ ROTX ROTY ROTZ
*WARNING*: Certain contact elements (for example 49083&49133) overlap each
other.
****************************************


*** NOTE ***                            CP =       3.359 TIME= 17:45:13
Rigid-constraint surface identified by real constant set 51 and contact
element type 51 has been set up. The degrees of freedom of the rigid
surface are driven by the pilot node 45099 which connects to other
element 38089. Internal MPC will be built.
This pair will be merged with other pair defined by real constant set 81.
The used degrees of freedom set is UX UY UZ ROTX ROTY ROTZ
*WARNING*: Certain contact elements (for example 49154&49173) overlap each
other.
****************************************


*** NOTE ***                            CP =       3.359 TIME= 17:45:13
Rigid-constraint surface identified by real constant set 53 and contact
element type 53 has been set up. The degrees of freedom of the rigid
surface are driven by the pilot node 45101 which connects to other
element 38090. Internal MPC will be built.
This pair will be merged with other pair defined by real constant set 83.
The used degrees of freedom set is UX UY UZ ROTX ROTY ROTZ
*WARNING*: Certain contact elements (for example 49222&49286) overlap each
other.
****************************************


*** NOTE ***                            CP =       3.359 TIME= 17:45:13
Rigid-constraint surface identified by real constant set 55 and contact
element type 55 has been set up. The degrees of freedom of the rigid
surface are driven by the pilot node 45103 which connects to other
element 38091. Internal MPC will be built.
This pair will be merged with other pair defined by real constant set 83.
The used degrees of freedom set is UX UY UZ ROTX ROTY ROTZ
*WARNING*: Certain contact elements (for example 49286&49201) overlap each
other.
****************************************


*** NOTE ***                            CP =       3.359 TIME= 17:45:13
Rigid-constraint surface identified by real constant set 57 and contact
element type 57 has been set up. The degrees of freedom of the rigid
surface are driven by the pilot node 45105 which connects to other
element 38092. Internal MPC will be built.
This pair will be merged with other pair defined by real constant set 85.
The used degrees of freedom set is UX UY UZ ROTX ROTY ROTZ
*WARNING*: Certain contact elements (for example 49374&49429) overlap each
other.
****************************************


*** NOTE ***                            CP =       3.359 TIME= 17:45:13
Rigid-constraint surface identified by real constant set 59 and contact
element type 59 has been set up. The degrees of freedom of the rigid
surface are driven by the pilot node 45107 which connects to other
element 38093. Internal MPC will be built.
This pair will be merged with other pair defined by real constant set 85.
The used degrees of freedom set is UX UY UZ ROTX ROTY ROTZ
```

```
*WARNING*: Certain contact elements (for example 49458&49508) overlap each
other.
****************************************


*** NOTE ***                            CP =       3.359 TIME= 17:45:13
Rigid-constraint surface identified by real constant set 61 and contact
element type 61 has been set up. The degrees of freedom of the rigid
surface are driven by the pilot node 45109 which connects to other
element 38094. Internal MPC will be built.
This pair will be merged with other pair defined by real constant set 87.
The used degrees of freedom set is UX UY UZ ROTX ROTY ROTZ
*WARNING*: Certain contact elements (for example 49529&49548) overlap each
other.
****************************************


*** NOTE ***                            CP =       3.359 TIME= 17:45:13
Rigid-constraint surface identified by real constant set 63 and contact
element type 63 has been set up. The degrees of freedom of the rigid
surface are driven by the pilot node 45111 which connects to other
element 38095. Internal MPC will be built.
This pair will be merged with other pair defined by real constant set 87.
The used degrees of freedom set is UX UY UZ ROTX ROTY ROTZ
*WARNING*: Certain contact elements (for example 49597&49661) overlap each
other.
****************************************


*** NOTE ***                            CP =       3.359 TIME= 17:45:13
Rigid-constraint surface identified by real constant set 65 and contact
element type 65 has been set up. The degrees of freedom of the rigid
surface are driven by the pilot node 45113 which connects to other
element 38096. Internal MPC will be built.
This pair will be merged with other pair defined by real constant set 89.
The used degrees of freedom set is UX UY UZ ROTX ROTY ROTZ
*WARNING*: Certain contact elements (for example 49661&49576) overlap each
other.
****************************************


*** NOTE ***                            CP =       3.359 TIME= 17:45:13
Rigid-constraint surface identified by real constant set 67 and contact
element type 67 has been set up. The degrees of freedom of the rigid
surface are driven by the pilot node 45115 which connects to other
element 38097. Internal MPC will be built.
This pair will be merged with other pair defined by real constant set 91.
The used degrees of freedom set is UX UY UZ ROTX ROTY ROTZ
*WARNING*: Certain contact elements (for example 49756&53423) overlap each
other.
****************************************


*** NOTE ***                            CP =       3.359 TIME= 17:45:13
Rigid-constraint surface identified by real constant set 69 and contact
element type 69 has been set up. The degrees of freedom of the rigid
surface are driven by the pilot node 45117 which connects to other
element 38098. Internal MPC will be built.
This pair will be merged with other pair defined by real constant set 135.
The used degrees of freedom set is UX UY UZ ROTX ROTY ROTZ
*WARNING*: Certain contact elements (for example 49833&54353) overlap each
other.
****************************************


*** NOTE ***                            CP =       3.359 TIME= 17:45:13
Rigid-constraint surface identified by real constant set 71 and contact
element type 71 has been set up. The degrees of freedom of the rigid
surface are driven by the pilot node 45119 which connects to other
element 38099. Internal MPC will be built.
This pair will be merged with other pair defined by real constant set 99.
The used degrees of freedom set is UX UY UZ ROTX ROTY ROTZ
*WARNING*: Certain contact elements (for example 50205&48465) overlap each
other.
****************************************


*** NOTE ***                            CP =       3.359 TIME= 17:45:13
Rigid-constraint surface identified by real constant set 73 and contact
element type 73 has been set up. The degrees of freedom of the rigid
surface are driven by the pilot node 45121 which connects to other
element 38100. Internal MPC will be built.
This pair will be merged with other pair defined by real constant set 125.
The used degrees of freedom set is UX UY UZ ROTX ROTY ROTZ
*WARNING*: Certain contact elements (for example 50566&48618) overlap each
other.
****************************************


*** NOTE ***                            CP =       3.359 TIME= 17:45:13
Rigid-constraint surface identified by real constant set 75 and contact
element type 75 has been set up. The degrees of freedom of the rigid
surface are driven by the pilot node 45123 which connects to other
element 38101. Internal MPC will be built.
This pair will be merged with other pair defined by real constant set 157.
The used degrees of freedom set is UX UY UZ ROTX ROTY ROTZ
*WARNING*: Certain contact elements (for example 50938&48759) overlap each
other.
****************************************


*** NOTE ***                            CP =       3.359 TIME= 17:45:13
Rigid-constraint surface identified by real constant set 77 and
```

```
contact element type 77 has been set up. The degrees of freedom of the
rigid surface are driven by the pilot node 45125 which connects to other
element 38102. Internal MPC will be built.
This pair will be merged with other pair defined by real constant set 161.
The used degrees of freedom set is UX UY UZ ROTX ROTY ROTZ
*WARNING*: Certain contact elements (for example 51308&48913) overlap each
other.
****************************************


*** NOTE ***                            CP =       3.359 TIME= 17:45:13
Rigid-constraint surface identified by real constant set 79 and contact
element type 79 has been set up. The degrees of freedom of the rigid
surface are driven by the pilot node 45127 which connects to other
element 38103. Internal MPC will be built.
This pair will be merged with other pair defined by real constant set 163.
The used degrees of freedom set is UX UY UZ ROTX ROTY ROTZ
*WARNING*: Certain contact elements (for example 51685&49068) overlap each
other.
****************************************


*** NOTE ***                            CP =       3.359 TIME= 17:45:13
Rigid-constraint surface identified by real constant set 81 and contact
element type 81 has been set up. The degrees of freedom of the rigid
surface are driven by the pilot node 45129 which connects to other
element 38104. Internal MPC will be built.
This pair will be merged with other pair defined by real constant set 53.
The used degrees of freedom set is UX UY UZ ROTX ROTY ROTZ
*WARNING*: Certain contact elements (for example 51952&52262) overlap each
other.
****************************************


*** NOTE ***                            CP =       3.359 TIME= 17:45:13
Rigid-constraint surface identified by real constant set 83 and contact
element type 83 has been set up. The degrees of freedom of the rigid
surface are driven by the pilot node 45131 which connects to other
element 38105. Internal MPC will be built.
This pair will be merged with other pair defined by real constant set 57.
The used degrees of freedom set is UX UY UZ ROTX ROTY ROTZ
*WARNING*: Certain contact elements (for example 52262&51889) overlap each
other.
****************************************


*** NOTE ***                            CP =       3.375 TIME= 17:45:13
Rigid-constraint surface identified by real constant set 85 and contact
element type 85 has been set up. The degrees of freedom of the rigid
surface are driven by the pilot node 45133 which connects to other
element 38106. Internal MPC will be built.
This pair will be merged with other pair defined by real constant set 61.
The used degrees of freedom set is UX UY UZ ROTX ROTY ROTZ
*WARNING*: Certain contact elements (for example 52627&52931) overlap each
other.
****************************************


*** NOTE ***                            CP =       3.375 TIME= 17:45:13
Rigid-constraint surface identified by real constant set 87 and contact
element type 87 has been set up. The degrees of freedom of the rigid
surface are driven by the pilot node 45135 which connects to other
element 38107. Internal MPC will be built.
This pair will be merged with other pair defined by real constant set 65.
The used degrees of freedom set is UX UY UZ ROTX ROTY ROTZ
*WARNING*: Certain contact elements (for example 53069&53375) overlap each
other.
****************************************


*** NOTE ***                            CP =       3.375 TIME= 17:45:13
Rigid-constraint surface identified by real constant set 89 and contact
element type 89 has been set up. The degrees of freedom of the rigid
surface are driven by the pilot node 45137 which connects to other
element 38108. Internal MPC will be built.
This pair will be merged with other pair defined by real constant set 91.
The used degrees of freedom set is UX UY UZ ROTX ROTY ROTZ
*WARNING*: Certain contact elements (for example 53538&49818) overlap each
other.
****************************************


*** NOTE ***                            CP =       3.375 TIME= 17:45:13
Rigid-constraint surface identified by real constant set 91 and contact
element type 91 has been set up. The degrees of freedom of the rigid
surface are driven by the pilot node 45139 which connects to other
element 38109. Internal MPC will be built.
This pair will be merged with other pair defined by real constant set 135.
The used degrees of freedom set is UX UY UZ ROTX ROTY ROTZ
*WARNING*: Certain contact elements (for example 53910&54373) overlap each
other.
****************************************


*** NOTE ***                            CP =       3.375 TIME= 17:45:13
Rigid-constraint surface identified by real constant set 93 and contact
element type 93 has been set up. The degrees of freedom of the rigid
surface are driven by the pilot node 45141 which connects to other
element 38110. Internal MPC will be built.
This pair will be merged with other pair defined by real constant set 95.
The used degrees of freedom set is UX UY UZ ROTX ROTY ROTZ
*WARNING*: Certain contact elements (for example 53943&48296) overlap
```

```
each other.
****************************************


*** NOTE ***                            CP =       3.375 TIME= 17:45:13
Rigid-constraint surface identified by real constant set 95 and contact
element type 95 has been set up. The degrees of freedom of the rigid
surface are driven by the pilot node 45035 which connects to other
element 38057. Internal MPC will be built.
This pair will be merged with other pair defined by real constant set 93.
The used degrees of freedom set is UX UY UZ ROTX ROTY ROTZ
*WARNING*: Certain contact elements (for example 53980&49967) overlap each
other.
****************************************


*** NOTE ***                            CP =       3.375 TIME= 17:45:13
Rigid-constraint surface identified by real constant set 97 and contact
element type 97 has been set up. The degrees of freedom of the rigid
surface are driven by the pilot node 45037 which connects to other
element 38058. Internal MPC will be built.
This pair will be merged with other pair defined by real constant set 71.
The used degrees of freedom set is UX UY UZ ROTX ROTY ROTZ
*WARNING*: Certain contact elements (for example 54044&54094) overlap each
other.
****************************************


*** NOTE ***                            CP =       3.375 TIME= 17:45:13
Rigid-constraint surface identified by real constant set 99 and contact
element type 99 has been set up. The degrees of freedom of the rigid
surface are driven by the pilot node 45039 which connects to other
element 38059. Internal MPC will be built.
This pair will be merged with other pair defined by real constant set 33.
The used degrees of freedom set is UX UY UZ ROTX ROTY ROTZ
*WARNING*: Certain contact elements (for example 54128&50261) overlap each
other.
****************************************


*** NOTE ***                            CP =       3.375 TIME= 17:45:13
Rigid-constraint surface identified by real constant set 101 and
contact element type 101 has been set up. The degrees of freedom of the
rigid surface are driven by the pilot node 45143 which connects to other
element 38114. Internal MPC will be built.
This pair will be merged with other pair defined by real constant set 137.
The used degrees of freedom set is UX UY UZ ROTX ROTY ROTZ
*WARNING*: Certain contact elements (for example 54505&54917) overlap each
other.
****************************************


*** NOTE ***                            CP =       3.375 TIME= 17:45:13
Rigid-constraint surface identified by real constant set 103 and
contact element type 103 has been set up. The degrees of freedom of the
rigid surface are driven by the pilot node 45041 which connects to other
element 38060. Internal MPC will be built.
This pair will be merged with other pair defined by real constant set 73.
The used degrees of freedom set is UX UY UZ ROTX ROTY ROTZ
*WARNING*: Certain contact elements (for example 54569&56550) overlap each
other.
****************************************


*** NOTE ***                            CP =       3.375 TIME= 17:45:13
Rigid-constraint surface identified by real constant set 105 and
contact element type 105 has been set up. The degrees of freedom of the
rigid surface are driven by the pilot node 45145 which connects to other
element 38118. Internal MPC will be built.
This pair will be merged with other pair defined by real constant set 139.
The used degrees of freedom set is UX UY UZ ROTX ROTY ROTZ
*WARNING*: Certain contact elements (for example 54921&54501) overlap each
other.
****************************************


*** NOTE ***                            CP =       3.375 TIME= 17:45:13
Rigid-constraint surface identified by real constant set 107 and
contact element type 107 has been set up. The degrees of freedom of the
rigid surface are driven by the pilot node 45147 which connects to other
element 38122. Internal MPC will be built.
This pair will be merged with other pair defined by real constant set 145.
The used degrees of freedom set is UX UY UZ ROTX ROTY ROTZ
*WARNING*: Certain contact elements (for example 55146&55450) overlap each
other.
****************************************


*** NOTE ***                            CP =       3.375 TIME= 17:45:13
Rigid-constraint surface identified by real constant set 109 and
contact element type 109 has been set up. The degrees of freedom of the
rigid surface are driven by the pilot node 45149 which connects to other
element 38126. Internal MPC will be built.
This pair will be merged with other pair defined by real constant set 151.
The used degrees of freedom set is UX UY UZ ROTX ROTY ROTZ
*WARNING*: Certain contact elements (for example 55588&55894) overlap each
other.
****************************************


*** NOTE ***                            CP =       3.375 TIME= 17:45:13
Rigid-constraint surface identified by real constant set 111 and contact
element type 111 has been set up. The degrees of freedom of
```

```
the rigid surface are driven by the pilot node 45151 which connects to
other element 38130. Internal MPC will be built.
This pair will be merged with other pair defined by real constant set 155.
The used degrees of freedom set is UX UY UZ ROTX ROTY ROTZ
*WARNING*: Boundary conditions, coupling, and/or constraint equations have
been applied on certain contact nodes (for example 6891).
*WARNING*: Certain contact elements (for example 55894&55518) overlap each
other.
****************************************


*** NOTE ***                            CP =       3.375 TIME= 17:45:13
Rigid-constraint surface identified by real constant set 113 and
contact element type 113 has been set up. The degrees of freedom of the
rigid surface are driven by the pilot node 45153 which connects to other
element 38134. Internal MPC will be built.
This pair will be merged with other pair defined by real constant set 101.
The used degrees of freedom set is UX UY UZ ROTX ROTY ROTZ
*WARNING*: Certain contact elements (for example 56131&53606) overlap each
other.
****************************************


*** NOTE ***                            CP =       3.391 TIME= 17:45:13
Rigid-constraint surface identified by real constant set 115 and
contact element type 115 has been set up. The degrees of freedom of the
rigid surface are driven by the pilot node 45155 which connects to other
element 38138. Internal MPC will be built.
This pair will be merged with other pair defined by real constant set 105.
The used degrees of freedom set is UX UY UZ ROTX ROTY ROTZ
*WARNING*: Certain contact elements (for example 56206&56963) overlap each
other.
****************************************


*** NOTE ***                            CP =       3.391 TIME= 17:45:13
Rigid-constraint surface identified by real constant set 117 and
contact element type 117 has been set up. The degrees of freedom of the
rigid surface are driven by the pilot node 45157 which connects to other
element 38142. Internal MPC will be built.
This pair will be merged with other pair defined by real constant set 139.
The used degrees of freedom set is UX UY UZ ROTX ROTY ROTZ
*WARNING*: Certain contact elements (for example 56281&54700) overlap each
other.
****************************************


*** NOTE ***                            CP =       3.391 TIME= 17:45:13
Rigid-constraint surface identified by real constant set 119 and
contact element type 119 has been set up. The degrees of freedom of the
rigid surface are driven by the pilot node 45159 which connects to other
element 38146. Internal MPC will be built.
This pair will be merged with other pair defined by real constant set 141.
The used degrees of freedom set is UX UY UZ ROTX ROTY ROTZ
*WARNING*: Certain contact elements (for example 56355&55075) overlap each
other.
****************************************


*** NOTE ***                            CP =       3.391 TIME= 17:45:13
Rigid-constraint surface identified by real constant set 121 and
contact element type 121 has been set up. The degrees of freedom of the
rigid surface are driven by the pilot node 45161 which connects to other
element 38150. Internal MPC will be built.
This pair will be merged with other pair defined by real constant set 107.
The used degrees of freedom set is UX UY UZ ROTX ROTY ROTZ
*WARNING*: Certain contact elements (for example 56433&57185) overlap each
other.
****************************************


*** NOTE ***                            CP =       3.391 TIME= 17:45:13
Rigid-constraint surface identified by real constant set 123 and
contact element type 123 has been set up. The degrees of freedom of the
rigid surface are driven by the pilot node 45163 which connects to other
element 38154. Internal MPC will be built.
This pair will be merged with other pair defined by real constant set 107.
The used degrees of freedom set is UX UY UZ ROTX ROTY ROTZ
*WARNING*: Certain contact elements (for example 56508&57254) overlap each
other.
****************************************


*** NOTE ***                            CP =       3.391 TIME= 17:45:13
Rigid-constraint surface identified by real constant set 125 and
contact element type 125 has been set up. The degrees of freedom of the
rigid surface are driven by the pilot node 45043 which connects to other
element 38061. Internal MPC will be built.
This pair will be merged with other pair defined by real constant set 37.
The used degrees of freedom set is UX UY UZ ROTX ROTY ROTZ
*WARNING*: Certain contact elements (for example 56582&50703) overlap each
other.
****************************************


*** NOTE ***                            CP =       3.391 TIME= 17:45:13
Rigid-constraint surface identified by real constant set 127 and
contact element type 127 has been set up. The degrees of freedom of the
rigid surface are driven by the pilot node 45165 which connects to other
element 38158. Internal MPC will be built.
This pair will be merged with other pair defined by real constant set 109.
The used degrees of freedom set is UX UY UZ ROTX ROTY ROTZ
```

```
*WARNING*: Certain contact elements (for example 56658&57415) overlap each
other.
****************************************


*** NOTE ***                            CP =       3.391 TIME= 17:45:13
Rigid-constraint surface identified by real constant set 129 and
contact element type 129 has been set up. The degrees of freedom of the
rigid surface are driven by the pilot node 45167 which connects to other
element 38162. Internal MPC will be built.
This pair will be merged with other pair defined by real constant set 109.
The used degrees of freedom set is UX UY UZ ROTX ROTY ROTZ
*WARNING*: Certain contact elements (for example 56733&57484) overlap each
other.
****************************************


*** NOTE ***                            CP =       3.391 TIME= 17:45:13
Rigid-constraint surface identified by real constant set 131 and
contact element type 131 has been set up. The degrees of freedom of the
rigid surface are driven by the pilot node 45169 which connects to other
element 38166. Internal MPC will be built.
This pair will be merged with other pair defined by real constant set 111.
The used degrees of freedom set is UX UY UZ ROTX ROTY ROTZ
*WARNING*: Certain contact elements (for example 56808&57551) overlap each
other.
****************************************


*** NOTE ***                            CP =       3.391 TIME= 17:45:13
Rigid-constraint surface identified by real constant set 133 and
contact element type 133 has been set up. The degrees of freedom of the
rigid surface are driven by the pilot node 45171 which connects to other
element 38170. Internal MPC will be built.
This pair will be merged with other pair defined by real constant set 155.
The used degrees of freedom set is UX UY UZ ROTX ROTY ROTZ
*WARNING*: Boundary conditions, coupling, and/or constraint equations have
been applied on certain contact nodes (for example 7484).
*WARNING*: Certain contact elements (for example 56849&55806) overlap each
other.
****************************************


*** NOTE ***                            CP =       3.391 TIME= 17:45:13
Rigid-constraint surface identified by real constant set 135 and
contact element type 135 has been set up. The degrees of freedom of the
rigid surface are driven by the pilot node 45173 which connects to other
element 38174. Internal MPC will be built.
This pair will be merged with other pair defined by real constant set 101.
The used degrees of freedom set is UX UY UZ ROTX ROTY ROTZ
*WARNING*: Certain contact elements (for example 56925&54781) overlap each
other.
****************************************


*** NOTE ***                            CP =       3.391 TIME= 17:45:13
Rigid-constraint surface identified by real constant set 137 and
contact element type 137 has been set up. The degrees of freedom of the
rigid surface are driven by the pilot node 45175 which connects to other
element 38178. Internal MPC will be built.
This pair will be merged with other pair defined by real constant set 105.
The used degrees of freedom set is UX UY UZ ROTX ROTY ROTZ
*WARNING*: Certain contact elements (for example 56990&57054) overlap each
other.
****************************************


*** NOTE ***                            CP =       3.391 TIME= 17:45:13
Rigid-constraint surface identified by real constant set 139 and
contact element type 139 has been set up. The degrees of freedom of the
rigid surface are driven by the pilot node 45177 which connects to other
element 38182. Internal MPC will be built.
This pair will be merged with other pair defined by real constant set 141.
The used degrees of freedom set is UX UY UZ ROTX ROTY ROTZ
*WARNING*: Certain contact elements (for example 57054&56969) overlap each
other.
****************************************


*** NOTE ***                            CP =       3.391 TIME= 17:45:13
Rigid-constraint surface identified by real constant set 141 and
contact element type 141 has been set up. The degrees of freedom of the
rigid surface are driven by the pilot node 45179 which connects to other
element 38186. Internal MPC will be built.
This pair will be merged with other pair defined by real constant set 107.
The used degrees of freedom set is UX UY UZ ROTX ROTY ROTZ
*WARNING*: Certain contact elements (for example 57142&57197) overlap each
other.
****************************************


*** NOTE ***                            CP =       3.391 TIME= 17:45:13
Rigid-constraint surface identified by real constant set 143 and
contact element type 143 has been set up. The degrees of freedom of the
rigid surface are driven by the pilot node 45181 which connects to other
element 38190. Internal MPC will be built.
This pair will be merged with other pair defined by real constant set 107.
The used degrees of freedom set is UX UY UZ ROTX ROTY ROTZ
*WARNING*: Certain contact elements (for example 57226&57276) overlap each
other.
****************************************
```

```
*** NOTE ***                            CP =       3.391 TIME= 17:45:13
Rigid-constraint surface identified by real constant set 145 and
contact element type 145 has been set up. The degrees of freedom of the
rigid surface are driven by the pilot node 45183 which connects to other
element 38194. Internal MPC will be built.
This pair will be merged with other pair defined by real constant set 109.
The used degrees of freedom set is UX UY UZ ROTX ROTY ROTZ
*WARNING*: Certain contact elements (for example 57297&57393) overlap each
other.
****************************************

*** NOTE ***                            CP =       3.391 TIME= 17:45:13
Rigid-constraint surface identified by real constant set 147 and
contact element type 147 has been set up. The degrees of freedom of the
rigid surface are driven by the pilot node 45045 which connects to other
element 38062. Internal MPC will be built.
This pair will be merged with other pair defined by real constant set 75.
The used degrees of freedom set is UX UY UZ ROTX ROTY ROTZ
*WARNING*: Certain contact elements (for example 57369&57679) overlap each
other.
****************************************

*** NOTE ***                            CP =       3.391 TIME= 17:45:13
Rigid-constraint surface identified by real constant set 149 and
contact element type 149 has been set up. The degrees of freedom of the
rigid surface are driven by the pilot node 45185 which connects to other
element 38198. Internal MPC will be built.
This pair will be merged with other pair defined by real constant set 109.
The used degrees of freedom set is UX UY UZ ROTX ROTY ROTZ
*WARNING*: Certain contact elements (for example 57442&57506) overlap each
other.
****************************************

*** NOTE ***                            CP =       3.391 TIME= 17:45:13
Rigid-constraint surface identified by real constant set 151 and
contact element type 151 has been set up. The degrees of freedom of the
rigid surface are driven by the pilot node 45187 which connects to other
element 38202. Internal MPC will be built.
This pair will be merged with other pair defined by real constant set 111.
The used degrees of freedom set is UX UY UZ ROTX ROTY ROTZ
*WARNING*: Certain contact elements (for example 57506&57421) overlap each
other.
****************************************

*** NOTE ***                            CP =       3.391 TIME= 17:45:13
Rigid-constraint surface identified by real constant set 153 and
contact element type 153 has been set up. The degrees of freedom of the
rigid surface are driven by the pilot node 45189 which connects to other
element 38206. Internal MPC will be built.
This pair will be merged with other pair defined by real constant set 111.
The used degrees of freedom set is UX UY UZ ROTX ROTY ROTZ
*WARNING*: Certain contact elements (for example 57594&57626) overlap each
other.
****************************************

*** NOTE ***                            CP =       3.391 TIME= 17:45:13
Rigid-constraint surface identified by real constant set 155 and
contact element type 155 has been set up. The degrees of freedom of the
rigid surface are driven by the pilot node 45191 which connects to other
element 38210. Internal MPC will be built.
This pair will be merged with other pair defined by real constant set 111.
The used degrees of freedom set is UX UY UZ ROTX ROTY ROTZ
*WARNING*: Boundary conditions, coupling, and/or constraint equations have
been applied on certain contact nodes (for example 8736).
*WARNING*: Certain contact elements (for example 57626&57571) overlap each
other.
****************************************

*** NOTE ***                            CP =       3.391 TIME= 17:45:13
Rigid-constraint surface identified by real constant set 157 and
contact element type 157 has been set up. The degrees of freedom of the
rigid surface are driven by the pilot node 45047 which connects to other
element 38063. Internal MPC will be built.
This pair will be merged with other pair defined by real constant set 41.
The used degrees of freedom set is UX UY UZ ROTX ROTY ROTZ
*WARNING*: Certain contact elements (for example 57710&51073) overlap each
other.
****************************************

*** NOTE ***                            CP =       3.391 TIME= 17:45:13
Rigid-constraint surface identified by real constant set 159 and
contact element type 159 has been set up. The degrees of freedom of the
rigid surface are driven by the pilot node 45049 which connects to other
element 38064. Internal MPC will be built.
This pair will be merged with other pair defined by real constant set 77.
The used degrees of freedom set is UX UY UZ ROTX ROTY ROTZ
*WARNING*: Certain contact elements (for example 57771&57832) overlap each
other.
****************************************

*** NOTE ***                            CP =       3.391 TIME= 17:45:13
Rigid-constraint surface identified by real constant set 161 and
contact element type 161 has been set up. The degrees of freedom of the
rigid surface are driven by the pilot node 45051 which connects to other
element 38065. Internal MPC will be built.
```

```
This pair will be merged with other pair defined by real constant set 45.
The used degrees of freedom set is UX UY UZ ROTX ROTY ROTZ
*WARNING*: Certain contact elements (for example 57861&51445) overlap each
other.
****************************************


*** NOTE ***                            CP =       3.391 TIME= 17:45:13
Rigid-constraint surface identified by real constant set 163 and
contact element type 163 has been set up. The degrees of freedom of the
rigid surface are driven by the pilot node 45053 which connects to other
element 38066. Internal MPC will be built.
This pair will be merged with other pair defined by real constant set 79.
The used degrees of freedom set is UX UY UZ ROTX ROTY ROTZ
*WARNING*: Certain contact elements (for example 57903&57854) overlap each
other.
****************************************


*** WARNING ***                         CP =       3.391 TIME= 17:45:13
Overconstraint may occur for Lagrange multiplier or MPC based contact
algorithm.
The reasons for possible overconstraint are:

*** WARNING ***                         CP =       3.406 TIME= 17:45:13
Boundary conditions, coupling, and/or constraint equations have been
applied on certain contact nodes (for example 8736).

*** WARNING ***                         CP =       3.406 TIME= 17:45:13
Certain contact elements (for example 57903 & 57854) overlap with
other.
****************************************



*** NOTE ***                            CP =       3.469 TIME= 17:45:13
Internal nodes from 45192 to 45270 are created.
79 internal nodes are used for handling degrees of freedom on pilot
nodes of rigid target surfaces.



D I S T R I B U T E D D O M A I N D E C O M P O S E R

...Number of elements: 29026
...Number of nodes:        9485
...Decompose to 2 CPU domains
...Element load balance ratio =         1.147


L O A D S T E P O P T I O N S LOAD STEP NUMBER. ........1
TIME AT END OF THE LOAD STEP. ........................1.0000
AUTOMATIC TIME STEPPING...............................ON
INITIAL NUMBER OF SUBSTEPS ...........................1
MAXIMUM NUMBER OF SUBSTEPS ...........................10
MINIMUM NUMBER OF SUBSTEPS ...........................1
MAXIMUM NUMBER OF EQUILIBRIUM ITERATIONS..............15
STEP CHANGE BOUNDARY CONDITIONS ......................NO
TERMINATE ANALYSIS IF NOT CONVERGED . . . . . .YES (EXIT)
CONVERGENCE CONTROLS. . . . . . . . . . . . . .USE DEFAULTS
PRINT OUTPUT CONTROLS . . . . . . . . . . . . .NO PRINTOUT
DATABASE OUTPUT CONTROLS
ITEM             FREQUENCY COMPONENT
ALL                NONE
NSOL                ALL
RSOL                ALL
EANG                ALL
ETMP                ALL
VENG                ALL
STRS                ALL
EPEL                ALL
EPPL                ALL
CONT                ALL
MISC                ALL       _ELMISC


SOLUTION MONITORING INFO IS WRITTEN TO FILE=
file.mntr

MAXIMUM NUMBER OF EQUILIBRIUM ITERATIONS HAS BEEN MODIFIED TO
BE, NEQIT = 26, BY SOLUTION CONTROL LOGIC.

*** NOTE ***                            CP =       5.438 TIME= 17:45:15
Predictor is ON by default for structural elements with rotational
degrees of freedom. Use the PRED,OFF command to turn the predictor OFF
if it adversely affects the convergence.


*** WARNING ***                         CP =       5.906 TIME= 17:45:16
Multiple constraints have been applied on degree of freedom 1 of
contact node 7629. The program will remove certain internal MPCs.
Please check the model carefully.

*** WARNING ***                         CP =       7.219 TIME= 17:45:17
The internal constraint equation 31684 has been deleted due to
redundancy. This is most likely caused by two or more constraint
equations that share too many degrees of freedom.


*********** PRECISE MASS SUMMARY *********** TOTAL RIGID BODY MASS MATRIX

ABOUT ORIGIN
Translational mass                               |  Coupled translational/rotational mass
          1.3453      0.0000          0.0000     |       0.0000      -0.33307E-15 -242.15
          0.0000      1.3453          0.0000     |     0.11102E-15    0.0000       -1.2931
          0.0000      0.0000          1.3453     |      242.15        1.2931        0.
```

```
|                                                          Rotational mass (inertia)
                                                 |   58144.          232.75       0.88818E-15
                                                 |   232.75           57.216      -0.17053E-12
|                                                     0.88818E-15 -0.17053E-12    58146.

TOTAL MASS =  1.3453
The mass principal axes coincide with the global Cartesian axes CENTER

OF MASS (X,Y,Z)=  -0.96117                    180.00      -0.24758E-15

TOTAL INERTIA ABOUT CENTER OF MASS
           14557.      -0.78109E-12  0.99489E-15
         -0.78109E-12    55.973      -0.23048E-12
0.99489E-15  -0.23048E-12             14557.
The inertia principal axes coincide with the global Cartesian axes


*** MASS SUMMARY BY ELEMENT TYPE ***

TYPE          MASS
1  1.34529

Range of element maximum matrix coefficients in global coordinates
Maximum = 1044638.37 at element 8042.
Minimum = 7.40931762 at element 46275.

*** ELEMENT MATRIX FORMULATION TIMES
       TYPE    NUMBER ENAME      TOTAL CP  AVE CP

          1      9216 SHELL181      6.312   0.000685
          5      9216 SURF154       0.828   0.000090
          6        32 SURF156       0.000   0.000000
          7        76 CONTA174      0.000   0.000000
          8         1 TARGE170      0.000   0.000000
          9        74 CONTA174      0.000   0.000000
         10         1 TARGE170      0.000   0.000000
         11        74 CONTA174      0.000   0.000000
         12         1 TARGE170      0.000   0.000000
         13        74 CONTA174      0.000   0.000000
         14         1 TARGE170      0.000   0.000000
         15        74 CONTA174      0.000   0.000000
         16         1 TARGE170      0.000   0.000000
         17        76 CONTA174      0.000   0.000000
         18         1 TARGE170      0.000   0.000000
         19        74 CONTA174      0.000   0.000000
         20         1 TARGE170      0.000   0.000000
         21        74 CONTA174      0.000   0.000000
         22         1 TARGE170      0.000   0.000000
         23        74 CONTA174      0.000   0.000000
         24         1 TARGE170      0.000   0.000000
         25        74 CONTA174      0.000   0.000000
         26         1 TARGE170      0.000   0.000000
         27        76 CONTA174      0.016   0.000206
         28         1 TARGE170      0.000   0.000000
         29        40 CONTA174      0.000   0.000000
         30         1 TARGE170      0.000   0.000000
         31        77 CONTA174      0.031   0.000406
         32         1 TARGE170      0.000   0.000000
         33        74 CONTA174      0.000   0.000000
         34         1 TARGE170      0.000   0.000000
         35        74 CONTA174      0.016   0.000211
         36         1 TARGE170      0.000   0.000000
         37        73 CONTA174      0.000   0.000000
         38         1 TARGE170      0.000   0.000000
         39        76 CONTA174      0.000   0.000000
         40         1 TARGE170      0.000   0.000000
         41        73 CONTA174      0.000   0.000000
         42         1 TARGE170      0.000   0.000000
         43        74 CONTA174      0.000   0.000000
         44         1 TARGE170      0.000   0.000000
         45        74 CONTA174      0.000   0.000000
         46         1 TARGE170      0.000   0.000000
         47        73 CONTA174      0.000   0.000000
         48         1 TARGE170      0.000   0.000000
         49        76 CONTA174      0.000   0.000000
         50         1 TARGE170      0.000   0.000000
         51        73 CONTA174      0.016   0.000214
         52         1 TARGE170      0.000   0.000000
         53        74 CONTA174      0.000   0.000000
         54         1 TARGE170      0.000   0.000000
         55        74 CONTA174      0.000   0.000000
         56         1 TARGE170      0.000   0.000000
         57        73 CONTA174      0.000   0.000000
         58         1 TARGE170      0.000   0.000000
         59        76 CONTA174      0.016   0.000206
         60         1 TARGE170      0.000   0.000000
         61        73 CONTA174      0.000   0.000000
         62         1 TARGE170      0.000   0.000000
         63        74 CONTA174      0.000   0.000000
         64         1 TARGE170      0.000   0.000000
         65        74 CONTA174      0.000   0.000000
         66         1 TARGE170      0.000   0.000000
         67        73 CONTA174      0.000   0.000000
         68         1 TARGE170      0.000   0.000000
         69        76 CONTA174      0.000   0.000000
         70         1 TARGE170      0.000   0.000000
         71       372 CONTA174      0.016   0.000042
         72         1 TARGE170      0.000   0.000000
         73       370 CONTA174      0.000   0.000000
         74         1 TARGE170      0.000   0.000000
         75       368 CONTA174      0.000   0.000000
         76         1 TARGE170      0.000   0.000000
         77       368 CONTA174      0.000   0.000000
         78         1 TARGE170      0.000   0.000000
         79       372 CONTA174      0.000   0.000000
         80         1 TARGE170      0.000   0.000000
```

81	372	CONTA174	0.031	0.000084
82	1	TARGE170	0.000	0.000000
83	368	CONTA174	0.016	0.000042
84	1	TARGE170	0.000	0.000000
85	368	CONTA174	0.016	0.000042

86	1	TARGE170	0.000	0.000000
87	368	CONTA174	0.016	0.000042
88	1	TARGE170	0.000	0.000000
89	372	CONTA174	0.016	0.000042
90	1	TARGE170	0.000	0.000000
91	368	CONTA174	0.000	0.000000
92	1	TARGE170	0.000	0.000000
93	32	CONTA175	0.000	0.000000
94	1	TARGE170	0.000	0.000000
95	38	CONTA174	0.000	0.000000
96	1	TARGE170	0.000	0.000000
97	74	CONTA174	0.000	0.000000
98	1	TARGE170	0.000	0.000000
99	74	CONTA174	0.000	0.000000
100	1	TARGE170	0.000	0.000000
101	372	CONTA174	0.000	0.000000
102	1	TARGE170	0.000	0.000000
103	74	CONTA174	0.000	0.000000
104	1	TARGE170	0.000	0.000000
105	368	CONTA174	0.016	0.000042
106	1	TARGE170	0.000	0.000000
107	368	CONTA174	0.000	0.000000
108	1	TARGE170	0.000	0.000000
109	368	CONTA174	0.000	0.000000
110	1	TARGE170	0.000	0.000000
111	372	CONTA174	0.000	0.000000
112	1	TARGE170	0.000	0.000000
113	74	CONTA174	0.000	0.000000
114	1	TARGE170	0.000	0.000000
115	74	CONTA174	0.000	0.000000
116	1	TARGE170	0.000	0.000000
117	74	CONTA174	0.016	0.000211
118	1	TARGE170	0.000	0.000000
119	74	CONTA174	0.000	0.000000
120	1	TARGE170	0.000	0.000000
121	76	CONTA174	0.000	0.000000
122	1	TARGE170	0.000	0.000000
123	74	CONTA174	0.000	0.000000
124	1	TARGE170	0.000	0.000000
125	74	CONTA174	0.000	0.000000
126	1	TARGE170	0.000	0.000000
127	74	CONTA174	0.000	0.000000
128	1	TARGE170	0.000	0.000000
129	74	CONTA174	0.000	0.000000
130	1	TARGE170	0.000	0.000000
131	74	CONTA174	0.000	0.000000
132	1	TARGE170	0.000	0.000000
133	38	CONTA174	0.000	0.000000
134	1	TARGE170	0.000	0.000000
135	73	CONTA174	0.000	0.000000
136	1	TARGE170	0.000	0.000000
137	74	CONTA174	0.000	0.000000
138	1	TARGE170	0.000	0.000000
139	74	CONTA174	0.000	0.000000
140	1	TARGE170	0.000	0.000000
141	73	CONTA174	0.000	0.000000
142	1	TARGE170	0.000	0.000000
143	76	CONTA174	0.000	0.000000
144	1	TARGE170	0.000	0.000000
145	73	CONTA174	0.000	0.000000
146	1	TARGE170	0.000	0.000000
147	76	CONTA174	0.000	0.000000
148	1	TARGE170	0.000	0.000000
149	74	CONTA174	0.000	0.000000
150	1	TARGE170	0.000	0.000000
151	74	CONTA174	0.000	0.000000
152	1	TARGE170	0.000	0.000000
153	73	CONTA174	0.000	0.000000
154	1	TARGE170	0.000	0.000000
155	38	CONTA174	0.000	0.000000
156	1	TARGE170	0.000	0.000000
157	74	CONTA174	0.000	0.000000
158	1	TARGE170	0.000	0.000000
159	74	CONTA174	0.000	0.000000
160	1	TARGE170	0.000	0.000000
161	74	CONTA174	0.000	0.000000
162	1	TARGE170	0.000	0.000000
163	74	CONTA174	0.000	0.000000
164	1	TARGE170	0.000	0.000000
165	1	COMBIN39	0.000	0.000000
166	1	COMBIN39	0.000	0.000000
167	1	COMBIN39	0.000	0.000000
168	1	COMBIN39	0.000	0.000000
169	1	COMBIN39	0.000	0.000000
170	1	COMBIN39	0.000	0.000000
171	1	COMBIN39	0.000	0.000000
172	1	COMBIN39	0.000	0.000000
173	1	COMBIN39	0.000	0.000000
174	1	COMBIN39	0.000	0.000000
175	1	COMBIN39	0.000	0.000000
176	1	COMBIN39	0.000	0.000000
177	1	COMBIN39	0.000	0.000000
178	1	COMBIN39	0.000	0.000000
179	1	COMBIN39	0.000	0.000000
180	1	COMBIN39	0.000	0.000000
181	1	COMBIN39	0.000	0.000000
182	1	COMBIN39	0.000	0.000000
183	1	COMBIN39	0.000	0.000000
184	1	COMBIN39	0.000	0.000000
185	1	COMBIN39	0.000	0.000000
186	1	COMBIN39	0.016	0.015625
187	1	COMBIN39	0.000	0.000000
188	1	COMBIN39	0.000	0.000000
189	1	COMBIN39	0.000	0.000000
190	1	COMBIN39	0.000	0.000000
191	1	COMBIN39	0.000	0.000000

192	1	COMBIN39	0.000	0.000000
193	1	COMBIN39	0.000	0.000000
194	1	COMBIN39	0.000	0.000000
195	1	COMBIN39	0.000	0.000000
196	1	COMBIN39	0.000	0.000000

```
       197         1 COMBIN39       0.000   0.000000
       198         1 COMBIN39       0.000   0.000000
       199         1 COMBIN39       0.000   0.000000
       200         1 COMBIN39       0.000   0.000000
       201         1 COMBIN39       0.000   0.000000
       202         1 COMBIN39       0.000   0.000000
       203         1 COMBIN39       0.000   0.000000
       204         1 COMBIN39       0.000   0.000000
       205         1 COMBIN39       0.000   0.000000
       206         1 COMBIN39       0.000   0.000000
       207         1 COMBIN39       0.000   0.000000
       208         1 COMBIN39       0.000   0.000000
       209         1 COMBIN39       0.000   0.000000
       210         1 COMBIN39       0.000   0.000000
       211         1 COMBIN39       0.000   0.000000
       212         1 COMBIN39       0.000   0.000000
       213         1 COMBIN39       0.000   0.000000
       214         1 COMBIN39       0.000   0.000000
       215         1 COMBIN39       0.000   0.000000
       216         1 COMBIN39       0.000   0.000000
       217         1 COMBIN39       0.000   0.000000
       218         1 COMBIN39       0.000   0.000000
       219         1 COMBIN39       0.000   0.000000
       220         1 COMBIN39       0.000   0.000000
       221         1 COMBIN39       0.000   0.000000
       222         1 COMBIN39       0.000   0.000000
       223         1 COMBIN39       0.000   0.000000
       224         1 COMBIN39       0.000   0.000000
       225         1 COMBIN39       0.000   0.000000
       226         1 COMBIN39       0.000   0.000000
       227         1 COMBIN39       0.000   0.000000
       228         1 COMBIN39       0.000   0.000000
       229         1 COMBIN39       0.000   0.000000
       230         1 COMBIN39       0.000   0.000000
       231         1 COMBIN39       0.000   0.000000
       232         1 COMBIN39       0.000   0.000000
       233         1 COMBIN39       0.000   0.000000
       234         1 COMBIN39       0.000   0.000000
       235         1 COMBIN39       0.000   0.000000
       236         1 COMBIN39       0.000   0.000000
       237         1 COMBIN39       0.000   0.000000
       238         1 COMBIN39       0.000   0.000000
       239         1 COMBIN39       0.000   0.000000
       240         1 COMBIN39       0.000   0.000000
       241         1 COMBIN39       0.000   0.000000
       242         1 COMBIN39       0.000   0.000000
       243         1 COMBIN39       0.000   0.000000
Time at end of element matrix formulation CP = 12.375.

ALL CURRENT ANSYS DATA WRITTEN TO FILE NAME= file.rdb
FOR POSSIBLE RESUME FROM THIS POINT
FORCE CONVERGENCE VALUE = 0.5032E+07 CRITERION= 0.2568E+05 MOMENT
CONVERGENCE VALUE = 0.2606E+07 CRITERION= 0.1329E+05

DISTRIBUTED SPARSE MATRIX DIRECT SOLVER.
Number of equations =           15236,    Maximum wavefront =     48

Local memory allocated for solver                 =   26.270   MB
Local memory  required  for  in-core  solution =   18.158  MB  Local
memory required for out-of-core solution =   15.254 MB

Total memory allocated for solver                 =   46.190   MB
Total  memory  required  for  in-core  solution =   29.962  MB  Total
memory required for out-of-core solution =   21.279 MB

*** NOTE ***                             CP =      13.750 TIME= 17:45:29
The Distributed Sparse Matrix Solver is currently running in the
in-core memory mode. This memory mode uses the most amount of memory in
order to avoid using the hard drive as much as possible, which most often
results in the fastest solution time. This mode is recommended if enough
physical memory is present to accommodate all of the solver data.
curEqn=  7636  totEqn=  7636 Job  CP sec=        13.797
Factor Done= 100% Factor Wall sec=              0.018 rate=    3800.5 Mflops
Distributed sparse solver maximum pivot= 27984857 at node 45147 UX.
Distributed sparse solver minimum pivot= 692.974243 at node 7333 ROTZ.
Distributed sparse solver minimum pivot in absolute value= 692.974243 at
node 7333 ROTZ.
DISP CONVERGENCE VALUE   =   4.000              CRITERION=  0.2041
EQUIL ITER   1 COMPLETED.  NEW TRIANG MATRIX.  MAX DOF INC=         4.000
DISP CONVERGENCE VALUE   =   4.000              CRITERION=  0.2082
LINE SEARCH PARAMETER =   1.000             SCALED MAX DOF INC =   4.000
FORCE CONVERGENCE VALUE  = 0.3344E+05  CRITERION=          1805.
MOMENT CONVERGENCE VALUE =  0.1363E-06 CRITERION=   1011.           <<< CONVERGED
EQUIL ITER 2 COMPLETED. NEW TRIANG MATRIX. MAX DOF INC=  0.3356E-01
DISP CONVERGENCE VALUE   =  0.3356E-01 CRITERION=  0.2125           <<< CONVERGED
LINE SEARCH PARAMETER =   1.000             SCALED MAX DOF INC =  0.3356E-01
FORCE CONVERGENCE VALUE  =   3431.              CRITERION=   1752.
MOMENT CONVERGENCE VALUE =  0.8066E-08 CRITERION=   982.2           <<< CONVERGED
EQUIL ITER 3 COMPLETED. NEW TRIANG MATRIX. MAX DOF INC=  0.3905E-02
DISP CONVERGENCE VALUE   =  0.3905E-02 CRITERION=  0.2168           <<< CONVERGED
LINE SEARCH PARAMETER =   1.000             SCALED MAX DOF INC =  0.3905E-02
FORCE CONVERGENCE VALUE  =  0.3669E-07 CRITERION=   1778.           <<< CONVERGED
MOMENT CONVERGENCE VALUE =  0.8134E-08 CRITERION=   996.7           <<< CONVERGED
>>> SOLUTION CONVERGED AFTER EQUILIBRIUM ITERATION         3

*** ELEMENT RESULT CALCULATION TIMES
       TYPE    NUMBER ENAME       TOTAL CP  AVE CP

          1      9216 SHELL181      8.641   0.000938
          5      9216 SURF154       0.969   0.000105
          6        32 SURF156       0.000   0.000000
          7        76 CONTA174      0.000   0.000000
          9        74 CONTA174      0.000   0.000000
         11        74 CONTA174      0.000   0.000000
         13        74 CONTA174      0.000   0.000000
         15        74 CONTA174      0.000   0.000000
```

17	76	CONTA174	0.000	0.000000
19	74	CONTA174	0.000	0.000000
21	74	CONTA174	0.000	0.000000
23	74	CONTA174	0.000	0.000000

25	74	CONTA174	0.000	0.000000
27	76	CONTA174	0.000	0.000000
29	40	CONTA174	0.000	0.000000
31	77	CONTA174	0.000	0.000000
33	74	CONTA174	0.000	0.000000
35	74	CONTA174	0.000	0.000000
37	73	CONTA174	0.000	0.000000
39	76	CONTA174	0.000	0.000000
41	73	CONTA174	0.000	0.000000
43	74	CONTA174	0.000	0.000000
45	74	CONTA174	0.000	0.000000
47	73	CONTA174	0.000	0.000000
49	76	CONTA174	0.000	0.000000
51	73	CONTA174	0.000	0.000000
53	74	CONTA174	0.000	0.000000
55	74	CONTA174	0.000	0.000000
57	73	CONTA174	0.000	0.000000
59	76	CONTA174	0.000	0.000000
61	73	CONTA174	0.000	0.000000
63	74	CONTA174	0.000	0.000000
65	74	CONTA174	0.000	0.000000
67	73	CONTA174	0.000	0.000000
69	76	CONTA174	0.000	0.000000
71	372	CONTA174	0.000	0.000000
73	370	CONTA174	0.000	0.000000
75	368	CONTA174	0.000	0.000000
77	368	CONTA174	0.000	0.000000
79	372	CONTA174	0.000	0.000000
81	372	CONTA174	0.000	0.000000
83	368	CONTA174	0.000	0.000000
85	368	CONTA174	0.000	0.000000
87	368	CONTA174	0.000	0.000000
89	372	CONTA174	0.000	0.000000
91	368	CONTA174	0.000	0.000000
93	32	CONTA175	0.000	0.000000
95	38	CONTA174	0.000	0.000000
97	74	CONTA174	0.000	0.000000
99	74	CONTA174	0.000	0.000000
101	372	CONTA174	0.000	0.000000
103	74	CONTA174	0.000	0.000000
105	368	CONTA174	0.000	0.000000
107	368	CONTA174	0.000	0.000000
109	368	CONTA174	0.000	0.000000
111	372	CONTA174	0.000	0.000000
113	74	CONTA174	0.000	0.000000
115	74	CONTA174	0.000	0.000000
117	74	CONTA174	0.000	0.000000
119	74	CONTA174	0.000	0.000000
121	76	CONTA174	0.000	0.000000
123	74	CONTA174	0.000	0.000000
125	74	CONTA174	0.000	0.000000
127	74	CONTA174	0.000	0.000000
129	74	CONTA174	0.000	0.000000
131	74	CONTA174	0.000	0.000000
133	38	CONTA174	0.000	0.000000
135	73	CONTA174	0.000	0.000000
137	74	CONTA174	0.000	0.000000
139	74	CONTA174	0.000	0.000000
141	73	CONTA174	0.000	0.000000
143	76	CONTA174	0.000	0.000000
145	73	CONTA174	0.000	0.000000
147	76	CONTA174	0.000	0.000000
149	74	CONTA174	0.000	0.000000
151	74	CONTA174	0.000	0.000000
153	73	CONTA174	0.000	0.000000
155	38	CONTA174	0.016	0.000411
157	74	CONTA174	0.000	0.000000
159	74	CONTA174	0.000	0.000000
161	74	CONTA174	0.000	0.000000
163	74	CONTA174	0.000	0.000000
165	1	COMBIN39	0.000	0.000000
166	1	COMBIN39	0.000	0.000000
167	1	COMBIN39	0.000	0.000000
168	1	COMBIN39	0.000	0.000000
169	1	COMBIN39	0.000	0.000000
170	1	COMBIN39	0.000	0.000000
171	1	COMBIN39	0.000	0.000000
172	1	COMBIN39	0.000	0.000000
173	1	COMBIN39	0.000	0.000000
174	1	COMBIN39	0.000	0.000000
175	1	COMBIN39	0.000	0.000000
176	1	COMBIN39	0.000	0.000000
177	1	COMBIN39	0.000	0.000000
178	1	COMBIN39	0.000	0.000000
179	1	COMBIN39	0.000	0.000000
180	1	COMBIN39	0.000	0.000000
181	1	COMBIN39	0.000	0.000000
182	1	COMBIN39	0.000	0.000000
183	1	COMBIN39	0.000	0.000000
184	1	COMBIN39	0.000	0.000000
185	1	COMBIN39	0.000	0.000000
186	1	COMBIN39	0.000	0.000000
187	1	COMBIN39	0.000	0.000000
188	1	COMBIN39	0.000	0.000000
189	1	COMBIN39	0.000	0.000000
190	1	COMBIN39	0.000	0.000000
191	1	COMBIN39	0.000	0.000000
192	1	COMBIN39	0.000	0.000000
193	1	COMBIN39	0.000	0.000000
194	1	COMBIN39	0.000	0.000000
195	1	COMBIN39	0.000	0.000000
196	1	COMBIN39	0.000	0.000000
197	1	COMBIN39	0.000	0.000000
198	1	COMBIN39	0.000	0.000000
199	1	COMBIN39	0.000	0.000000
200	1	COMBIN39	0.000	0.000000

201	1	COMBIN39	0.000	0.000000
202	1	COMBIN39	0.000	0.000000
203	1	COMBIN39	0.000	0.000000
204	1	COMBIN39	0.000	0.000000
205	1	COMBIN39	0.000	0.000000
206	1	COMBIN39	0.000	0.000000
207	1	COMBIN39	0.000	0.000000
208	1	COMBIN39	0.000	0.000000
209	1	COMBIN39	0.000	0.000000
210	1	COMBIN39	0.000	0.000000
211	1	COMBIN39	0.000	0.000000
212	1	COMBIN39	0.000	0.000000
213	1	COMBIN39	0.000	0.000000
214	1	COMBIN39	0.000	0.000000
215	1	COMBIN39	0.000	0.000000
216	1	COMBIN39	0.000	0.000000
217	1	COMBIN39	0.000	0.000000
218	1	COMBIN39	0.000	0.000000
219	1	COMBIN39	0.000	0.000000
220	1	COMBIN39	0.000	0.000000
221	1	COMBIN39	0.000	0.000000
222	1	COMBIN39	0.000	0.000000
223	1	COMBIN39	0.000	0.000000
224	1	COMBIN39	0.000	0.000000
225	1	COMBIN39	0.000	0.000000
226	1	COMBIN39	0.000	0.000000
227	1	COMBIN39	0.000	0.000000
228	1	COMBIN39	0.000	0.000000
229	1	COMBIN39	0.000	0.000000
230	1	COMBIN39	0.000	0.000000
231	1	COMBIN39	0.000	0.000000
232	1	COMBIN39	0.000	0.000000
233	1	COMBIN39	0.000	0.000000
234	1	COMBIN39	0.000	0.000000
235	1	COMBIN39	0.000	0.000000
236	1	COMBIN39	0.000	0.000000
237	1	COMBIN39	0.000	0.000000
238	1	COMBIN39	0.000	0.000000
239	1	COMBIN39	0.000	0.000000
240	1	COMBIN39	0.000	0.000000
241	1	COMBIN39	0.000	0.000000
242	1	COMBIN39	0.000	0.000000
243	1	COMBIN39	0.000	0.000000

*** NODAL LOAD CALCULATION TIMES

TYPE	NUMBER	ENAME	TOTAL CP	AVE CP
1	9216	SHELL181	0.062	0.000007
5	9216	SURF154	0.016	0.000002
6	32	SURF156	0.000	0.000000
7	76	CONTA174	0.000	0.000000
9	74	CONTA174	0.000	0.000000
11	74	CONTA174	0.000	0.000000
13	74	CONTA174	0.000	0.000000
15	74	CONTA174	0.000	0.000000
17	76	CONTA174	0.000	0.000000
19	74	CONTA174	0.000	0.000000
21	74	CONTA174	0.000	0.000000
23	74	CONTA174	0.000	0.000000
25	74	CONTA174	0.000	0.000000
27	76	CONTA174	0.000	0.000000
29	40	CONTA174	0.000	0.000000
31	77	CONTA174	0.000	0.000000
33	74	CONTA174	0.000	0.000000
35	74	CONTA174	0.000	0.000000
37	73	CONTA174	0.000	0.000000
39	76	CONTA174	0.000	0.000000
41	73	CONTA174	0.000	0.000000
43	74	CONTA174	0.000	0.000000
45	74	CONTA174	0.000	0.000000
47	73	CONTA174	0.000	0.000000
49	76	CONTA174	0.000	0.000000
51	73	CONTA174	0.000	0.000000
53	74	CONTA174	0.000	0.000000
55	74	CONTA174	0.000	0.000000
57	73	CONTA174	0.000	0.000000
59	76	CONTA174	0.000	0.000000
61	73	CONTA174	0.000	0.000000
63	74	CONTA174	0.000	0.000000
65	74	CONTA174	0.000	0.000000
67	73	CONTA174	0.000	0.000000
69	76	CONTA174	0.000	0.000000
71	372	CONTA174	0.000	0.000000
73	370	CONTA174	0.000	0.000000
75	368	CONTA174	0.000	0.000000
77	368	CONTA174	0.000	0.000000
79	372	CONTA174	0.000	0.000000
81	372	CONTA174	0.000	0.000000
83	368	CONTA174	0.000	0.000000
85	368	CONTA174	0.000	0.000000
87	368	CONTA174	0.000	0.000000
89	372	CONTA174	0.000	0.000000
91	368	CONTA174	0.000	0.000000
93	32	CONTA175	0.000	0.000000
95	38	CONTA174	0.000	0.000000
97	74	CONTA174	0.000	0.000000
99	74	CONTA174	0.000	0.000000
101	372	CONTA174	0.000	0.000000
103	74	CONTA174	0.000	0.000000
105	368	CONTA174	0.000	0.000000
107	368	CONTA174	0.000	0.000000
109	368	CONTA174	0.000	0.000000
111	372	CONTA174	0.000	0.000000
113	74	CONTA174	0.000	0.000000
115	74	CONTA174	0.000	0.000000
117	74	CONTA174	0.000	0.000000

119	74	CONTA174	0.000	0.000000
121	76	CONTA174	0.000	0.000000
123	74	CONTA174	0.000	0.000000
125	74	CONTA174	0.000	0.000000
127	74	CONTA174	0.000	0.000000
129	74	CONTA174	0.000	0.000000
131	74	CONTA174	0.000	0.000000
133	38	CONTA174	0.000	0.000000
135	73	CONTA174	0.000	0.000000
137	74	CONTA174	0.000	0.000000

```
       139        74 CONTA174       0.000    0.000000
       141        73 CONTA174       0.000    0.000000
       143        76 CONTA174       0.000    0.000000
       145        73 CONTA174       0.000    0.000000
       147        76 CONTA174       0.000    0.000000
       149        74 CONTA174       0.000    0.000000
       151        74 CONTA174       0.000    0.000000
       153        73 CONTA174       0.000    0.000000
       155        38 CONTA174       0.000    0.000000
       157        74 CONTA174       0.000    0.000000
       159        74 CONTA174       0.000    0.000000
       161        74 CONTA174       0.000    0.000000
       163        74 CONTA174       0.000    0.000000
       165         1 COMBIN39       0.000    0.000000
       166         1 COMBIN39       0.000    0.000000
       167         1 COMBIN39       0.000    0.000000
       168         1 COMBIN39       0.000    0.000000
       169         1 COMBIN39       0.000    0.000000
       170         1 COMBIN39       0.000    0.000000
       171         1 COMBIN39       0.000    0.000000
       172         1 COMBIN39       0.000    0.000000
       173         1 COMBIN39       0.000    0.000000
       174         1 COMBIN39       0.000    0.000000
       175         1 COMBIN39       0.000    0.000000
       176         1 COMBIN39       0.000    0.000000
       177         1 COMBIN39       0.000    0.000000
       178         1 COMBIN39       0.000    0.000000
       179         1 COMBIN39       0.000    0.000000
       180         1 COMBIN39       0.000    0.000000
       181         1 COMBIN39       0.000    0.000000
       182         1 COMBIN39       0.000    0.000000
       183         1 COMBIN39       0.000    0.000000
       184         1 COMBIN39       0.000    0.000000
       185         1 COMBIN39       0.000    0.000000
       186         1 COMBIN39       0.000    0.000000
       187         1 COMBIN39       0.000    0.000000
       188         1 COMBIN39       0.000    0.000000
       189         1 COMBIN39       0.000    0.000000
       190         1 COMBIN39       0.000    0.000000
       191         1 COMBIN39       0.000    0.000000
       192         1 COMBIN39       0.000    0.000000
       193         1 COMBIN39       0.000    0.000000
       194         1 COMBIN39       0.000    0.000000
       195         1 COMBIN39       0.000    0.000000
       196         1 COMBIN39       0.000    0.000000
       197         1 COMBIN39       0.000    0.000000
       198         1 COMBIN39       0.000    0.000000
       199         1 COMBIN39       0.000    0.000000
       200         1 COMBIN39       0.000    0.000000
       201         1 COMBIN39       0.000    0.000000
       202         1 COMBIN39       0.000    0.000000
       203         1 COMBIN39       0.000    0.000000
       204         1 COMBIN39       0.000    0.000000
       205         1 COMBIN39       0.000    0.000000
       206         1 COMBIN39       0.000    0.000000
       207         1 COMBIN39       0.000    0.000000
       208         1 COMBIN39       0.000    0.000000
       209         1 COMBIN39       0.000    0.000000
       210         1 COMBIN39       0.000    0.000000
       211         1 COMBIN39       0.000    0.000000
       212         1 COMBIN39       0.000    0.000000
       213         1 COMBIN39       0.000    0.000000
       214         1 COMBIN39       0.000    0.000000
       215         1 COMBIN39       0.000    0.000000
       216         1 COMBIN39       0.000    0.000000
       217         1 COMBIN39       0.000    0.000000
       218         1 COMBIN39       0.000    0.000000
       219         1 COMBIN39       0.000    0.000000
       220         1 COMBIN39       0.000    0.000000
       221         1 COMBIN39       0.000    0.000000
       222         1 COMBIN39       0.000    0.000000
       223         1 COMBIN39       0.000    0.000000
       224         1 COMBIN39       0.000    0.000000
       225         1 COMBIN39       0.000    0.000000
       226         1 COMBIN39       0.000    0.000000
       227         1 COMBIN39       0.000    0.000000
       228         1 COMBIN39       0.000    0.000000
       229         1 COMBIN39       0.000    0.000000
       230         1 COMBIN39       0.000    0.000000
       231         1 COMBIN39       0.000    0.000000
       232         1 COMBIN39       0.000    0.000000
       233         1 COMBIN39       0.000    0.000000
       234         1 COMBIN39       0.000    0.000000
       235         1 COMBIN39       0.000    0.000000
       236         1 COMBIN39       0.000    0.000000
       237         1 COMBIN39       0.000    0.000000
       238         1 COMBIN39       0.000    0.000000
       239         1 COMBIN39       0.000    0.000000
       240         1 COMBIN39       0.000    0.000000
       241         1 COMBIN39       0.000    0.000000
       242         1 COMBIN39       0.000    0.000000
       243         1 COMBIN39       0.000    0.000000
*** LOAD STEP     1   SUBSTEP     1  COMPLETED.    CUM ITER =      3
*** TIME =   1.00000          TIME INC =   1.00000


*** ANSYS BINARY FILE STATISTICS BUFFER
SIZE USED= 16384
5.375 MB WRITTEN ON ELEMENT MATRIX FILE: file0.emat 667.688 MB
WRITTEN ON ELEMENT SAVED DATA FILE: file0.esav
14.125 MB WRITTEN ON ASSEMBLED MATRIX FILE: file0.full
93.000 MB WRITTEN ON RESULTS FILE: file0.rst
*************** Write FE CONNECTORS *********

WRITE OUT CONSTRAINT EQUATIONS TO FILE=
file.ce
```

```
****************************************************
*************** FINISHED SOLVE FOR LS 1 *************

*GET _WALLASOL FROM ACTI ITEM=TIME WALL VALUE= 17.7766667
```

```
PRINTOUT RESUMED BY /GOP

FINISH SOLUTION PROCESSING


***** ROUTINE COMPLETED ***** CP =           61.562



*** ANSYS - ENGINEERING ANALYSIS SYSTEM RELEASE 2019 R2             19.4     ***
DISTRIBUTED ANSYS Academic Research

00427805  VERSION=WINDOWS x64  17:46:40  APR 03, 2020 CP=        61.609

Longer pile--Static Structural (B3)



***** ANSYS RESULTS INTERPRETATION (POST1) *****

*** NOTE ***                              CP =      61.609 TIME= 17:46:40
Reading results into the database (SET command) will update the current
displacement and force boundary conditions in the database with the
values from the results file for that load set. Note that any subsequent
solutions will use these values unless action is taken to either SAVE the
current values or not overwrite them (/EXIT,NOSAVE).

Set Encoding of XML File to:ISO-8859-1

Set Output of XML File to:
PARM,            ,     ,     ,     ,     ,     ,     ,     ,     ,     ,     ,
,                ,     ,     ,     ,     ,     ,

DATABASE WRITTEN ON FILE
parm.xml


EXIT THE ANSYS POST1 DATABASE PROCESSOR


***** ROUTINE COMPLETED ***** CP =           61.641



PRINTOUT RESUMED BY /GOP

*GET _WALLDONE FROM ACTI ITEM=TIME WALL VALUE= 17.7777778

PARAMETER _PREPTIME =        1.000000000

PARAMETER _SOLVTIME =        84.00000000

PARAMETER _POSTTIME =        4.000000000

PARAMETER _TOTALTIM =        89.00000000

*GET _DLBRATIO FROM ACTI ITEM=SOLU DLBR VALUE= 1.14719901
--- Number of total nodes = 9406
--- Number of total elements = 29026
--- Element load balance ratio = 1.14719901

EXIT ANSYS WITHOUT SAVING DATABASE


NUMBER OF WARNING MESSAGES ENCOUNTERED=             7
NUMBER OF ERROR  MESSAGES ENCOUNTERED=             0

+--------- D I S T R I B U T E D   A N S Y S   S T A T I S T I C S -------------- +

Release: 2019 R2              Build: 19.4 Update:  UP20190416  Platform:  WINDOWS  x64
Date Run: 04/03/2020  Time: 17:46       Process ID: 6684
Operating System: Windows Server 2012 R2 (Build: 9600)

Processor Model: Intel(R) Xeon(R) CPU E5-2667 v4 @ 3.20GHz

Compiler: Intel(R) FORTRAN Compiler Version 17.0.6 (Build: 20171215)
Intel(R) C/C++ Compiler Version 17.0.6 (Build: 20171215)
Intel(R) Math Kernel Library Version 2017.0.3 Product Build 20170413

  Number of machines requested                   :   1

  Total number of cores available                :   8

  Number of physical cores available             :   8
MPI Version: Intel(R) MPI Library 2018 Update 3 for Windows* OS


GPU Acceleration: Not Requested

Job Name: file0
Input File: \\engrfs904v\VCL.userspace\kavach\Documents\Thesis Sections\Octagonal\V Stiff Clay\_ProjectScratch\ScrD3F9\dummy.dat

    Core                Machine Name  Working Directory
   ----------------------------------------------------------------------------------------------------------------
       0      ENGRVDA9401V.AD.UMD.EDU  U:\Documents\Thesis Sections\Octagonal\V Stiff Clay\_ProjectScratch\ScrD3F9
       1      ENGRVDA9401V.AD.UMD.EDU  U:\Documents\Thesis Sections\Octagonal\V Stiff Clay\_ProjectScratch\ScrD3F9

Latency time from master to core       1 =    0.976 microseconds

Communication speed from master to core 1 = 3373.77 MB/sec

Total CPU time for main thread                    :       59.7 seconds
Total CPU time summed for all threads             :       61.8 seconds
```

```
Elapsed time spent pre-processing model (/PREP7) : 1.4 seconds Elapsed
time spent solution - preprocessing   :   1.6 seconds Elapsed time spent
computing solution                                :    81.8    seconds
Elapsed time spent solution - postprocessing     :       2.8 seconds
```

```
Elapsed time spent post-processing model (/POST1) :          0.0 seconds

Equation solver used                                :           Sparse (symmetric)
Equation solver computational rate                  :        1.7 Gflops

Maximum total memory used                           :      543.0 MB
Maximum total memory allocated                      :     3136.0 MB
Total physical memory available                     :         64 GB

Total amount of I/O written to disk                 :        5.7 GB
Total amount of I/O read from disk                  :        9.8 GB

+------ E N D   D I S T R I B U T E D   A N S Y S   S T A T I S T I C S ---------+


   *------------------------------------------------------------------------*
   |                                                                          |
   |                  DISTRIBUTED ANSYS RUN COMPLETED                         |
   |                                                                          |
   |------------------------------------------------------------------------|
   |                                                                          |
   | Ansys 2019 R2     Build 19.4              UP20190416         WINDOWS x64 |
   |                                                                          |
|----------------------------------------------------------------------------|
|                                                                            |
| Database Requested(-db)  1024 MB       Scratch Memory Requested      1024 MB |
| Maximum Database Used         43 MB    Maximum Scratch Memory Used    244 MB |
|                                                                            |
|----------------------------------------------------------------------------|
|                                                                            |
|          CP Time      (sec) =         61.828       Time  =  17:46:40        |
|          Elapsed Time (sec) =         92.000       Date  =  04/03/2020      |
|                                                                            |
*----------------------------------------------------------------------------
```

Project*

First Saved	Saturday, February 15, 2020
Last Saved	Monday, April 6, 2020
Product Version	2019 R2
Save Project Before Solution	No
Save Project After Solution	No

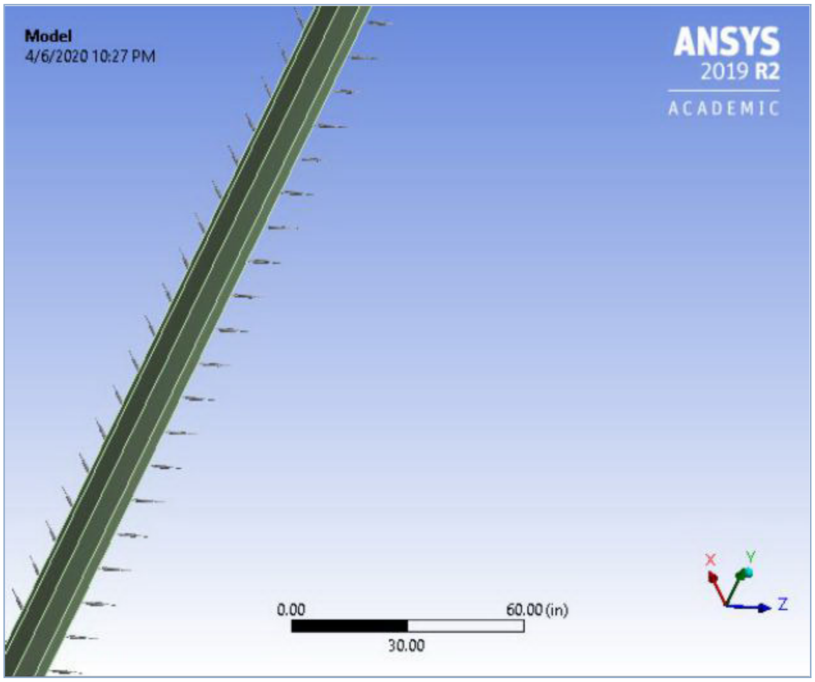

Contents

Units

TABLE 1

Unit System	U.S. Customary (in, lbm, lbf, s, V, A) Degrees rad/s Fahrenheit
Angle	Degrees
Rotational Velocity	rad/s
Temperature	Fahrenheit

Model (B2)

Geometry

TABLE 2
Model (B2) > Geometry

Object Name	*Geometry*
State	Fully Defined
Definition	
Source	U:\Documents\Thesis Sections\Octagonal\V Stiff Clay\Longer pile_files\dp0\global\MECH\SYS\AssembledModel\SYS.pmdb
Type	ACP
Length Unit	Meters
Element Control	Program Controlled
Display Style	Body Color
Bounding Box	
Length X	13.066 in
Length Y	360. in
Length Z	13.066 in
Properties	
Volume	1440. in³
Mass	104.05 lbm
Statistics	
Bodies	2
Active Bodies	1
Nodes	9248
Elements	9216
Mesh Metric	None
Update Options	
Assign Default Material	No
Advanced Geometry Options	
Analysis Type	3-D

TABLE 3
Model (B2) > Geometry > Parts

Object Name	*Surface Body(ACP (Pre))*	*Solid(ACP (Pre))*
State	Meshed	Suppressed
Graphics Properties		
Visible	Yes	No
Transparency	1	
Definition		
Suppressed	No	Yes
Dimension	3D	
Stiffness Behavior	Flexible	
Coordinate System	Default Coordinate System	Global Coordinate System(ACP (Pre))
Reference Temperature	By Environment	
Thickness	Defined By Composites	
Thickness Mode	Manual	
Offset Type	Defined By Composites	
Treatment	None	
Material		
Assignment	Composite Material	Concrete
Nonlinear Effects	Yes	
Thermal Strain Effects	Yes	
Bounding Box		
Length X	13.066 in	
Length Y	360. in	
Length Z	13.066 in	
Properties		
Volume	1440. in³	43456 in³
Centroid X	-0.96117 in	
Centroid Y	180. in	
Centroid Z	1.1762e-016 in	-2.3977e-017 in
Surface Area(approx.)	14400 in²	
Mass		3610.9 lbm
Moment of Inertia Ip1		3.9032e+007 lbm·in²

Moment of Inertia Ip2		69529 lbm·in²
Moment of Inertia Ip3		3.9032e+007 lbm·in²
Statistics		
Nodes	9248	0
Elements	9216	0
Mesh Metric	None	
Transfer Properties		
Source	A5::ACP (Pre)	
Read Only	Yes	

TABLE 4
Model (B2) > Materials

Object Name	*Materials*
State	Fully Defined
Statistics	
Materials	2
Material Assignments	0

Coordinate Systems

TABLE 5
Model (B2) > Coordinate Systems > Coordinate System

Object Name	*Global Coordinate System*	*Global Coordinate System(ACP (Pre))*
State	Fully Defined	
Definition		
Type	Cartesian	
Coordinate System ID	0.	
Coordinate System		Program Controlled
APDL Name		
Suppressed		No
Origin		
Origin X	0. in	
Origin Y	0. in	
Origin Z	0. in	
Define By		Global Coordinates
Location		Defined
Directional Vectors		
X Axis Data	[1. 0. 0.]	
Y Axis Data	[0. 1. 0.]	
Z Axis Data	[0. 0. 1.]	
Principal Axis		
Axis		X
Define By		Fixed Vector
Orientation About Principal Axis		
Axis		Y
Define By		Fixed Vector
Transfer Properties		
Source		A5::ACP (Pre)
Read Only		Yes
Transformations		
Base Configuration		Absolute
Transformed Configuration		[0. 0. 0.]

Connections

TABLE 6
Model (B2) > Connections

Object Name	*Connections*
State	Fully Defined
Auto Detection	
Generate Automatic Connection On Refresh	Yes
Transparency	
Enabled	Yes

TABLE 7
Model (B2) > Connections > Contacts(ACP (Pre))

Object Name	*Contacts(ACP (Pre))*
State	Suppressed
Definition	
Connection Type	Contact
Scope	
Scoping Method	Source Assembly
Source Assembly	A5::ACP (Pre)
Auto Detection	
Tolerance Type	Slider
Tolerance Slider	0.
Tolerance Value	0.90118 in
Use Range	No

Face/Face	Yes
Face-Face Angle Tolerance	75. °
Face Overlap Tolerance	Off
Cylindrical Faces	Include
Face/Edge	No
Edge/Edge	No
Priority	Include All
Group By	Bodies
Search Across	Bodies
Statistics	
Connections	1
Active Connections	0
Transfer Properties	
Source	A5::ACP (Pre)
Read Only	Yes

TABLE 8
Model (B2) > Connections > Contacts(ACP (Pre)) > Contact Regions

Object Name	*Contact Region(ACP (Pre))*
State	Suppressed
Scope	
Scoping Method	Geometry Selection
Contact	8 Faces
Target	No Selection
Contact Bodies	Surface Body(ACP (Pre))
Target Bodies	Solid(ACP (Pre))
Contact Shell Face	Program Controlled
Shell Thickness Effect	No
Protected	No
Definition	
Type	Bonded
Scope Mode	Automatic
Behavior	Program Controlled
Trim Contact	Program Controlled
Trim Tolerance	0.90118 in
Suppressed	No
Advanced	
Formulation	Program Controlled
Small Sliding	Program Controlled
Detection Method	Program Controlled
Penetration Tolerance	Program Controlled
Elastic Slip Tolerance	Program Controlled
Normal Stiffness	Program Controlled
Update Stiffness	Program Controlled
Pinball Region	Program Controlled
Geometric Modification	
Contact Geometry Correction	None
Target Geometry Correction	None
Transfer Properties	
Source	A5::ACP (Pre)
Read Only	Yes

TABLE 9
Model (B2) > Connections > Springs

Object Name	*Longitudinal - Ground To Surface Body(ACP (Pre))*	*Longitudinal - Ground To Surface Body(ACP (Pre)) 2*	*Longitudinal - Ground To Surface Body(ACP (Pre)) 3*	*Longitudinal - Ground To Surface Body(ACP (Pre)) 4*	*Longitudinal - Ground To Surface Body(ACP (Pre)) 5*	*Longitudinal - Ground To Surface Body(ACP (Pre)) 6*	*Longitudinal - Ground To Surface Body(ACP (Pre)) 7*	*Longitudinal - Ground To Surface Body(ACP (Pre)) 8*	*Longitudinal - Ground To Surface Body(ACP (Pre)) 9*	*Longitudinal - Ground To Surface Body(ACP (Pre)) 10*	*Longitudinal - Ground To Surface Body(ACP (Pre)) 11*
State	Fully Defined										
Graphics Properties											
Visible	Yes										
Definition											
Material	None										
Type	Longitudinal										
Spring Behavior	Both										
Longitudinal Stiffness	Tabular Data										
Longitudinal Damping	0. lbf·s/in										
Preload	None										
Suppressed	No										
Spring Length	12. in										
Element APDL Name											
Scope											
Scope	Body-Ground										

Reference											
Coordinate System	Global Coordinate System										
Reference X Coordinate	17.572 in										
Reference Y Coordinate	0. in	12. in	24. in	36. in	48. in	60. in	72. in	84. in	96. in	108. in	120. in
Reference Z Coordinate	0. in	1.3688e-017 in	7.8541e-016 in								
Reference Location	Defined										
Mobile											
Scoping Method	Geometry Selection										
Applied By	Remote Attachment										
Scope	8 Faces										
Body	Surface Body(ACP (Pre))										
Coordinate System	Global Coordinate System										
Mobile X Coordinate	5.5716 in										
Mobile Y Coordinate	0. in	12. in	24. in	36. in	48. in	60. in	72. in	84. in	96. in	108. in	120. in
Mobile Z Coordinate	0. in	1.3688e-017 in	7.8541e-016 in								
Mobile Location	Defined										
Behavior	Rigid										
Pinball Region	6. in										

FIGURE 1
Model (B2) > Connections > Longitudinal - Ground To Surface Body(ACP (Pre))

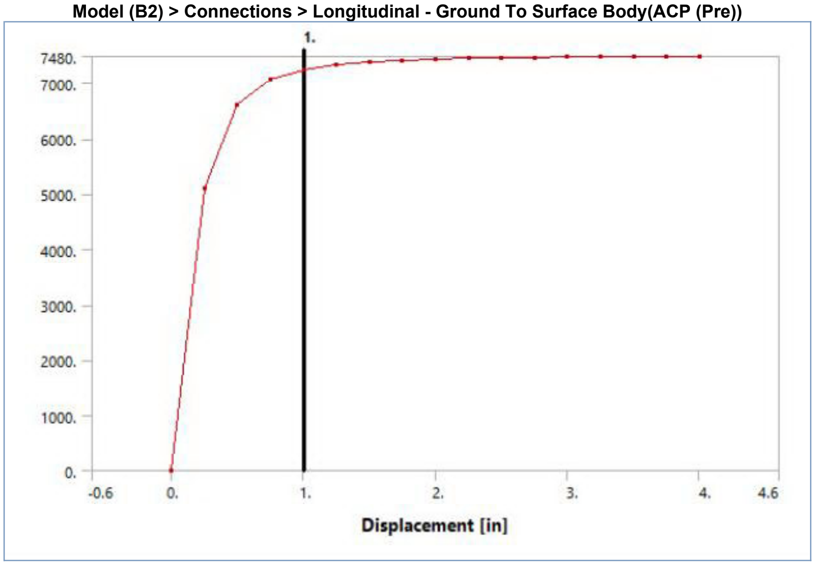

TABLE 10
Model (B2) > Connections > Longitudinal - Ground To Surface Body(ACP (Pre))

Displacement [in]	Force [lbf]
0.	0.
0.25	5110.
0.5	6610.
0.75	7060.
1.	7240.
1.25	7330.
1.5	7380.
1.75	7410.
2.	7430.
2.25	7450.
2.5	7460.
2.75	
3.	7470.
3.25	
3.5	7480.
3.75	
4.	

FIGURE 2
Model (B2) > Connections > Longitudinal - Ground To Surface Body(ACP (Pre)) 2

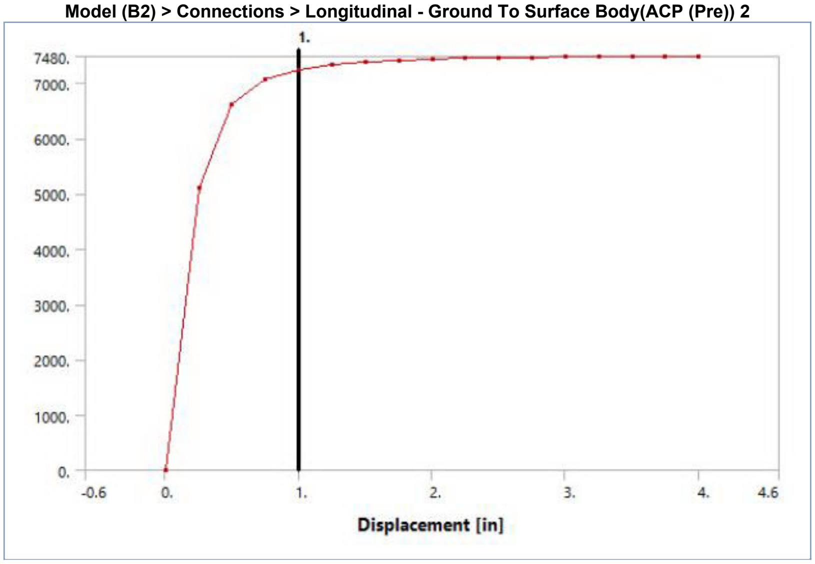

TABLE 11
Model (B2) > Connections > Longitudinal - Ground To Surface Body(ACP (Pre)) 2

Displacement [in]	Force [lbf]
0.	0.
0.25	5110.
0.5	6610.
0.75	7060.
1.	7240.
1.25	7330.
1.5	7380.
1.75	7410.
2.	7430.
2.25	7450.
2.5	7460.
2.75	
3.	7470.
3.25	
3.5	7480.
3.75	
4.	

FIGURE 3
Model (B2) > Connections > Longitudinal - Ground To Surface Body(ACP (Pre)) 3

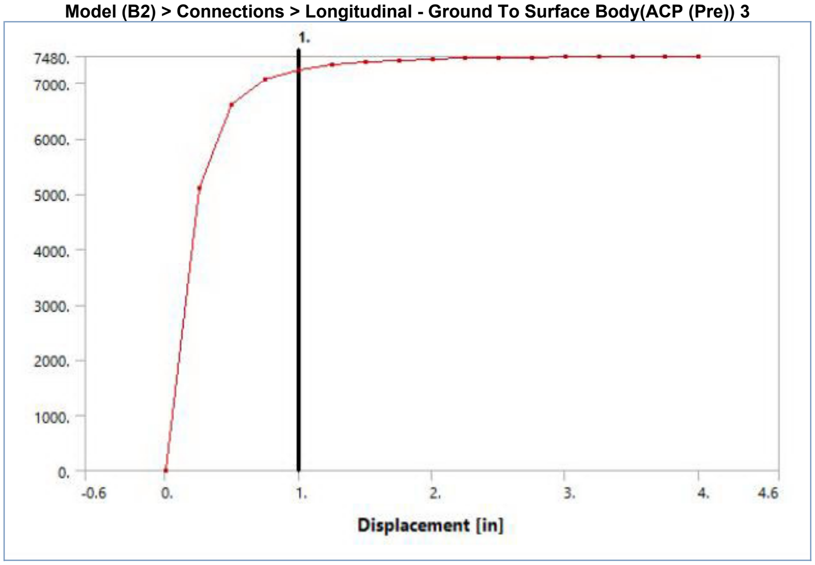

TABLE 12
Model (B2) > Connections > Longitudinal - Ground To Surface Body(ACP (Pre)) 3

Displacement [in]	Force [lbf]
0.	0.
0.25	5110.

0.5	6610.
0.75	7060.
1.	7240.
1.25	7330.
1.5	7380.
1.75	7410.
2.	7430.
2.25	7450.
2.5	7460.
2.75	
3.	7470.
3.25	
3.5	7480.
3.75	
4.	

FIGURE 4
Model (B2) > Connections > Longitudinal - Ground To Surface Body(ACP (Pre)) 4

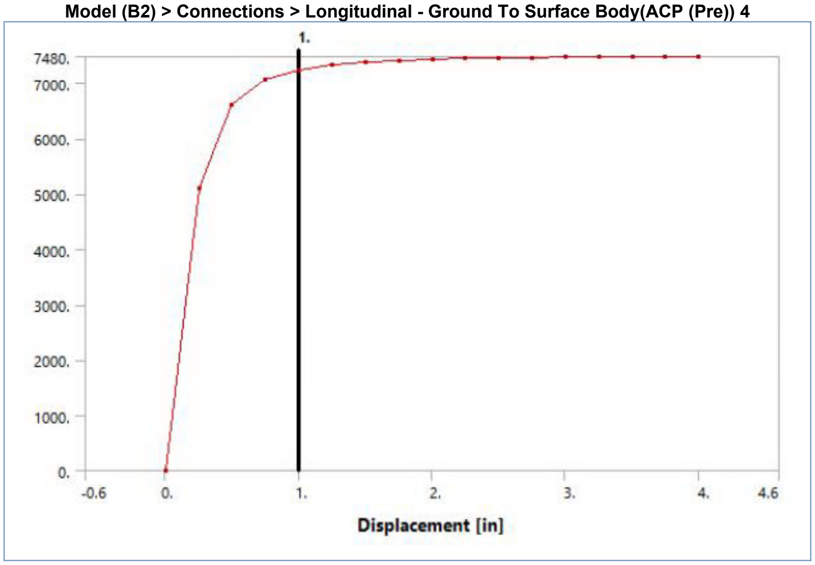

TABLE 13
Model (B2) > Connections > Longitudinal - Ground To Surface Body(ACP (Pre)) 4

Displacement [in]	Force [lbf]
0.	0.
0.25	5110.
0.5	6610.
0.75	7060.
1.	7240.
1.25	7330.
1.5	7380.
1.75	7410.
2.	7430.
2.25	7450.
2.5	7460.
2.75	
3.	7470.
3.25	
3.5	7480.
3.75	
4.	

FIGURE 5
Model (B2) > Connections > Longitudinal - Ground To Surface Body(ACP (Pre)) 5

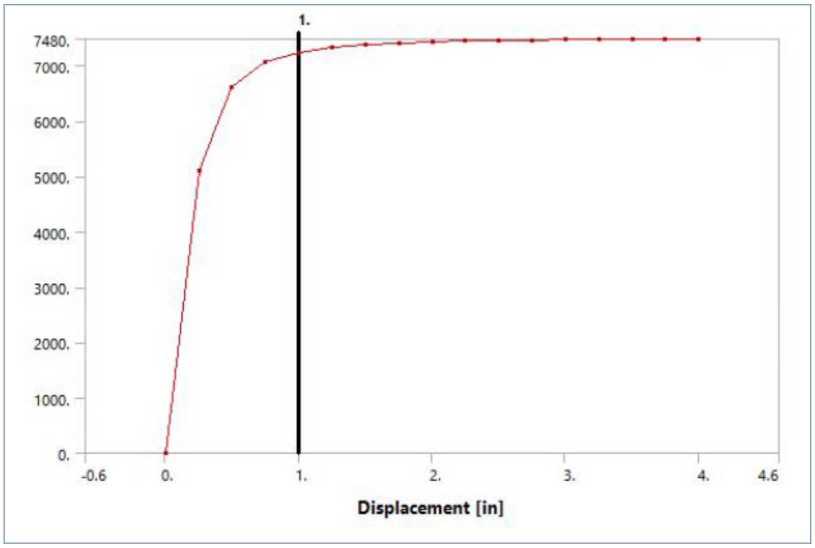

TABLE 14
Model (B2) > Connections > Longitudinal - Ground To Surface Body(ACP (Pre)) 5

Displacement [in]	Force [lbf]
0.	0.
0.25	5110.
0.5	6610.
0.75	7060.
1.	7240.
1.25	7330.
1.5	7380.
1.75	7410.
2.	7430.
2.25	7450.
2.5	7460.
2.75	
3.	7470.
3.25	
3.5	7480.
3.75	
4.	

FIGURE 6
Model (B2) > Connections > Longitudinal - Ground To Surface Body(ACP (Pre)) 6

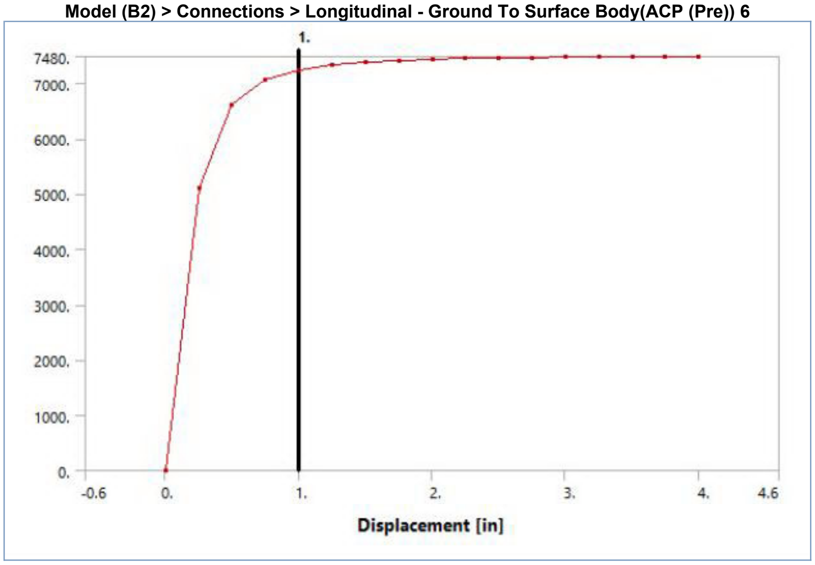

TABLE 15
Model (B2) > Connections > Longitudinal - Ground To Surface Body(ACP (Pre)) 6

Displacement [in]	Force [lbf]
0.	0.
0.25	5110.
0.5	6610.
0.75	7060.

1.	7240.
1.25	7330.
1.5	7380.
1.75	7410.
2.	7430.
2.25	7450.
2.5	7460.
2.75	
3.	7470.
3.25	
3.5	7480.
3.75	
4.	

FIGURE 7
Model (B2) > Connections > Longitudinal - Ground To Surface Body(ACP (Pre)) 7

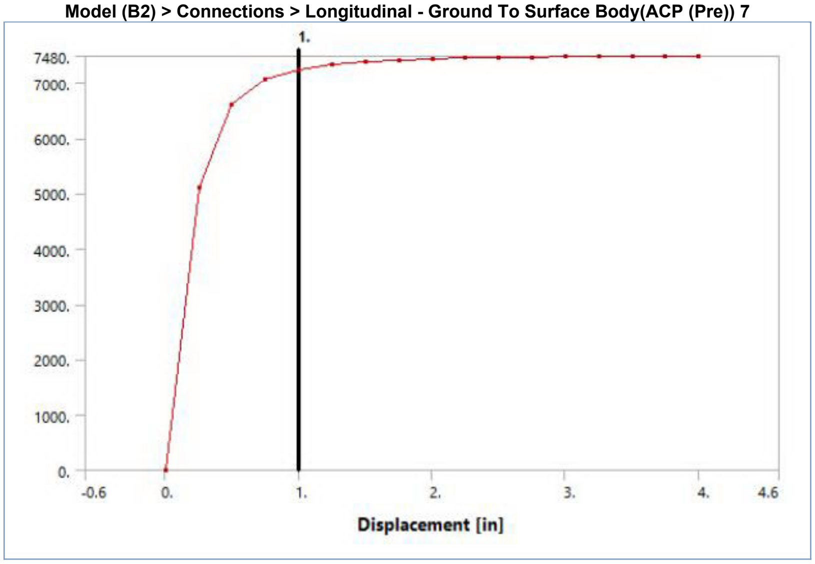

TABLE 16
Model (B2) > Connections > Longitudinal - Ground To Surface Body(ACP (Pre)) 7

Displacement [in]	Force [lbf]
0.	0.
0.25	5110.
0.5	6610.
0.75	7060.
1.	7240.
1.25	7330.
1.5	7380.
1.75	7410.
2.	7430.
2.25	7450.
2.5	7460.
2.75	
3.	7470.
3.25	
3.5	7480.
3.75	
4.	

FIGURE 8
Model (B2) > Connections > Longitudinal - Ground To Surface Body(ACP (Pre)) 8

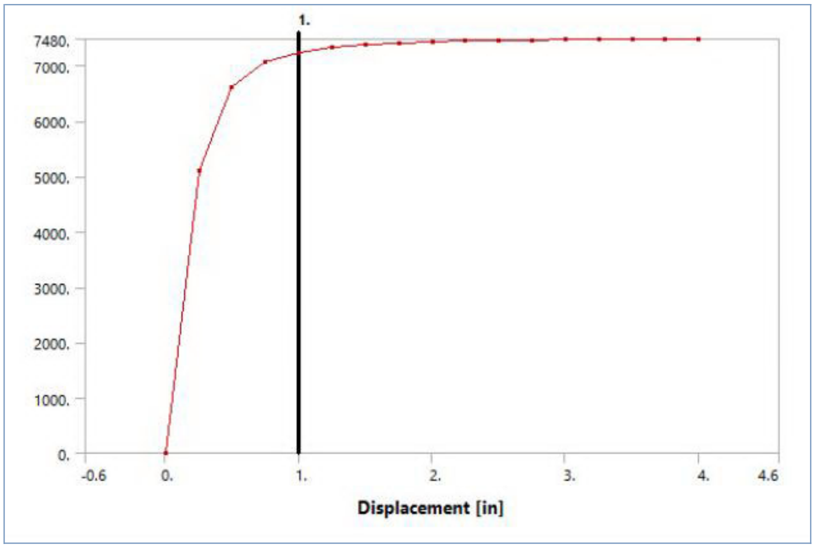

TABLE 17
Model (B2) > Connections > Longitudinal - Ground To Surface Body(ACP (Pre)) 8

Displacement [in]	Force [lbf]
0.	0.
0.25	5110.
0.5	6610.
0.75	7060.
1.	7240.
1.25	7330.
1.5	7380.
1.75	7410.
2.	7430.
2.25	7450.
2.5	7460.
2.75	
3.	7470.
3.25	
3.5	7480.
3.75	
4.	

FIGURE 9
Model (B2) > Connections > Longitudinal - Ground To Surface Body(ACP (Pre)) 9

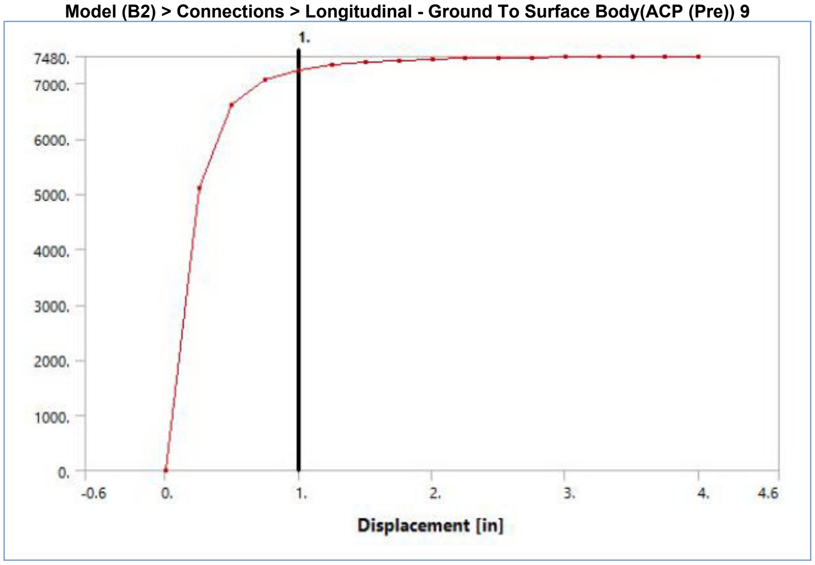

TABLE 18
Model (B2) > Connections > Longitudinal - Ground To Surface Body(ACP (Pre)) 9

Displacement [in]	Force [lbf]
0.	0.
0.25	5110.
0.5	6610.
0.75	7060.

1.	7240.
1.25	7330.
1.5	7380.
1.75	7410.
2.	7430.
2.25	7450.
2.5	7460.
2.75	
3.	7470.
3.25	
3.5	7480.
3.75	
4.	

FIGURE 10
Model (B2) > Connections > Longitudinal - Ground To Surface Body(ACP (Pre)) 10

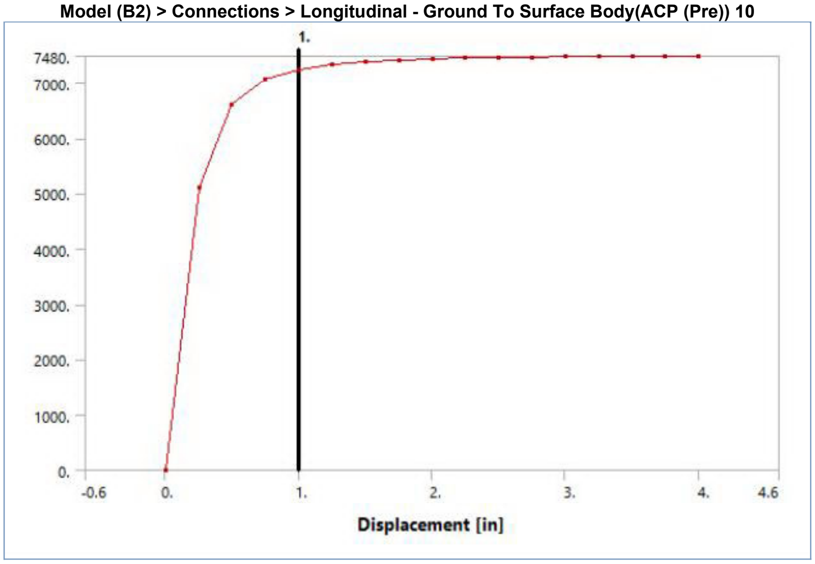

TABLE 19
Model (B2) > Connections > Longitudinal - Ground To Surface Body(ACP (Pre)) 10

Displacement [in]	Force [lbf]
0.	0.
0.25	5110.
0.5	6610.
0.75	7060.
1.	7240.
1.25	7330.
1.5	7380.
1.75	7410.
2.	7430.
2.25	7450.
2.5	7460.
2.75	
3.	7470.
3.25	
3.5	7480.
3.75	
4.	

FIGURE 11
Model (B2) > Connections > Longitudinal - Ground To Surface Body(ACP (Pre)) 11

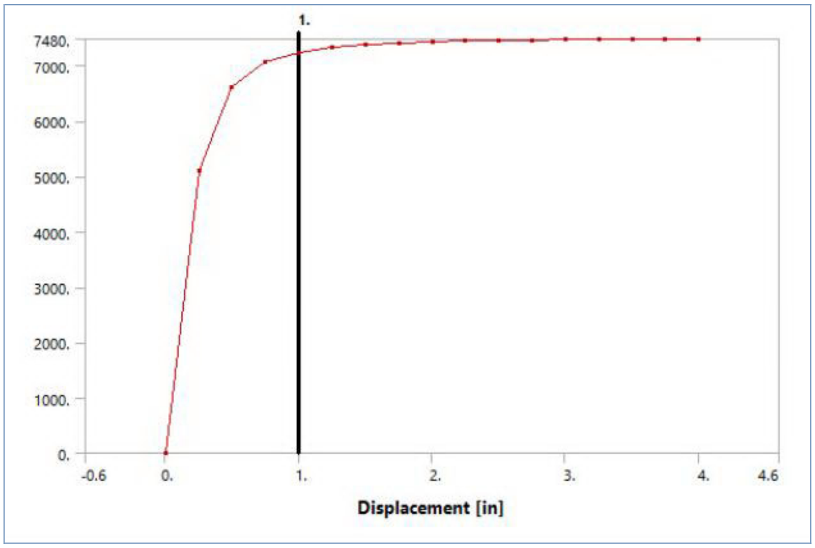

TABLE 20
Model (B2) > Connections > Longitudinal - Ground To Surface Body(ACP (Pre)) 11

Displacement [in]	Force [lbf]
0.	0.
0.25	5110.
0.5	6610.
0.75	7060.
1.	7240.
1.25	7330.
1.5	7380.
1.75	7410.
2.	7430.
2.25	7450.
2.5	7460.
2.75	
3.	7470.
3.25	
3.5	7480.
3.75	
4.	

TABLE 21
Model (B2) > Connections > Springs

Object Name	*Longitudinal - Ground To Surface Body(ACP (Pre)) 12*	*Longitudinal - Ground To Surface Body(ACP (Pre)) 13*	*Longitudinal - Ground To Surface Body(ACP (Pre)) 14*	*Longitudinal - Ground To Surface Body(ACP (Pre)) 15*	*Longitudinal - Ground To Surface Body(ACP (Pre)) 16*	*Longitudinal - Ground To Surface Body(ACP (Pre)) 17*	*Longitudinal - Ground To Surface Body(ACP (Pre)) 18*	*Longitudinal - Ground To Surface Body(ACP (Pre)) 19*	*Longitudinal - Ground To Surface Body(ACP (Pre)) 20*	*Longitudinal - Ground To Surface Body(ACP (Pre)) 21*	*Z Axis Spring*
State	Fully Defined										
Graphics Properties											
Visible	Yes										
Definition											
Material	None										
Type	Longitudinal										
Spring Behavior	Both										
Longitudinal Stiffness	Tabular Data										
Longitudinal Damping	0. lbf·s/in										
Preload	None										
Suppressed	No										
Spring Length	12. in										
Element APDL Name											
Scope											
Scope	Body-Ground										
Reference											
Coordinate System	Global Coordinate System										
Reference X Coordinate	17.572 in										0. in
Reference											

Y Coordinate	132. in	144. in	156. in	168. in	180. in	192. in	204. in	216. in	228. in	240. in	0. in
Reference Z Coordinate	7.8541e-016 in										17.572 in
Reference Location	Defined										
Mobile											
Scoping Method	Geometry Selection										
Applied By	Remote Attachment										
Scope	8 Faces										
Body	Surface Body(ACP (Pre))										
Coordinate System	Global Coordinate System										
Mobile X Coordinate	5.5716 in										0. in
Mobile Y Coordinate	132. in	144. in	156. in	168. in	180. in	192. in	204. in	216. in	228. in	240. in	0. in
Mobile Z Coordinate	7.8541e-016 in										5.5716 in
Mobile Location	Defined										
Behavior	Rigid										
Pinball Region	6. in										

FIGURE 12
Model (B2) > Connections > Longitudinal - Ground To Surface Body(ACP (Pre)) 12

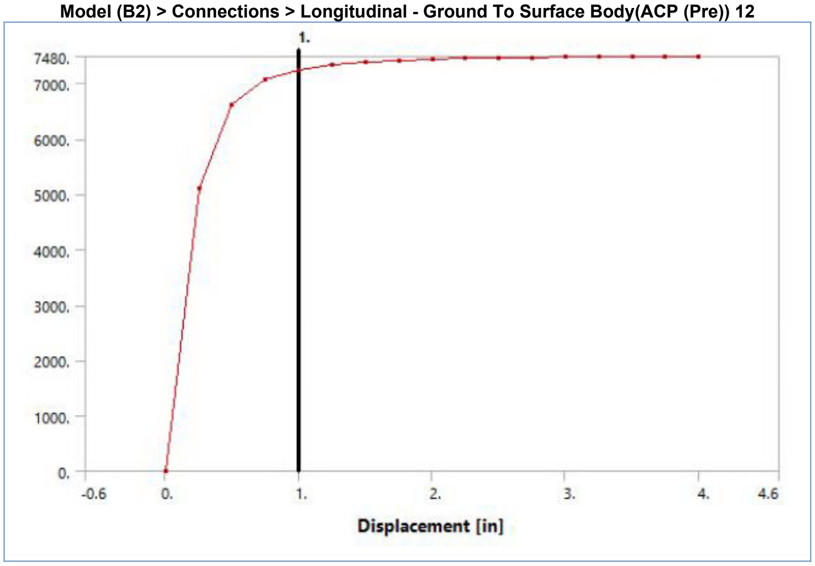

TABLE 22
Model (B2) > Connections > Longitudinal - Ground To Surface Body(ACP (Pre)) 12

Displacement [in]	Force [lbf]
0.	0.
0.25	5110.
0.5	6610.
0.75	7060.
1.	7240.
1.25	7330.
1.5	7380.
1.75	7410.
2.	7430.
2.25	7450.
2.5	7460.
2.75	
3.	7470.
3.25	
3.5	7480.
3.75	
4.	

FIGURE 13
Model (B2) > Connections > Longitudinal - Ground To Surface Body(ACP (Pre)) 13

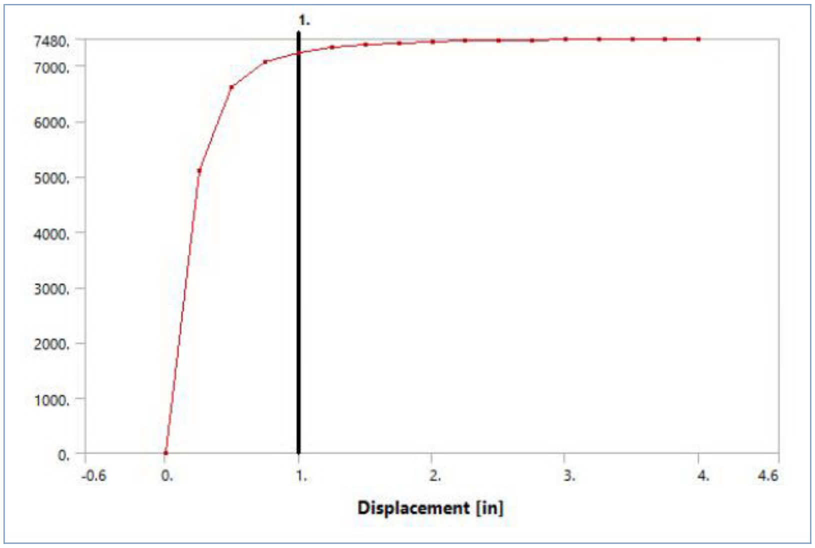

TABLE 23
Model (B2) > Connections > Longitudinal - Ground To Surface Body(ACP (Pre)) 13

Displacement [in]	Force [lbf]
0.	0.
0.25	5110.
0.5	6610.
0.75	7060.
1.	7240.
1.25	7330.
1.5	7380.
1.75	7410.
2.	7430.
2.25	7450.
2.5	7460.
2.75	
3.	7470.
3.25	
3.5	7480.
3.75	
4.	

FIGURE 14
Model (B2) > Connections > Longitudinal - Ground To Surface Body(ACP (Pre)) 14

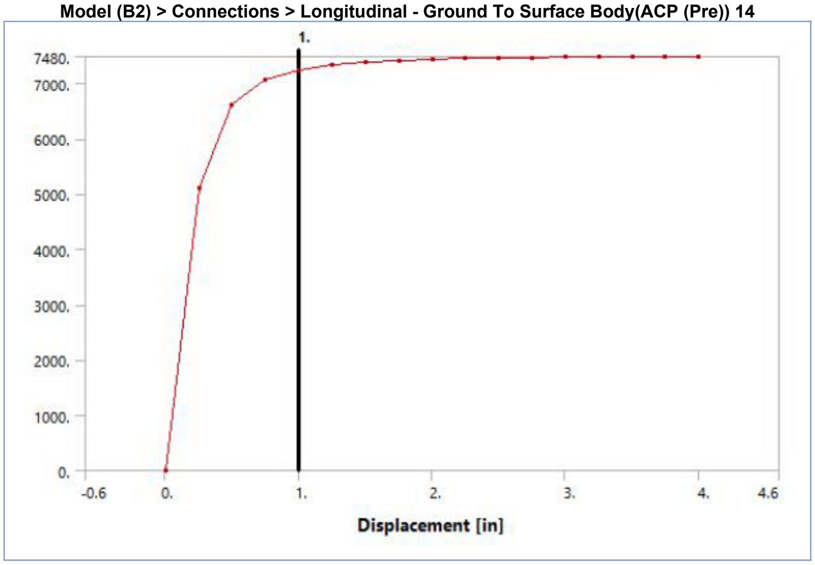

TABLE 24
Model (B2) > Connections > Longitudinal - Ground To Surface Body(ACP (Pre)) 14

Displacement [in]	Force [lbf]
0.	0.
0.25	5110.
0.5	6610.
0.75	7060.

1.	7240.
1.25	7330.
1.5	7380.
1.75	7410.
2.	7430.
2.25	7450.
2.5	7460.
2.75	
3.	7470.
3.25	
3.5	7480.
3.75	
4.	

FIGURE 15
Model (B2) > Connections > Longitudinal - Ground To Surface Body(ACP (Pre)) 15

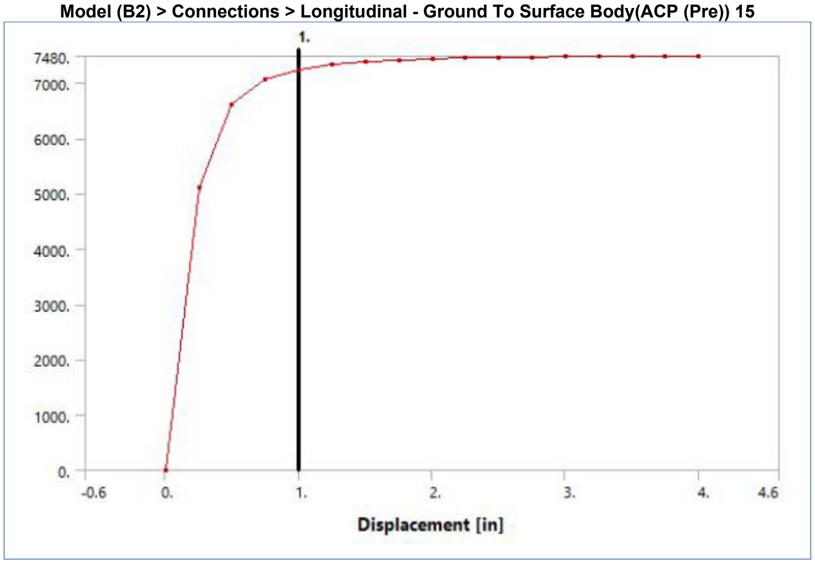

TABLE 25
Model (B2) > Connections > Longitudinal - Ground To Surface Body(ACP (Pre)) 15

Displacement [in]	Force [lbf]
0.	0.
0.25	5110.
0.5	6610.
0.75	7060.
1.	7240.
1.25	7330.
1.5	7380.
1.75	7410.
2.	7430.
2.25	7450.
2.5	7460.
2.75	
3.	7470.
3.25	
3.5	7480.
3.75	
4.	

FIGURE 16
Model (B2) > Connections > Longitudinal - Ground To Surface Body(ACP (Pre)) 16

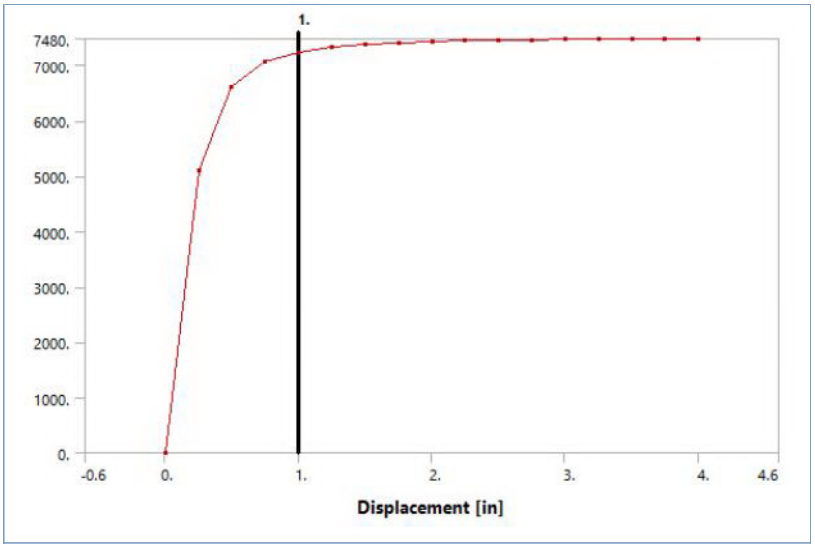

TABLE 26
Model (B2) > Connections > Longitudinal - Ground To Surface Body(ACP (Pre)) 16

<table>
<tr><th>Displacement [in]</th><th>Force [lbf]</th></tr>
<tr><td>0.</td><td>0.</td></tr>
<tr><td>0.25</td><td>5110.</td></tr>
<tr><td>0.5</td><td>6610.</td></tr>
<tr><td>0.75</td><td>7060.</td></tr>
<tr><td>1.</td><td>7240.</td></tr>
<tr><td>1.25</td><td>7330.</td></tr>
<tr><td>1.5</td><td>7380.</td></tr>
<tr><td>1.75</td><td>7410.</td></tr>
<tr><td>2.</td><td>7430.</td></tr>
<tr><td>2.25</td><td>7450.</td></tr>
<tr><td>2.5</td><td rowspan="2">7460.</td></tr>
<tr><td>2.75</td></tr>
<tr><td>3.</td><td rowspan="2">7470.</td></tr>
<tr><td>3.25</td></tr>
<tr><td>3.5</td><td rowspan="3">7480.</td></tr>
<tr><td>3.75</td></tr>
<tr><td>4.</td></tr>
</table>

FIGURE 17
Model (B2) > Connections > Longitudinal - Ground To Surface Body(ACP (Pre)) 17

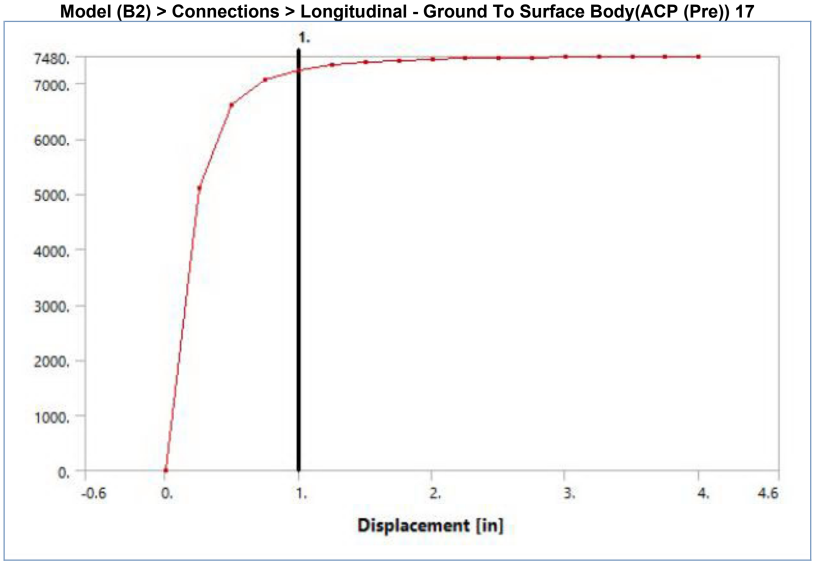

TABLE 27
Model (B2) > Connections > Longitudinal - Ground To Surface Body(ACP (Pre)) 17

Displacement [in]	Force [lbf]
0.	0.
0.25	5110.
0.5	6610.
0.75	7060.

1.	7240.
1.25	7330.
1.5	7380.
1.75	7410.
2.	7430.
2.25	7450.
2.5	7460.
2.75	
3.	7470.
3.25	
3.5	7480.
3.75	
4.	

FIGURE 18
Model (B2) > Connections > Longitudinal - Ground To Surface Body(ACP (Pre)) 18

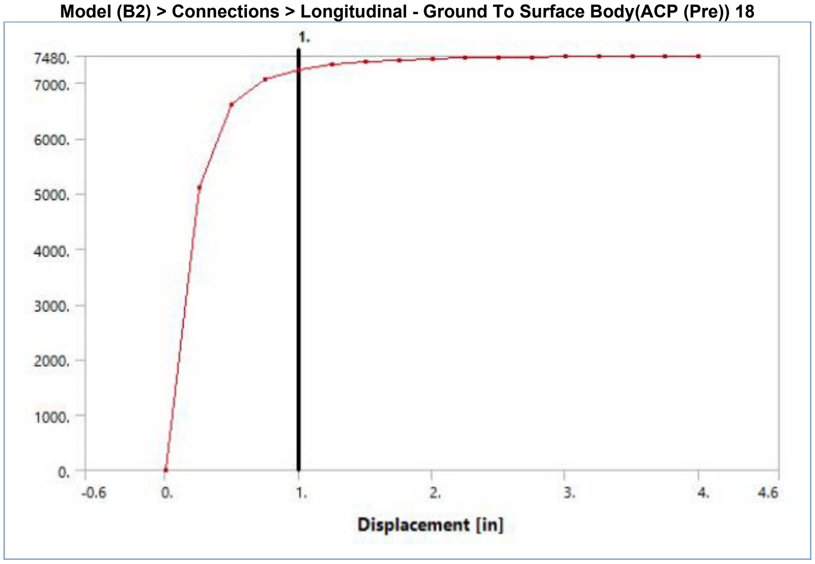

TABLE 28
Model (B2) > Connections > Longitudinal - Ground To Surface Body(ACP (Pre)) 18

Displacement [in]	Force [lbf]
0.	0.
0.25	5110.
0.5	6610.
0.75	7060.
1.	7240.
1.25	7330.
1.5	7380.
1.75	7410.
2.	7430.
2.25	7450.
2.5	7460.
2.75	
3.	7470.
3.25	
3.5	7480.
3.75	
4.	

FIGURE 19
Model (B2) > Connections > Longitudinal - Ground To Surface Body(ACP (Pre)) 19

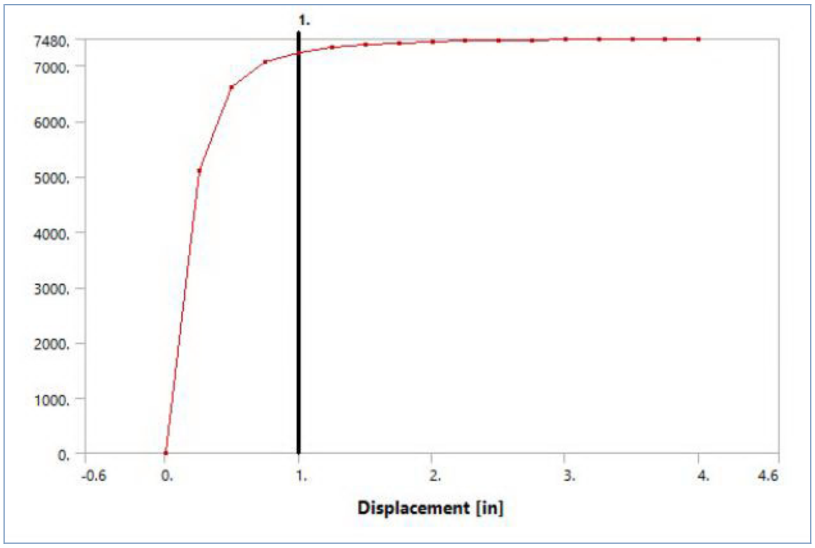

TABLE 29
Model (B2) > Connections > Longitudinal - Ground To Surface Body(ACP (Pre)) 19

Displacement [in]	Force [lbf]
0.	0.
0.25	5110.
0.5	6610.
0.75	7060.
1.	7240.
1.25	7330.
1.5	7380.
1.75	7410.
2.	7430.
2.25	7450.
2.5	7460.
2.75	
3.	7470.
3.25	
3.5	7480.
3.75	
4.	

FIGURE 20
Model (B2) > Connections > Longitudinal - Ground To Surface Body(ACP (Pre)) 20

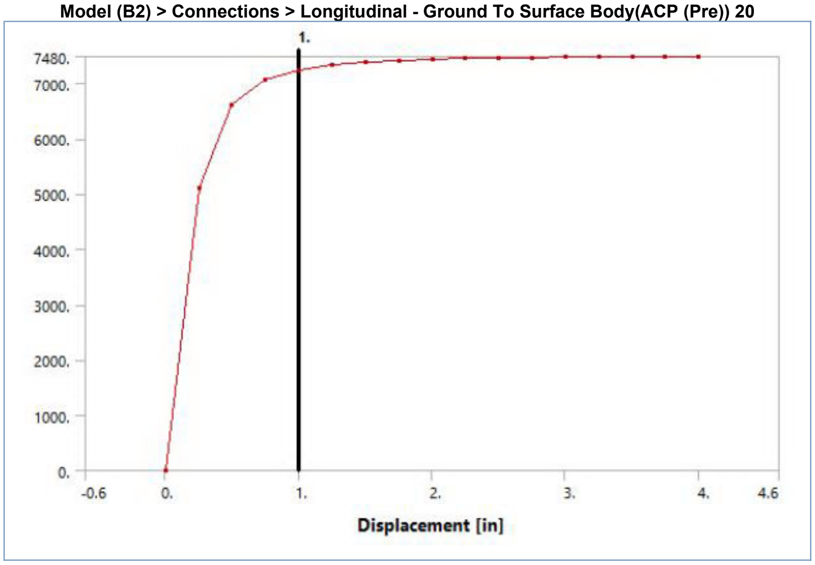

TABLE 30
Model (B2) > Connections > Longitudinal - Ground To Surface Body(ACP (Pre)) 20

Displacement [in]	Force [lbf]
0.	0.
0.25	5110.
0.5	6610.
0.75	7060.

1.	7240.
1.25	7330.
1.5	7380.
1.75	7410.
2.	7430.
2.25	7450.
2.5	7460.
2.75	
3.	7470.
3.25	
3.5	7480.
3.75	
4.	

FIGURE 21
Model (B2) > Connections > Longitudinal - Ground To Surface Body(ACP (Pre)) 21

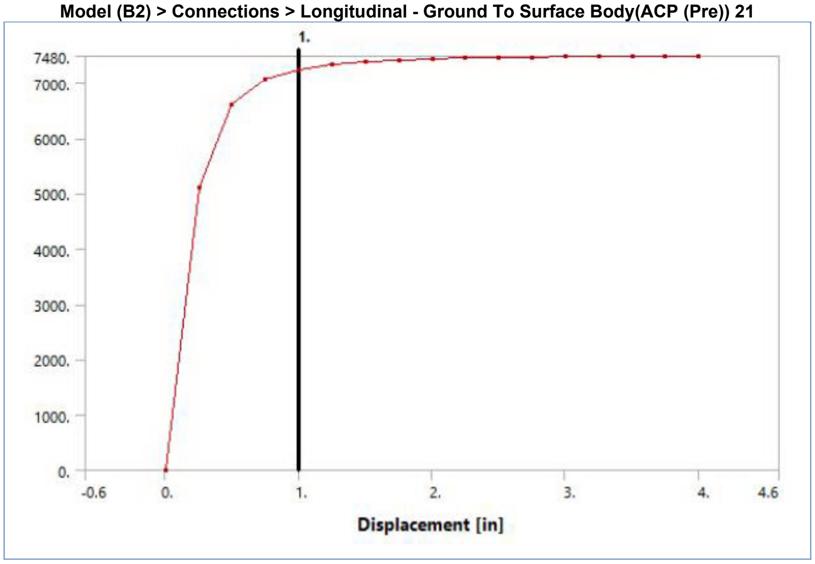

TABLE 31
Model (B2) > Connections > Longitudinal - Ground To Surface Body(ACP (Pre)) 21

Displacement [in]	Force [lbf]
0.	0.
0.25	5110.
0.5	6610.
0.75	7060.
1.	7240.
1.25	7330.
1.5	7380.
1.75	7410.
2.	7430.
2.25	7450.
2.5	7460.
2.75	
3.	7470.
3.25	
3.5	7480.
3.75	
4.	

FIGURE 22
Model (B2) > Connections > Z Axis Spring

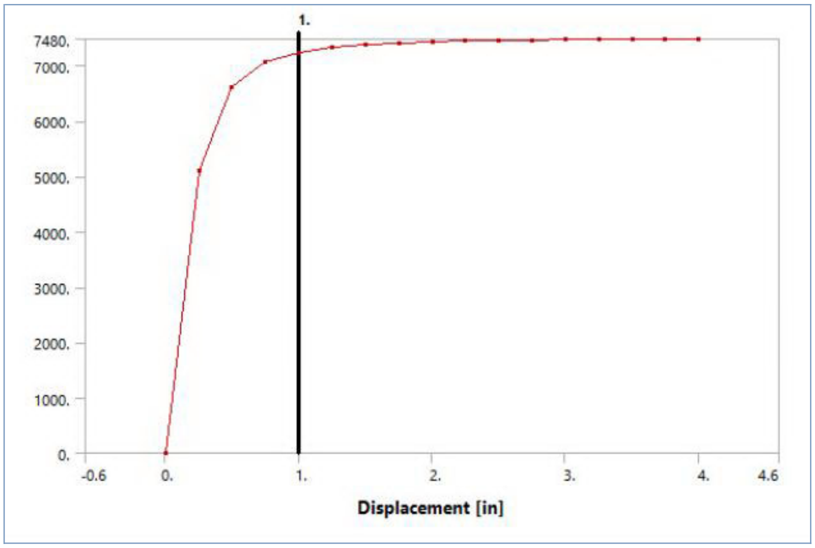

TABLE 32
Model (B2) > Connections > Z Axis Spring

Displacement [in]	Force [lbf]
0.	0.
0.25	5110.
0.5	6610.
0.75	7060.
1.	7240.
1.25	7330.
1.5	7380.
1.75	7410.
2.	7430.
2.25	7450.
2.5	7460.
2.75	
3.	7470.
3.25	
3.5	7480.
3.75	
4.	

TABLE 33
Model (B2) > Connections > Springs

Object Name	*Z Axis Spring 2*	*Z Axis Spring 3*	*Z Axis Spring 4*	*Z Axis Spring 5*	*Z Axis Spring 6*	*Z Axis Spring 7*	*Z Axis Spring 8*	*Z Axis Spring 9*	*Z Axis Spring 10*	*Z Axis Spring 11*	*Z Axis Spring 12*
State	Fully Defined										
Graphics Properties											
Visible	Yes										
Definition											
Material	None										
Type	Longitudinal										
Spring Behavior	Both										
Longitudinal Stiffness	Tabular Data										
Longitudinal Damping	0. lbf·s/in										
Preload	None										
Suppressed	No										
Spring Length	12. in										
Element APDL Name											
Scope											
Scope	Body-Ground										
Reference											
Coordinate System	Global Coordinate System										
Reference X Coordinate	0. in										
Reference Y Coordinate	12. in	24. in	36. in	48. in	60. in	72. in	84. in	96. in	108. in	120. in	132. in
Reference Z Coordinate	17.572 in	18.53 in									
Reference Location	Defined										
Mobile											
Scoping Method	Geometry Selection										

Applied By	Remote Attachment										
Scope	8 Faces										
Body	Surface Body(ACP (Pre))										
Coordinate System	Global Coordinate System										
Mobile X Coordinate	0. in										
Mobile Y Coordinate	12. in	24. in	36. in	48. in	60. in	72. in	84. in	96. in	108. in	120. in	132. in
Mobile Z Coordinate	5.5716 in	6.53 in									
Mobile Location	Defined										
Behavior	Rigid										
Pinball Region	6. in										

FIGURE 23
Model (B2) > Connections > Z Axis Spring 2

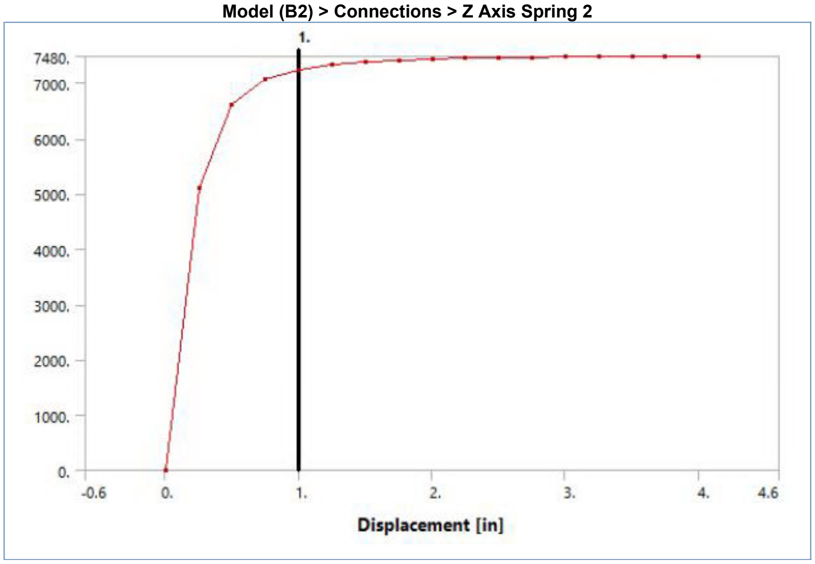

TABLE 34
Model (B2) > Connections > Z Axis Spring 2

Displacement [in]	Force [lbf]
0.	0.
0.25	5110.
0.5	6610.
0.75	7060.
1.	7240.
1.25	7330.
1.5	7380.
1.75	7410.
2.	7430.
2.25	7450.
2.5	7460.
2.75	
3.	7470.
3.25	
3.5	7480.
3.75	
4.	

FIGURE 24
Model (B2) > Connections > Z Axis Spring 3

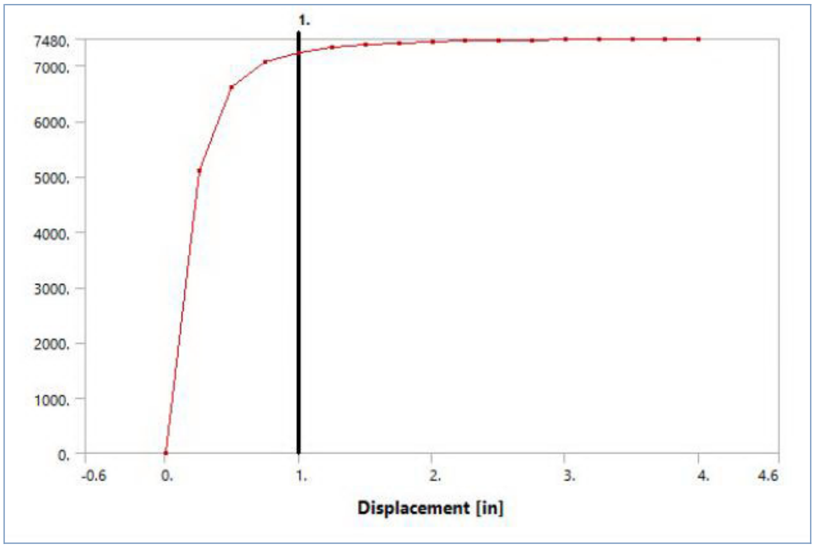

TABLE 35
Model (B2) > Connections > Z Axis Spring 3

Displacement [in]	Force [lbf]
0.	0.
0.25	5110.
0.5	6610.
0.75	7060.
1.	7240.
1.25	7330.
1.5	7380.
1.75	7410.
2.	7430.
2.25	7450.
2.5	7460.
2.75	
3.	7470.
3.25	
3.5	7480.
3.75	
4.	

FIGURE 25
Model (B2) > Connections > Z Axis Spring 4

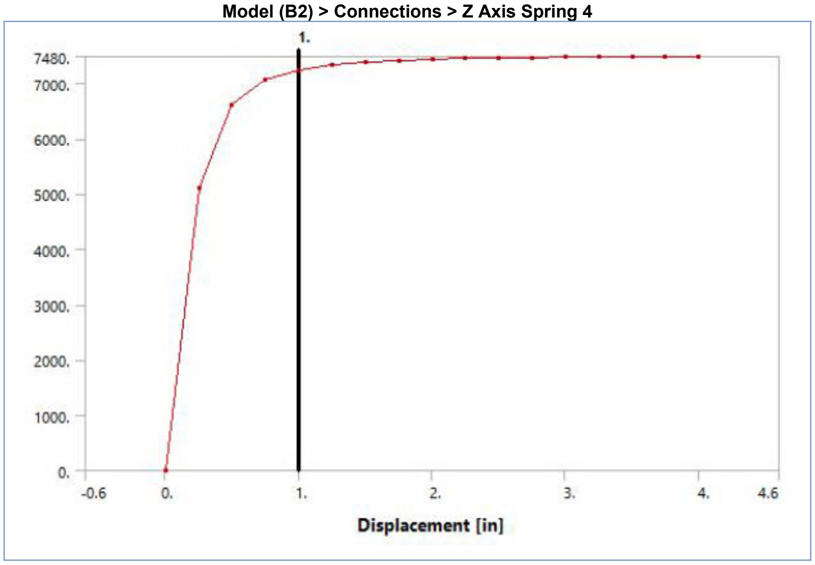

TABLE 36
Model (B2) > Connections > Z Axis Spring 4

Displacement [in]	Force [lbf]
0.	0.
0.25	5110.
0.5	6610.
0.75	7060.

1.	7240.
1.25	7330.
1.5	7380.
1.75	7410.
2.	7430.
2.25	7450.
2.5	7460.
2.75	
3.	7470.
3.25	
3.5	7480.
3.75	
4.	

FIGURE 26
Model (B2) > Connections > Z Axis Spring 5

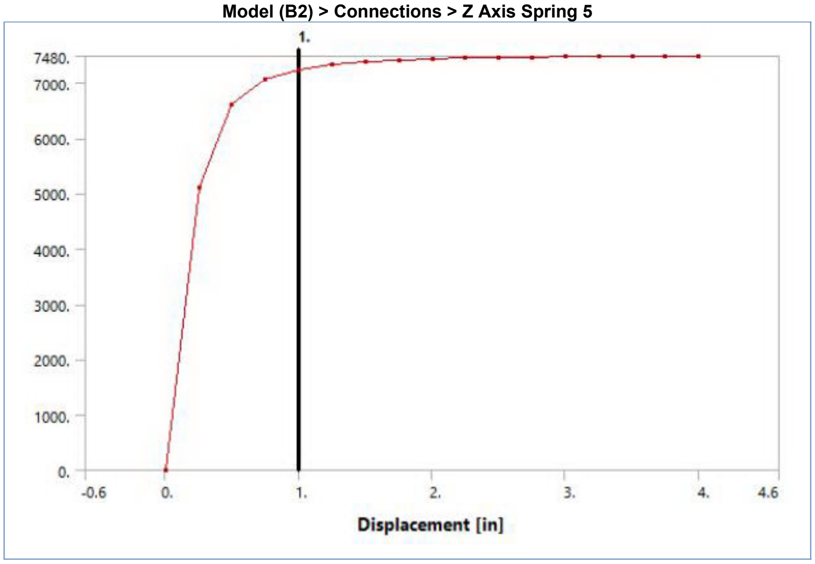

TABLE 37
Model (B2) > Connections > Z Axis Spring 5

Displacement [in]	Force [lbf]
0.	0.
0.25	5110.
0.5	6610.
0.75	7060.
1.	7240.
1.25	7330.
1.5	7380.
1.75	7410.
2.	7430.
2.25	7450.
2.5	7460.
2.75	
3.	7470.
3.25	
3.5	7480.
3.75	
4.	

FIGURE 27
Model (B2) > Connections > Z Axis Spring 6

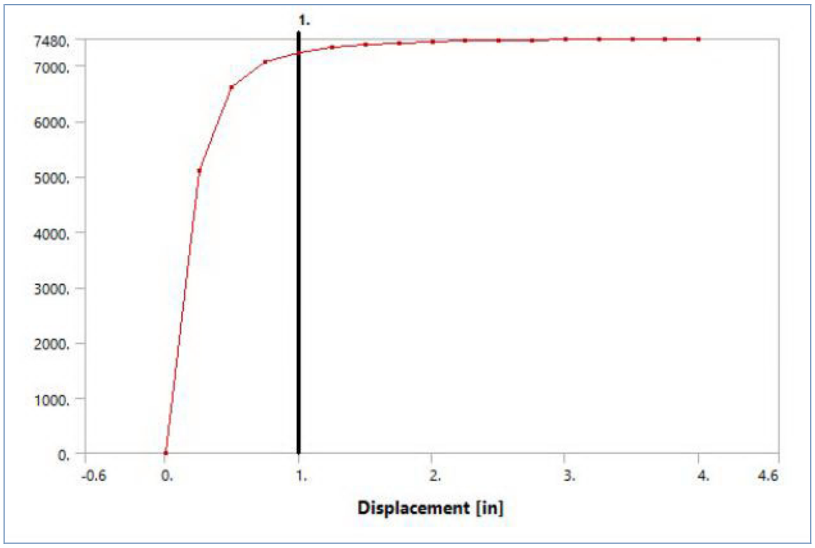

TABLE 38
Model (B2) > Connections > Z Axis Spring 6

Displacement [in]	Force [lbf]
0.	0.
0.25	5110.
0.5	6610.
0.75	7060.
1.	7240.
1.25	7330.
1.5	7380.
1.75	7410.
2.	7430.
2.25	7450.
2.5	7460.
2.75	
3.	7470.
3.25	
3.5	7480.
3.75	
4.	

FIGURE 28
Model (B2) > Connections > Z Axis Spring 7

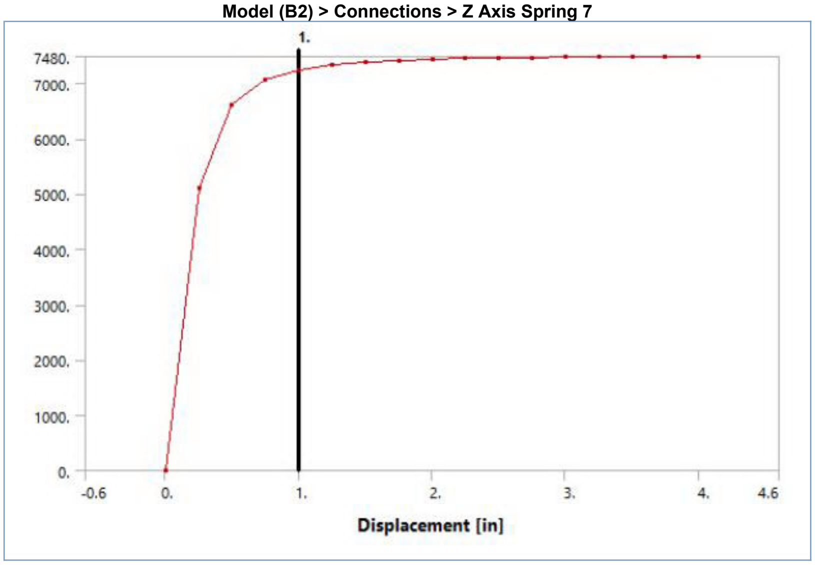

TABLE 39
Model (B2) > Connections > Z Axis Spring 7

Displacement [in]	Force [lbf]
0.	0.
0.25	5110.
0.5	6610.
0.75	7060.

1.	7240.
1.25	7330.
1.5	7380.
1.75	7410.
2.	7430.
2.25	7450.
2.5	7460.
2.75	
3.	7470.
3.25	
3.5	7480.
3.75	
4.	

FIGURE 29
Model (B2) > Connections > Z Axis Spring 8

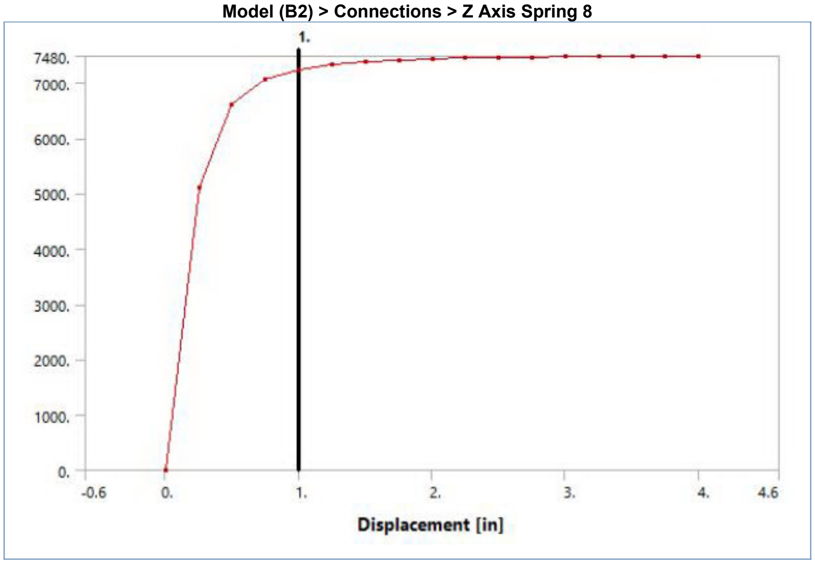

TABLE 40
Model (B2) > Connections > Z Axis Spring 8

Displacement [in]	Force [lbf]
0.	0.
0.25	5110.
0.5	6610.
0.75	7060.
1.	7240.
1.25	7330.
1.5	7380.
1.75	7410.
2.	7430.
2.25	7450.
2.5	7460.
2.75	
3.	7470.
3.25	
3.5	7480.
3.75	
4.	

FIGURE 30
Model (B2) > Connections > Z Axis Spring 9

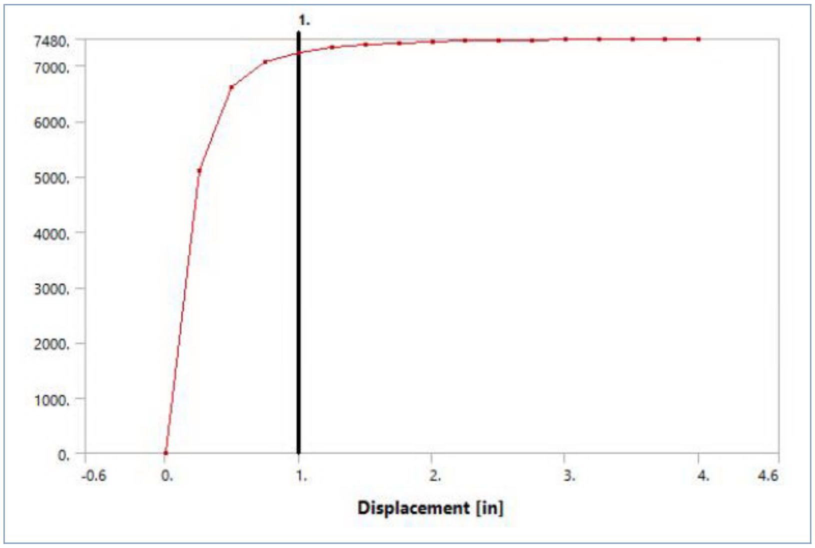

TABLE 41
Model (B2) > Connections > Z Axis Spring 9

Displacement [in]	Force [lbf]
0.	0.
0.25	5110.
0.5	6610.
0.75	7060.
1.	7240.
1.25	7330.
1.5	7380.
1.75	7410.
2.	7430.
2.25	7450.
2.5	7460.
2.75	
3.	7470.
3.25	
3.5	7480.
3.75	
4.	

FIGURE 31
Model (B2) > Connections > Z Axis Spring 10

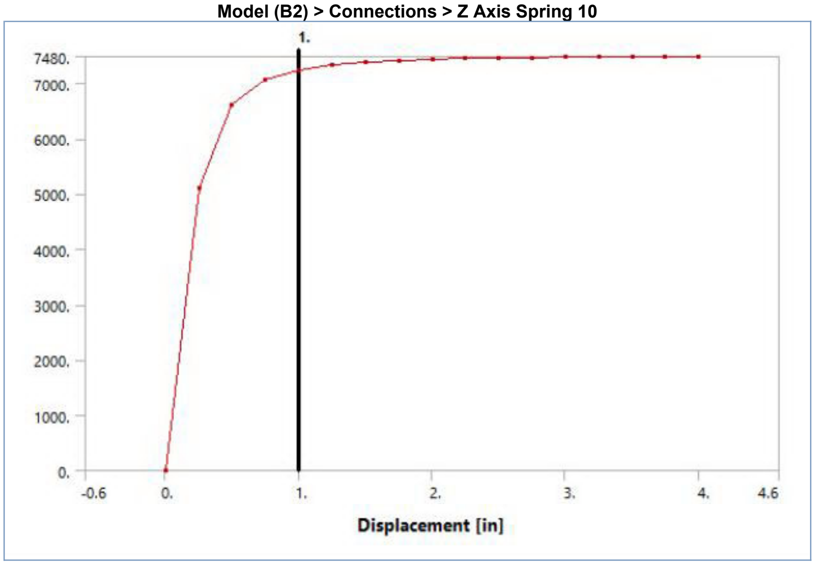

TABLE 42
Model (B2) > Connections > Z Axis Spring 10

Displacement [in]	Force [lbf]
0.	0.
0.25	5110.
0.5	6610.
0.75	7060.

1.	7240.
1.25	7330.
1.5	7380.
1.75	7410.
2.	7430.
2.25	7450.
2.5	7460.
2.75	
3.	7470.
3.25	
3.5	7480.
3.75	
4.	

FIGURE 32
Model (B2) > Connections > Z Axis Spring 11

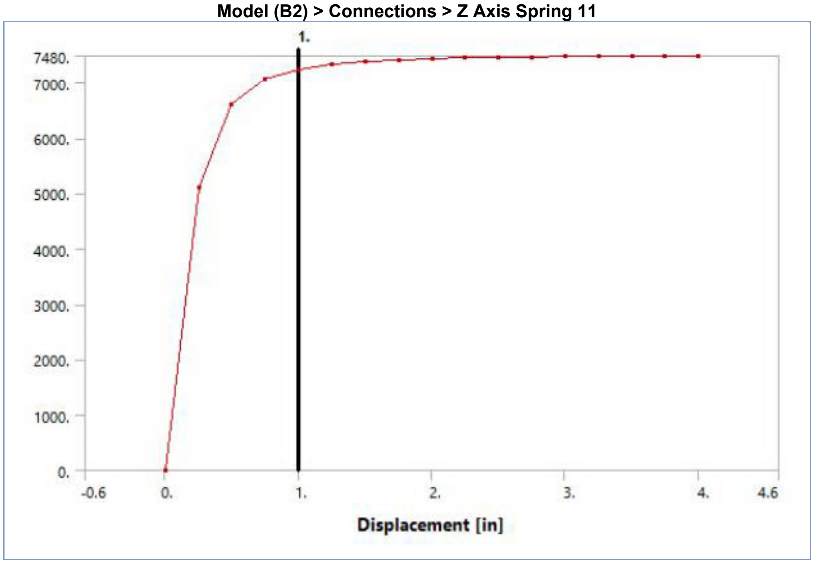

TABLE 43
Model (B2) > Connections > Z Axis Spring 11

Displacement [in]	Force [lbf]
0.	0.
0.25	5110.
0.5	6610.
0.75	7060.
1.	7240.
1.25	7330.
1.5	7380.
1.75	7410.
2.	7430.
2.25	7450.
2.5	7460.
2.75	
3.	7470.
3.25	
3.5	7480.
3.75	
4.	

FIGURE 33
Model (B2) > Connections > Z Axis Spring 12

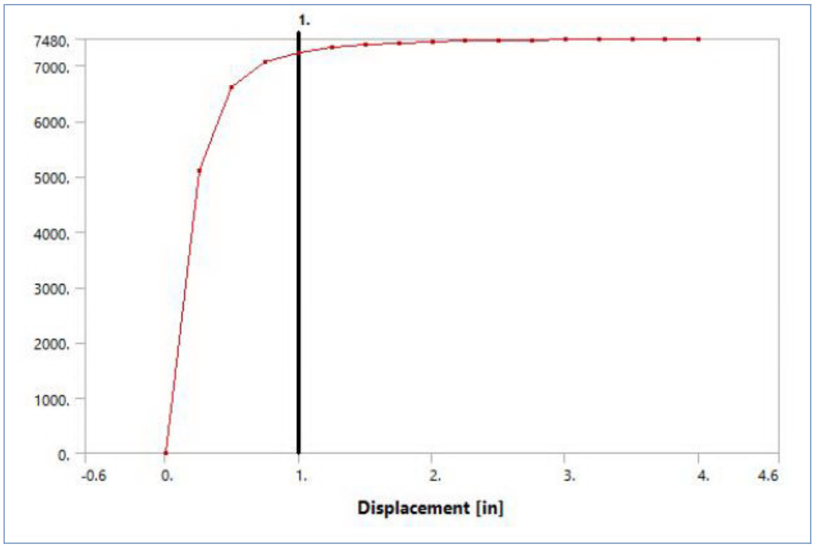

TABLE 44
Model (B2) > Connections > Z Axis Spring 12

Displacement [in]	Force [lbf]
0.	0.
0.25	5110.
0.5	6610.
0.75	7060.
1.	7240.
1.25	7330.
1.5	7380.
1.75	7410.
2.	7430.
2.25	7450.
2.5	7460.
2.75	
3.	7470.
3.25	
3.5	7480.
3.75	
4.	

TABLE 45
Model (B2) > Connections > Springs

Object Name	*Z Axis Spring 13*	*Z Axis Spring 14*	*Z Axis Spring 15*	*Z Axis Spring 16*	*Z Axis Spring 17*	*Z Axis Spring 18*	*Z Axis Spring 19*	*Z Axis Spring 20*	*Z Axis Spring 21*	*Slip Resistance Spring*	*Slip Resistance Spring 2*
State	Fully Defined										
Graphics Properties											
Visible	Yes										
Definition											
Material	None										
Type	Longitudinal										
Spring Behavior	Both										
Longitudinal Stiffness	Tabular Data										
Longitudinal Damping	0. lbf·s/in										
Preload	None										
Suppressed	No										
Spring Length	12. in										
Element APDL Name											
Scope											
Scope	Body-Ground										
Reference											
Coordinate System	Global Coordinate System										
Reference X Coordinate	0. in									1.3485 in	
Reference Y Coordinate	144. in	156. in	168. in	180. in	192. in	204. in	216. in	228. in	240. in	0. in	24. in
Reference Z Coordinate	18.53 in									5.5761 in	
Reference Location	Defined										
Mobile											
Scoping Method	Geometry Selection										

<table>
<tr><td>Applied By</td><td colspan="11">Remote Attachment</td></tr>
<tr><td>Scope</td><td colspan="11">8 Faces</td></tr>
<tr><td>Body</td><td colspan="11">Surface Body(ACP (Pre))</td></tr>
<tr><td>Coordinate System</td><td colspan="11">Global Coordinate System</td></tr>
<tr><td>Mobile X Coordinate</td><td colspan="9">0. in</td><td colspan="2">1.3485 in</td></tr>
<tr><td>Mobile Y Coordinate</td><td>144. in</td><td>156. in</td><td>168. in</td><td>180. in</td><td>192. in</td><td>204. in</td><td>216. in</td><td>228. in</td><td>240. in</td><td>12. in</td><td>36. in</td></tr>
<tr><td>Mobile Z Coordinate</td><td colspan="9">6.53 in</td><td>5.5761 in</td><td>5.57 in</td></tr>
<tr><td>Mobile Location</td><td colspan="11">Defined</td></tr>
<tr><td>Behavior</td><td colspan="11">Rigid</td></tr>
<tr><td>Pinball Region</td><td colspan="9">6. in</td><td colspan="2">12. in</td></tr>
</table>

FIGURE 34
Model (B2) > Connections > Z Axis Spring 13

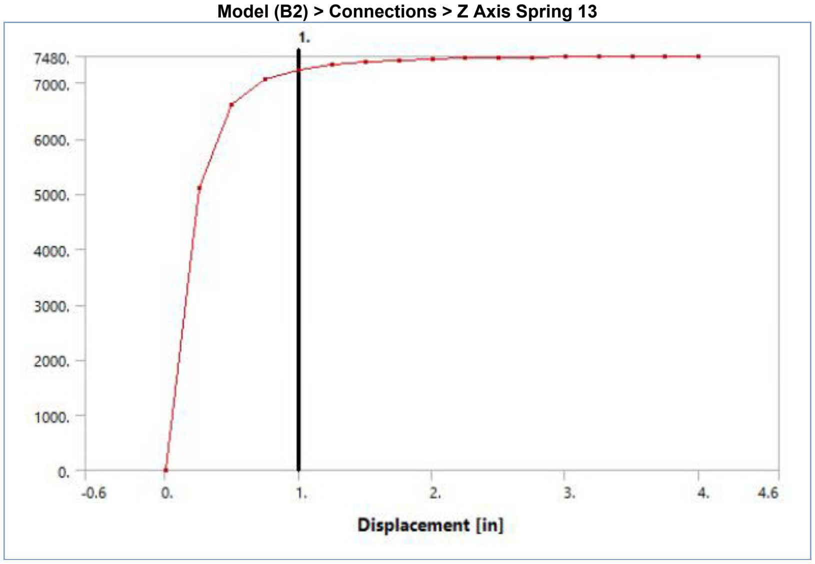

TABLE 46
Model (B2) > Connections > Z Axis Spring 13

<table>
<tr><th>Displacement [in]</th><th>Force [lbf]</th></tr>
<tr><td>0.</td><td>0.</td></tr>
<tr><td>0.25</td><td>5110.</td></tr>
<tr><td>0.5</td><td>6610.</td></tr>
<tr><td>0.75</td><td>7060.</td></tr>
<tr><td>1.</td><td>7240.</td></tr>
<tr><td>1.25</td><td>7330.</td></tr>
<tr><td>1.5</td><td>7380.</td></tr>
<tr><td>1.75</td><td>7410.</td></tr>
<tr><td>2.</td><td>7430.</td></tr>
<tr><td>2.25</td><td>7450.</td></tr>
<tr><td>2.5</td><td rowspan="2">7460.</td></tr>
<tr><td>2.75</td></tr>
<tr><td>3.</td><td rowspan="2">7470.</td></tr>
<tr><td>3.25</td></tr>
<tr><td>3.5</td><td rowspan="3">7480.</td></tr>
<tr><td>3.75</td></tr>
<tr><td>4.</td></tr>
</table>

FIGURE 35
Model (B2) > Connections > Z Axis Spring 14

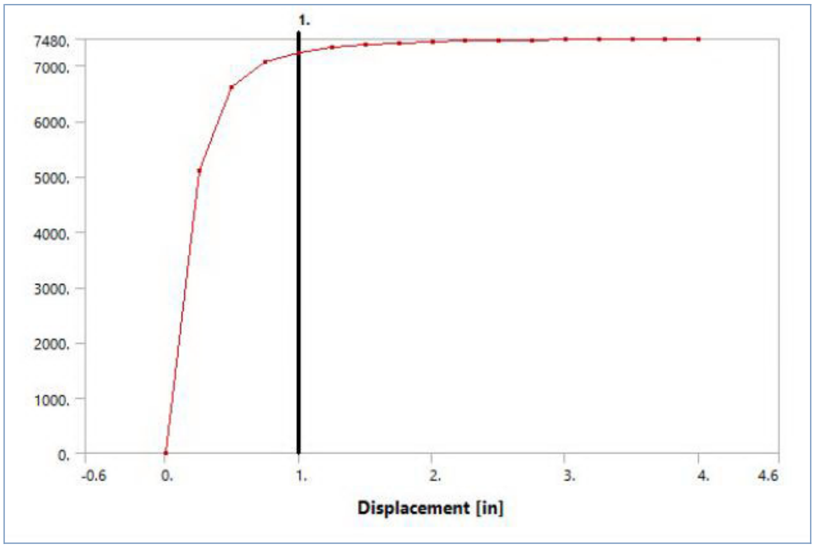

TABLE 47
Model (B2) > Connections > Z Axis Spring 14

Displacement [in]	Force [lbf]
0.	0.
0.25	5110.
0.5	6610.
0.75	7060.
1.	7240.
1.25	7330.
1.5	7380.
1.75	7410.
2.	7430.
2.25	7450.
2.5	7460.
2.75	
3.	7470.
3.25	
3.5	7480.
3.75	
4.	

FIGURE 36
Model (B2) > Connections > Z Axis Spring 15

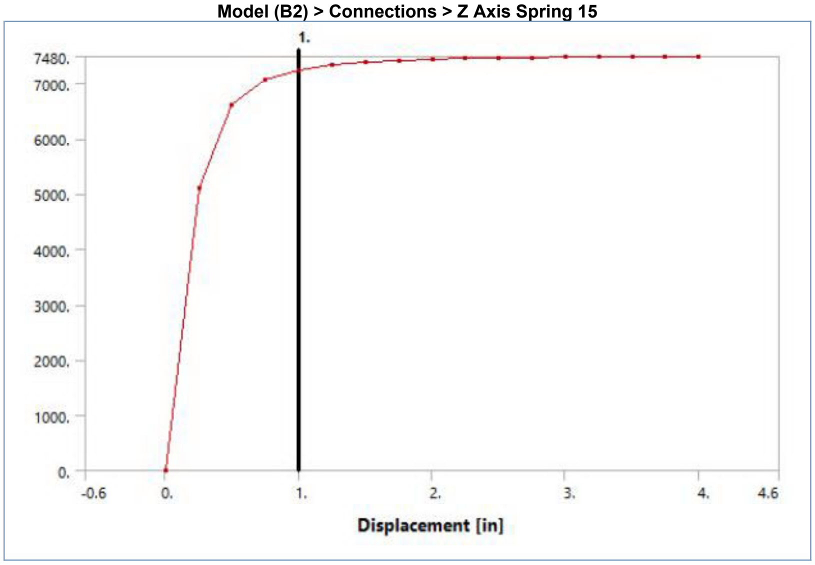

TABLE 48
Model (B2) > Connections > Z Axis Spring 15

Displacement [in]	Force [lbf]
0.	0.
0.25	5110.
0.5	6610.
0.75	7060.

1.	7240.
1.25	7330.
1.5	7380.
1.75	7410.
2.	7430.
2.25	7450.
2.5	7460.
2.75	
3.	7470.
3.25	
3.5	7480.
3.75	
4.	

FIGURE 37
Model (B2) > Connections > Z Axis Spring 16

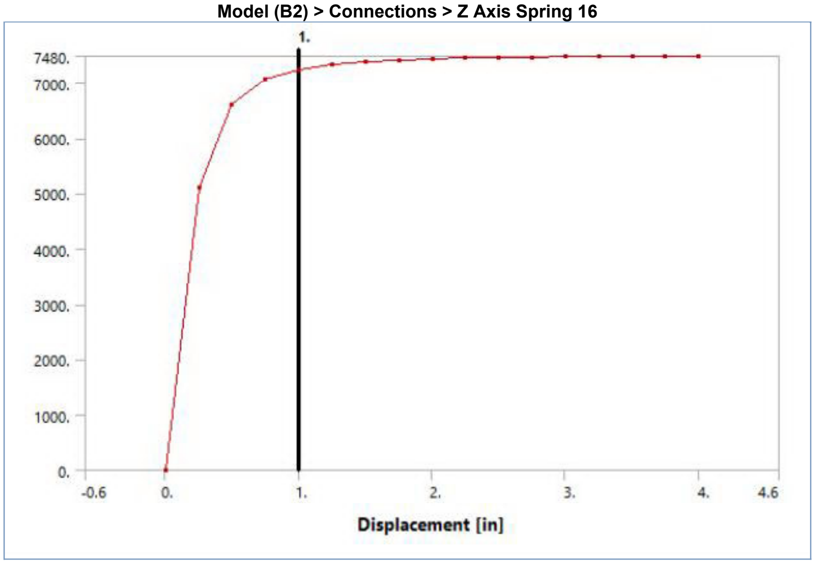

TABLE 49
Model (B2) > Connections > Z Axis Spring 16

Displacement [in]	Force [lbf]
0.	0.
0.25	5110.
0.5	6610.
0.75	7060.
1.	7240.
1.25	7330.
1.5	7380.
1.75	7410.
2.	7430.
2.25	7450.
2.5	7460.
2.75	
3.	7470.
3.25	
3.5	7480.
3.75	
4.	

FIGURE 38
Model (B2) > Connections > Z Axis Spring 17

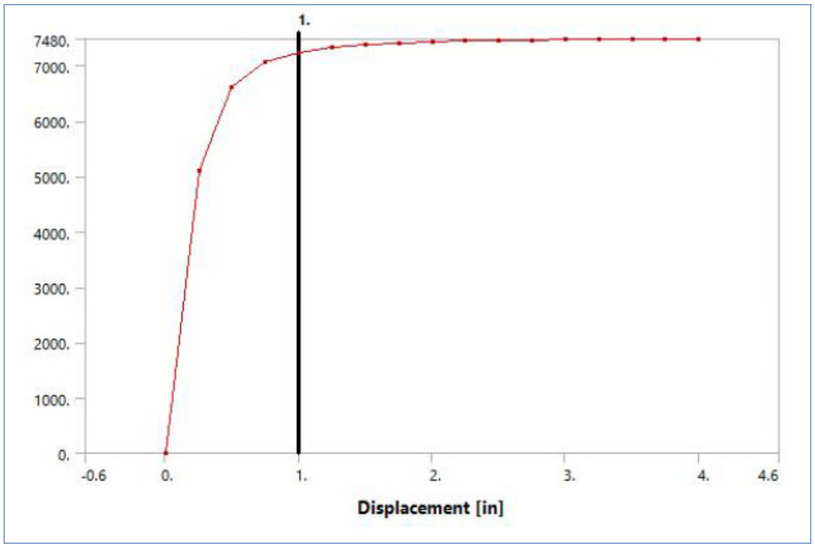

TABLE 50
Model (B2) > Connections > Z Axis Spring 17

<table>
<tr><th>Displacement [in]</th><th>Force [lbf]</th></tr>
<tr><td>0.</td><td>0.</td></tr>
<tr><td>0.25</td><td>5110.</td></tr>
<tr><td>0.5</td><td>6610.</td></tr>
<tr><td>0.75</td><td>7060.</td></tr>
<tr><td>1.</td><td>7240.</td></tr>
<tr><td>1.25</td><td>7330.</td></tr>
<tr><td>1.5</td><td>7380.</td></tr>
<tr><td>1.75</td><td>7410.</td></tr>
<tr><td>2.</td><td>7430.</td></tr>
<tr><td>2.25</td><td>7450.</td></tr>
<tr><td>2.5</td><td rowspan="2">7460.</td></tr>
<tr><td>2.75</td></tr>
<tr><td>3.</td><td rowspan="2">7470.</td></tr>
<tr><td>3.25</td></tr>
<tr><td>3.5</td><td rowspan="3">7480.</td></tr>
<tr><td>3.75</td></tr>
<tr><td>4.</td></tr>
</table>

FIGURE 39
Model (B2) > Connections > Z Axis Spring 18

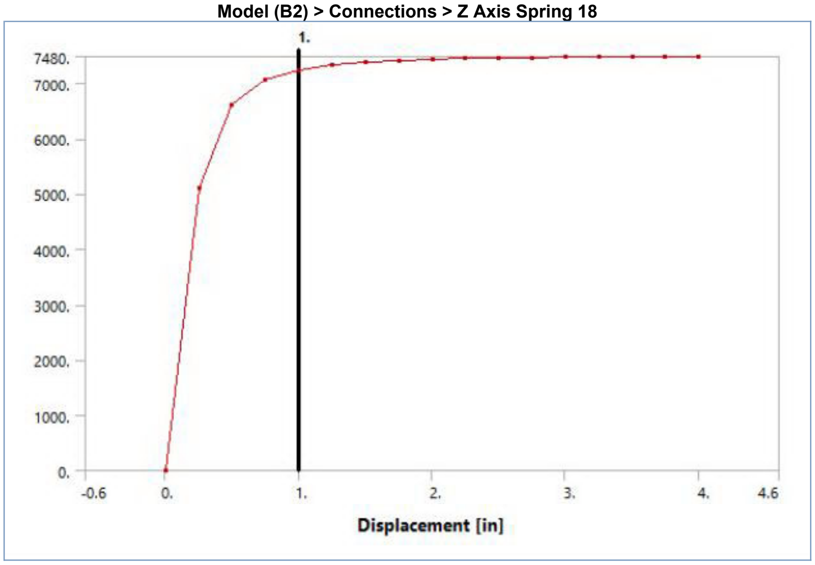

TABLE 51
Model (B2) > Connections > Z Axis Spring 18

Displacement [in]	Force [lbf]
0.	0.
0.25	5110.
0.5	6610.
0.75	7060.

1.	7240.
1.25	7330.
1.5	7380.
1.75	7410.
2.	7430.
2.25	7450.
2.5	7460.
2.75	
3.	7470.
3.25	
3.5	7480.
3.75	
4.	

FIGURE 40
Model (B2) > Connections > Z Axis Spring 19

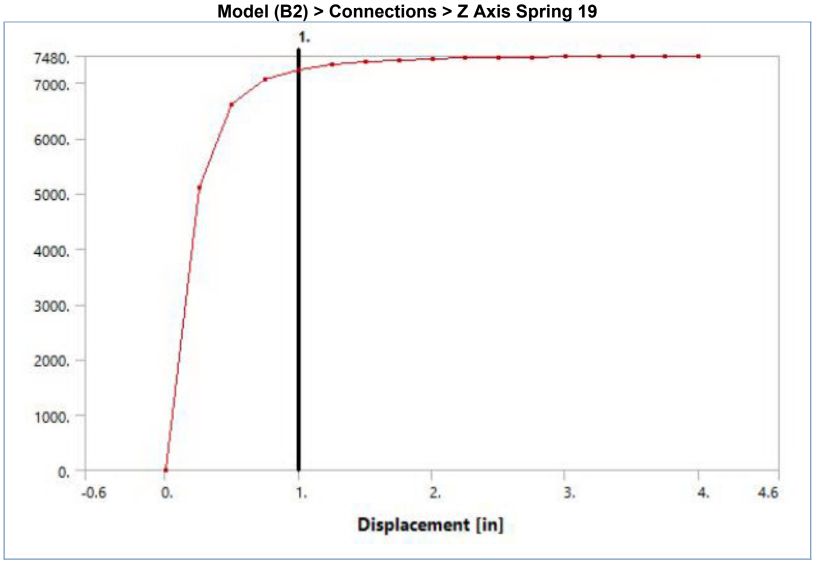

TABLE 52
Model (B2) > Connections > Z Axis Spring 19

Displacement [in]	Force [lbf]
0.	0.
0.25	5110.
0.5	6610.
0.75	7060.
1.	7240.
1.25	7330.
1.5	7380.
1.75	7410.
2.	7430.
2.25	7450.
2.5	7460.
2.75	
3.	7470.
3.25	
3.5	7480.
3.75	
4.	

FIGURE 41
Model (B2) > Connections > Z Axis Spring 20

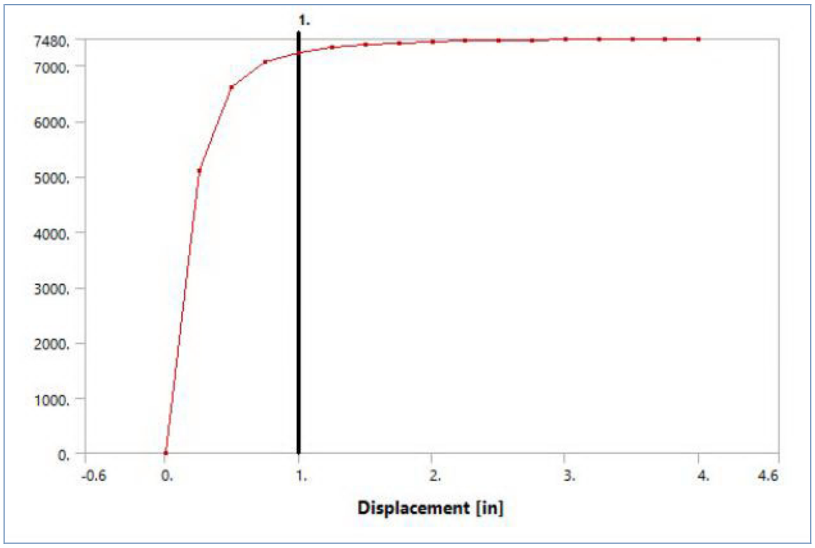

TABLE 53
Model (B2) > Connections > Z Axis Spring 20

<table>
<tr><th>Displacement [in]</th><th>Force [lbf]</th></tr>
<tr><td>0.</td><td>0.</td></tr>
<tr><td>0.25</td><td>5110.</td></tr>
<tr><td>0.5</td><td>6610.</td></tr>
<tr><td>0.75</td><td>7060.</td></tr>
<tr><td>1.</td><td>7240.</td></tr>
<tr><td>1.25</td><td>7330.</td></tr>
<tr><td>1.5</td><td>7380.</td></tr>
<tr><td>1.75</td><td>7410.</td></tr>
<tr><td>2.</td><td>7430.</td></tr>
<tr><td>2.25</td><td>7450.</td></tr>
<tr><td>2.5</td><td rowspan="2">7460.</td></tr>
<tr><td>2.75</td></tr>
<tr><td>3.</td><td rowspan="2">7470.</td></tr>
<tr><td>3.25</td></tr>
<tr><td>3.5</td><td rowspan="3">7480.</td></tr>
<tr><td>3.75</td></tr>
<tr><td>4.</td></tr>
</table>

FIGURE 42
Model (B2) > Connections > Z Axis Spring 21

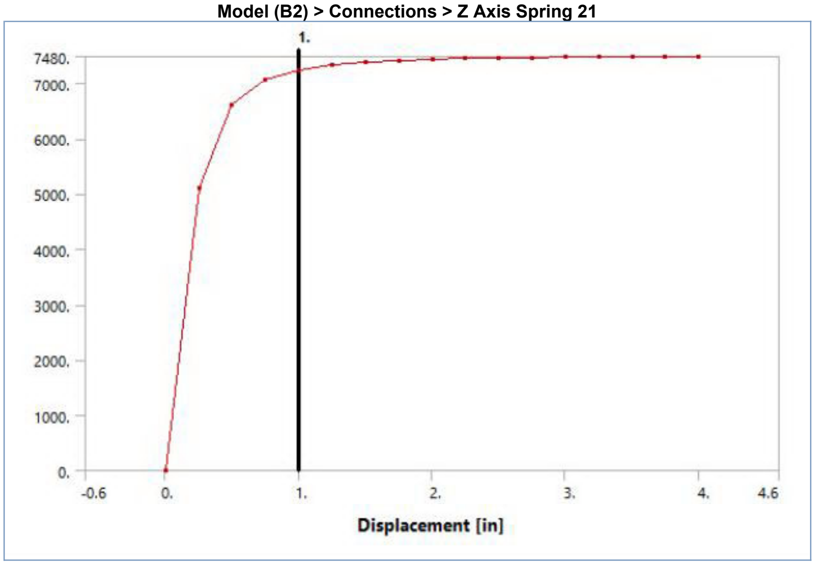

TABLE 54
Model (B2) > Connections > Z Axis Spring 21

Displacement [in]	Force [lbf]
0.	0.
0.25	5110.
0.5	6610.
0.75	7060.

1.	7240.
1.25	7330.
1.5	7380.
1.75	7410.
2.	7430.
2.25	7450.
2.5	7460.
2.75	
3.	7470.
3.25	
3.5	7480.
3.75	
4.	

FIGURE 43
Model (B2) > Connections > Slip Resistance Spring

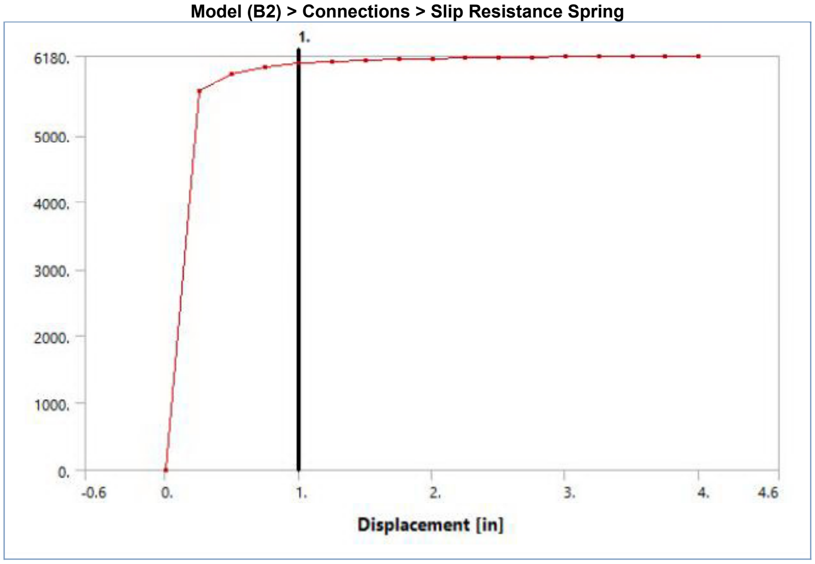

TABLE 55
Model (B2) > Connections > Slip Resistance Spring

Displacement [in]	Force [lbf]
0.	0.
0.25	5650.
0.5	5920.
0.75	6020.
1.	6070.
1.25	6100.
1.5	6120.
1.75	6130.
2.	6140.
2.25	6150.
2.5	6160.
2.75	
3.	6170.
3.25	
3.5	6180.
3.75	
4.	

FIGURE 44
Model (B2) > Connections > Slip Resistance Spring 2

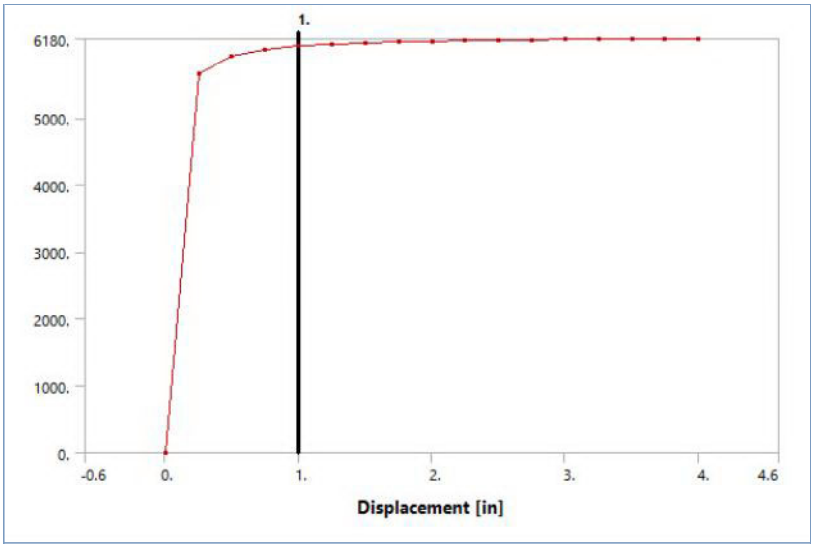

TABLE 56
Model (B2) > Connections > Slip Resistance Spring 2

Displacement [in]	Force [lbf]
0.	0.
0.25	5650.
0.5	5920.
0.75	6020.
1.	6070.
1.25	6100.
1.5	6120.
1.75	6130.
2.	6140.
2.25	6150.
2.5	6160.
2.75	
3.	6170.
3.25	
3.5	6180.
3.75	
4.	

TABLE 57
Model (B2) > Connections > Springs

Object Name	*Slip Resistance Spring 3*	*Slip Resistance Spring 4*	*Slip Resistance Spring 5*	*Slip Resistance Spring 6*	*Slip Resistance Spring 7*	*Slip Resistance Spring 8*	*Slip Resistance Spring 9*	*Slip Resistance Spring 10*	*Longitudinal - Ground To Surface Body (ACP (Pre))*	*End Bearing Spring*	*Slip Resistance Spring 11*
State	Fully Defined										
Graphics Properties											
Visible	Yes										
Definition											
Material	None										
Type	Longitudinal										
Spring Behavior	Both										
Longitudinal Stiffness	Tabular Data										
Longitudinal Damping	0. lbf·s/in										
Preload	None										
Suppressed	No										
Spring Length	12. in										
Element APDL Name											
Scope											
Scope	Body-Ground										
Reference											
Coordinate System	Global Coordinate System										
Reference X Coordinate	1.3485 in									-3.2709 in	1.3485 in
Reference Y Coordinate	48. in	72. in	96. in	120. in	144. in	168. in	192. in	216. in	252. in	0. in	240. in
Reference Z Coordinate	5.5761 in										

Reference Location	Defined										
Mobile											
Scoping Method	Geometry Selection										
Applied By	Remote Attachment										
Scope	8 Faces									8 Edges	8 Faces
Body	Surface Body(ACP (Pre))										
Coordinate System	Global Coordinate System										
Mobile X Coordinate	1.3485 in									-3.2709 in	1.3485 in
Mobile Y Coordinate	60. in	84. in	108. in	132. in	156. in	180. in	204. in	228. in	240. in	-12. in	252. in
Mobile Z Coordinate	5.5761 in										
Mobile Location	Defined										
Behavior	Rigid										
Pinball Region	12. in									All	12. in

FIGURE 45
Model (B2) > Connections > Slip Resistance Spring 3

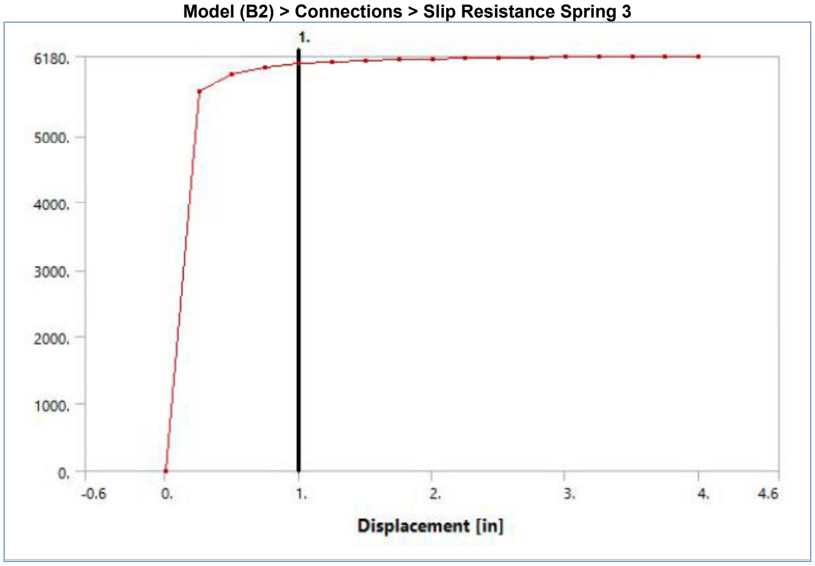

TABLE 58
Model (B2) > Connections > Slip Resistance Spring 3

Displacement [in]	Force [lbf]
0.	0.
0.25	5650.
0.5	5920.
0.75	6020.
1.	6070.
1.25	6100.
1.5	6120.
1.75	6130.
2.	6140.
2.25	6150.
2.5	6160.
2.75	
3.	6170.
3.25	
3.5	6180.
3.75	
4.	

FIGURE 46
Model (B2) > Connections > Slip Resistance Spring 4

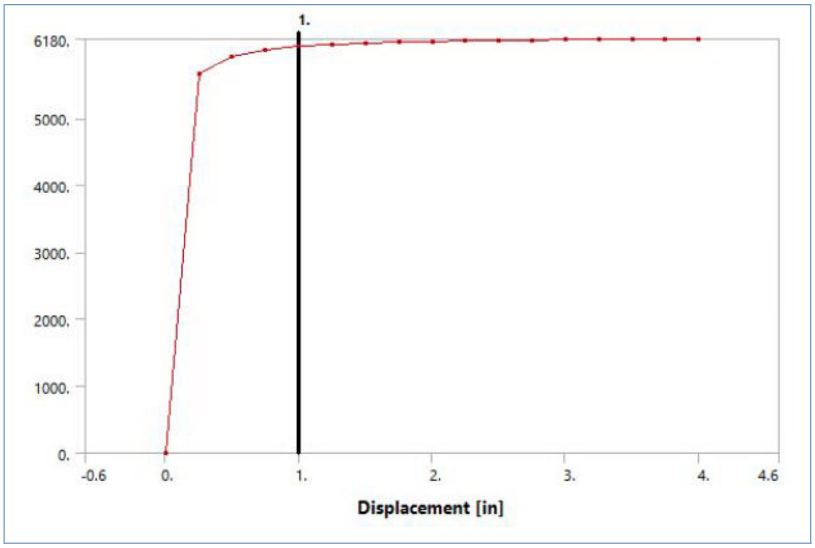

TABLE 59
Model (B2) > Connections > Slip Resistance Spring 4

Displacement [in]	Force [lbf]
0.	0.
0.25	5650.
0.5	5920.
0.75	6020.
1.	6070.
1.25	6100.
1.5	6120.
1.75	6130.
2.	6140.
2.25	6150.
2.5	6160.
2.75	
3.	6170.
3.25	
3.5	6180.
3.75	
4.	

FIGURE 47
Model (B2) > Connections > Slip Resistance Spring 5

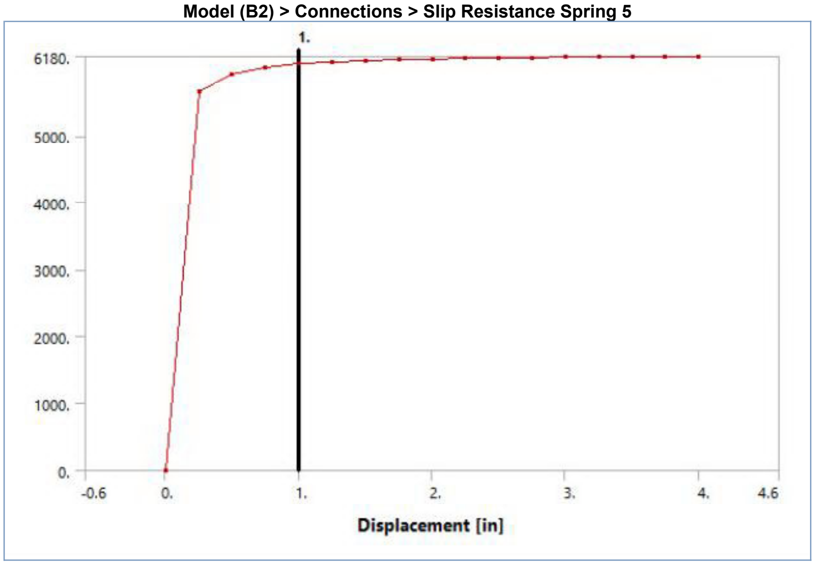

TABLE 60
Model (B2) > Connections > Slip Resistance Spring 5

Displacement [in]	Force [lbf]
0.	0.
0.25	5650.
0.5	5920.
0.75	6020.

1.	6070.
1.25	6100.
1.5	6120.
1.75	6130.
2.	6140.
2.25	6150.
2.5	6160.
2.75	
3.	6170.
3.25	
3.5	6180.
3.75	
4.	

FIGURE 48
Model (B2) > Connections > Slip Resistance Spring 6

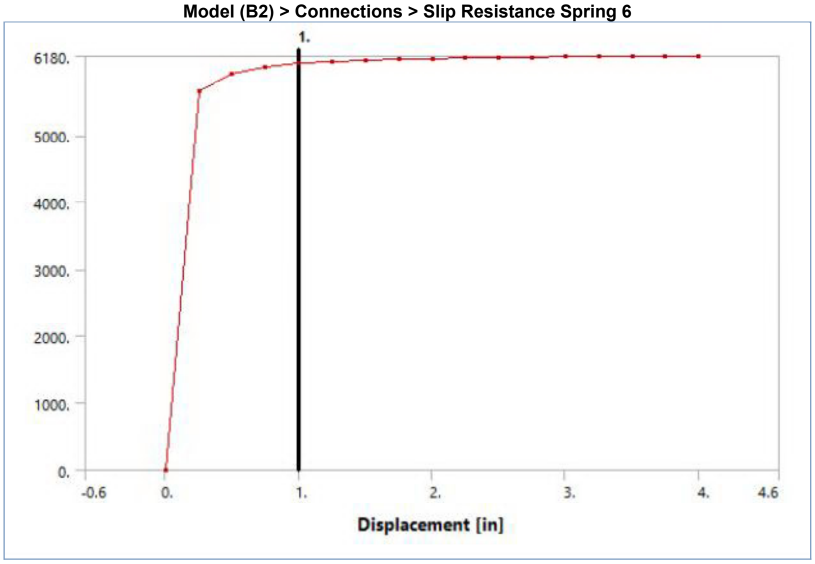

TABLE 61
Model (B2) > Connections > Slip Resistance Spring 6

Displacement [in]	Force [lbf]
0.	0.
0.25	5650.
0.5	5920.
0.75	6020.
1.	6070.
1.25	6100.
1.5	6120.
1.75	6130.
2.	6140.
2.25	6150.
2.5	6160.
2.75	
3.	6170.
3.25	
3.5	6180.
3.75	
4.	

FIGURE 49
Model (B2) > Connections > Slip Resistance Spring 7

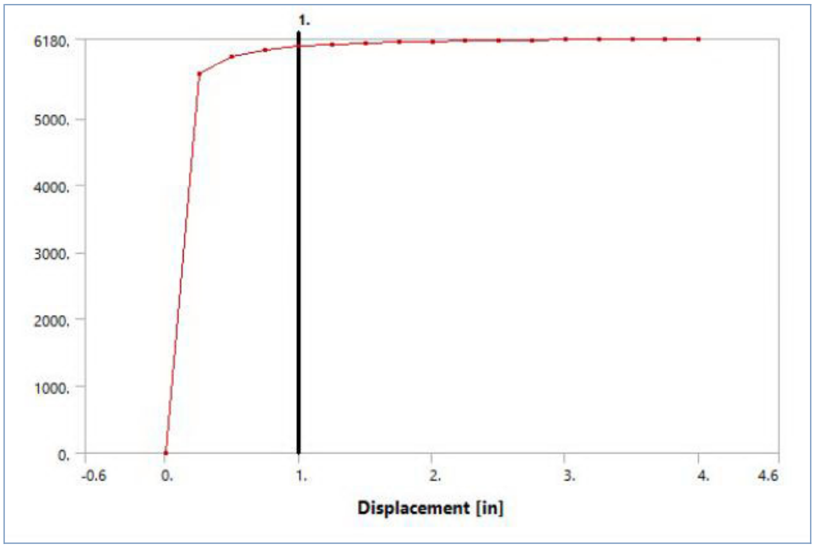

TABLE 62
Model (B2) > Connections > Slip Resistance Spring 7

Displacement [in]	Force [lbf]
0.	0.
0.25	5650.
0.5	5920.
0.75	6020.
1.	6070.
1.25	6100.
1.5	6120.
1.75	6130.
2.	6140.
2.25	6150.
2.5	6160.
2.75	
3.	6170.
3.25	
3.5	6180.
3.75	
4.	

FIGURE 50
Model (B2) > Connections > Slip Resistance Spring 8

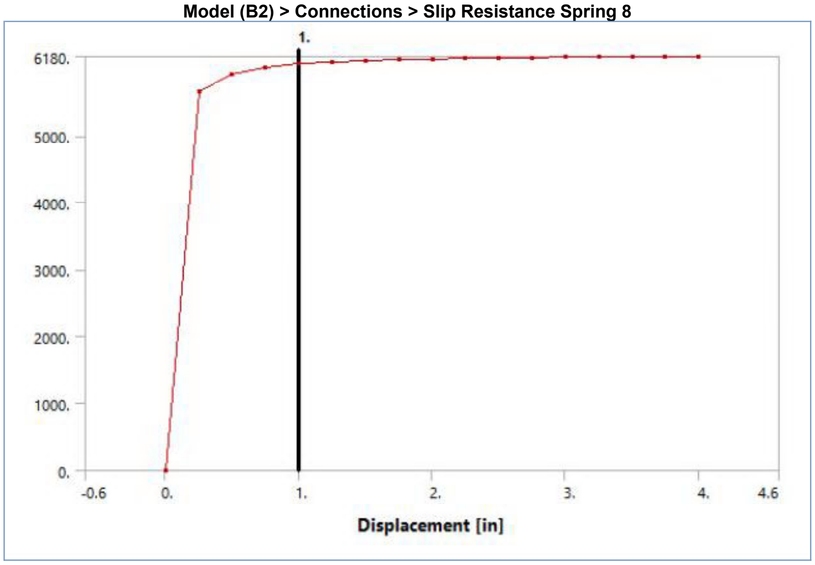

TABLE 63
Model (B2) > Connections > Slip Resistance Spring 8

Displacement [in]	Force [lbf]
0.	0.
0.25	5650.
0.5	5920.
0.75	6020.

1.	6070.
1.25	6100.
1.5	6120.
1.75	6130.
2.	6140.
2.25	6150.
2.5	6160.
2.75	
3.	6170.
3.25	
3.5	6180.
3.75	
4.	

FIGURE 51
Model (B2) > Connections > Slip Resistance Spring 9

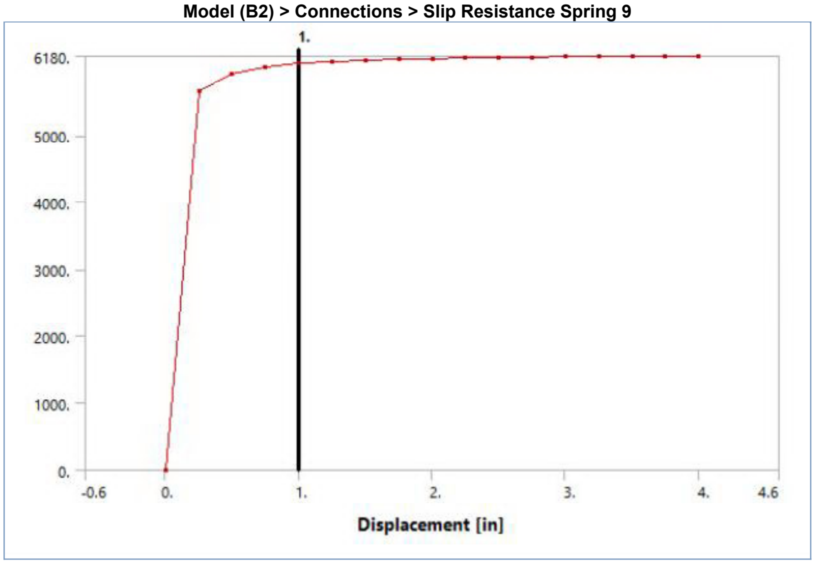

TABLE 64
Model (B2) > Connections > Slip Resistance Spring 9

Displacement [in]	Force [lbf]
0.	0.
0.25	5650.
0.5	5920.
0.75	6020.
1.	6070.
1.25	6100.
1.5	6120.
1.75	6130.
2.	6140.
2.25	6150.
2.5	6160.
2.75	
3.	6170.
3.25	
3.5	6180.
3.75	
4.	

FIGURE 52
Model (B2) > Connections > Slip Resistance Spring 10

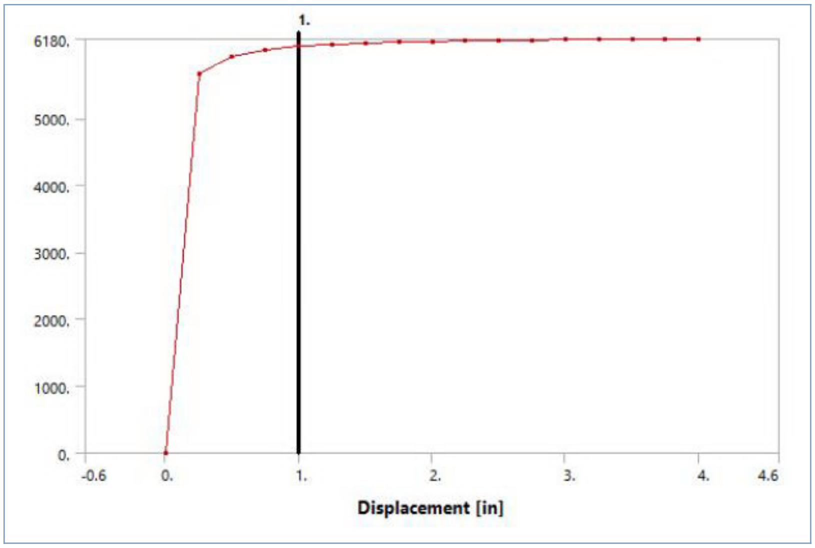

TABLE 65
Model (B2) > Connections > Slip Resistance Spring 10

Displacement [in]	Force [lbf]
0.	0.
0.25	5650.
0.5	5920.
0.75	6020.
1.	6070.
1.25	6100.
1.5	6120.
1.75	6130.
2.	6140.
2.25	6150.
2.5	6160.
2.75	
3.	6170.
3.25	
3.5	6180.
3.75	
4.	

FIGURE 53
Model (B2) > Connections > Longitudinal - Ground To Surface Body(ACP (Pre))

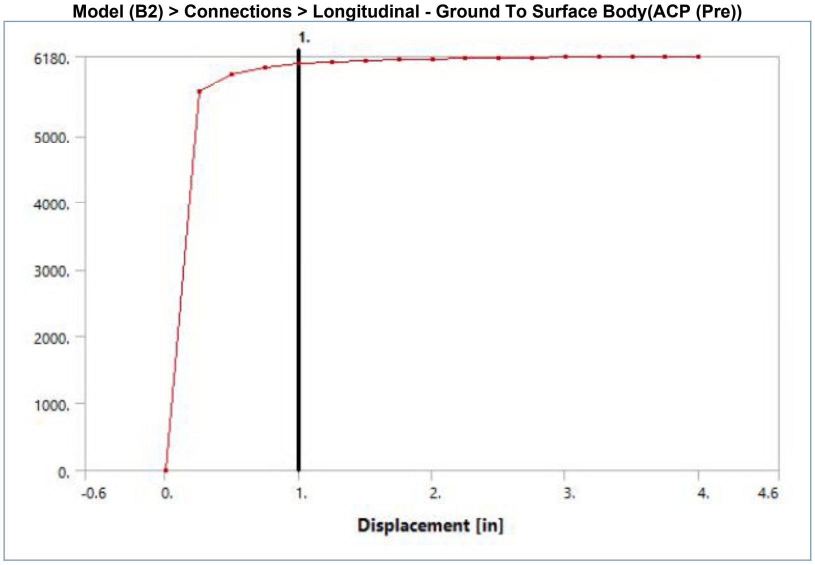

TABLE 66
Model (B2) > Connections > Longitudinal - Ground To Surface Body(ACP (Pre))

Displacement [in]	Force [lbf]
0.	0.
0.25	5650.
0.5	5920.
0.75	6020.

1.	6070.
1.25	6100.
1.5	6120.
1.75	6130.
2.	6140.
2.25	6150.
2.5	6160.
2.75	
3.	6170.
3.25	
3.5	6180.
3.75	
4.	

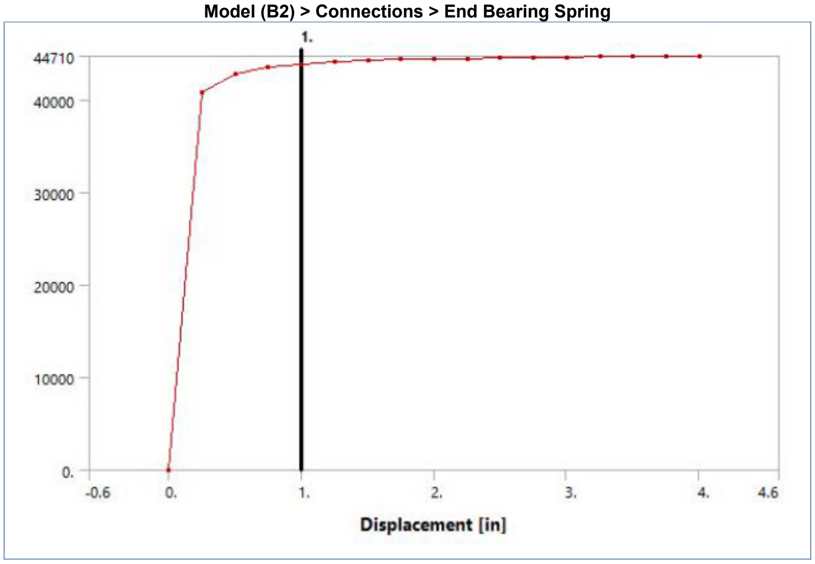

FIGURE 54
Model (B2) > Connections > End Bearing Spring

TABLE 67
Model (B2) > Connections > End Bearing Spring

Displacement [in]	Force [lbf]
0.	0.
0.25	40800
0.5	42800
0.75	43510
1.	43870
1.25	44090
1.5	44240
1.75	44350
2.	44430
2.25	44490
2.5	44540
2.75	44580
3.	44620
3.25	44650
3.5	44670
3.75	44690
4.	44710

FIGURE 55
Model (B2) > Connections > Slip Resistance Spring 11

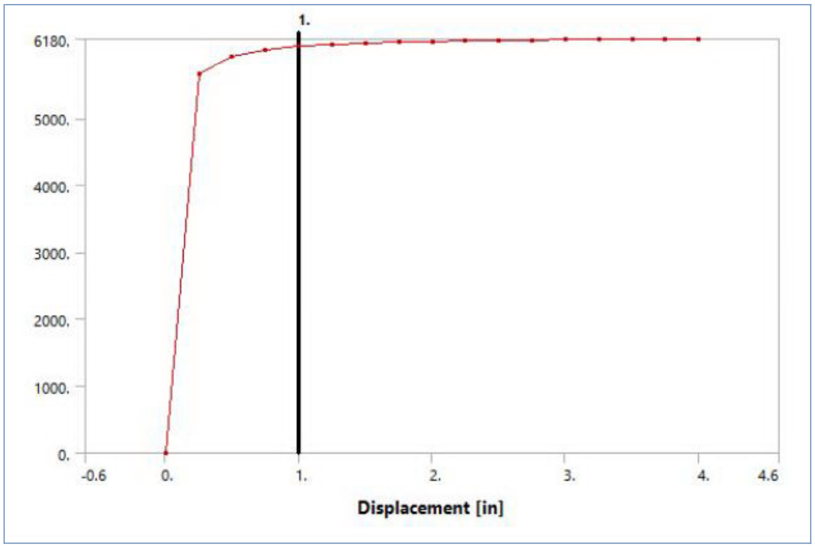

TABLE 68
Model (B2) > Connections > Slip Resistance Spring 11

Displacement [in]	Force [lbf]
0.	0.
0.25	5650.
0.5	5920.
0.75	6020.
1.	6070.
1.25	6100.
1.5	6120.
1.75	6130.
2.	6140.
2.25	6150.
2.5	6160.
2.75	
3.	6170.
3.25	
3.5	6180.
3.75	
4.	

TABLE 69
Model (B2) > Connections > Springs

Object Name	*Slip Resistance Spring 12*	*Slip Resistance Spring 13*	*Slip Resistance Spring 14*	*Slip Resistance Spring 15*	*Longitudinal - Ground To Surface Body(ACP (Pre)) 23*	*Longitudinal - Ground To Surface Body(ACP (Pre)) 24*	*Longitudinal - Ground To Surface Body(ACP (Pre)) 25*	*Longitudinal - Ground To Surface Body(ACP (Pre)) 26*	*Longitudinal - Ground To Surface Body(ACP (Pre)) 27*	*Longitudinal - Ground To Surface Body(ACP (Pre)) 28*	*Longitudinal - Ground To Surface Body(ACP (Pre)) 29*
State	Fully Defined										
Graphics Properties											
Visible	Yes										
Definition											
Material	None										
Type	Longitudinal										
Spring Behavior	Both										
Longitudinal Stiffness	Tabular Data										
Longitudinal Damping	0. lbf·s/in										
Preload	None										
Suppressed	No										
Spring Length	12. in										
Element APDL Name											
Scope											
Scope	Body-Ground										
Reference											
Coordinate System	Global Coordinate System										
Reference X Coordinate	1.3485 in				17.572 in						
Reference											

Y Coordinate	276. in	288. in	312. in	336. in	252. in	264. in	276. in	288. in	300. in	312. in	324. in
Reference Z Coordinate	5.5761 in				7.8541e-016 in						
Reference Location	Defined										
Mobile											
Scoping Method	Geometry Selection										
Applied By	Remote Attachment										
Scope	8 Faces										
Body	Surface Body(ACP (Pre))										
Coordinate System	Global Coordinate System										
Mobile X Coordinate	1.3485 in				5.5716 in						
Mobile Y Coordinate	264. in	300. in	324. in	348. in	252. in	264. in	276. in	288. in	300. in	312. in	324. in
Mobile Z Coordinate	5.5761 in				7.8541e-016 in						
Mobile Location	Defined										
Behavior	Rigid										
Pinball Region	12. in				6. in						

FIGURE 56
Model (B2) > Connections > Slip Resistance Spring 12

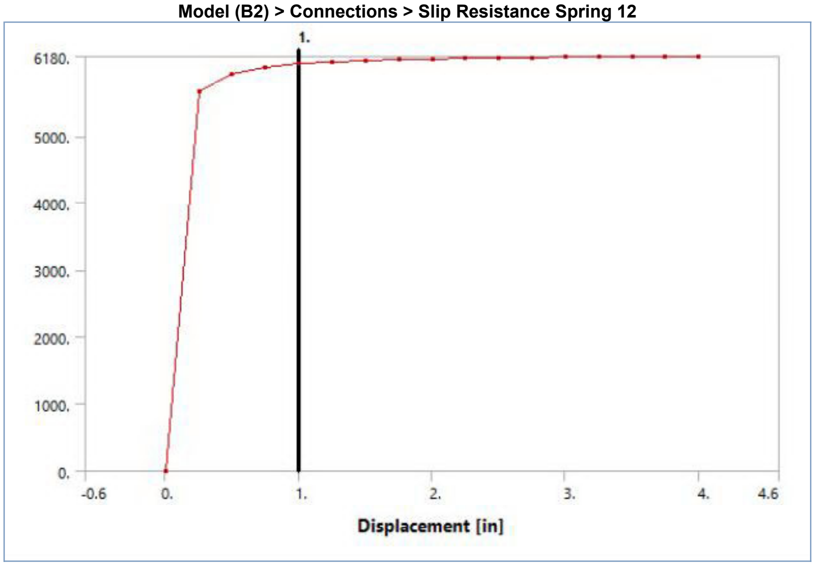

TABLE 70
Model (B2) > Connections > Slip Resistance Spring 12

Displacement [in]	Force [lbf]
0.	0.
0.25	5650.
0.5	5920.
0.75	6020.
1.	6070.
1.25	6100.
1.5	6120.
1.75	6130.
2.	6140.
2.25	6150.
2.5	6160.
2.75	
3.	6170.
3.25	
3.5	6180.
3.75	
4.	

FIGURE 57
Model (B2) > Connections > Slip Resistance Spring 13

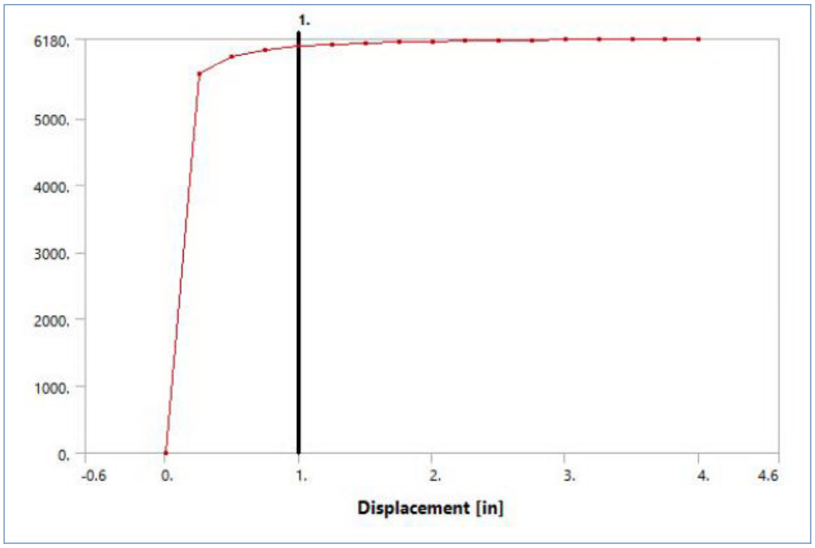

TABLE 71
Model (B2) > Connections > Slip Resistance Spring 13

<table>
<tr><th>Displacement [in]</th><th>Force [lbf]</th></tr>
<tr><td>0.</td><td>0.</td></tr>
<tr><td>0.25</td><td>5650.</td></tr>
<tr><td>0.5</td><td>5920.</td></tr>
<tr><td>0.75</td><td>6020.</td></tr>
<tr><td>1.</td><td>6070.</td></tr>
<tr><td>1.25</td><td>6100.</td></tr>
<tr><td>1.5</td><td>6120.</td></tr>
<tr><td>1.75</td><td>6130.</td></tr>
<tr><td>2.</td><td>6140.</td></tr>
<tr><td>2.25</td><td>6150.</td></tr>
<tr><td>2.5</td><td rowspan="2">6160.</td></tr>
<tr><td>2.75</td></tr>
<tr><td>3.</td><td rowspan="2">6170.</td></tr>
<tr><td>3.25</td></tr>
<tr><td>3.5</td><td rowspan="3">6180.</td></tr>
<tr><td>3.75</td></tr>
<tr><td>4.</td></tr>
</table>

FIGURE 58
Model (B2) > Connections > Slip Resistance Spring 14

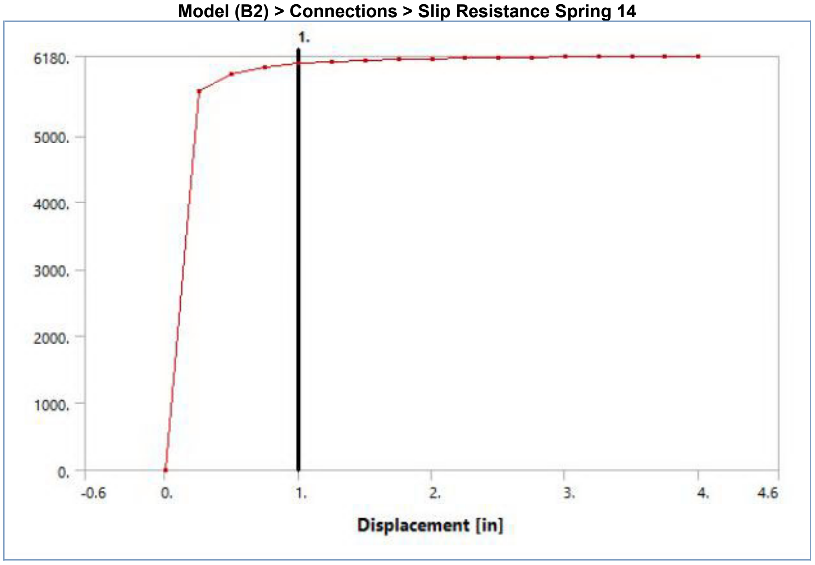

TABLE 72
Model (B2) > Connections > Slip Resistance Spring 14

Displacement [in]	Force [lbf]
0.	0.
0.25	5650.
0.5	5920.
0.75	6020.

1.	6070.
1.25	6100.
1.5	6120.
1.75	6130.
2.	6140.
2.25	6150.
2.5	6160.
2.75	
3.	6170.
3.25	
3.5	6180.
3.75	
4.	

FIGURE 59
Model (B2) > Connections > Slip Resistance Spring 15

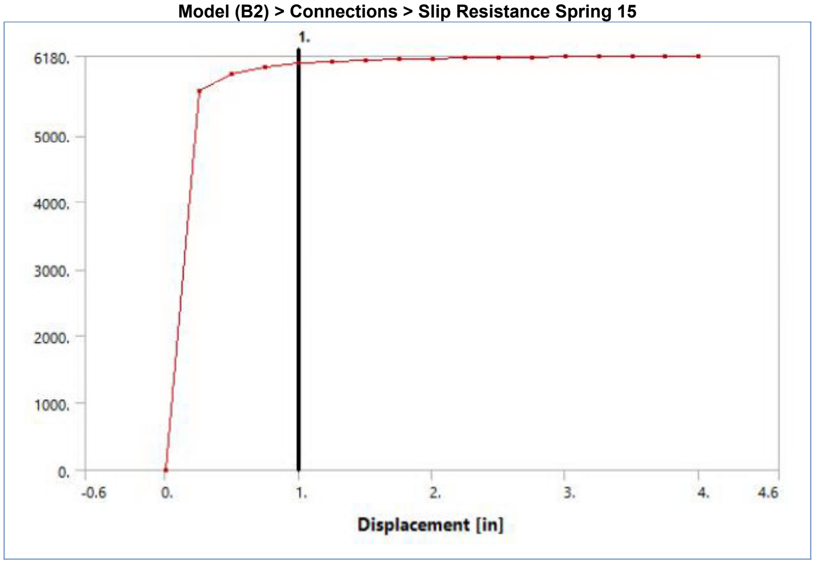

TABLE 73
Model (B2) > Connections > Slip Resistance Spring 15

Displacement [in]	Force [lbf]
0.	0.
0.25	5650.
0.5	5920.
0.75	6020.
1.	6070.
1.25	6100.
1.5	6120.
1.75	6130.
2.	6140.
2.25	6150.
2.5	6160.
2.75	
3.	6170.
3.25	
3.5	6180.
3.75	
4.	

FIGURE 60
Model (B2) > Connections > Longitudinal - Ground To Surface Body(ACP (Pre)) 23

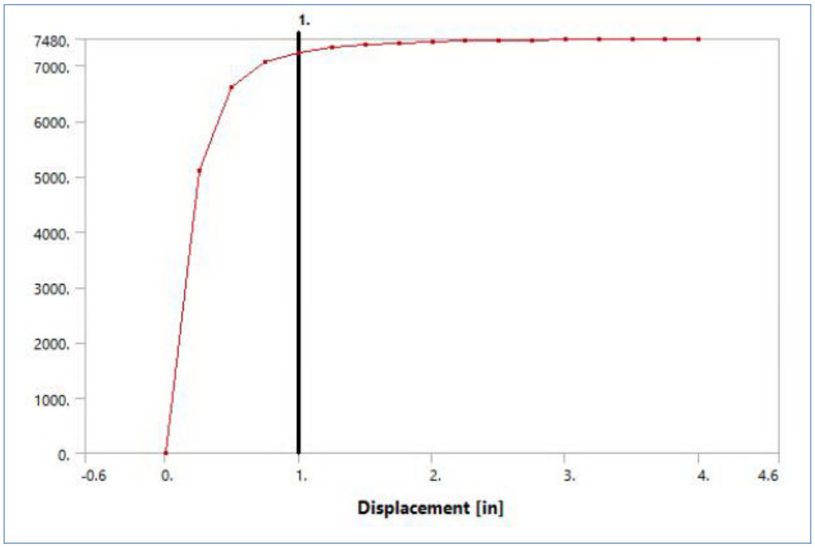

TABLE 74
Model (B2) > Connections > Longitudinal - Ground To Surface Body(ACP (Pre)) 23

Displacement [in]	Force [lbf]
0.	0.
0.25	5110.
0.5	6610.
0.75	7060.
1.	7240.
1.25	7330.
1.5	7380.
1.75	7410.
2.	7430.
2.25	7450.
2.5	7460.
2.75	
3.	7470.
3.25	
3.5	7480.
3.75	
4.	

FIGURE 61
Model (B2) > Connections > Longitudinal - Ground To Surface Body(ACP (Pre)) 24

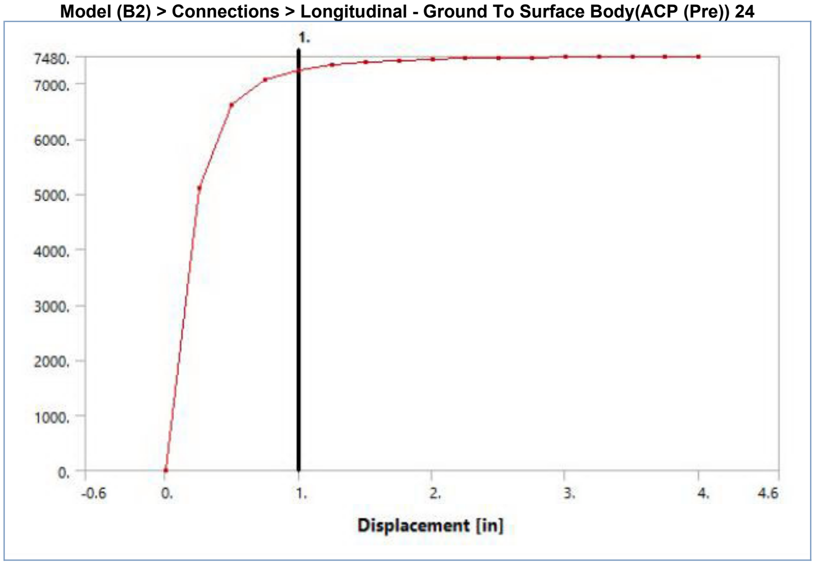

TABLE 75
Model (B2) > Connections > Longitudinal - Ground To Surface Body(ACP (Pre)) 24

Displacement [in]	Force [lbf]
0.	0.
0.25	5110.
0.5	6610.
0.75	7060.

1.	7240.
1.25	7330.
1.5	7380.
1.75	7410.
2.	7430.
2.25	7450.
2.5	7460.
2.75	
3.	7470.
3.25	
3.5	7480.
3.75	
4.	

FIGURE 62
Model (B2) > Connections > Longitudinal - Ground To Surface Body(ACP (Pre)) 25

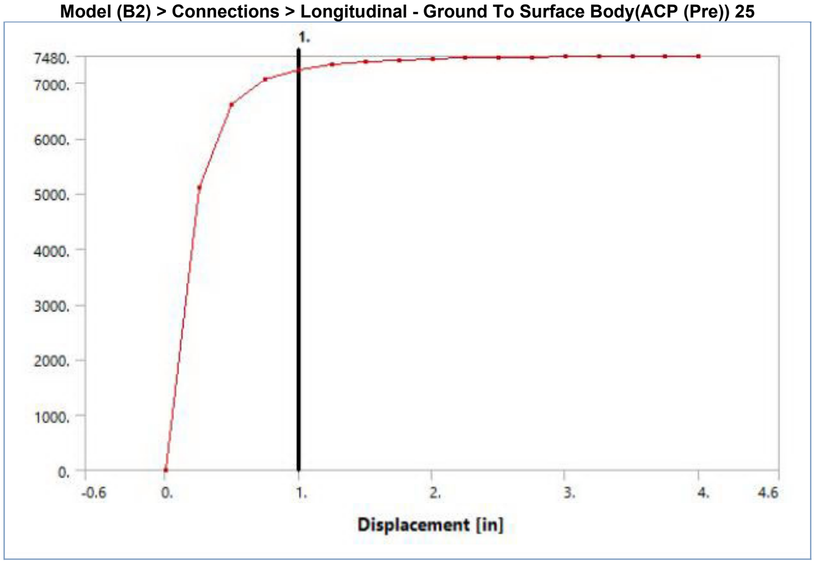

TABLE 76
Model (B2) > Connections > Longitudinal - Ground To Surface Body(ACP (Pre)) 25

Displacement [in]	Force [lbf]
0.	0.
0.25	5110.
0.5	6610.
0.75	7060.
1.	7240.
1.25	7330.
1.5	7380.
1.75	7410.
2.	7430.
2.25	7450.
2.5	7460.
2.75	
3.	7470.
3.25	
3.5	7480.
3.75	
4.	

FIGURE 63
Model (B2) > Connections > Longitudinal - Ground To Surface Body(ACP (Pre)) 26

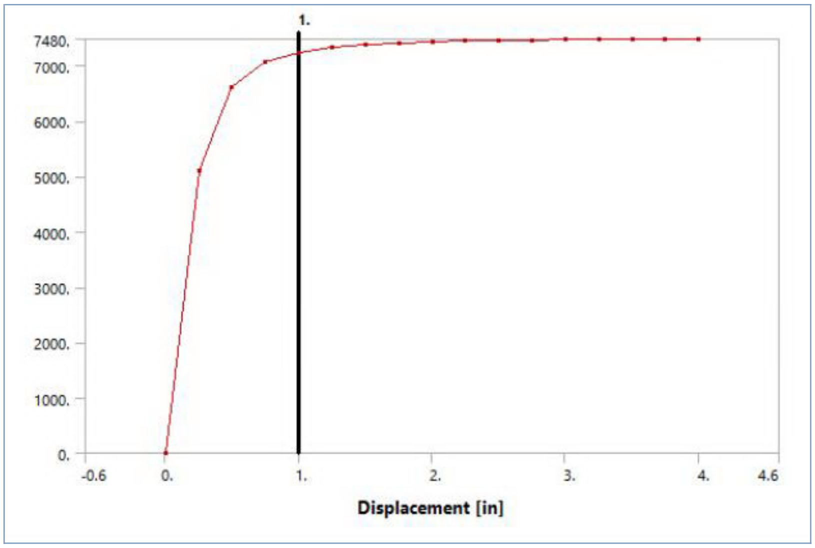

TABLE 77
Model (B2) > Connections > Longitudinal - Ground To Surface Body(ACP (Pre)) 26

Displacement [in]	Force [lbf]
0.	0.
0.25	5110.
0.5	6610.
0.75	7060.
1.	7240.
1.25	7330.
1.5	7380.
1.75	7410.
2.	7430.
2.25	7450.
2.5	7460.
2.75	
3.	7470.
3.25	
3.5	7480.
3.75	
4.	

FIGURE 64
Model (B2) > Connections > Longitudinal - Ground To Surface Body(ACP (Pre)) 27

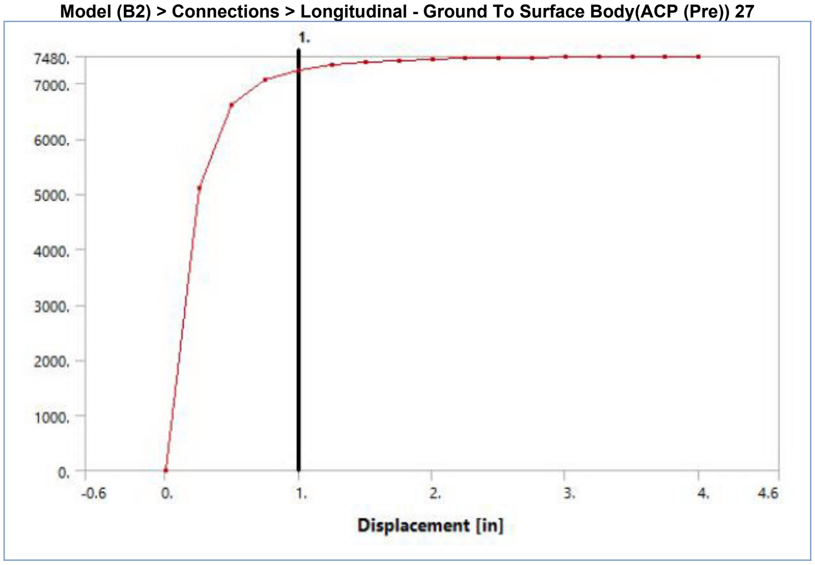

TABLE 78
Model (B2) > Connections > Longitudinal - Ground To Surface Body(ACP (Pre)) 27

Displacement [in]	Force [lbf]
0.	0.
0.25	5110.
0.5	6610.
0.75	7060.

1.	7240.
1.25	7330.
1.5	7380.
1.75	7410.
2.	7430.
2.25	7450.
2.5	7460.
2.75	
3.	7470.
3.25	
3.5	7480.
3.75	
4.	

FIGURE 65
Model (B2) > Connections > Longitudinal - Ground To Surface Body(ACP (Pre)) 28

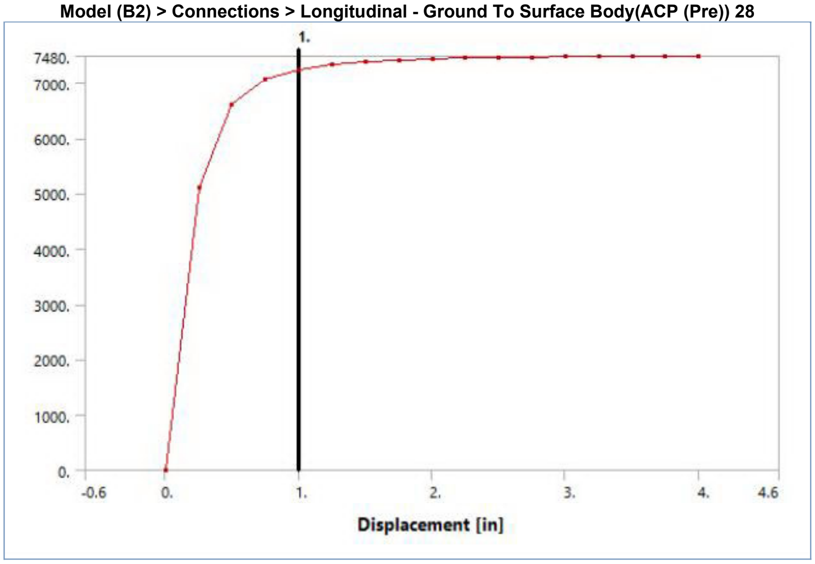

TABLE 79
Model (B2) > Connections > Longitudinal - Ground To Surface Body(ACP (Pre)) 28

Displacement [in]	Force [lbf]
0.	0.
0.25	5110.
0.5	6610.
0.75	7060.
1.	7240.
1.25	7330.
1.5	7380.
1.75	7410.
2.	7430.
2.25	7450.
2.5	7460.
2.75	
3.	7470.
3.25	
3.5	7480.
3.75	
4.	

FIGURE 66
Model (B2) > Connections > Longitudinal - Ground To Surface Body(ACP (Pre)) 29

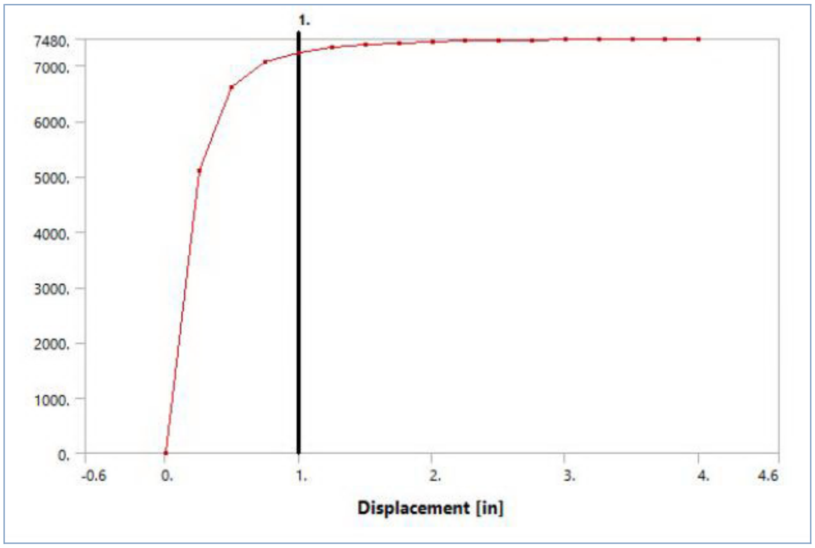

TABLE 80
Model (B2) > Connections > Longitudinal - Ground To Surface Body(ACP (Pre)) 29

Displacement [in]	Force [lbf]
0.	0.
0.25	5110.
0.5	6610.
0.75	7060.
1.	7240.
1.25	7330.
1.5	7380.
1.75	7410.
2.	7430.
2.25	7450.
2.5	7460.
2.75	
3.	7470.
3.25	
3.5	7480.
3.75	
4.	

TABLE 81
Model (B2) > Connections > Springs

Object Name	*Longitudinal - Ground To Surface Body (ACP (Pre)) 30*	*Longitudinal - Ground To Surface Body (ACP (Pre)) 31*	*Longitudinal - Ground To Surface Body (ACP (Pre)) 32*	*Z Axis Spring 22*	*Z Axis Spring 23*	*Z Axis Spring 24*	*Z Axis Spring 25*	*Z Axis Spring 26*	*Z Axis Spring 27*	*Z Axis Spring 28*	*Z Axis Spring 29*
State	Fully Defined										
Graphics Properties											
Visible	Yes										
Definition											
Material	None										
Type	Longitudinal										
Spring Behavior	Both										
Longitudinal Stiffness	Tabular Data										
Longitudinal Damping	0. lbf·s/in										
Preload	None										
Suppressed	No										
Spring Length	12. in										
Element APDL Name											
Scope											
Scope	Body-Ground										
Reference											
Coordinate System	Global Coordinate System										
Reference X Coordinate	17.572 in			0. in							
Reference Y Coordinate	336. in	348. in	360. in	252. in	264. in	276. in	288. in	300. in	312. in	324. in	336. in
Reference Z Coordinate	7.8541e-016 in			18.53 in							
Reference Location	Defined										

Mobile											
Scoping Method	Geometry Selection										
Applied By	Remote Attachment										
Scope	8 Faces										
Body	Surface Body(ACP (Pre))										
Coordinate System	Global Coordinate System										
Mobile X Coordinate	5.5716 in			0. in							
Mobile Y Coordinate	336. in	348. in	360. in	252. in	264. in	276. in	288. in	300. in	312. in	324. in	336. in
Mobile Z Coordinate	7.8541e-016 in			6.53 in							
Mobile Location	Defined										
Behavior	Rigid										
Pinball Region	6. in										

FIGURE 67
Model (B2) > Connections > Longitudinal - Ground To Surface Body(ACP (Pre)) 30

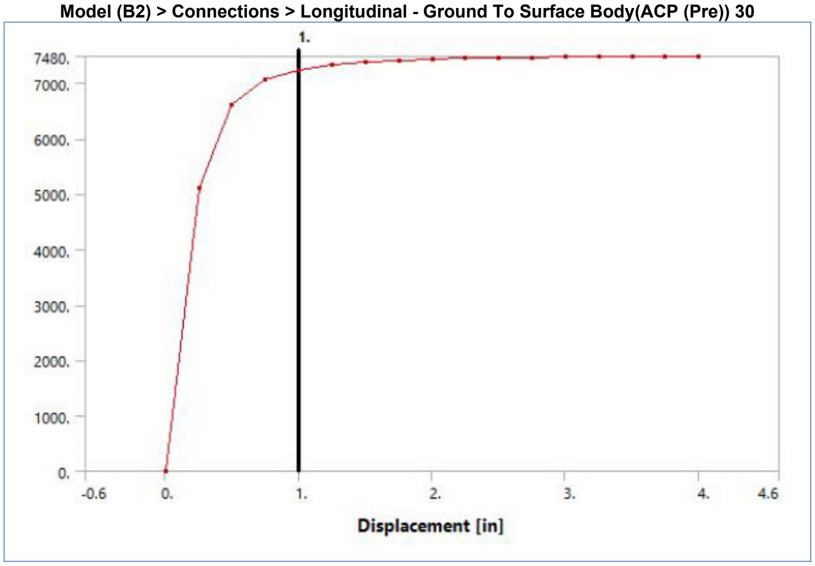

TABLE 82
Model (B2) > Connections > Longitudinal - Ground To Surface Body(ACP (Pre)) 30

Displacement [in]	Force [lbf]
0.	0.
0.25	5110.
0.5	6610.
0.75	7060.
1.	7240.
1.25	7330.
1.5	7380.
1.75	7410.
2.	7430.
2.25	7450.
2.5	7460.
2.75	
3.	7470.
3.25	
3.5	7480.
3.75	
4.	

FIGURE 68
Model (B2) > Connections > Longitudinal - Ground To Surface Body(ACP (Pre)) 31

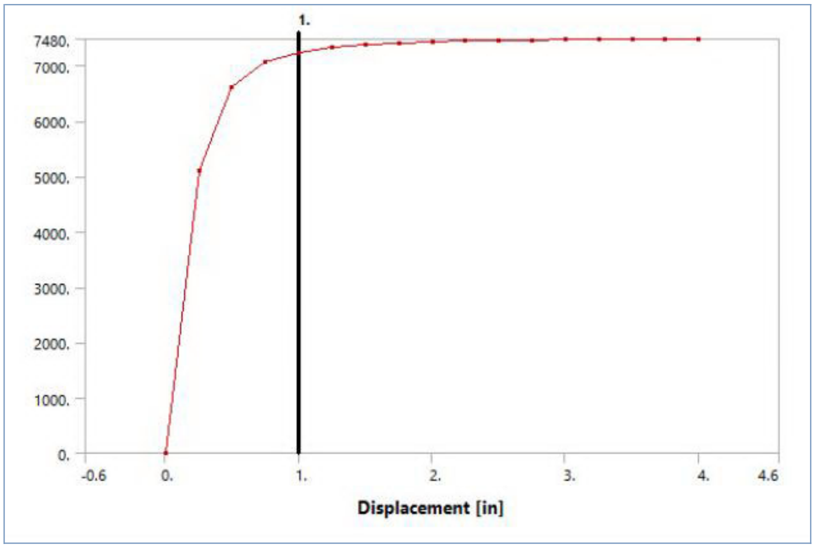

TABLE 83
Model (B2) > Connections > Longitudinal - Ground To Surface Body(ACP (Pre)) 31

Displacement [in]	Force [lbf]
0.	0.
0.25	5110.
0.5	6610.
0.75	7060.
1.	7240.
1.25	7330.
1.5	7380.
1.75	7410.
2.	7430.
2.25	7450.
2.5	7460.
2.75	
3.	7470.
3.25	
3.5	7480.
3.75	
4.	

FIGURE 69
Model (B2) > Connections > Longitudinal - Ground To Surface Body(ACP (Pre)) 32

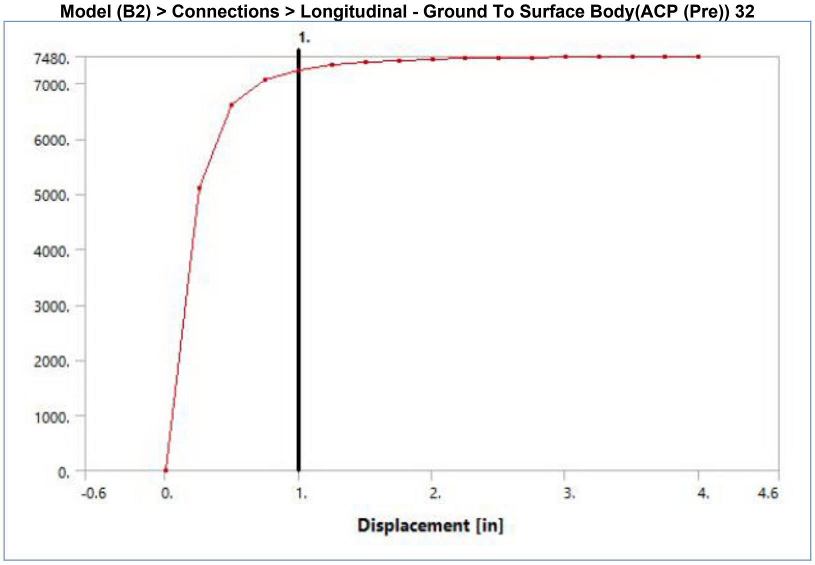

TABLE 84
Model (B2) > Connections > Longitudinal - Ground To Surface Body(ACP (Pre)) 32

Displacement [in]	Force [lbf]
0.	0.
0.25	5110.
0.5	6610.
0.75	7060.

1.	7240.
1.25	7330.
1.5	7380.
1.75	7410.
2.	7430.
2.25	7450.
2.5	7460.
2.75	
3.	7470.
3.25	
3.5	7480.
3.75	
4.	

FIGURE 70
Model (B2) > Connections > Z Axis Spring 22

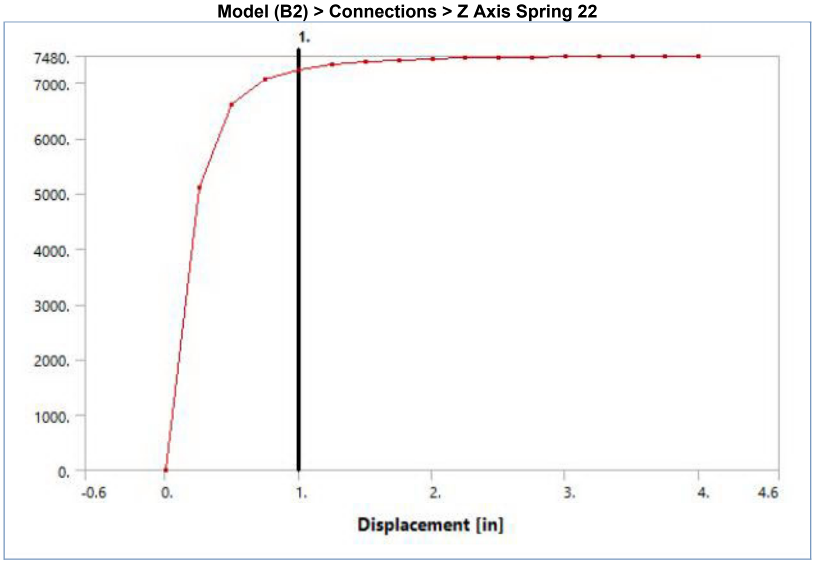

TABLE 85
Model (B2) > Connections > Z Axis Spring 22

Displacement [in]	Force [lbf]
0.	0.
0.25	5110.
0.5	6610.
0.75	7060.
1.	7240.
1.25	7330.
1.5	7380.
1.75	7410.
2.	7430.
2.25	7450.
2.5	7460.
2.75	
3.	7470.
3.25	
3.5	7480.
3.75	
4.	

FIGURE 71
Model (B2) > Connections > Z Axis Spring 23

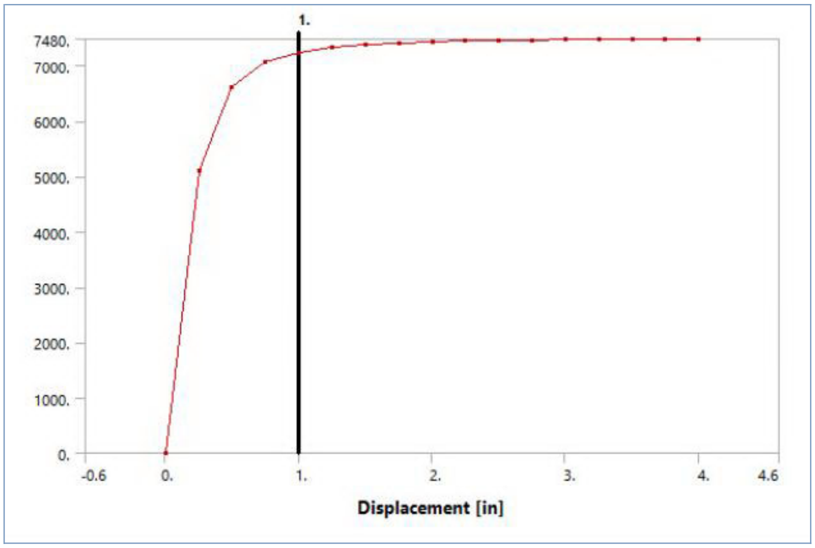

TABLE 86
Model (B2) > Connections > Z Axis Spring 23

Displacement [in]	Force [lbf]
0.	0.
0.25	5110.
0.5	6610.
0.75	7060.
1.	7240.
1.25	7330.
1.5	7380.
1.75	7410.
2.	7430.
2.25	7450.
2.5	7460.
2.75	
3.	7470.
3.25	
3.5	7480.
3.75	
4.	

FIGURE 72
Model (B2) > Connections > Z Axis Spring 24

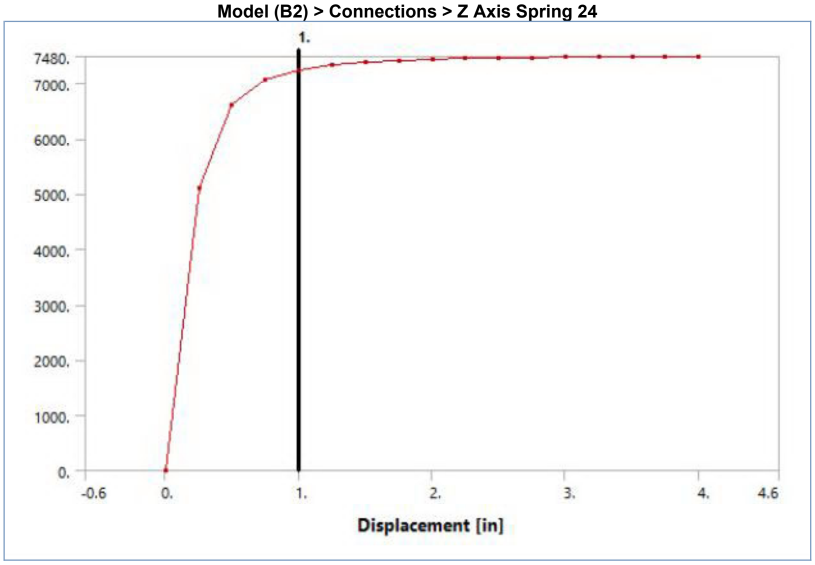

TABLE 87
Model (B2) > Connections > Z Axis Spring 24

Displacement [in]	Force [lbf]
0.	0.
0.25	5110.
0.5	6610.
0.75	7060.

1.	7240.
1.25	7330.
1.5	7380.
1.75	7410.
2.	7430.
2.25	7450.
2.5	7460.
2.75	
3.	7470.
3.25	
3.5	7480.
3.75	
4.	

FIGURE 73
Model (B2) > Connections > Z Axis Spring 25

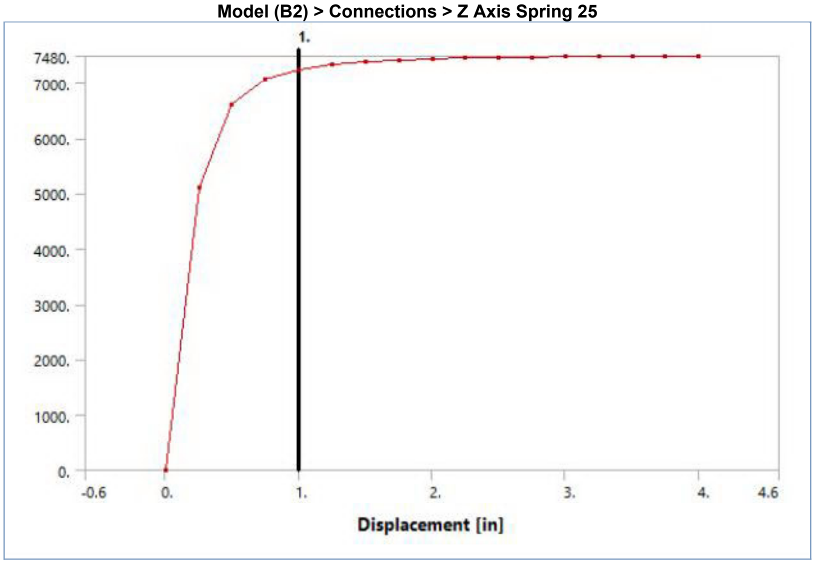

TABLE 88
Model (B2) > Connections > Z Axis Spring 25

Displacement [in]	Force [lbf]
0.	0.
0.25	5110.
0.5	6610.
0.75	7060.
1.	7240.
1.25	7330.
1.5	7380.
1.75	7410.
2.	7430.
2.25	7450.
2.5	7460.
2.75	
3.	7470.
3.25	
3.5	7480.
3.75	
4.	

FIGURE 74
Model (B2) > Connections > Z Axis Spring 26

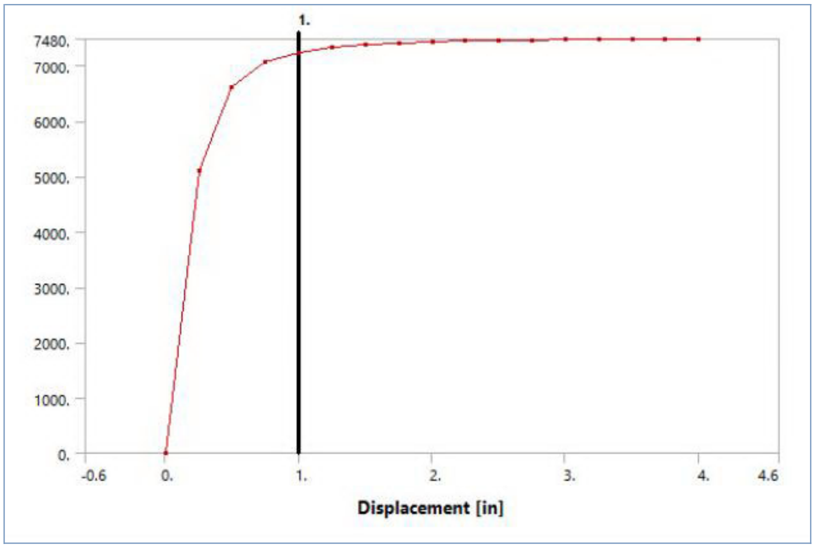

TABLE 89
Model (B2) > Connections > Z Axis Spring 26

Displacement [in]	Force [lbf]
0.	0.
0.25	5110.
0.5	6610.
0.75	7060.
1.	7240.
1.25	7330.
1.5	7380.
1.75	7410.
2.	7430.
2.25	7450.
2.5	7460.
2.75	
3.	7470.
3.25	
3.5	7480.
3.75	
4.	

FIGURE 75
Model (B2) > Connections > Z Axis Spring 27

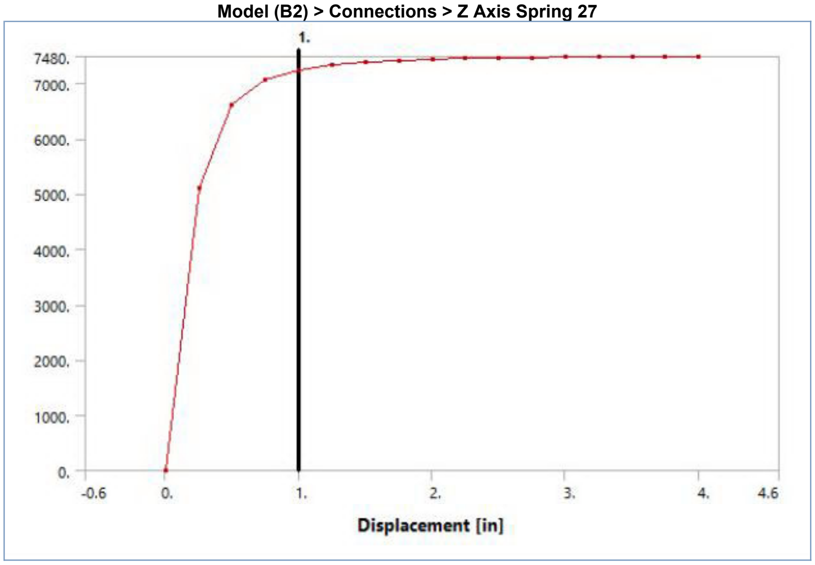

TABLE 90
Model (B2) > Connections > Z Axis Spring 27

Displacement [in]	Force [lbf]
0.	0.
0.25	5110.
0.5	6610.
0.75	7060.

1.	7240.
1.25	7330.
1.5	7380.
1.75	7410.
2.	7430.
2.25	7450.
2.5	7460.
2.75	
3.	7470.
3.25	
3.5	7480.
3.75	
4.	

FIGURE 76
Model (B2) > Connections > Z Axis Spring 28

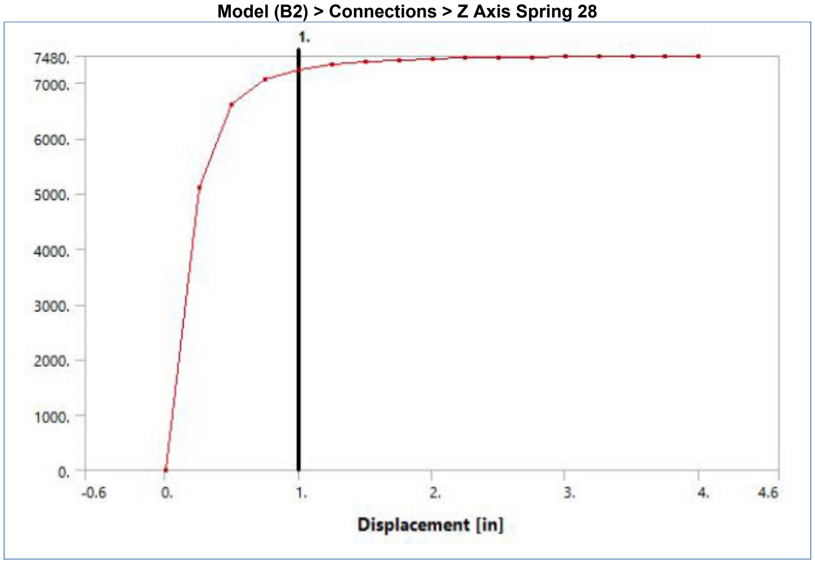

TABLE 91
Model (B2) > Connections > Z Axis Spring 28

Displacement [in]	Force [lbf]
0.	0.
0.25	5110.
0.5	6610.
0.75	7060.
1.	7240.
1.25	7330.
1.5	7380.
1.75	7410.
2.	7430.
2.25	7450.
2.5	7460.
2.75	
3.	7470.
3.25	
3.5	7480.
3.75	
4.	

FIGURE 77
Model (B2) > Connections > Z Axis Spring 29

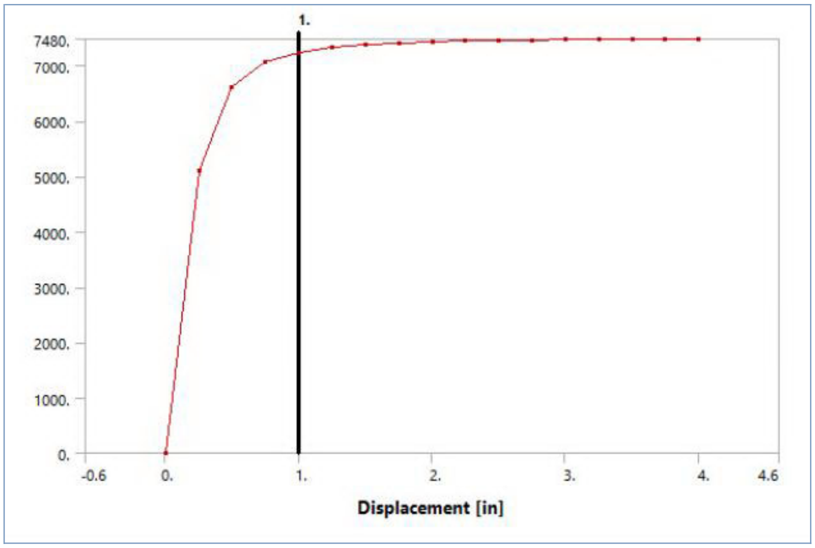

TABLE 92
Model (B2) > Connections > Z Axis Spring 29

<table>
<tr><th>Displacement [in]</th><th>Force [lbf]</th></tr>
<tr><td>0.</td><td>0.</td></tr>
<tr><td>0.25</td><td>5110.</td></tr>
<tr><td>0.5</td><td>6610.</td></tr>
<tr><td>0.75</td><td>7060.</td></tr>
<tr><td>1.</td><td>7240.</td></tr>
<tr><td>1.25</td><td>7330.</td></tr>
<tr><td>1.5</td><td>7380.</td></tr>
<tr><td>1.75</td><td>7410.</td></tr>
<tr><td>2.</td><td>7430.</td></tr>
<tr><td>2.25</td><td>7450.</td></tr>
<tr><td>2.5</td><td rowspan="2">7460.</td></tr>
<tr><td>2.75</td></tr>
<tr><td>3.</td><td rowspan="2">7470.</td></tr>
<tr><td>3.25</td></tr>
<tr><td>3.5</td><td rowspan="3">7480.</td></tr>
<tr><td>3.75</td></tr>
<tr><td>4.</td></tr>
</table>

TABLE 93
Model (B2) > Connections > Springs

Object Name	*Z Axis Spring 30*	*Z Axis Spring 31*
State	Fully Defined	
Graphics Properties		
Visible	Yes	
Definition		
Material	None	
Type	Longitudinal	
Spring Behavior	Both	
Longitudinal Stiffness	Tabular Data	
Longitudinal Damping	0. lbf·s/in	
Preload	None	
Suppressed	No	
Spring Length	12. in	
Element APDL Name		
Scope		
Scope	Body-Ground	
Reference		
Coordinate System	Global Coordinate System	
Reference X Coordinate	0. in	
Reference Y Coordinate	348. in	360. in
Reference Z Coordinate	18.53 in	
Reference Location	Defined	
Mobile		
Scoping Method	Geometry Selection	
Applied By	Remote Attachment	
Scope	8 Faces	
Body	Surface Body(ACP (Pre))	
Coordinate System	Global Coordinate System	
Mobile X Coordinate	0. in	
Mobile Y Coordinate	348. in	360. in
Mobile Z Coordinate	6.53 in	

Mobile Location	Defined
Behavior	Rigid
Pinball Region	6. in

FIGURE 78
Model (B2) > Connections > Z Axis Spring 30

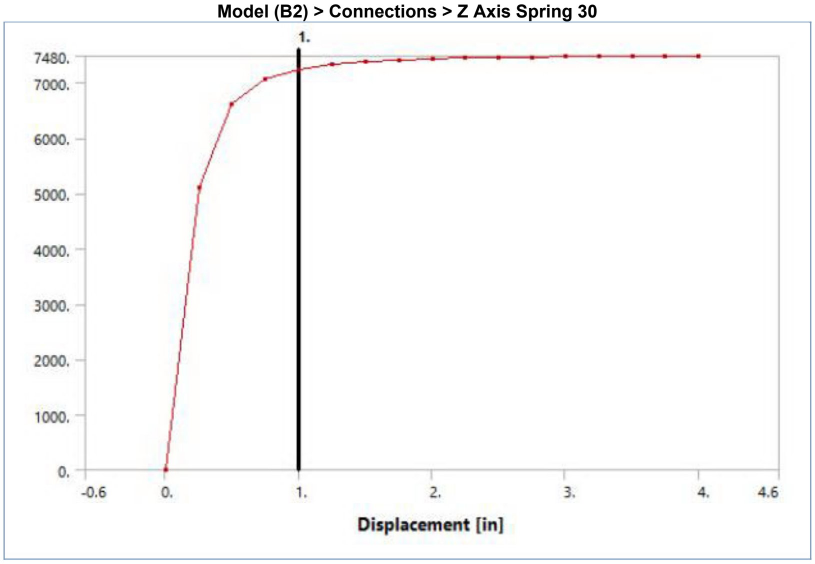

TABLE 94
Model (B2) > Connections > Z Axis Spring 30

<table>
<tr><th>Displacement [in]</th><th>Force [lbf]</th></tr>
<tr><td>0.</td><td>0.</td></tr>
<tr><td>0.25</td><td>5110.</td></tr>
<tr><td>0.5</td><td>6610.</td></tr>
<tr><td>0.75</td><td>7060.</td></tr>
<tr><td>1.</td><td>7240.</td></tr>
<tr><td>1.25</td><td>7330.</td></tr>
<tr><td>1.5</td><td>7380.</td></tr>
<tr><td>1.75</td><td>7410.</td></tr>
<tr><td>2.</td><td>7430.</td></tr>
<tr><td>2.25</td><td>7450.</td></tr>
<tr><td>2.5</td><td rowspan="2">7460.</td></tr>
<tr><td>2.75</td></tr>
<tr><td>3.</td><td rowspan="2">7470.</td></tr>
<tr><td>3.25</td></tr>
<tr><td>3.5</td><td rowspan="3">7480.</td></tr>
<tr><td>3.75</td></tr>
<tr><td>4.</td></tr>
</table>

FIGURE 79
Model (B2) > Connections > Z Axis Spring 31

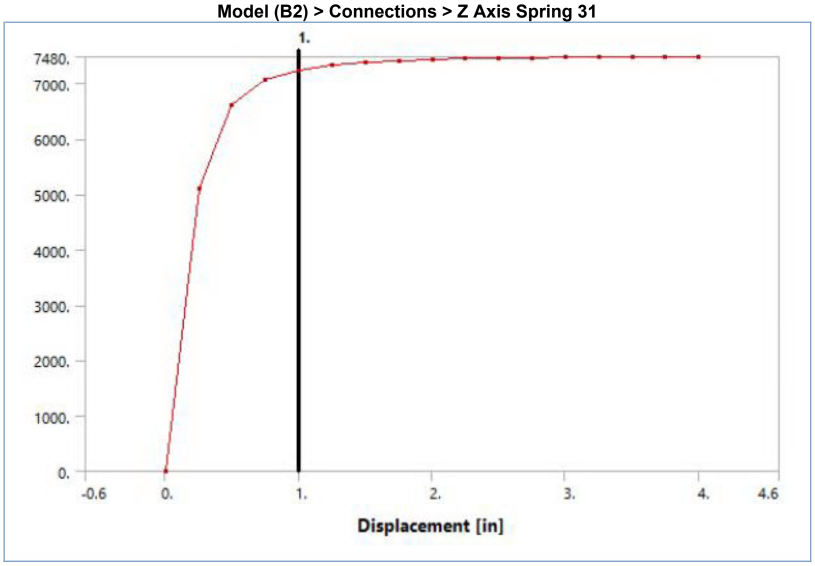

TABLE 95

Model (B2) > Connections > Z Axis Spring 31

Displacement [in]	Force [lbf]
0.	0.
0.25	5110.
0.5	6610.
0.75	7060.
1.	7240.
1.25	7330.
1.5	7380.
1.75	7410.
2.	7430.
2.25	7450.
2.5	7460.
2.75	
3.	7470.
3.25	
3.5	7480.
3.75	
4.	

Mesh

TABLE 96
Model (B2) > Mesh

Object Name	*Mesh*
State	Solved
Display	
Display Style	Use Geometry Setting
Quality	
Check Mesh Quality	Yes, Errors
Error Limits	Standard Mechanical
Mesh Metric	None
Statistics	
Nodes	9248
Elements	9216
Model Assembly	
Read Only	Yes

TABLE 97
Model (B2) > Imported Plies

Object Name	*Imported Plies*
State	Solved
Definition	
Type	Imported Plies
Suppressed	No
Material	
Nonlinear Effects	Yes
Thermal Strain Effects	Yes
Graphics Properties	
Layer To Display	All Layers

ACP (Pre)

ModelingGroup.1(ACP (Pre))

ModelingPly.1(ACP (Pre))

P1__ModelingPly.1(ACP (Pre))

TABLE 98
Model (B2) > Imported Plies > ACP (Pre) > ModelingGroup.1(ACP (Pre)) > ModelingPly.1(ACP (Pre)) > P1__ModelingPly.1(ACP (Pre)) > P1L1__ModelingPly.1 (ACP (Pre))

Object Name	*P1L1__ModelingPly.1(ACP (Pre))*
State	Fully Defined
Definition	
Name in Source	P1L1__ModelingPly.1
ID in Source	P1L1__ModelingPly.1
Material	Epoxy E-Glass UD
Thickness	2.08e-002 in
Angle	0. °
Number of Elements	9216.
Transfer Properties	
Source	A5::ACP (Pre)

P2__ModelingPly.1(ACP (Pre))

TABLE 99
Model (B2) > Imported Plies > ACP (Pre) > ModelingGroup.1(ACP (Pre)) > ModelingPly.1(ACP (Pre)) > P2__ModelingPly.1(ACP (Pre)) > P2L1__ModelingPly.1

(ACP (Pre))	
Object Name	*P2L1__ModelingPly.1(ACP (Pre))*
State	Fully Defined
Definition	
Name in Source	P2L1__ModelingPly.1
ID in Source	P2L1__ModelingPly.1
Material	Epoxy E-Glass UD
Thickness	2.08e-002 in
Angle	0. °
Number of Elements	9216.
Transfer Properties	
Source	A5::ACP (Pre)

P3__ModelingPly.1(ACP (Pre))

TABLE 100
Model (B2) > Imported Plies > ACP (Pre) > ModelingGroup.1(ACP (Pre)) > ModelingPly.1(ACP (Pre)) > P3__ModelingPly.1(ACP (Pre)) > P3L1__ModelingPly.1 (ACP (Pre))

Object Name	*P3L1__ModelingPly.1(ACP (Pre))*
State	Fully Defined
Definition	
Name in Source	P3L1__ModelingPly.1
ID in Source	P3L1__ModelingPly.1
Material	Epoxy E-Glass UD
Thickness	2.08e-002 in
Angle	0. °
Number of Elements	9216.
Transfer Properties	
Source	A5::ACP (Pre)

P4__ModelingPly.1(ACP (Pre))

TABLE 101
Model (B2) > Imported Plies > ACP (Pre) > ModelingGroup.1(ACP (Pre)) > ModelingPly.1(ACP (Pre)) > P4__ModelingPly.1(ACP (Pre)) > P4L1__ModelingPly.1 (ACP (Pre))

Object Name	*P4L1__ModelingPly.1(ACP (Pre))*
State	Fully Defined
Definition	
Name in Source	P4L1__ModelingPly.1
ID in Source	P4L1__ModelingPly.1
Material	Epoxy E-Glass UD
Thickness	2.08e-002 in
Angle	0. °
Number of Elements	9216.
Transfer Properties	
Source	A5::ACP (Pre)

P5__ModelingPly.1(ACP (Pre))

TABLE 102
Model (B2) > Imported Plies > ACP (Pre) > ModelingGroup.1(ACP (Pre)) > ModelingPly.1(ACP (Pre)) > P5__ModelingPly.1(ACP (Pre)) > P5L1__ModelingPly.1 (ACP (Pre))

Object Name	*P5L1__ModelingPly.1(ACP (Pre))*
State	Fully Defined
Definition	
Name in Source	P5L1__ModelingPly.1
ID in Source	P5L1__ModelingPly.1
Material	Epoxy E-Glass UD
Thickness	2.08e-002 in
Angle	0. °
Number of Elements	9216.
Transfer Properties	
Source	A5::ACP (Pre)

P6__ModelingPly.1(ACP (Pre))

TABLE 103
Model (B2) > Imported Plies > ACP (Pre) > ModelingGroup.1(ACP (Pre)) > ModelingPly.1(ACP (Pre)) > P6__ModelingPly.1(ACP (Pre)) > P6L1__ModelingPly.1 (ACP (Pre))

Object Name	*P6L1__ModelingPly.1(ACP (Pre))*
State	Fully Defined
Definition	
Name in Source	P6L1__ModelingPly.1
ID in Source	P6L1__ModelingPly.1
Material	Epoxy E-Glass UD
Thickness	2.08e-002 in
Angle	0. °
Number of Elements	9216.
Transfer Properties	

Source	A5::ACP (Pre)

P7__ModelingPly.1(ACP (Pre))

TABLE 104
Model (B2) > Imported Plies > ACP (Pre) > ModelingGroup.1(ACP (Pre)) > ModelingPly.1(ACP (Pre)) > P7__ModelingPly.1(ACP (Pre)) > P7L1__ModelingPly.1 (ACP (Pre))

Object Name	*P7L1__ModelingPly.1(ACP (Pre))*
State	Fully Defined
Definition	
Name in Source	P7L1__ModelingPly.1
ID in Source	P7L1__ModelingPly.1
Material	Epoxy E-Glass UD
Thickness	2.08e-002 in
Angle	0. °
Number of Elements	9216.
Transfer Properties	
Source	A5::ACP (Pre)

P8__ModelingPly.1(ACP (Pre))

TABLE 105
Model (B2) > Imported Plies > ACP (Pre) > ModelingGroup.1(ACP (Pre)) > ModelingPly.1(ACP (Pre)) > P8__ModelingPly.1(ACP (Pre)) > P8L1__ModelingPly.1 (ACP (Pre))

Object Name	*P8L1__ModelingPly.1(ACP (Pre))*
State	Fully Defined
Definition	
Name in Source	P8L1__ModelingPly.1
ID in Source	P8L1__ModelingPly.1
Material	Epoxy E-Glass UD
Thickness	2.08e-002 in
Angle	0. °
Number of Elements	9216.
Transfer Properties	
Source	A5::ACP (Pre)

P9__ModelingPly.1(ACP (Pre))

TABLE 106
Model (B2) > Imported Plies > ACP (Pre) > ModelingGroup.1(ACP (Pre)) > ModelingPly.1(ACP (Pre)) > P9__ModelingPly.1(ACP (Pre)) > P9L1__ModelingPly.1 (ACP (Pre))

Object Name	*P9L1__ModelingPly.1(ACP (Pre))*
State	Fully Defined
Definition	
Name in Source	P9L1__ModelingPly.1
ID in Source	P9L1__ModelingPly.1
Material	Epoxy E-Glass UD
Thickness	2.08e-002 in
Angle	0. °
Number of Elements	9216.
Transfer Properties	
Source	A5::ACP (Pre)

P10__ModelingPly.1(ACP (Pre))

TABLE 107
Model (B2) > Imported Plies > ACP (Pre) > ModelingGroup.1(ACP (Pre)) > ModelingPly.1(ACP (Pre)) > P10__ModelingPly.1(ACP (Pre)) > P10L1__ModelingPly.1 (ACP (Pre))

Object Name	*P10L1__ModelingPly.1(ACP (Pre))*
State	Fully Defined
Definition	
Name in Source	P10L1__ModelingPly.1
ID in Source	P10L1__ModelingPly.1
Material	Epoxy E-Glass UD
Thickness	2.08e-002 in
Angle	0. °
Number of Elements	9216.
Transfer Properties	
Source	A5::ACP (Pre)

P11__ModelingPly.1(ACP (Pre))

TABLE 108
Model (B2) > Imported Plies > ACP (Pre) > ModelingGroup.1(ACP (Pre)) > ModelingPly.1(ACP (Pre)) > P11__ModelingPly.1(ACP (Pre)) > P11L1__ModelingPly.1 (ACP (Pre))

Object Name	*P11L1__ModelingPly.1(ACP (Pre))*
State	Fully Defined
Definition	

Name in Source	P11L1__ModelingPly.1
ID in Source	P11L1__ModelingPly.1
Material	Epoxy E-Glass UD
Thickness	2.08e-002 in
Angle	0. °
Number of Elements	9216.
Transfer Properties	
Source	A5::ACP (Pre)

P12__ModelingPly.1(ACP (Pre))

TABLE 109
Model (B2) > Imported Plies > ACP (Pre) > ModelingGroup.1(ACP (Pre)) > ModelingPly.1(ACP (Pre)) > P12__ModelingPly.1(ACP (Pre)) > P12L1__ModelingPly.1 (ACP (Pre))

Object Name	*P12L1__ModelingPly.1(ACP (Pre))*
State	Fully Defined
Definition	
Name in Source	P12L1__ModelingPly.1
ID in Source	P12L1__ModelingPly.1
Material	Epoxy E-Glass UD
Thickness	2.08e-002 in
Angle	0. °
Number of Elements	9216.
Transfer Properties	
Source	A5::ACP (Pre)

P13__ModelingPly.1(ACP (Pre))

TABLE 110
Model (B2) > Imported Plies > ACP (Pre) > ModelingGroup.1(ACP (Pre)) > ModelingPly.1(ACP (Pre)) > P13__ModelingPly.1(ACP (Pre)) > P13L1__ModelingPly.1 (ACP (Pre))

Object Name	*P13L1__ModelingPly.1(ACP (Pre))*
State	Fully Defined
Definition	
Name in Source	P13L1__ModelingPly.1
ID in Source	P13L1__ModelingPly.1
Material	Epoxy E-Glass UD
Thickness	2.08e-002 in
Angle	0. °
Number of Elements	9216.
Transfer Properties	
Source	A5::ACP (Pre)

P14__ModelingPly.1(ACP (Pre))

TABLE 111
Model (B2) > Imported Plies > ACP (Pre) > ModelingGroup.1(ACP (Pre)) > ModelingPly.1(ACP (Pre)) > P14__ModelingPly.1(ACP (Pre)) > P14L1__ModelingPly.1 (ACP (Pre))

Object Name	*P14L1__ModelingPly.1(ACP (Pre))*
State	Fully Defined
Definition	
Name in Source	P14L1__ModelingPly.1
ID in Source	P14L1__ModelingPly.1
Material	Epoxy E-Glass UD
Thickness	2.08e-002 in
Angle	0. °
Number of Elements	9216.
Transfer Properties	
Source	A5::ACP (Pre)

P15__ModelingPly.1(ACP (Pre))

TABLE 112
Model (B2) > Imported Plies > ACP (Pre) > ModelingGroup.1(ACP (Pre)) > ModelingPly.1(ACP (Pre)) > P15__ModelingPly.1(ACP (Pre)) > P15L1__ModelingPly.1 (ACP (Pre))

Object Name	*P15L1__ModelingPly.1(ACP (Pre))*
State	Fully Defined
Definition	
Name in Source	P15L1__ModelingPly.1
ID in Source	P15L1__ModelingPly.1
Material	Epoxy E-Glass UD
Thickness	2.08e-002 in
Angle	0. °
Number of Elements	9216.
Transfer Properties	
Source	A5::ACP (Pre)

P16__ModelingPly.1(ACP (Pre))

TABLE 113
Model (B2) > Imported Plies > ACP (Pre) > ModelingGroup.1(ACP (Pre)) > ModelingPly.1(ACP (Pre)) > P16__ModelingPly.1(ACP (Pre)) > P16L1__ModelingPly.1 (ACP (Pre))

Object Name	*P16L1__ModelingPly.1(ACP (Pre))*
State	Fully Defined
Definition	
Name in Source	P16L1__ModelingPly.1
ID in Source	P16L1__ModelingPly.1
Material	Epoxy E-Glass UD
Thickness	2.08e-002 in
Angle	0. °
Number of Elements	9216.
Transfer Properties	
Source	A5::ACP (Pre)

P17__ModelingPly.1(ACP (Pre))

TABLE 114
Model (B2) > Imported Plies > ACP (Pre) > ModelingGroup.1(ACP (Pre)) > ModelingPly.1(ACP (Pre)) > P17__ModelingPly.1(ACP (Pre)) > P17L1__ModelingPly.1 (ACP (Pre))

Object Name	*P17L1__ModelingPly.1(ACP (Pre))*
State	Fully Defined
Definition	
Name in Source	P17L1__ModelingPly.1
ID in Source	P17L1__ModelingPly.1
Material	Epoxy E-Glass UD
Thickness	2.08e-002 in
Angle	0. °
Number of Elements	9216.
Transfer Properties	
Source	A5::ACP (Pre)

P18__ModelingPly.1(ACP (Pre))

TABLE 115
Model (B2) > Imported Plies > ACP (Pre) > ModelingGroup.1(ACP (Pre)) > ModelingPly.1(ACP (Pre)) > P18__ModelingPly.1(ACP (Pre)) > P18L1__ModelingPly.1 (ACP (Pre))

Object Name	*P18L1__ModelingPly.1(ACP (Pre))*
State	Fully Defined
Definition	
Name in Source	P18L1__ModelingPly.1
ID in Source	P18L1__ModelingPly.1
Material	Epoxy E-Glass UD
Thickness	2.08e-002 in
Angle	0. °
Number of Elements	9216.
Transfer Properties	
Source	A5::ACP (Pre)

P19__ModelingPly.1(ACP (Pre))

TABLE 116
Model (B2) > Imported Plies > ACP (Pre) > ModelingGroup.1(ACP (Pre)) > ModelingPly.1(ACP (Pre)) > P19__ModelingPly.1(ACP (Pre)) > P19L1__ModelingPly.1 (ACP (Pre))

Object Name	*P19L1__ModelingPly.1(ACP (Pre))*
State	Fully Defined
Definition	
Name in Source	P19L1__ModelingPly.1
ID in Source	P19L1__ModelingPly.1
Material	Epoxy E-Glass UD
Thickness	2.08e-002 in
Angle	0. °
Number of Elements	9216.
Transfer Properties	
Source	A5::ACP (Pre)

P20__ModelingPly.1(ACP (Pre))

TABLE 117
Model (B2) > Imported Plies > ACP (Pre) > ModelingGroup.1(ACP (Pre)) > ModelingPly.1(ACP (Pre)) > P20__ModelingPly.1(ACP (Pre)) > P20L1__ModelingPly.1 (ACP (Pre))

Object Name	*P20L1__ModelingPly.1(ACP (Pre))*
State	Fully Defined
Definition	
Name in Source	P20L1__ModelingPly.1
ID in Source	P20L1__ModelingPly.1
Material	Epoxy E-Glass UD
Thickness	2.08e-002 in
Angle	0. °

Number of Elements	9216.
Transfer Properties	
Source	A5::ACP (Pre)

P21__ModelingPly.1(ACP (Pre))

TABLE 118
Model (B2) > Imported Plies > ACP (Pre) > ModelingGroup.1(ACP (Pre)) > ModelingPly.1(ACP (Pre)) > P21__ModelingPly.1(ACP (Pre)) > P21L1__ModelingPly.1 (ACP (Pre))

Object Name	*P21L1__ModelingPly.1(ACP (Pre))*
State	Fully Defined
Definition	
Name in Source	P21L1__ModelingPly.1
ID in Source	P21L1__ModelingPly.1
Material	Epoxy E-Glass UD
Thickness	2.08e-002 in
Angle	0. °
Number of Elements	9216.
Transfer Properties	
Source	A5::ACP (Pre)

P22__ModelingPly.1(ACP (Pre))

TABLE 119
Model (B2) > Imported Plies > ACP (Pre) > ModelingGroup.1(ACP (Pre)) > ModelingPly.1(ACP (Pre)) > P22__ModelingPly.1(ACP (Pre)) > P22L1__ModelingPly.1 (ACP (Pre))

Object Name	*P22L1__ModelingPly.1(ACP (Pre))*
State	Fully Defined
Definition	
Name in Source	P22L1__ModelingPly.1
ID in Source	P22L1__ModelingPly.1
Material	Epoxy E-Glass UD
Thickness	2.08e-002 in
Angle	0. °
Number of Elements	9216.
Transfer Properties	
Source	A5::ACP (Pre)

P23__ModelingPly.1(ACP (Pre))

TABLE 120
Model (B2) > Imported Plies > ACP (Pre) > ModelingGroup.1(ACP (Pre)) > ModelingPly.1(ACP (Pre)) > P23__ModelingPly.1(ACP (Pre)) > P23L1__ModelingPly.1 (ACP (Pre))

Object Name	*P23L1__ModelingPly.1(ACP (Pre))*
State	Fully Defined
Definition	
Name in Source	P23L1__ModelingPly.1
ID in Source	P23L1__ModelingPly.1
Material	Epoxy E-Glass UD
Thickness	2.08e-002 in
Angle	0. °
Number of Elements	9216.
Transfer Properties	
Source	A5::ACP (Pre)

P24__ModelingPly.1(ACP (Pre))

TABLE 121
Model (B2) > Imported Plies > ACP (Pre) > ModelingGroup.1(ACP (Pre)) > ModelingPly.1(ACP (Pre)) > P24__ModelingPly.1(ACP (Pre)) > P24L1__ModelingPly.1 (ACP (Pre))

Object Name	*P24L1__ModelingPly.1(ACP (Pre))*
State	Fully Defined
Definition	
Name in Source	P24L1__ModelingPly.1
ID in Source	P24L1__ModelingPly.1
Material	Epoxy E-Glass UD
Thickness	2.08e-002 in
Angle	0. °
Number of Elements	9216.
Transfer Properties	
Source	A5::ACP (Pre)

Static Structural (B3)

TABLE 122
Model (B2) > Analysis

Object Name	*Static Structural (B3)*
State	Solved

Definition	
Physics Type	Structural
Analysis Type	Static Structural
Solver Target	Mechanical APDL
Options	
Environment Temperature	71.6 °F
Generate Input Only	No

TABLE 123
Model (B2) > Static Structural (B3) > Analysis Settings

Object Name	*Analysis Settings*
State	Fully Defined
Step Controls	
Number Of Steps	1.
Current Step Number	1.
Step End Time	1. s
Auto Time Stepping	Program Controlled
Solver Controls	
Solver Type	Program Controlled
Weak Springs	Off
Solver Pivot Checking	Program Controlled
Large Deflection	Off
Inertia Relief	Off
Rotordynamics Controls	
Coriolis Effect	Off
Restart Controls	
Generate Restart Points	Program Controlled
Retain Files After Full Solve	No
Combine Restart Files	Program Controlled
Nonlinear Controls	
Newton-Raphson Option	Program Controlled
Force Convergence	Program Controlled
Moment Convergence	Program Controlled
Displacement Convergence	Program Controlled
Rotation Convergence	Program Controlled
Line Search	Program Controlled
Stabilization	Program Controlled
Output Controls	
Stress	Yes
Surface Stress	No
Back Stress	No
Strain	Yes
Contact Data	Yes
Nonlinear Data	No
Nodal Forces	No
Contact Miscellaneous	No
General Miscellaneous	No
Store Results At	All Time Points
Result File Compression	Program Controlled
Analysis Data Management	
Solver Files Directory	U:\Documents\Thesis Sections\Octagonal\V Stiff Clay\Longer pile_files\dp0\SYS\MECH\
Future Analysis	None
Scratch Solver Files Directory	
Save MAPDL db	No
Contact Summary	Program Controlled
Delete Unneeded Files	Yes
Nonlinear Solution	Yes
Solver Units	Active System
Solver Unit System	Bin

TABLE 124
Model (B2) > Static Structural (B3) > Loads

Object Name	*Displacement*	*Force*	*Elastic Support*
State	Fully Defined		
Scope			
Scoping Method	Geometry Selection		
Geometry	8 Edges		8 Faces
Definition			
Type	Displacement	Force	Elastic Support
Define By	Components		
Coordinate System	Global Coordinate System(ACP (Pre))	Global Coordinate System	
X Component	4. in (ramped)	0. lbf (ramped)	
Y Component	Free	-1.e+005 lbf (ramped)	
Z Component	Free	0. lbf (ramped)	
Suppressed	No		
Foundation Stiffness			50. lbf/in³

FIGURE 80
Model (B2) > Static Structural (B3) > Displacement

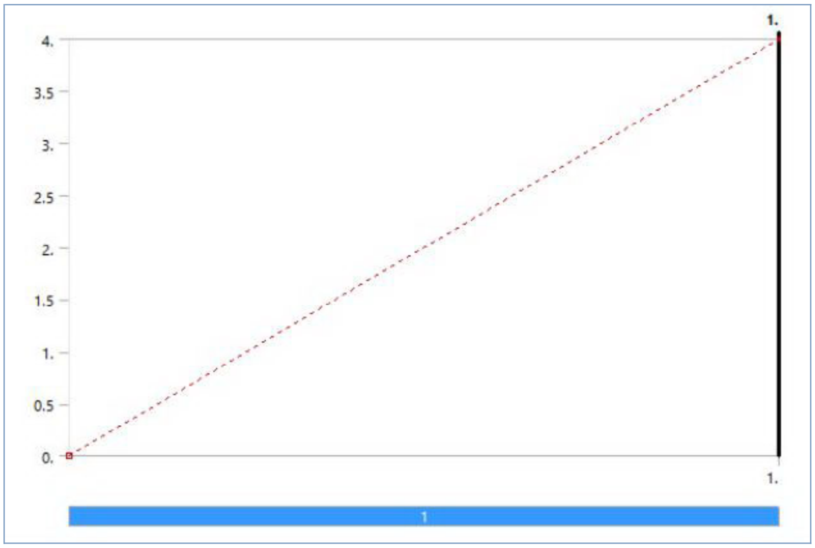

FIGURE 81
Model (B2) > Static Structural (B3) > Force

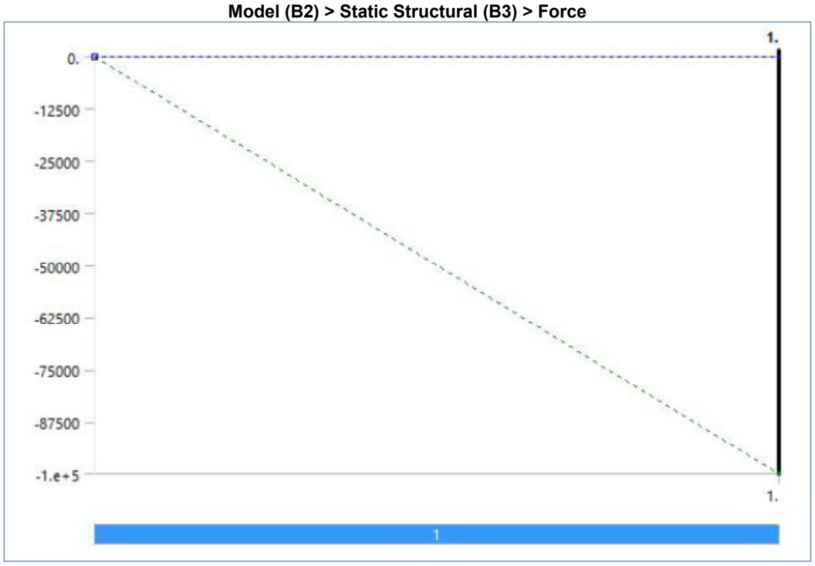

Solution (B4)

TABLE 125
Model (B2) > Static Structural (B3) > Solution

Object Name	*Solution (B4)*
State	Solved
Adaptive Mesh Refinement	
Max Refinement Loops	1.
Refinement Depth	2.
Information	
Status	Done
MAPDL Elapsed Time	1 m 32 s
MAPDL Memory Used	543. MB
MAPDL Result File Size	139.81 MB
Post Processing	
Beam Section Results	No
On Demand Stress/Strain	No

TABLE 126
Model (B2) > Static Structural (B3) > Solution (B4) > Solution Information

Object Name	*Solution Information*
State	Solved
Solution Information	
Solution Output	Solver Output
Newton-Raphson Residuals	0
Identify Element Violations	0
Update Interval	2.5 s
Display Points	All

FE Connection Visibility	
Activate Visibility	Yes
Display	All FE Connectors
Draw Connections Attached To	All Nodes
Line Color	Connection Type
Visible on Results	No
Line Thickness	Single
Display Type	Lines

TABLE 127
Model (B2) > Static Structural (B3) > Solution (B4) > Results

Object Name	*Directional Deformation*	*Maximum Principal Stress*	*Maximum Shear Stress*	*Total Deformation*
State	Solved			
Scope				
Scoping Method	Geometry Selection			
Geometry	All Bodies			
Sub Scope By		Layer		
Layer		Entire Section		
Position		Top/Bottom		
Definition				
Type	Directional Deformation	Maximum Principal Stress	Maximum Shear Stress	Total Deformation
Orientation	Y Axis			
By	Time			
Display Time	Last			
Coordinate System	Global Coordinate System			
Calculate Time History	Yes			
Identifier				
Suppressed	No			
Results				
Minimum	-0.28357 in	-2713.8 psi	2.4186e-012 psi	6.9749e-002 in
Maximum	-6.8022e-002 in	13850 psi	11412 psi	4.01 in
Average	-0.17663 in	234.82 psi	210.51 psi	1.6884 in
Minimum Occurs On	Surface Body(ACP (Pre))			
Maximum Occurs On	Surface Body(ACP (Pre))			
Information				
Time	1. s			
Load Step	1			
Substep	1			
Iteration Number	3			
Integration Point Results				
Display Option		Averaged		
Average Across Bodies		No		

FIGURE 82
Model (B2) > Static Structural (B3) > Solution (B4) > Directional Deformation

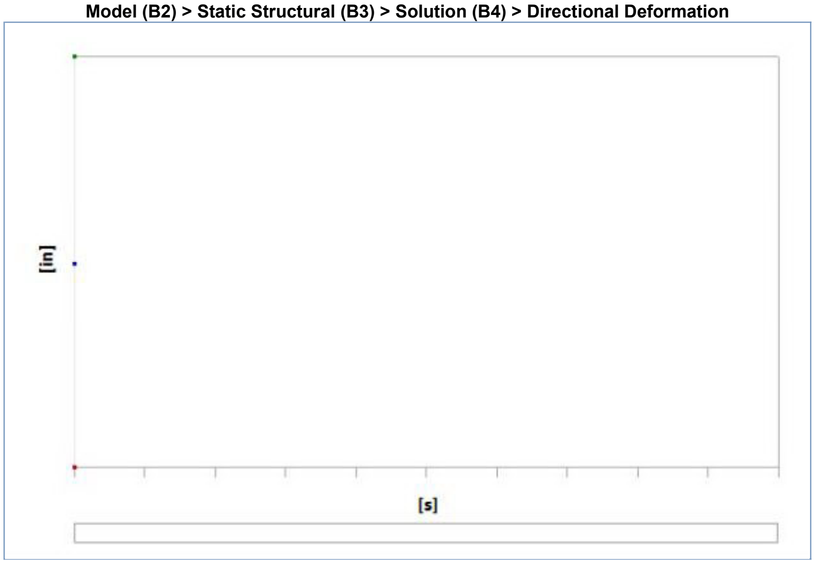

TABLE 128
Model (B2) > Static Structural (B3) > Solution (B4) > Directional Deformation

Time [s]	Minimum [in]	Maximum [in]	Average [in]
1.	-0.28357	-6.8022e-002	-0.17663

FIGURE 83
Model (B2) > Static Structural (B3) > Solution (B4) > Maximum Principal Stress

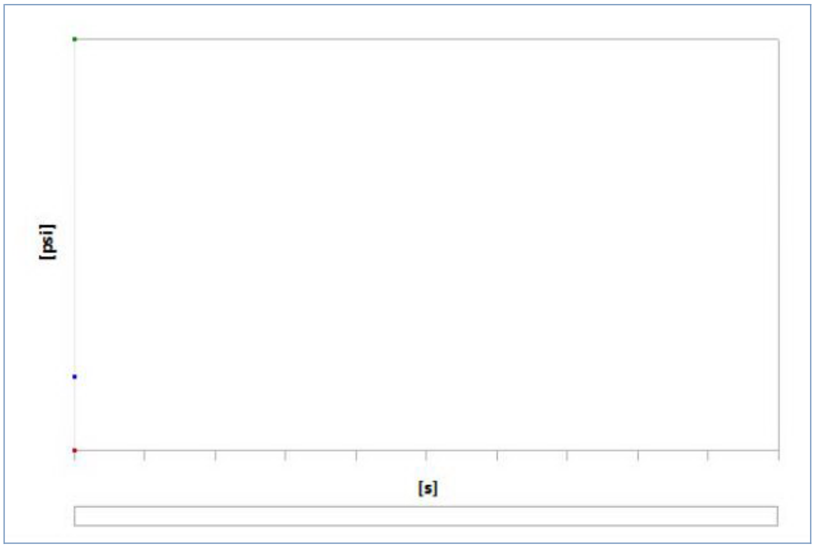

TABLE 129
Model (B2) > Static Structural (B3) > Solution (B4) > Maximum Principal Stress

Time [s]	Minimum [psi]	Maximum [psi]	Average [psi]
1.	-2713.8	13850	234.82

FIGURE 84
Model (B2) > Static Structural (B3) > Solution (B4) > Maximum Shear Stress

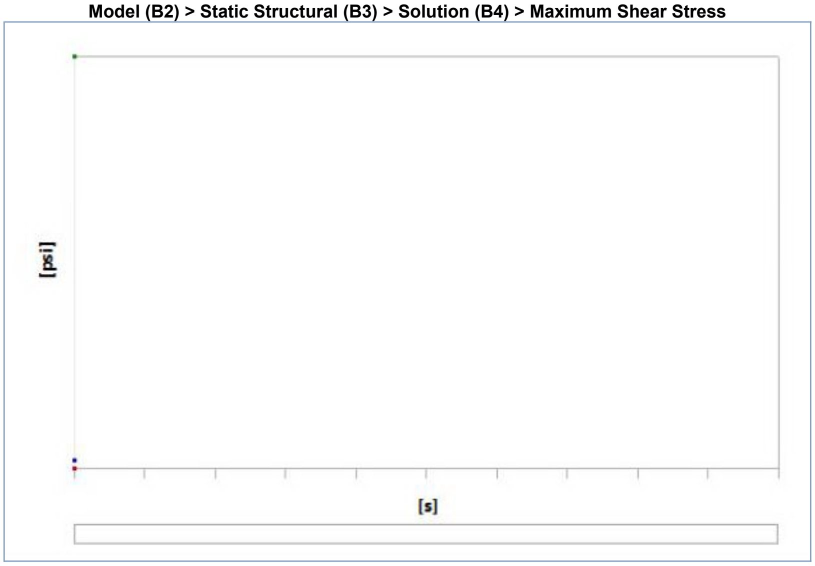

TABLE 130
Model (B2) > Static Structural (B3) > Solution (B4) > Maximum Shear Stress

Time [s]	Minimum [psi]	Maximum [psi]	Average [psi]
1.	2.4186e-012	11412	210.51

FIGURE 85
Model (B2) > Static Structural (B3) > Solution (B4) > Total Deformation

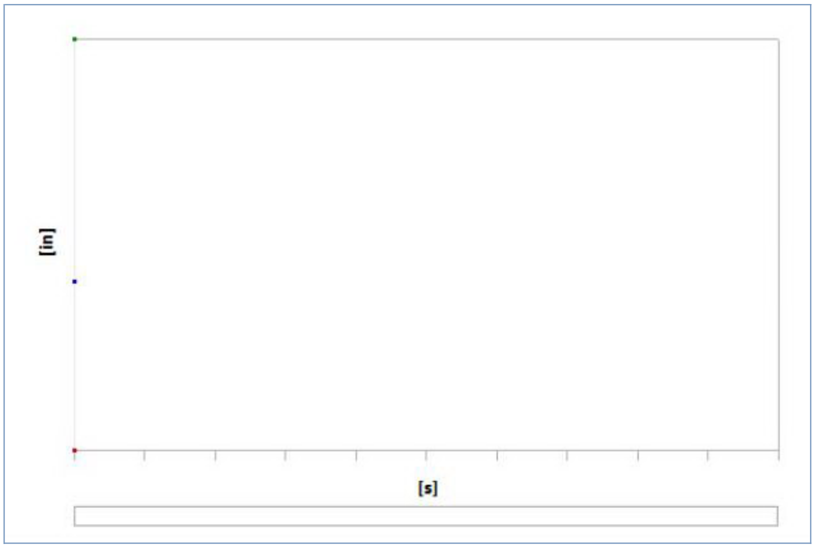

TABLE 131
Model (B2) > Static Structural (B3) > Solution (B4) > Total Deformation

Time [s]	Minimum [in]	Maximum [in]	Average [in]
1.	6.9749e-002	4.01	1.6884

TABLE 132
Model (B2) > Static Structural (B3) > Solution (B4) > Probes

Object Name	*Force Reaction*
State	Solved
Definition	
Type	Force Reaction
Location Method	Spring
Orientation	Global Coordinate System
Spring	End Bearing Spring
Suppressed	No
Options	
Result Selection	All
Display Time	End Time
Results	
X Axis	0. lbf
Y Axis	22585 lbf
Z Axis	0. lbf
Total	22585 lbf
Maximum Value Over Time	
X Axis	0. lbf
Y Axis	22585 lbf
Z Axis	0. lbf
Total	22585 lbf
Minimum Value Over Time	
X Axis	0. lbf
Y Axis	22585 lbf
Z Axis	0. lbf
Total	22585 lbf
Information	
Time	1. s
Load Step	1
Substep	1
Iteration Number	3

FIGURE 86
Model (B2) > Static Structural (B3) > Solution (B4) > Force Reaction

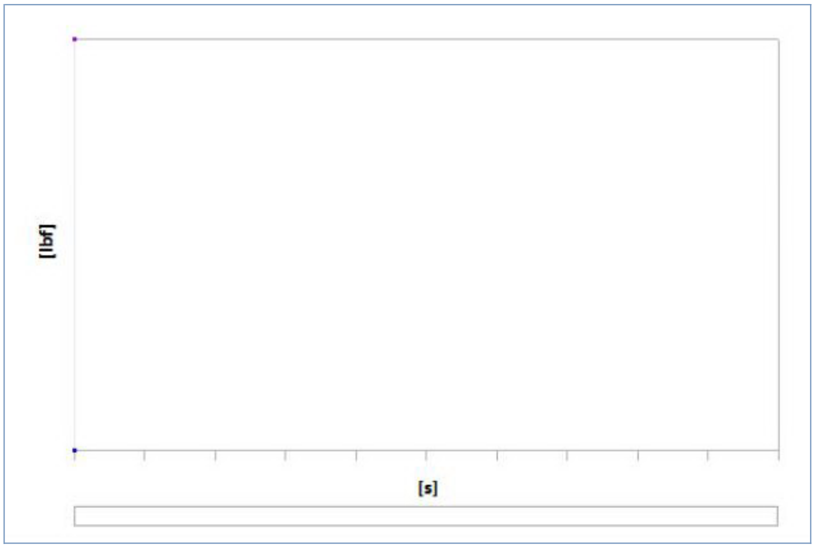

TABLE 133
Model (B2) > Static Structural (B3) > Solution (B4) > Force Reaction

Time [s]	Force Reaction (X) [lbf]	Force Reaction (Y) [lbf]	Force Reaction (Z) [lbf]	Force Reaction (Total) [lbf]
1.	0.	22585	0.	22585

TABLE 134
Model (B2) > Static Structural (B3) > Solution (B4) > Composite Failure Tool

Object Name	*Composite Failure Tool*
State	Solved
Definition	
Type	Composite Failure Tool
Reference	
Defined By	Direct Input
Reinforced Ply Criteria	
Maximum Strain	On
Maximum Stress	On
Tsai-Wu	On
Tsai-Hill	On
Hoffman	Off
Hashin	Off
Puck	On
LaRC	Off
Cuntze	Off
Sandwich Criteria	
Face Sheet Wrinkling	Off
Core Failure	Off
Shear Crimping	Off
Isotropic Material Criteria	
Von Mises	Off

TABLE 135
Model (B2) > Static Structural (B3) > Solution (B4) > Composite Failure Tool > Results

Object Name	*Inverse Reserve Factor*	*Safety Factor*
State	Solved	
Scope		
Scoping Method	Geometry Selection	
Geometry	All Bodies	
Sub Scope By	Entire Section	
Definition		
Type	Inverse Reserve Factor	Safety Factor
Show Critical Failure Mode	Yes	
Show Critical Layer	Yes	No
Threshold for Text Visualization	Auto	
--Value	0.25	4.
By	Time	
Display Time	Last	
Calculate Time History	No	
Suppressed	No	
Integration Point Results		
Display Option	Elemental Maximum	
Results		
Minimum	2.725e-015	0.80895
Maximum	1.2362	1000.
Average	2.4509e-002	696.2
Minimum Occurs On	Surface Body(ACP (Pre))	

Maximum Occurs On	Surface Body(ACP (Pre))
Information	
Time	1. s
Load Step	1
Substep	1
Iteration Number	3

FIGURE 87
Model (B2) > Static Structural (B3) > Solution (B4) > Composite Failure Tool > Inverse Reserve Factor

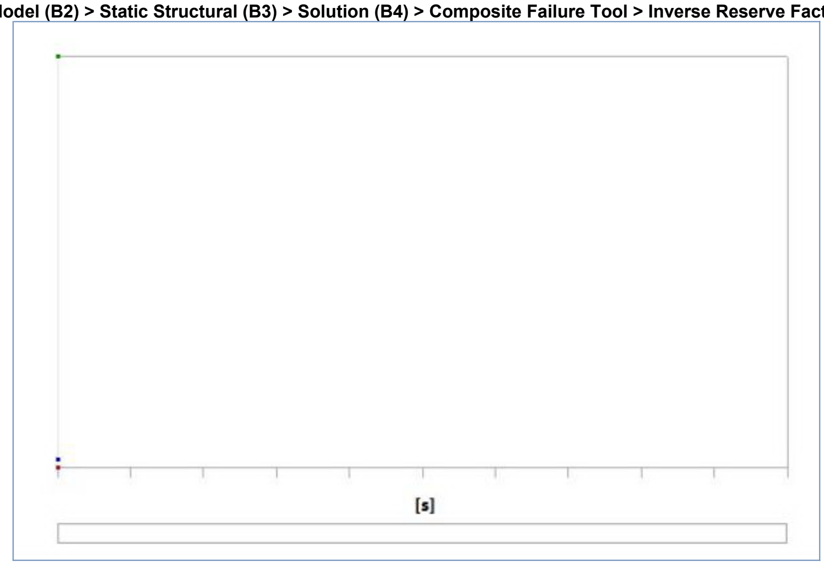

TABLE 136
Model (B2) > Static Structural (B3) > Solution (B4) > Composite Failure Tool > Inverse Reserve Factor

Time [s]	Minimum	Maximum	Average
1.	2.725e-015	1.2362	2.4509e-002

FIGURE 88
Model (B2) > Static Structural (B3) > Solution (B4) > Composite Failure Tool > Safety Factor

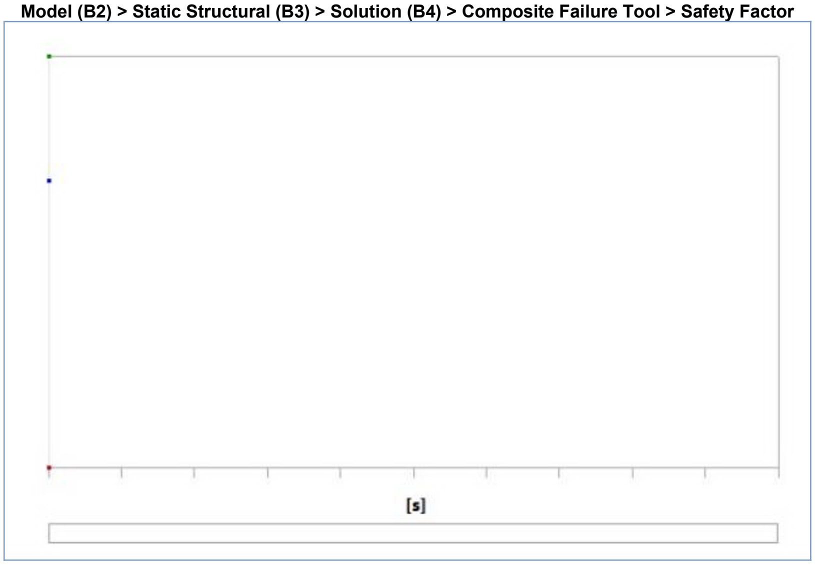

TABLE 137
Model (B2) > Static Structural (B3) > Solution (B4) > Composite Failure Tool > Safety Factor

Time [s]	Minimum	Maximum	Average
1.	0.80895	1000.	696.2

Material Data

Epoxy E-Glass UD

TABLE 138
Epoxy E-Glass UD > Density

Density lbm in^-3
7.2255e-002

TABLE 139
Epoxy E-Glass UD > Orthotropic Elasticity

Young's Modulus X direction psi	Young's Modulus Y direction psi	Young's Modulus Z direction psi	Poisson's Ratio XY	Poisson's Ratio YZ	Poisson's Ratio XZ	Shear Modulus XY psi	Shear Modulus YZ psi	Shear Modulus XZ psi
6.5267e+006	1.4504e+006	1.4504e+006	0.3	0.4	0.3	7.2519e+005	5.5784e+005	7.2519e+005

TABLE 140
Epoxy E-Glass UD > Orthotropic Strain Limits

Tensile X direction	Tensile Y direction	Tensile Z direction	Compressive X direction	Compressive Y direction	Compressive Z direction	Shear XY	Shear YZ	Shear XZ
2.44e-002	3.5e-003	3.5e-003	-1.5e-002	-1.2e-002	-1.2e-002	1.6e-002	1.2e-002	1.6e-002

TABLE 141
Epoxy E-Glass UD > Orthotropic Stress Limits

Tensile X direction psi	Tensile Y direction psi	Tensile Z direction psi	Compressive X direction psi	Compressive Y direction psi	Compressive Z direction psi	Shear XY psi	Shear YZ psi	Shear XZ psi
1.5954e+005	5076.3	5076.3	-97900	-17405	-17405	11603	6694	11603

TABLE 142
Epoxy E-Glass UD > Puck Constants

Compressive Inclination XZ	Compressive Inclination YZ	Tensile Inclination XZ	Tensile Inclination YZ
0.25	0.2	0.3	0.2

TABLE 143
Epoxy E-Glass UD > Additional Puck Constants

Interface Weakening Factor	Degradation Parameter s	Degradation Parameter M
0.8	0.5	0.5

TABLE 144
Epoxy E-Glass UD > Tsai-Wu Constants

Temperature F	Coupling Coefficient XY	Coupling Coefficient YZ	Coupling Coefficient XZ
	-1	-1	-1

TABLE 145
Epoxy E-Glass UD > Color

Red	Green	Blue
184	235	197

Concrete

TABLE 146
Concrete > Constants

Density	8.3093e-002 lbm in^-3
Coefficient of Thermal Expansion	7.7778e-006 F^-1
Specific Heat	0.1863 BTU lbm^-1 F^-1
Thermal Conductivity	9.6298e-006 BTU s^-1 in^-1 F^-1

TABLE 147
Concrete > Color

Red	Green	Blue
180	173	167

TABLE 148
Concrete > Compressive Ultimate Strength

Compressive Ultimate Strength psi
5946.5

TABLE 149
Concrete > Compressive Yield Strength

Compressive Yield Strength psi
0

TABLE 150
Concrete > Tensile Yield Strength

Tensile Yield Strength psi
0

TABLE 151
Concrete > Tensile Ultimate Strength

Tensile Ultimate Strength psi
725.19

TABLE 152
Concrete > Isotropic Secant Coefficient of Thermal Expansion

Zero-Thermal-Strain Reference Temperature F
71.6

TABLE 153
Concrete > Isotropic Elasticity

Young's Modulus psi	Poisson's Ratio	Bulk Modulus psi	Shear Modulus psi	Temperature F
4.3511e+006	0.18	2.2662e+006	1.8437e+006	

Bibliography

[1] P. S. Yang, A. M. Wolde-Tinsae and L. F. Greimann, "Nonlinear Finite Element Study of Piles in Integral Abutment Bridges Part 2," 1982.

[2] C. Tuakta, "USE OF FIBER REINFORCED POLYMER COMPOSITE IN BRIDGE STRUCTURES," 2005.

[3] H. A. Shaia, "BEHAVIOUR OF FIBRE REINFORCED POLYMER COMPOSITE PILES: EXPERIMENTAL AND NUMERICAL STUDY," 2013.

[4] M. Sakr, M. H. E. Naggar and M. Nehdi, "Novel toe driving for thin-walled piles and performance of fiberglass-reinforced polymer (FRP) pile segments," 14 04 2004. [Online]. Available: http://cgj.nrc.ca.

[5] A. Paraschos and A. M. Amde, "A survey on the status of use, problems, and costs associated with Integral Abutment Bridges," 2010.

[6] M. A. Pando, "Durability of Concrete-Filled Tubular FRP Piles," 2002.

[7] R. Najib and A. M. Amde, "Effect of Pile Orientation in Skewed Integral Abutment Bridges," 2010.

[8] M. A. Masuelli, "Introduction of Fibre-Reinforced Polymers − Polymers and Composites: Concepts, Properties and Processes," 23 01 2013. [Online]. Available: https://www.intechopen.com/books/fiber-reinforced-polymers-the-technology-applied-for-concrete-repair/introduction-of-fibre-reinforced-polymers-polymers-and-composites-concepts-properties-and-processes. [Accessed 28 02 2020].

[9] D. Lawrence, "EXPERIMENTAL EVALUATION OF FIBER REINFORCED POLYMER PILES IN LOAD-BEARING APPLICATIONS," Maine DOT, 2015.

[10] J. Kunin and S. Alampalli, "INTEGRAL ABUTMENT BRIDGES: CURRENT PRACTICE IN UNITED STATES AND CANADA," *Journal of Performance of Constructed Facilities,* vol. 14, no. 3, pp. 104-111, 2000.

[11] Y. Jaradat, "SOIL-STRUCTURE INTERACTION OF FRP PILES IN INTEGRAL ABUTMENT BRIDGES," 2005.

[12] M. G. Iskander and M. Hassan, "STATE OF THE PRACTICE REVIEW IN FRP COMPOSITE PILING," *Journal of Composites for Construction,* vol. 2, no. 3, 1998.

[13] M. Iskander, "Recent Developments in FRP Composite Piling Practice," in *TRB 2002 Session on Composite Piles (Committee A2K03)*, 2002.

[14] M. Iskander, A. Mohamed and M. Hassan, "Durability of FRP piling piling in aggressive environments," 2002.

[15] R. B. Holland, "DURABILITY OF PRECAST PRESTRESSED CONCRETE PILES IN MARINE ENVIRONMENTS," 2012.

[16] J. Giraldo and M. Rayhani, "Load transfer of hollow Fiber-Reinforced Polymer (FRP) piles," *Transportation Geotechnics,* vol. 1, no. 2, pp. 63-73, 2014.

[17] A. . Z. Fam and S. . H. Rizkalla, "Confinement Model for Axially Loaded Concrete Confined by Circular Fiber-Reinforced Polymer Tubes," *ACI Structural Journal,* vol. 98, no. 4, pp. 451-461, 2001.

[18] A. Z. Fam and S. H. Rizkalla, "Behavior of Axially Loaded Concrete-Filled Circular FRP Tubes," 2001.

[19] U. D. O. Defense, Composite Materials Handbook-MIL 17: Materials Usage, Design, and Analysis, CRC Press.

[20] I. M. Daniel and O. Ishai, Engineering Mechanics of Composite Materials, New York: Oxford University Press, 2006.

[21] S. A. Civjan, C. Bonczar, S. F. Breña, J. T. DeJong and D. S. Crovo, "Integral Abutment Bridge Behavior: Parametric Analysis of a Massachusetts Bridge," *Journal of Bridge Engineering,* vol. 12, no. 1, pp. 64-71, 2007.

[22] S. A. Ashford and W. Jakrapiyanun, "Drivability of Glass FRP Composite Piling," *Journal of Composites for Construction,* vol. 5, no. 1, pp. 58-60, 2001.

[23] Y. Aliabadizadeh, "BEHAVIOR OF FIBER REINFORCED POLYMER COMPOSITE PILES WITH ELLIPTICAL CROSS SECTIONS IN INTEGRAL ABUTMENT BRIDGE FOUNDATIONS," 2016.

[24] Creative Pultrusions, "SUPERPILE® - PIPE PILE," [Online]. Available: https://www.creativepultrusions.com/index.cfm/data/product-literature/waterfront-products-literature/superpile-technical-brochure/. [Accessed 12 02 2020].

[25] Autodesk, "Puck Criterion," 21 10 2016. [Online]. Available: https://knowledge.autodesk.com/support/helius-composite/learn-explore/caas/CloudHelp/cloudhelp/2017/ENU/ACMPDS/files/GUID-7343646B-039D-4CF1-BBBE-B453FF8C6877-htm.html. [Accessed 29 03 2020].

[26] Dupont, "Kevlar® Fibers," [Online]. Available: https://www.dupont.com/products/dupont-kevlar-fiber.html. [Accessed 12 03 2020].

[27] DOFRP, "Fiberglass Reinforced Plastic," [Online]. Available: https://www.dofrp.com. [Accessed 16 03 2020].

[28] Federal Highway Administration, "FHWA-HRT-04-043," 03 2006. [Online]. Available: https://www.fhwa.dot.gov/publications/research/infrastructure/structures/04043/02.cfm. [Accessed 17 03 2020].

[29] U.S. Department of Transportation Federal Highway Administration, "Behavior of Fiber-Reinforced Polymer Composite Piles Under Vertical Loads," 2006.

[30] A. Paraschos, "Effects of Wingwall Configurations on the Behavior of Integral Abutment Bridges".